

**The Long-term Weathering of Pulverised Fuel Ash  
and its Implications for Groundwater Pollution**

by

Sanghoon Lee  
Department of Earth Sciences  
University of Sheffield

Thesis submitted in fulfilment of  
the Requirements for the Degree of  
Doctor of Philosophy

May, 1994

## **Abstract**

The current, non-marketed, production of PFA in the UK amounts to approximately  $6.5 \times 10^6$  tonnes per year. This waste is disposed of in lagoons, land-fill sites or mounds. Many trace elements are concentrated in PFA and their association with either unstable high temperature glass phases or surfaces of particles creates potential environmental problems of leachates contributing to groundwater. Natural weathering of PFA are not well documented and form the basis of this study. PFA samples were taken from boreholes in ash mound associated with two UK power stations. The PFA on these mounds date back 17 and approximately 40 years. In addition, effluents samples were taken from one of the ash mounds.

Reaction of PFA with the infiltrating porewaters in the boreholes are indicated from the depth-related trend of elements both in the porewater and in the PFA. This allows an assessment of the mobility of element. Losses of elements from the PFA to the porewater are also detected in the whole PFA and this provides confirmation of some of the porewater depth trend. Although the chemical analyses demonstrated that reactions are taking place, secondary reaction products have not been unambiguously detected using SEM and XRD analyses. The feedback based investigations have been supplemented in the laboratory using batch and column leaching tests. The performance of weathered and fresh PFA has been compared with the result from the field investigation and also the feasibility of weathered PFA providing some amelioration for land-fill leachate has been investigated.

The results from the field and laboratory investigations imply that not only fresh ash, but also weathered ash, yields elemental concentrations that exceed the drinking water quality standards. More importantly, the release of elements from the weathered ash decreases slowly with time and therefore weathered PFA, could be a potential source of groundwater pollution, without proper protection, even after a long period of disposal.

## **Acknowledgement**

First of all I would like thank Professor D. A. Spears who broadened my outlook on science, for his great support and guidance throughout the whole period of this project.

I would like to thank the National Power for the financial support for the laboratory experiments and Mr. Malcolm Hill, former ash and coal manager, and staff in Drax Power Station for their support. The support and expertise of Dr. S. Waygood and other staff in National Power are greatly acknowledged.

In analytical works in Earth Sciences department, Sheffield, I am especially indebted to Dr. R. Kanaris-Sotiriou, for his help and guidance in the use of XRD and XRF analysis, to Alan Saxby for his help on AAS and wet chemical analysis. I also greatly appreciate the assistance of A.W Fairburn, Animal and plant sciences, for his works on AAS and Ion chromatography and Dr. P. Korgul, Sorby centre, for his works of semi-quantitative analysis with SEM. In addition to those who are in the university, I would like to thank Mr. M. Dobby, the Assay Office, Sheffield and Dr, N. Walsh, Royal Holloway and Bedford New College, for their valuable works on ICP analyses. Graham Mulhearn helped me to set up the experimental settings for the leaching and column leaching tests with his great craftsmanship and sense of humour. Paul Higham, departmental superintendent, has been always helpful for my various trifles. I am very grateful to Wyn James, who proof-reads my thesis, turning my thesis into more readable one.

I would like to express my deep sense of gratitude to my parents, parents in law and my wife, Eunkyong, for their great encouragement and devoting support during the whole period of the course.

Finally, I feel a great gratitude to Professor H. S. Moon in Yonsei University, Korea, who persuaded me to resume the research course and helped me to start in Sheffield in the end. Without him, I would never have felt the pleasure of completing this work.

# Contents

	Initial page
<b>Abstracts</b>	i
<b>Acknowledgement</b>	ii
<b>Contents</b>	iii
<b>List of Figures</b>	viii
<b>List of Tables</b>	xii
<b>List of Plates</b>	xiii
<b>Chapter 1 Introduction</b>	1
1.1 Overview	1
1.2 Previous and current research	2
1.2.1 Studies on the chemical, mineralogical and physical properties of PFA	4
1.2.2 PFA batch/column leaching test	6
1.2.3 Field based studies	8
1.2.4 Thermochemical approach	8
1.3 Aims of study	9
1.4 Study area	11
<b>Chapter 2 Site Description and Method</b>	13
2.1 Site Description	13
2.1.1. Drax Power Station	13
2.2.2. Meaford Power Station	17
2.2 Sampling of PFA and porewater	18
2.2.1 Barlow PFA Mound	18
2.2.2 PFA sampling at the Meaford site	21
2.3 Pore water extraction	21
2.4 Analytical methods	22

2.4.1 Whole PFA analysis	23
2.4.2 Water analysis	25
2.4.3 Assessing analytical results	26
2.5. Geochemical modelling	27
<b>Chapter 3 Field investigation of Porewater</b>	<b>29</b>
3.1 Introduction	29
3.2. Investigation of depth profiles in Drax porewater	30
3.2.1 Introduction	30
3.2.2 Depth profiles of major elements	32
3.2.3 Depth profiles of minor elements	37
3.3 Geochemical reactions in porewater	41
3.3.1 Introduction	41
3.3.2 Major ions	42
3.3.3 Minor ions	45
3.4 Elements with an external origin	49
3.5 Chemistry of Meaford porewater	50
3.5.1 Chemical composition of Meaford porewater	51
3.5.2 Depth profiles of Meaford porewater	54
3.6 Geochemistry of porewater and its long-term influence on groundwater	57
3.6.1 Comparison of Drax and Meaford porewater	57
3.6.2 Evolution of porewater and implications for groundwater pollution	59
3.7 Conclusion	60
<b>Chapter 4 Chemistry and mineralogy of PFA and their changes during weathering</b>	<b>62</b>
4.1 Introduction	62
4.2 Mineralogy and chemistry of fresh PFA	63
4.2.1 Mineralogy of fresh Drax PFA	63
4.2.2 Chemistry of fresh Drax PFA	68

4.2.3 Comparison between fresh and weathered Drax PFA	69
4.3 Chemical changes in Drax PFA during weathering	70
4.3.1 Depth profiles of major elements	70
4.3.2 Depth profiles of trace elements	73
4.4 Mineralogical changes in Drax PFA during weathering	75
4.4.1 Introduction	75
4.4.2 XRD investigation of clay fractionated samples	75
4.4.3 SEM	77
4.5 Weathered Meaford PFA	82
4.5.1 Introduction	82
4.5.2 Depth profiles of major elements in Meaford PFA	83
4.5.3 Depth profiles of trace elements in Meaford PFA	85
4.5.4 Mineralogy of Meaford PFA	86
4.6 Geochemistry of PFA and its relationship to porewater composition	91
4.6.1 Geochemical associations in PFA	91
4.6.2 Weathering of PFA and its implications for porewater chemistry	95
4.7 Conclusion	96
<b>Chapter 5 Chemistry of effluents from the Barlow ash mound</b>	<b>98</b>
5.1 Introduction	98
5.2 Chemistry of effluent from the Barlow mound	99
5.2.1 Leachate water	99
5.2.2 Chemistry of ditch water	100
5.2.3 Geochemical associations	103
5.4 Rate of infiltration of porewater in the Barlow ash mound	105
5.5 Comparison of leachate water with porewater	107
5.6. Comparison of the chemistry of leachate water with water quality standard	109
5.7 Conclusion	110
<b>Chapter 6. Batch leaching tests</b>	<b>112</b>

6.1 Introduction	112
6.2 Experiments	113
6.2.1 Material	113
6.2.2 Experimental procedures	115
6.3 Batch leaching with deionised water	116
6.3.1 Introduction	116
6.3.2 Leaching behaviour of PFA with deionised water	117
6.3.3 Mobility of elements and leaching behaviour - data from the batch leaching tests with deionised water	120
6.3.4 Comparison of eluates from deionised water with water quality standards	125
6.4 Electrical conductivity and leachate quality	126
6.5 Reaction of PFA with synthetic leachate	128
6.5.1 Introduction	128
6.5.2 Batch leaching of fresh Drax PFA with synthetic leachate	129
6.5.3 Batch leaching of weathered Drax PFA with synthetic leachate	131
6.5.4 Batch leaching of weathered Meaford PFA with synthetic leachate	132
6.5.5 Trace elements retention from synthetic leachate	133
6.6 Conclusion	137
<b>Chapter 7 Column leaching tests</b>	<b>139</b>
7.1 Introduction	139
7.2 Experimental method	140
7.2.1 Samples with synthetic leachate	140
7.2.2 Design of columns and experimental procedure	141
7.3 Column leaching with deionised water	143
7.3.1 Fresh Drax PFA with deionised water	143
7.3.2 Weathered Drax and Meaford PFA with deionised water	148
7.4 Leaching behaviour of elements from the column leaching tests	152

7.4.1 Introduction	152
7.4.2 Leaching behaviour of major elements	152
7.4.3 Leaching behaviour of trace elements	162
7.4.4 Comparison of batch and column leaching tests	172
7.5 Comparison of column leaching results with water quality standards	172
7.6 Column leaching tests with synthetic leachate	176
7.3.1 Fresh Drax PFA with synthetic leachate	176
7.3.2 Weathered Drax and Meaford PFA with synthetic leachate	177
7.3.3 Comparison of leaching of fresh and weathered PFA	180
7.7 Conclusion	181
<b>Chapter 8 Geochemical modelling of water/PFA interaction</b>	<b>184</b>
8.1 Introduction	184
8.2 Major elements	185
8.2.1 Silicon	185
8.2.2 Alumina	188
8.2.3 Calcium	191
8.2.4 Iron	195
8.3 Trace elements	197
8.3.1 Copper	199
8.3.2 Zinc	198
8.3.3 Lead	200
8.4 Conclusion	201
<b>Chapter 9 Conclusions</b>	<b>202</b>
<b>References</b>	<b>208</b>
<b>Appendix A. Additional experimental methods</b>	<b>A1</b>
<b>Appendix B. Geochemical modelling</b>	<b>B1</b>
<b>Appendix C. Data</b>	<b>C1</b>

## List of Figures

	Initial page
Figure 2.1	Drax Power Station and the Barlow PFA disposal site 15
Figure 2.2	Vertical section of the rocks below the Barlow PFA mound 16
Figure 2.3	Meaford Power Station and disposal of PFA 19
Figure 2.3	Schematic diagram of drilling of weathered PFA using hand-auger drill in the Barlow and Meaford PFA mound 20
Figure 2.5	Centrifuge liner assemblies for extracting porewater from PFA 22
Figure 3.1	Depth profiles of Na (a) and K (b) of porewater from boreholes in Drax PFA. 32
Figure 3.2	Depth profiles of Mg (a) and Ca (b) in Drax porewater 33
Figure 3.3	Depth profiles of SO <sub>4</sub> (II-) (a) and comparison with Ca (b) in Drax porewater 35
Figure 3.4	Depth profiles of Cl <sup>-</sup> (a) and NO <sub>3</sub> <sup>-</sup> (b) in Drax porewater 36
Figure 3.5	Depth profile of Si in Drax porewater, borehole 4 37
Figure 3.6	Depth profiles of trace elements, showing increase with depth, in Drax porewater, borehole 4 38
Figure 3.7	Depth profiles of trace elements (Ba, Sr, Zn, Cu) in Drax porewater, borehole 4 40
Figure 3.8	Plot of Ca and SO <sub>4</sub> (II-) activities in Drax porewater along with the calculated activities in equilibrium with gypsum and anhydrite (a), saturation indices with respect to gypsum (b) 43
Figure 3.9	Relationship between Mg and SO <sub>4</sub> (II-) 44
Figure 3.10	Relationship of Na, K vs. TDS (a) and Na vs. K (b) 45
Figure 3.11	Relationship between SiO <sub>2</sub> vs. B and B vs. Li and Mo (b) 46
Figure 3.12	Relationship between B vs. K and Mg (a) B vs. Ni and Pb (b) 47
Figure 3.13	Relationship between Ba vs. SO <sub>4</sub> (II-) (a) and Sr vs. SO <sub>4</sub> (II-) (b) 48
Figure 3.14	Relationship between NO <sub>3</sub> <sup>-</sup> and Cl <sup>-</sup> in porewater of borehole 4 50
Figure 3.15	Comparison of average concentrations of the major ions in Meaford and Drax porewater 51
Figure 3.16	Variation of pH in Meaford porewater with depth 52
Figure 3.17	Depth profiles of major elements (Na, K, Ca, Mg) in Meaford porewater 54
Figure 3.18	Depth profiles of SiO <sub>2</sub> (a) and al (b) in Meaford porewater 55
Figure 3.19	Depth profiles of anions in Meaford porewater 56
Figure 3.20	Depth profiles of minor ions in Meaford porewater 56

Figure 4.1	X-ray diffractogram of whole Drax and Meaford ash	65
Figure 4.3	Classification of PFA used in this study, after the scheme of Roy and Griffin (1982)	69
Figure 4.4	Depth profiles of major elements in weathered PFA, Barlow	71
Figure 4.5	Depth profiles of trace elements in weathered PFA, Barlow	74
Figure 4.6	X-ray diffractogram of clay size-fractionated samples from Drax borehole 2	76
Figure 4.8	Depth profiles of major elements in weathered Meaford PFA	83
Figure 4.9	Depth profiles of trace elements in weathered Meaford PFA	85
Figure 4.10	X-ray diffractogram of weathered Meaford PFA samples, collected at various depth	87
Figure 4.12	Al <sub>2</sub> O <sub>3</sub> vs. K <sub>2</sub> O in weathered Drax PFA	91
Figure 4.13	Relationships between Fe <sub>2</sub> O <sub>3</sub> and SiO <sub>2</sub> vs. L.O.I. in weathered Drax PFA	92
Figure 4.14	Relationships between Zn and Pb in weathered Drax PFA	94
Figure 4.15	Relationships of Zn and Pb with L.O.I. in weathered Drax PFA	95
Figure 5.1	The major ionic compositions of Drax leachate water samples	100
Figure 5.2	Ionic concentration vs. TDS in Barlow leachate water	104
Figure 5.3	Schematic diagram for the calculation of percolation rate in ash disposal mound	106
Figure 5.4	Schematic diagram for the infiltration of rainwater on the slope of the ash mound	109
Figure 6.1	Classification of trace elements by their behaviour during combustion and gasification	124
Figure 6.2	Correlation between total ion concentration and electrical conductivity in the ash leachate	127
Figure 6.3	Change of concentration of the major elements in the first leachates of Drax and Meaford ashes after treatment with synthetic leachate	130
Figure 6.4	Changes in the percentage of trace elements (Fe, Cd, Cr, Cu, Ni, Zn, Hg) in eluates after treatment with synthetic leachate	130
Figure 6.5	Changes in the concentrations of trace elements (B, Ba, As, Se, Mo, Mn, Sr) in eluates after treatment with synthetic leachate	136
Figure 7.1	Set-up for column leaching tests in down flow configuration	142
Figure 7.2	Variations in elemental concentrations in fresh Drax PFA eluate treated with deionised water	147
Figure 7.3	Variations in elemental concentrations in weathered Drax and Meaford PFA eluate treated with deionised water	149

Figure 7.4	Comparisons of solution concentrations of Ca vs. SO <sub>4</sub> (II-) in fresh ash eluate of column leaching tests	154
Figure 7.5	Plot of Ca vs. SO <sub>4</sub> (II-) concentrations in weathered ash eluate	154
Figure 7.6	Plot of Ca vs. Mg concentrations in weathered ash eluate	155
Figure 7.7	Plot of Na vs. K in column leaching tests	156
Figure 7.8	Variation of Al concentrations with pH in the eluates from the column leaching tests	157
Figure 7.9	Plot of Na vs. Si in column leaching tests	158
Figure 7.10	Plot of Mg vs. Si in column leaching tests	160
Figure 7.11	Plot of Si vs. Ca of weathered ashes in column leaching tests	160
Figure 7.12	Variation of Fe concentrations with pH in the eluates from the column leaching tests	161
Figure 7.13	Plot of Si vs. Cr in column leaching tests	164
Figure 7.14	Plot of Si vs. B in column leaching tests	165
Figure 7.15	Plot of Si vs. Li of the fresh PFA (a) and weathered PFA in column leaching tests	166
Figure 7.16	Plot of Si vs. Mo in column leaching tests	167
Figure 7.17	Variation of Pb concentration in fresh (a) and weathered ash eluates	169
Figure 7.18	Plots of Si vs. As (a) and Fe vs. As (b) of the weathered ash in column leaching tests	171
Figure 8.1	Plot of calculated activities of H <sub>4</sub> SiO <sub>4</sub> vs. pH from the batch leaching tests, along with calculated activities in equilibrium with SiO <sub>2</sub> (am) and SiO <sub>2</sub> (quartz)	186
Figure 8.2	Plot of calculated activities of H <sub>4</sub> SiO <sub>4</sub> vs. pH from the column leaching tests, along with calculated activities in equilibrium with SiO <sub>2</sub> (am) and SiO <sub>2</sub> (quartz)	187
Figure 8.3	Plot of calculated activities of H <sub>4</sub> SiO <sub>4</sub> vs. wairakite and the predicted activity of H <sub>4</sub> SiO <sub>4</sub> in equilibrium with wairakite	188
Figure 8.4	Variation of Al concentration in the eluate from the batch leaching test as a function of pH	189
Figure 8.5	pAl <sub>3+</sub> vs. pH for the eluates from batch leaching tests, along with the calculated activities of Al <sub>3+</sub> (solid lines) in equilibrium with crystalline and amorphous Al(OH) <sub>3</sub>	190
Figure 8.6	Plot of measured activity of Al <sub>3+</sub> against pH for the eluates from column leaching tests, along with the calculated activities of Al <sub>3+</sub> (solid lines) in equilibrium with crystalline and amorphous Al(OH) <sub>3</sub>	190

Figure 8.7	Plot of measured $\text{Ca}^{2+}$ activity in eluates from batch leaching tests versus pH, along with the calculated activities in equilibrium with gypsum and calcite	192
Figure 8.8	Plot of calculated activities of $\text{SO}_4(\text{II}-)$ vs. $\text{Ca}^{2+}$ in eluate from batch leaching tests, along with predicted activities of gypsum and anhydrite	193
Figure 8.9	Plot of measured activity of $\text{Ca}^{2+}$ and $\text{SO}_4(\text{II}-)$ in eluates from column leaching tests, along with calculated activities of Ca in equilibrium with gypsum	194
Figure 8.10	Plot of Ca activities against pH for eluates obtained from column leaching tests using distilled water, along with lines representing activities in equilibrium with calcite at various $\text{pCO}_2$ conditions	195
Figure 8.11	Plot of measured $\text{Fe}^{3+}$ activity versus pH, along with calculated $\text{Fe}^{3+}$ activity in equilibrium with $\text{Fe}(\text{OH})_3$ (am), batch leaching tests	196
Figure 8.12	Plot of measured $\text{Fe}^{3+}$ activity versus pH, along with calculated $\text{Fe}^{3+}$ activity in equilibrium with $\text{Fe}(\text{OH})_3$ (am), column leaching tests	196
Figure 8.13	Activities of $\text{Cu}^{2+}$ against pH in eluates, along with the calculated $\text{Cu}^{2+}$ activities at various pH in equilibrium with tenorite, malachite and soil-Cu, batch leaching tests	197
Figure 8.14	Plot of calculated $\text{Cu}^{2+}$ activities versus pH, along with predicted activities of Cu in equilibrium with tenorite and malachite at given pH values, column leaching tests	198
Figure 8.15	Plot of Zn activities with pH, along with calculated activities of Zn in equilibrium with Soil-Zn and $\text{ZnCO}_3$ at given pH values (solid lines), batch leaching tests	199
Figure 8.16	Plot of Zn activities with pH, along with calculated activities of Zn in equilibrium with Soil-Zn, ZnO and $\text{ZnCO}_3$ at given pH values (solid lines), column leaching tests	200
Figure 8.17	Plot of measured Pb activities with pH, along with calculated activities of Pb in equilibrium with $\text{PbCO}_3$ at given pH and $\text{pCO}_2$ values (solid lines), column leaching tests	200

## List of Tables

	Initial page
Table 2.1	Analysis of water Samples 23
Table 3.1	Chemical composition of whole porewater samples from the Barlow PFA mound, Drax 31
Table 3.2	Chemical composition of Meaford porewater 53
Table 3.3	Porewater analyses from PFA emplaced in 1975 and subjected to natural weathering in the PFA disposal mound 59
Table 4.1	Chemical composition of fresh Drax PFA 70
Table 4.2	Semi-quantitative analyses of weathered Drax PFA particles 81
Table 4.3	Average chemical analysis of weathered Meaford PFA 82
Table 4.4	Semi-quantitative analyses of weathered Meaford PFA particles 90
Table 5.1	Chemical composition of Barlow leachate water collected in May, 1992 101
Table 5.2	Chemical composition of ditch water, Barlow ash mound 102
Table 5.3	Comparison of the porewater composition collected at 4 m depth and average leachate water composition 107
Table 5.4	Comparison of average PFA leachate with standards for drinking water and landfill leachate discharge 110
Table 6.1	Composition of the synthetic leachate used in the batch leaching tests 114
Table 6.2	Analytical results of the eluates from the batch leaching test with deionised water 119
Table 6.3	Variations in aqueous Ca species distribution in the eluates using deionised water 121
Table 6.4	Variation of aquatic Fe species in the eluates obtained by deionised water 122
Table 6.5	Comparison of eluates from fresh and weathered PFA with the EEC Landfill Directive 126
Table 6.6	Analytical results of the eluate from the batch leaching test with synthetic leachate 134
Table 6.7	Composition of PFA before and after treatment with distilled water (d) and synthetic leachate (s) 135
Table 7.1	Composition of the synthetic leachate used in the column leaching tests 140
Table 7.2	Test conditions for column leaching tests 141

Table 7.3	Comparison of the PFA eluate from column leaching tests with drinking water and landfill leachate quality standards	144
Table 7.4	Analytical results of eluates from column leaching tests with deionised water	174
Table 7.5	Analytical results of eluates from column leaching tests with synthetic leachate	178
Table 8.1	Saturation indices with respect to Ca-bearing mineral phases possibly affecting the eluate	193

### **List of Plates**

		Initial page
Plate 4.2	SEM photographs of fresh Drax PFA	66
Plate 4.7	SEM photographs of weathered Drax PFA	78
Plate 4.11	SEM photographs of weathered Meaford PFA	88
Plate A.1	Laboratory set-up for column leaching tests	Appendix A

# Chapter 1

## Introduction

### **1.1 Overview**

The burning of coal to generate electric power for industry and domestic use produces large quantities of unwanted by-products, pulverised fuel ash (PFA) and furnace bottom ash (FBA). PFA consists of particles sufficiently small to be extracted in flue gases, whereas FBA consists of larger particles that sink to the bottom of the furnace of the power station and also contains molten materials fallen from the walls of the furnace. Approximately 80% of the ash produced is PFA.

The mineral matter present in coals is a major contributor to the composition of PFA. In PFA, elements are more concentrated than in coal because of the loss of carbon on ignition. For those elements mainly associated with the detrital minerals, concentrations in the coal ash are comparable with adjacent shales and mudstones. Other elements, however, are associated either with the organic matter or with minerals which formed in the coal, such as pyrite. These latter elements are concentrated in PFA and are present at much higher levels than in most geological materials (Data from: Lindsay, 1979; Adriano and Page *et al.*, 1980; Ainsworth and Rai *et al.*, 1987). Many of these trace elements (As, B, Cd, Mo, Ni, Pb, Se, V, Zn) are especially concentrated on the surfaces of PFA particles as a consequence of volatilisation and subsequent condensation onto the particles during combustion at high temperature (1000-1500°C) (Natusch and Wallace, 1974; Smith, 1980).

In 1990,  $48.6 \times 10^6$  tonnes of coal were consumed in coal-fired power stations (Central Statistical Office, 1992) in the UK and about  $10 \times 10^6$  tonnes of PFA were produced. One third to half of the PFA is commercially utilised

as materials for the construction industry, such as in road bases, structural fills, cement/concrete mixtures and soil amendments. However, the excess, non-marketed, production of PFA in the UK amounts to approximately  $6.5 \times 10^6$  tonnes per year and almost all of the waste PFA is currently being disposed of in lagoons, land-fill sites, or mounds. In future there may be less PFA in the UK to be disposed of, and disposal sites are carefully engineered to reduce the risk of groundwater contamination. However, past disposal practice has not always been so sound and there is the possibility of long-term weathering reactions influencing groundwater composition. Furthermore, elsewhere in the World the production of coal for power generation is rapidly increasing, particularly in China and India, and there is the threat of both short and long term weathering reactions adversely influencing groundwater composition.

## 1.2 Previous research

PFA has been recognised as a potential contaminant of groundwater in many studies, which have attempted to gain an understanding of the chemical toxicity of PFA and its leachate to the environment. These studies could be categorised as follows:

(1) Characterising chemical, mineralogical, and physical properties of PFA (Simons and Jeffery, 1960; Watt and Thorne, 1965; Natusch and Wallace *et al.*, 1974; Theis and Wirth, 1977; Campbell and Laul *et al.*, 1978; Smith and Campbell *et al.*, 1979; Hansen and Fisher, 1980; Henry and Knapp, 1980; Hulett and Weinberger *et al.*, 1980; Hulett and Weinberger, 1980; Bauer and Natusch, 1981; Hart, 1981; Mattigod, 1982; McElroy and Carr *et al.*, 1982; Harris and Silberman, 1983; McCarthy and Swanson *et al.*, 1983; Suloway and Skelly *et al.*, 1983; Hubbard and McGill *et al.*, 1984; Kaufherr and Lichtman, 1984; Kaufherr and Shenasa *et al.*, 1985; Hubbard and Dhir *et al.*, 1985; Lichtman and Mroczkowski, 1985; Markowski and Filby, 1985; Norton and

Markuszewski *et al.*, 1986; Wadge and Hutton *et al.*, 1986; Ainsworth and Rai, 1987; Furuya and Miyajima *et al.*, 1987; Dudas and Warren, 1988; Qian and Glasser, 1988; McCarthy and Solem *et al.*, 1990; Vassilev, 1992).

(2) Batch/column leaching tests to investigate the extent of elemental leachability from PFA using different reagents (Jones and Lewis, 1960; Brown and Ray *et al.*, 1976; Theis and Wirth, 1977; Cox and Lundquist *et al.*, 1978; Eggett and Thorpe, 1978; Talbot and Anderson *et al.*, 1978; Phung and Lund *et al.*, 1979; Elseewi and Page *et al.*, 1980; Dudas, 1981; Kopsik and Angino, 1981; Turner, 1981; Hodgson and Dryer *et al.*, 1982; James and Graham *et al.*, 1982; van der Sloot and Wijkstra *et al.*, 1982; Harris and Silberman, 1983; Liem and Sandstrom *et al.*, 1983; Mattigod, 1983; Roy and Griffin *et al.*, 1984; Roy and Griffin, 1984; Warren and Dudas, 1984, 1985, 1986; Holcombe and Eynon *et al.*, 1985; Ainsworth and Rai, 1987; Rai and Ainsworth *et al.*, 1987; Wadge and Hutton *et al.*, 1987; Alberts and Weber *et al.*, 1988; Grisafe and Angino, 1988; Hollis and Keren, 1988; Villaume and Bell *et al.*, 1988; Fruchter and Rai *et al.*, 1988, 1990; van der sloot and Hjelmars *et al.*, 1989; Hjelmars, 1990; Rai and Szelmezcza, 1990).

(3) Field based studies, which have mainly focused on PFA lagoons because of the high initial water content and the rapid release of elements into solution (Cherry and Guthrie, 1977; Dreesen and Gladney *et al.*, 1977; Talbot and Anderson *et al.*, 1978; Theis and Westrick *et al.*, 1978; Theis and Richter, 1979, Hardy, 1981; Alberts and Newman *et al.*, 1985; Simsiman and Chesters *et al.*, 1987). Although many works were conducted based in the field, only a small number of studies have involved PFA mounds, particularly paying attention to the longer term changes. Available studies covering the relatively long term periods are; Spencer and Drake (1987); Sakata, (1988); Regage and Holcombe (1990); Hockley and van der Sloot (1991).

Past studies were have also been extensively reviewed by several workers, including; Adriano and Page *et al.* (1980); Roy and Thiery *et al.*

(1981); Gay and Davis (1987); Rai and Ainsworth *et al.* (1987); Eary and Rai *et al.* (1990); Mattigod and Rai *et al.* (1990). These past studies are briefly reviewed as follows:

### **1.2.1 Studies of the chemical, mineralogical and physical properties of PFA**

Total elemental concentrations of the major and trace elements in PFA have been determined (Natusch and Wallace *et al.*, 1974; Suloway and Skelly *et al.*, 1983; Markowski and Filby, 1985; Ainsworth and Rai, 1987). The distribution of specific elements within particles has been extensively studied, due to its importance in controlling the initial solubility of elements. Numerous studies have shown that many trace elements (As, B, Cd, Hg, Mo, Ni, Pb, Se, V, Zn) are concentrated on the surfaces of PFA particles and the smaller particles to varying degrees (Natusch and Wallace *et al.*, 1974; Theis and Wirth, 1977; Hansen and Fisher, 1980; Smith and Campbell *et al.*, 1979; McElroy and Carr *et al.*, 1982; Harris and Silberman, 1984; Kaufherr and Shenasa *et al.*, 1985; Markowski and Filby, 1985; Wadge and Hutton *et al.*, 1986). In PFA, the ratio of total surface area to volume increases with decreasing particle size, and therefore increasing trace element enrichment with decreasing particle size indicates that these elements are concentrated on the particle surfaces. Enrichment occurs because the elements that are volatilised during combustion condense onto solid particles as combustion gases cool to differing degrees (Natusch and Wallace *et al.*, 1974; Smith and Campbell *et al.*, 1979; Campbell and Laue *et al.*, 1978).

Some of the studies have investigated the composition of either primary solid phase in PFA or secondary compounds which are formed from the weathering reaction of the primary phases (Simons and Jeffery, 1960; Watt and thorn, 1965; Hulett and Weinberger, 1980; Hulett and Weinberger *et al.*, 1980;

Bauer and Natusch, 1981; Turner, 1981; Mattigod, 1982; Roy and Griffin, 1984; Warren and Dudas, 1984, 1985, 1986; Ainsworth and Rai, 1987; Dudas and Warren, 1988; Fruchter and Rai *et al.*, 1988; Rai and Szelmeckna, 1990). In PFA, the primary phases containing most of the major elements include various refractory solids, such as Si-Al glass, mullite, iron oxides, and in lesser amounts, alkali and alkaline earth oxides and carbonates (Mattigod and Rai *et al.*, 1990). However, trace elements are generally low in concentration in PFA and few occur as discrete primary compounds. These include  $As_2O_3$  (Turner, 1981),  $BaSO_4$  (Fruchter and Rai *et al.*, 1988), spinel (Hulett and Weinberger, 1980), and  $SrCO_3$  (Bauer and Natusch, 1981). Trace elements may also be incorporated into the structures of the major phases of PFA glass matrices. Many of the first row transition metals (Cr, Cu, Mn, Ni, V, Zn) are distributed preferentially in the magnetic fraction of PFA, probably as solid-solution substitutions in spinel molecules with the formula  $Fe_{3-x}M_xO_4$  (Hulett and Weinberger, 1980), where M is a transition metal. The more volatile chalcophile elements (As, Hg, Pb, Se) and alkaline elements (Ba, Sr), however, are reported to be associated most strongly with the glassy fraction of PFA (Hulett and Weinberger *et al.*, 1980; Hulett and Weinberger, 1980).

Some studies have dealt with the mineralogy of PFA using X-ray technique and, or, SEM (Simons and Jeffery, 1960; Watt and Thorne, 1965; Mattigod, 1982; McCarthy and Swanson *et al.*, 1983; Hubbard and McGill *et al.*, 1984; Kaufherr and Lichtman, 1984; Hubbard and Dhir *et al.*, 1985; Kaufherr and Shenasa *et al.*, 1985; Lichtman and Mroczkowski, 1985; Warren and Dudas, 1985; Furuya and Miyajima *et al.*, 1987). Dudas and Warren (1988) characterised the glass phases and evaluated the chemical and morphological changes, by artificial weathering of PFA using column/batch leaching methods. These previous studies show that PFA is mainly composed of glass materials (50 to 70%), and the remaining fraction is composed of crystalline phases, including mullite, magnetite, haematite, quartz, and

occasionally gypsum. Due to the leaching of elements from these glassy materials and the crystalline phases, some secondary phases are believed to be formed during the weathering of PFA, including clay materials and easily soluble phases, such as gypsum and anhydrite. However, there are few studies of the secondary minerals formed in ash mounds during weathering. Prototypes of clays, such as allophane and proto-imogolite, have been observed in weathered PFA subjected artificial weathering (Warren and Dudas, 1985). This observation implies the possible formation of secondary clay minerals in the field. In a recent study of weathered PFA samples collected from ash mounds in the field, only secondary gypsum and calcite were detected, but not clay minerals (Rehage and Holcomb, 1990).

### 1.2.2 PFA batch/column leaching test

Major and trace elements in PFA are released to varying extents to the surrounding environment on contact with water. Many studies have focused on the extractability of the elements in PFA, using batch leaching tests with various reactants (Theis and Wirth, 1977; Cox and Lundquist *et al.*, 1978; Eggett and Thorpe, 1978; Talbot and Anderson *et al.*, 1978; Phung and Lund *et al.*, 1979; Cox and Lundquist *et al.*, 1980; Elseewi and Page *et al.*, 1980; Kopsik and Angino, 1981; Turner, 1981; Hodgson and Brown, 1982; James and Graham *et al.*, 1982; van der Sloot and Wijkstra *et al.*, 1982; Harris and Silberman, 1983; Liem and Sandstrom *et al.*, 1983; Mattigod, 1983; Roy and Griffin *et al.*, 1984; Roy and Griffin, 1984; Holcombe and Eynon *et al.*, 1985; Wadge and Hutton *et al.*, 1987; Ainsworth and Rai, 1987; Rai and Ainsworth *et al.*, 1987; Alberts and Weber *et al.*, 1988; Grisafe and Angino, 1988; Hollis and Keren, 1988; Rai and Szelmezcza, 1990). The agents used in the studies include distilled and demineralised water, hot water, dilute or strong acids, alkalines, and other solvents. The major factors that affect the extractability of

the elements are: the solid-solution ratio, the type and concentrations of the reactants, and the duration and temperature of the extraction (Mattigod and Rai *et al.*, 1990).

The results of the leaching experiments show large variations in the water-soluble concentrations of all major and trace elements. Ca, Na, S are the major elements in the extracts, ranging from tens to thousands of mg/l, whereas the concentrations of K and Mg show up to several hundred mg/l in some extracts. The pH of the water extract from the PFA is extremely variable, and it ranges from 3.3 to 12.3 for all types of PFA. The trace elements that are known to be enriched on the surface of PFA particles, such as As, B, Cd, Cr, Cu, Mo, Zn, show higher concentrations in extracts (Theis and Wirth, 1977; Hansen and Fisher, 1980; Turner, 1981; Alberts and Newman *et al.*, 1985; Ainsworth and Rai, 1987). The concentrations of trace elements are higher in acid extracts than in water extracts. These extraction studies have been conducted on a short-term basis and under conditions such as acid extraction and vigorous shakings, that do not conform to natural condition in the field. The data lack quantitative and thermochemical constraints and seem to be only applicable to the characterisation of the individual PFA extracts or explaining of the leaching behaviour during the early stage of PFA leaching.

Some studies used the column leaching method (Jones and Lewis, 1960; Brown and Ray *et al.*, 1976; Dudas, 1981; van der Sloot and Wijkstra *et al.*, 1982; Warren and Dudas, 1984, 1985, 1986; Ainsworth and Rai, 1987; Villaume and Bell *et al.*, 1988; Fruchter and Rai *et al.*, 1988, 1990; Hjelm, 1990) or field lysimeters (Brown and Ray *et al.*, 1976; Dudas, 1981; Ainsworth and Rai, 1987; Hjelm, 1990). Mattigod and Rai *et al.* (1990) summarised the leaching trend from continuous column leaching tests into two categories. Ca, Na, K, and S follow the first pattern, in which these elements show higher concentrations in the initial leachate, and thereafter the concentrations decline rapidly and then reach a steady state. In contrast, the elements in the second

pattern, such as Al and K, are very low in concentration in the early leaching stages, but increase with the progress of leaching.

The continuous column leaching test and the field lysimeter are better methods for understanding longer-period leaching behaviour than the batch leaching test. Combined study of field data and laboratory experiments could provide better understanding of the practical leaching behaviour of PFA.

### 1.2.3 Field based studies

Many field studies focused on PFA settling pond, or lagoons, due to the high initial water content and the rapid release of elements into solution. These include Cherry and Guthrie (1977), Dreesen and Gladney *et al.* (1977), Talbot and Anderson *et al.* (1978), Theis and Westrick *et al.* (1978), Theis and Richter (1979), Hardy (1981), Alberts and Newman (1985).

Studies of ash pond effluents show similar trends to those of column leaching tests, with Ca and  $\text{SO}_4$  as principal cationic and anionic constituents respectively. B appears to be one of the most readily dissolved trace elements (Jones and Lewis; 1960, Hardy, 1981). Spencer and Drake *et al.* (1987) reported detectable amounts of As and Se in the leachate of alkaline PFA ash mounds as well as high amounts of B. Sakata (1988) reported Ca and  $\text{SO}_4^{2-}$  as major ions in the leachate of weathered PFA from ash mounds, in the field and also showed that inorganic elements infiltrated into the underlying soil layer. The infiltration of ash leachate into underlying soil and elevated concentrations of B, Mo, Mn, Ca,  $\text{SO}_4^{2-}$ , Sr in shallow groundwater were also reported by Rehage and Holcombe (1990).

### 1.2.2.4 Thermochemical approach

Among the studies of environmental aspects of PFA mentioned in previous sections some studies adopted more quantitative approach, using mechanistic

methods: Roy and Griffin (1984), Ainsworth and Rai (1987), Rai and Ainsworth *et al.* (1987b), Fruchter and Rai *et al.* (1988, 1990), Rai and Mattigod *et al.* (1988). These studies are comprised of an evaluation of solubility relationships from various leaching tests in the laboratory or in the field lysimeter. This approach is more useful in that it relates the aqueous concentrations in leachates to solubility-controlling or adsorption-controlling solid phases and considers the dominant weathering reactions that will control the solubility and the mobility of the elements in long-term weathering processes.

### 1.3 Aims of study

Not adequately covered in previous studies are, however, the longer term weathering effects on PFA either by field study or by laboratory work. Specific laboratory experiments using strong agent do not provide realistic to assessment of such effects in the field.

PFA consists of minerals, glass and sublimates. Quartz, mullite and hematite/magnetite are the main minerals present. Reaction rates involving these minerals in groundwater systems will generally be slow. Reaction rates for the aluminosilicate glass will be faster and the sublimates could be readily soluble on contact with water. Thus not only are elements concentrated in PFA but elements are also associated with reactive phases. The rate of release of elements from the mineral and glass phases in PFA into solution may be sufficiently slow that the environmental impact on surface waters might be negligible because of dilution effects, but this need not apply to groundwaters.

In this study particular attention is paid to the longer-term leaching behaviour of PFA in field ash mounds under natural weathering conditions, and its potential influence on groundwater composition. This involves the investigation of weathering reactions in PFA involving glassy and crystalline

phases as well as the relatively rapidly dissolved phases. In order to support the field investigations, complementary experimental works were done in the laboratory, including batch and column leaching test, which simulate natural weathering under controlled conditions. Thereby, it is possible to get balanced information regarding the practical leaching behaviour of PFA, which can fill the present gap between laboratory results and field conditions.

The main aspects and framework of this study are summarised as follows:

(1) Investigation of porewater collected from weathered PFA in field ash mounds. Depth related variations in porewater chemistry are of particular interest. Trends of increasing porewater concentration with depth are consistent with increased reaction of PFA as a function of contact time. Reactions with the infiltrating porewaters are determined from the depth changes in the composition of the porewater, allowing assessment of the mobility of the major and trace elements (Chapter 3).

(2) Determination of the chemical concentrations of fresh and weathered PFA and assessing their geochemical significance. Investigation of chemical change with weathering as a function of depth and time were also done, to compare solid PFA composition with corresponding porewater and thereby detect the degree of weathering (Chapter 4).

(3) Investigation of the primary and secondary mineralogical phases in the fresh (Drax) and weathered PFA. As porewater infiltrates into the PFA it will react with the PFA and consequently secondary weathering products will be formed. These secondary phases, mainly clay minerals, yield valuable information as to the extent of weathering reaction of PFA glass, using stability field for the clay minerals (Chapter 4).

(4) Analysis of leachate water collected from the Drax PFA disposal mound. This leachate was generated within the ash mound and the composition is regarded as being the same as that of leachate which has

migrated into the soil beneath the mound. This will provide information as to the practical extent and effect of PFA leachate on groundwater composition. In addition, comparison of the leachate with porewater will yield information as to the evolution and reaction path of porewater composition during its downward seepage in the ash mound (Chapter 5).

(5) Simulation tests of the weathering interactions of PFA were conducted in the laboratory and these included batch leaching tests by the end-over-end shaker, and continuous column leaching tests for a longer-term simulation. Laboratory experiments are a good way of simulating the natural weathering of PFA under controlled conditions, and can be expected to yield generalised results which can be applied to predicting leachate chemistry and the extent of the influence of PFA on the environment (Chapter 6 and 7).

(6) A geochemical simulating, computer program, WATEQ4F (Ball and Nordstrom *et al.*, 1988), was used to evaluate the water analytical data (from porewater, leachate collected from ash mounds and solutions produced by laboratory experiments) more quantitatively, and to further establish the geochemical factors controlling the natural weathering reactions of PFA (Chapter 8).

## 1.4 Study area

The study is based on two different sites. One is based at the PFA mound at Barlow (National Grid ref. SE 655 277) adjacent to Drax Power Station, located near Selby, East Yorkshire, UK, and the other is based at the Meaford Power station in Stoke-on-Trent, Staffordshire (National Grid ref. SJ 896 373). The former is a well-engineered and leachate-controlled site with a good documentation. The latter is an older, less-engineered site in which the leachate generated in the PFA mound may be infiltrating downwards into the bedrock below the site. The rationale behind selecting these two sites was as

follows: in the well-engineered site the aim was to examine natural weathering interactions of the disposed PFA, with good controls on the sampling of PFA, with known ages of the leachates generated in the PFA mound. At Meaford, where the age of the oldest PFA in the area is 40 years old, the aim was basically to sample older ash to extend the age range of the PFA investigated. However, with the older site, which is less well-engineered, leachate samples are diluted by the groundwater and it is difficult to get uncontaminated leachate samples. The Drax Power Station has all the desired conditions which will be described later (Chapter 2) as a first approach.

## Chapter 2

### Site Description and Method

#### **2.1 Site description**

##### **2.1.1 Drax Power Station**

###### *2.1.1.1 General description of Drax Power Station*

Drax Power Station has a 4,000 mega watt generating capacity and produces approximately  $1.4 \times 10^6$  tonnes of PFA annually. The Drax Power Station is the largest in its generating capacity of the European coal-fired power plants and is one of Britain's modern thermal power stations. The site is run by National Power and has three generators.

Drax Power Station burns about  $7 \times 10^6$  tonnes of coal annually and most of the coal is mined locally in the Selby area. Approximately  $1.4 \times 10^6$  tonnes of PFA is produced per year. The waste PFA produced in the Drax power station is directly transferred to and disposed, on the Barlow PFA mound, adjacent to the power station, since the early 1970s. The schematic diagrams of overviews of the Drax Power Station and the Barlow mound are shown in Figure 2.1.

The total area of the Barlow mound is 120 Hectares. It has a longitudinal shape and the estimated amount of the disposed PFA emplaced by 1987 was approximately  $6.3 \times 10^6 \text{ m}^3$ . The maximum height of the site is 36 m and the surface of the mound is smooth and flat. The site is located on a series of glacial boulder clays overlying the Permo-Triassic Bunter Sandstone (Dobie and Newman, 1986). The clays are generally laminated, with the frequency and thickness of partings varying. The silt and sand content of the clay

increases with increasing depth, and at the base of the clay there is a layer of silt. The Bunter Sandstone consists of sandstone with occasional bands of mudstone or siltstone, and is weathered at its junction with the overlying clays to an uncemented sand (Figure 2.2).

### ***2.1.1.2 Disposal of PFA in Barlow mound***

The PFA is tipped on a thin layer of the permeable furnace bottom ash, with field drains, which overlies impermeable boulder clays. The PFA is transported and tipped on the mound by the belt conveyer and boom stackers. The PFA mound grows by lateral accumulation. Once the PFA is emplaced to the desired height, a thin layer of top soil (generally about 30 cm) is added to return the land to agricultural use. Many varieties of crops grow on the site, and cattle and sheep are being bred. There are also many wild animals living on the site such as rabbits and pheasants. The site is well-engineered and the subsurface is well protected from leakage of the leachate. It also has a good drainage system inside and around the mound. The field drains inside the mound are discharged to the outer dike, that surrounds the mound, through outlet pipes installed in the mound. The dike is also fed directly by surface run-off following precipitation.

Due to the lateral accumulation and the good documentation, it was possible to sample weathered PFA (and pore fluids) of varying and known ages, dating back to the early 70's. In addition to this, the good drainage system also makes it possible to obtain pore fluids generated within the mound that have not been mixed with groundwater. It has been proved to be an ideal place for establishing the practical leaching behaviour of disposed PFA, with good control on the sampling strategy, the result of which can be applied to a less well-engineered site, such as Meaford ash mound (Figure 2.3).

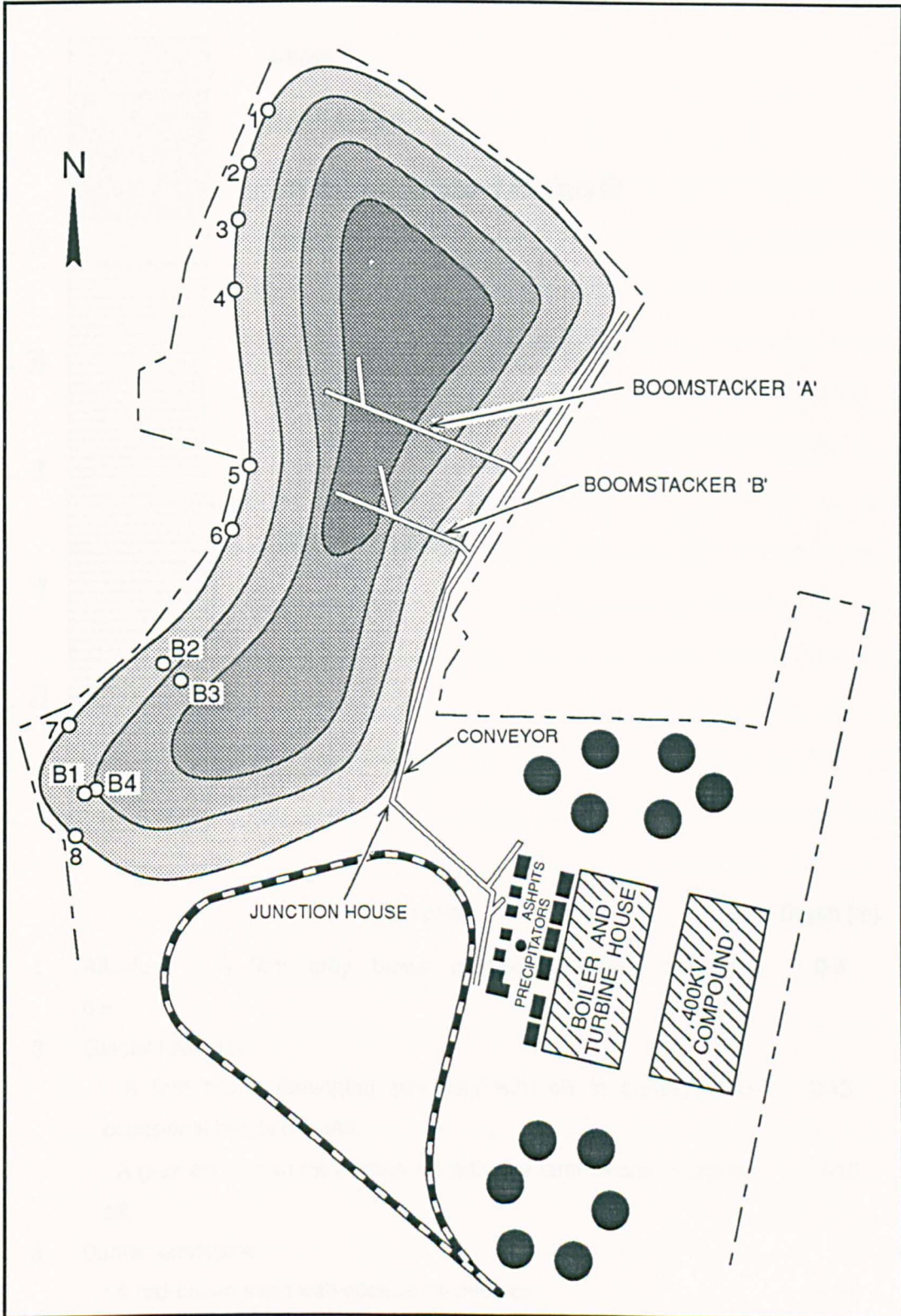
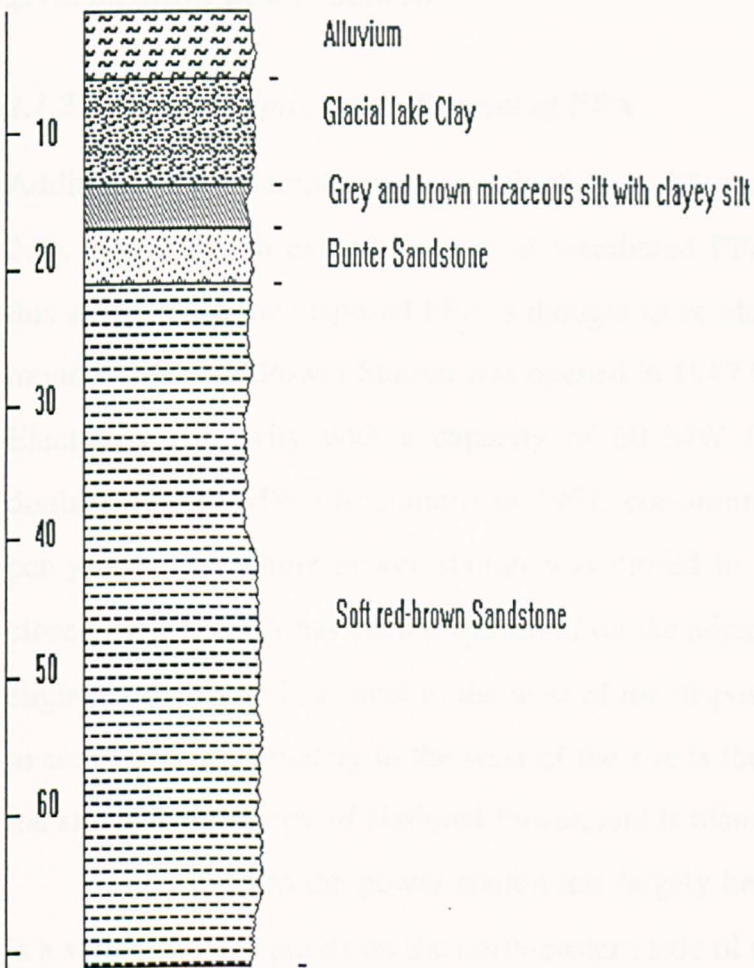


**Figure 2.1** Drax Power station and the Barlow PFA disposal site (The numbers 1-8 denote locations of outlet pipes for leachate water samples and the B1-B4 represent the locations of PFA boreholes. Not in scale)



	Description	Depth (m)
1	Alluvium : A firm grey brown mottled laminated silt clay	0-5
2	Glacial lake clay	
	: A firm brown laminated silty clay with silt in partings and occasional bands of sand.	2-13
	: A grey and brown micaceous silt with fine laminations of clayey silt	13-16
3	Bunter sandstone	
	: A red-brown sand with occasional pebbles	16-20
4	A soft red-brown sandstone	20-

**Figure 2.2 Vertical section of the rocks below the Barlow PFA mound (Not in scale)**

## 2.1.2 Meaford power station

### 2.1.2.1 Site description and disposal of PFA

Additional PFA samples were obtained from Meaford Power Station (Figure 2.3), essentially to extend the age of weathered PFA samples investigated in this study, since the disposed PFA is thought to be older than that of the Barlow mound. Meaford Power Station was opened in 1947 by the Northwest Joint Electricity Authority with a capacity of 60 MW ('A' station) and this was doubled to 120 MW ('B' station) in 1951, consuming 600,000 tonnes of coal per year. The whole power station was closed in 1989 although 'A' station closed earlier. PFA has been disposed of on the adjacent site, which is not well engineered. There is a canal to the west of the disposal site flowing from north to south and immediately to the west of the site is the River Trent. Nowadays, the site is the property of National Power, and is managed by security guards.

The ash from the power station has largely been dumped *in situ*. There is a series of three ponds on the north-eastern side of the site where ash from 'A' has been disposed of. Some years after the ash was dumped, the ash was removed from this pond and dragged up onto the hillside above the station. Thin layers of the top soil were added after the tipping on the hill and it is now converted to grazing land where cattle and sheep are bred. The land is stable in all area except one-in the centre of the slope-where inadequate top soiling and convergent subsurface drainage has led to severe erosion and gullyng into the underlying ash, resulting in deep gashes in the hillside of 10-20 m depth.

PFA from the 'B' station was disposed of in ponds to the south, the engineering of which appears to have been slightly better. The PFA was pumped to the lagoon and mixed with water. The lagoons are used alternately, and overflow from one drains into the other. Part of the PFA from the 'B' station lagoons has been piled up to one side, exposing the sandstone bedrock beneath.

### ***2.1.2.2 Geology of the disposal site at Meaford Power Station***

The Meaford area is composed of two major lithologies. One comprises late Carboniferous red-brown, purple, grey-green siltstones and mudstones and red-brown, grey sandstones, which are part of the Keele Formation. These are overlain unconformably by a lenticular body of Triassic rocks of the Kidderminster Formation. They are composed of pebbly sandstones with subordinate conglomerates and siltstones.

At the Meaford disposal site, most of the waste PFA disposal site and the lagoons are located on the Keele Formation, which dips to the west at between 5 and 37 degrees. The rocks are mainly permeable sandstones, which implies that the groundwater is migrating to the west along the bedding planes and the pore spaces of the rocks. Migration of pollutants could be affecting the Trent drainage system.

## **2.2 Sampling of PFA and porewater**

### **2.2.1 Barlow PFA mound**

#### ***2.2.1.1 Sampling strategy***

The PFA was sampled by means of boreholes. In each borehole, the PFA is of the same age. As infiltrating porewaters pass vertically through the PFA elements are leached into solution and the composition of the PFA is changed. By extracting and analysing porewaters from borehole samples it is possible to study the effect of reactions down the infiltration pathway. Changes in PFA composition with depth provide confirmation of the cumulative effect of the weathering reactions since the time of emplacement. Further confirmation of the reactions should be provided by comparison with samples from other boreholes where the PFA is of a different age.

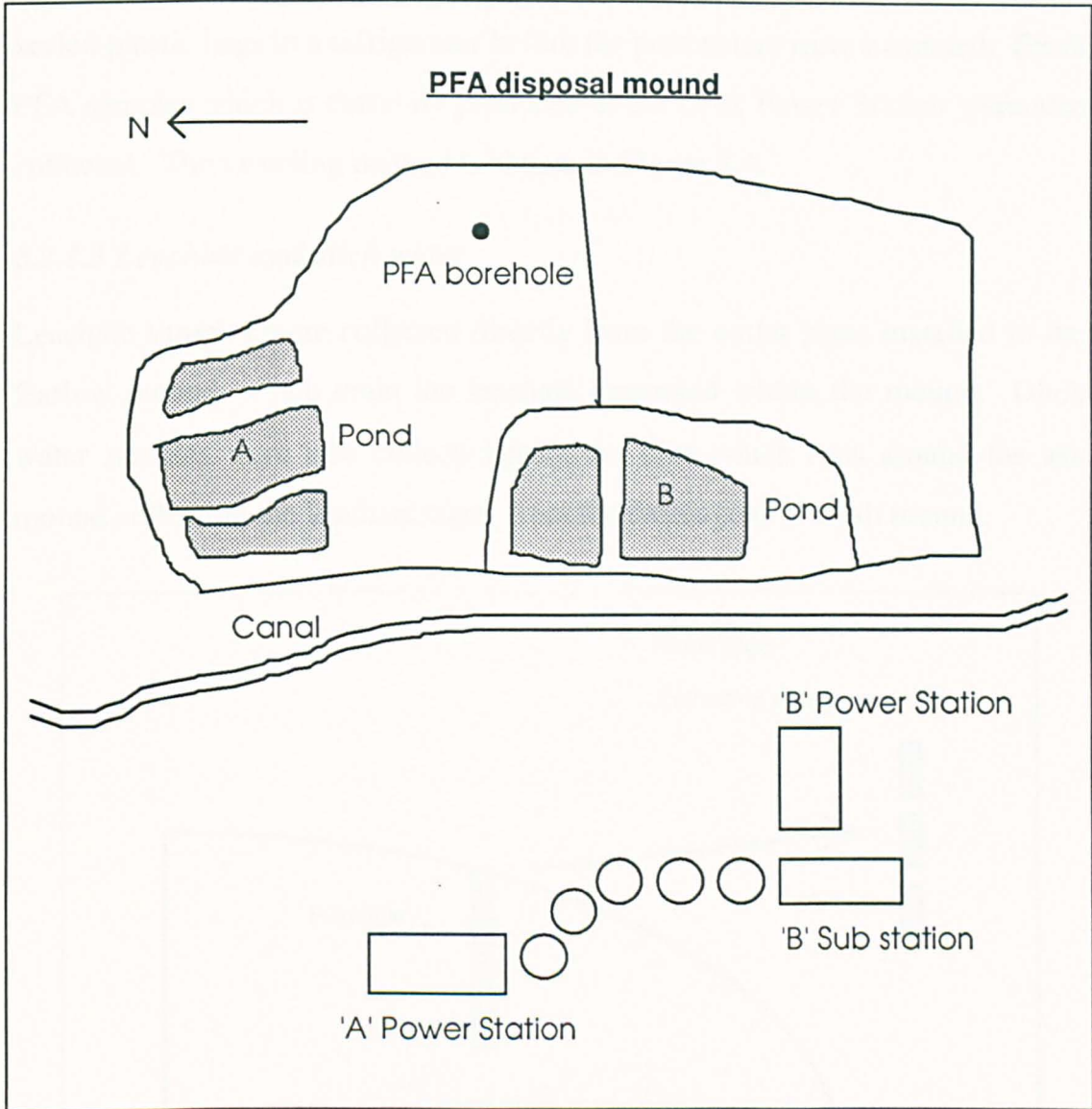


**Figure 2.3 Meaford Power station and disposal of PFA (Not in scale)**

### 2.2.1.2 PFA samples

A hand auger drill was used to take samples from four boreholes on the Barlow mound drilled to between 3 and 5 metres. Two of the boreholes (No. 2 and 3) are located in PFA emplaced in 1978 but differing in slope position on the mound. The other two boreholes (No. 1 and 4) were from the oldest part of the mound, where the PFA was emplaced in 1975. In general PFA samples were collected at 0.3 m depth interval. About 700 to 1000 g of PFA sample were

collected from each interval. The PFA samples from boreholes were stored in sealed plastic bags in a refrigerator before the porewaters were extracted. Fresh PFA samples which is currently produced at the Drax Power Station were also collected. The sampling method is shown in Figure 2.4.

### 2.2.1.3 Leachate and ditch water

Leachate samples were collected directly from the outlet pipes installed in the Barlow mound, which drain the leachate generated within the mound. Ditch water samples were also collected from the dike which runs around the ash mound collecting the leachate water from the drainage of the ash mound.

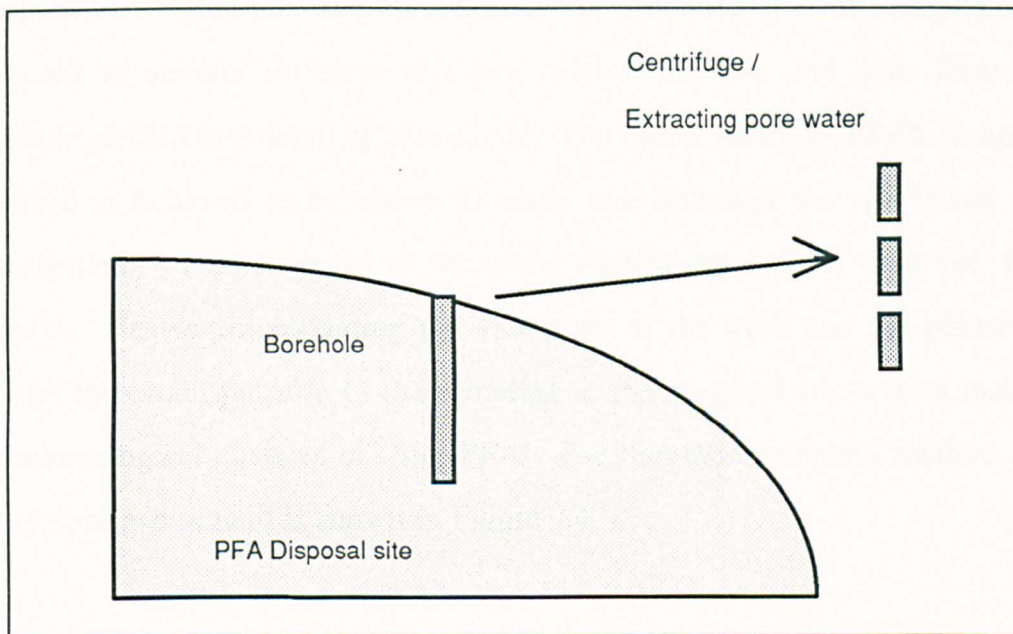


**Figure 2.4 Schematic diagram of drilling of weathered PFA using hand-auger drill in the Barlow and Meaford PFA mound**

Both the leachate and ditch water samples from each site were stored in 70 ml and 250 ml plastic bottles, the former were for anion analysis and the latter were for cation analysis. New sample bottles were used in most cases and all the bottles were soaked in diluted HCl acid overnight and rinsed with distilled and deionised water before use. The sample bottles were rinsed with

the leachate and ditch water several times before collecting. As soon as possible, in the laboratory, all the water samples were filtered through Millipore 0.45 $\mu$  micro filter, by vacuum suction. After filtration, aristar HNO<sub>3</sub> was added to the water samples for cation analysis making the solution up to 1% in HNO<sub>3</sub> to prevent adsorption and precipitation of cations during storage. Aliquots for the anion analysis were untreated. The water samples were then stored in the refrigerator to minimise biological activity before analysis. The pH, Eh were measured in the field.

### **2.2.2 PFA sampling at the Meaford site**

Meaford Power Station was closed in 1989. Weathered PFA samples were collected at several different locations within the site and also from one borehole, drilled to a depth of around 5m. The oldest weathered PFA sample at Meaford is believed to be about 40 years old, although the site is not well documented. This material is therefore significantly older than the Drax samples. Besides investigating the chemistry of the PFA and the porewater, another important purpose of the sampling at the Meaford site was to look for the mineralogical changes in older PFA. The borehole sampling method used at Meaford ash mound is shown in Figure 2.4.

### **2.3 Porewater extraction**

In the laboratory, the porewaters were extracted from the borehole PFA samples by a modification of the method of Edmunds and Bath (1976). Borehole PFA samples were put in PVC tubes, the bottoms of which had a detachable cup with a stainless net on it (Figure 2.5). About 100 g of sample was put in each tube. A Whatman No. 540 filter paper was inserted on top of the stainless net and the tubes were spun for 60 minutes at speed of 3,000 rpm. In the case of chalk samples (Edmunds and Bath, 1976), the recovery rate is

about 20-25 % of the total porewater at this speed. For PFA, which is unconsolidated and has bigger pores, about 30 to 35 % of the porewater was extracted at this speed. According to the experimental data of Edmunds and Bath (1976), this amount should increase to 90 % by increasing the speed of the centrifugation by 12,000 rpm. About 20 to 30 ml of porewater as extracted from samples of each depth and these extracts were transferred to 10 ml sample tubes and 70 ml plastic bottles for further analysis. Samples for the cation analysis were acidified up to 1 % in  $\text{HNO}_3$  and were then also stored in the refrigerator until the analysis, whereas aliquots for the anions were untreated.

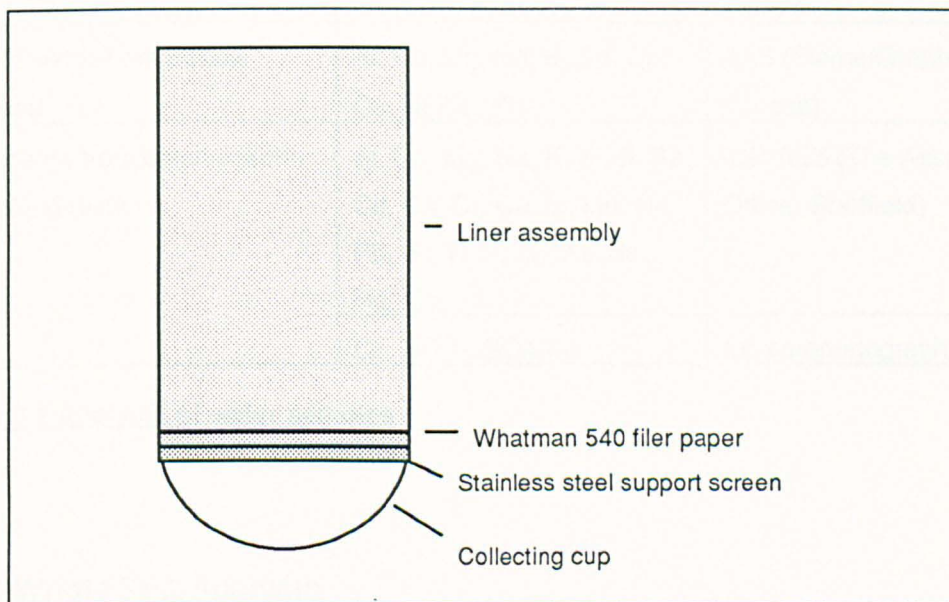


Figure 2.5 Centrifuge liner assemblies for extracting porewater from PFA (Modified after Edmunds and Bath (1976))

## 2.4 Analytical methods

An outline of analytical methods used in this study are described here. The analytical schemes for water samples are shown in Table 2.1. Detailed analytical techniques, procedures, and operating conditions or additional techniques used, which have not covered here are described in Appendix A.

Sample	Elements	Equipment
Drax Borehole 1	Al, Ca, Mg, Na, K, Cd, Cr, Cu, Ni, Pb, Zn	AAS (Flame/Graphite furnace)
Drax Borehole 2, 3	Al, Ca, Mg, Na, K, Cd, Cr, Cu, Ni, Pb, Zn	AAS (Flame/Graphite furnace)
	Cl-, NO <sub>3</sub> -, SO <sub>4</sub> (II-)	Ion chromatography
Drax borehole 4/Meaford borehole/Leachate water from Barlow mound (Outlet pipes)	Al, Ca, Mg, Na, K, Si, B, Ba, Cd, Co, Cr, Cu, Li, Mn, Ni, Pb, Sr, Ti, V, Zn	ICP-AES (Royal Holloway and Bedford New college)
	Cl-, NO <sub>3</sub> -, SO <sub>4</sub> (II-)	Ion chromatography
	As, Se, Hg, Mo	AAS-Hydride generating system
Ditch water from Barlow mound	Al, Ca, Mg, Na, K, Cd, Cr, Cu, Ni, Pb, Zn	AAS (Flame/Graphite furnace)
Leachate from batch/column leaching tests	Al, Ca, Mg, Na, K, Si, B, Ba, Cd, Co, Cr, Cu, Li, Mn, Ni, Pb, Sr, Ti, V, Zn, As, Se, Hg, Mo	ICP-AES (The Assay Office, Sheffield)
	Cl-, NO <sub>3</sub> -, SO <sub>4</sub> (II-)	Ion chromatography

**Table 2.1 Analysis of water samples**

## 2.4.1 Whole PFA analysis

### 2.4.1.1 X-ray Diffractometer (XRD)

An X-ray diffractometer (Phillips PW1349), employing a Cu-X-ray tube powered by a PW 1130/90 generator, was used to determine the mineralogy of the PFA and soils. Samples for whole PFA analysis were prepared by grinding them in on agate mortar. For selected samples, clays size fractions (< 2 µm) were separated following the method of Starkey and Blackmon *et al.* (1984), from weathered PFA samples with the aim of enhancing the detection of possible secondary clay fractions. Soil samples were treated to remove the high

organic content and free iron oxides by the method of Bullock and Loveland (1974). Both powder smears on the glass slide and back filled powder mount were prepared for the mineral analyses. All samples were run air-dried from 4-44° 2 $\theta$ .

#### ***2.4.1.2 Scanning electron microscope (SEM)***

Scanning electron microscopes (JEOL JSM 6400 attached with Link eXL pentafet turreted detector from Oxford instrument and Camscan MarkII) were used to study grain morphology and detect possible secondary precipitates in weathered PFA samples. This technique is especially effective for observing and analysing submicron glass particles. PFA particles were mounted on double adhesive tape affixed to carbon stubs and then evaporatively coated with carbon or gold to help reduce the charging effect. For the samples for analyses, only carbon was used. In addition to the stubs, polished sections were prepared for semi-quantitative analysis using an energy dispersive X-ray spectrometer equipped in SEM. The polished sections were also coated with carbon and prepared by mixing and solidifying PFA with resin.

#### ***2.4.1.3 X-ray fluorescence spectrometry (XRF)***

Determination of the chemical concentrations of major, minor and trace elements except for volatile trace elements (As, Se, Hg, Mo, B) in PFA was performed with an X-ray fluorescence spectrometer (Phillips PW 1400), using lithium tetraborate glass fusion samples. Both fresh and weathered PFA were screened by a 2 mm sieve and then crushed to less than 200 mesh in size using a Tema disc mill. After the grinding the PFA samples were oven-dried at 105° C overnight to remove adsorbed water and then loss on ignition was determined after heating for 4 hours at 850°C in the electric furnace. Loss in weight is mainly attributable to the loss of organic materials and easily decomposed

carbonaceous minerals but there is a balancing gain in weight as a result of the oxidation of reduced chemical species such as  $\text{Fe}^{2+}$ .

#### ***2.4.1.4 Soil and PFA pH***

Soil and PFA pH was measured by a modification of the method of White (1969). Soil or PFA and distilled water were mixed in a 1:2 ratio and then measured after agitating the suspension for 10 minutes by a magnetic stirrer. White (1969), in his study of the measurement of soil pH, recommended using 100 M  $\text{CaCl}_2$  solution, but in measuring the pH of PFA it was not deemed necessary, due to the non-organic nature of the PFA.

### **2.4.2 Water analysis**

#### ***2.4.2.1 pH and Eh***

pH and Eh were measured both in the field and laboratory. In the field, direct measurement of leachate and ditch water was done using an Orion 407A meter with combinations pH electrode (Orion 91-05) and combination redox electrode (Orion 96-78, 97-78). In the laboratory, the Orion 601 meter, with same electrodes, was used for porewaters extracted from PFA, and the leachate of both batch and column leaching tests.

#### ***2.4.2.2 Atomic absorption spectrophotometry (AAS)***

Atomic Absorption Spectrophotometers (Perkin Elmer M 2100 and Perkin Elmer 480) were used for the analysis of cations in the porewaters of Drax borehole 1, 2 and 3. Either flame or flameless graphite furnaces were used for analysing major and minor cations. The As, Se, Hg and Mo content of porewater samples of borehole 4 and the leachate water of the Barlow ash mound were analysed by the Perkin Elmer M 2100 AAS with a hydride generating system attached.

### ***2.4.2.3 Inductively Coupled Plasma spectrometer (ICP-AES)***

Inductively Coupled Plasma Spectrometry (Phillips PV8210 1.5-m ICP-AES / ICP model ARL 3580 mini torch) at Royal Holloway and Bedford New College and the Assay Office, Sheffield were used to determine all the cations, including B, except for the volatile elements such as As, Mo, Se, Hg in the Drax borehole 4 samples and leachate water from the Barlow mound. The latter instrument was especially used for analysing all cations, including the volatile elements, As, Se, Mo, B and Hg, in the leachate samples collected from laboratory batch/column leaching tests.

### ***2.4.2.4 Ion chromatography***

The concentrations of anions, including  $\text{SO}_4^{2-}$ ,  $\text{Cl}^-$ ,  $\text{NO}_3^-$ , were determined by Dionex 2000i Ion Chromatography for all solutions.

## **2.4.3 Assessing analytical results**

In all analyses of solid PFA and water samples, the accuracy and precision of the results were checked using standard samples and duplicates. For water analyses by AAS, ICP-AES and IC, some selected samples were duplicated by dilution and these diluted samples were frequently run together with the main samples to be analysed to monitor precision and accuracy. Accuracy was also checked by a standard sample.

## **2.5 Geochemical modelling**

In this study, the water analytical data were analysed using geochemical modelling computer codes to explain them quantitatively and to simulate their reactions in the aqueous environment. The concept of chemical modelling in natural hydrologic systems was initiated by Garrels and Thompson in their

pioneering work on the distribution of species in sea water, in 1962 (Bassett and Melchior, 1990). Until now, more than 50 different computing codes have been developed for the geochemical modelling of natural water.

The chemical reaction modelling the solid PFA-water system was facilitated by calculations of (1) equilibrium speciation (speciation-solubility) and (2) reaction-path. The equilibrium speciation calculations determine the speciation of the ions in solutions and the state of saturation of the solution with respect to a range based on a static thermodynamic model and analysed water data. This is also called a solubility-speciation calculation. The output of a speciation-solubility calculations comprises two parts. One is the speciation: the concentration and the thermodynamic activity, including activities and activity coefficients, of dissolved species. The other is the solubility, and this consists of saturation indices for the various reactions, and this informs of us whether a particular mineral phase would tend to dissolve or precipitate in a given aqueous environment. Widely used computer codes for the purpose of equilibrium calculation include GEOCHEM (Spotigo and Mattigod, 1980), WATEQ4F (Ball and Nordstrom *et al.*, 1987), EQ3NR (Wolery, 1992). Computer program, such as PHREEQE (Parkhurst and Thorstenson *et al.*, 1980), EQ6 (Wolery and Daveler, 1992) were developed for the modelling of reaction path in water-rock interaction.

Both EQ3/6NR and WATEQ4F were available in this study but the WATEQ4F was used in this study. The main reason was that the WATEQ4F was designed to run on a personal computer whereas the EQ3/6 needs workstation, such as Sunsparc system, which takes more time in installing and running the program. In addition to the advantage of running the program with more easeness, the WATEQ4F computes larger number of elements (34), species (500) and minerals (375) than the EQ3/6NR, which computes 18, 140, 250 respectively for the elements, species and minerals.

WATEQ4F calculates: (1) speciation of the ions in the solution; (2) saturation indices. WATEQ4F has been evolved through several revised modifications from the WATEQ computer program that was originally developed by the U.S. Geological Survey in 1974. WATEQ4F is the most recent version in the WATEQ series with an updated database and adopted to run on IBM PCs, which is written in FORTRAN 77. The program and data are run on 486 processor-based IBM PCs. The theoretical background and the constraints on the geochemical modelling of natural water is described in detail in Appendix B, with calculation examples.

## Chapter 3

### Field investigation of PFA Porewater

#### **3.1 Introduction**

Porewater from PFA mounds is the most sensitive medium that records reactions of the PFA by infiltration during weathering. The concentrations of most ions in interstitial water are small compared with those in solid phases and therefore the changes in porewater with depth induced by the interaction between the solid and water, are much larger and easier to detect in the porewater (Drever, 1988). Porewater extracted from weathered PFA boreholes of the Barlow disposal mound was analysed to investigate the chemical composition of the porewater as a function of PFA weathering reaction. In this work not only are the concentrations in porewater of interest, but also the way concentrations vary as a function of depth is of particular interest. Variations of ionic concentrations in porewater extracted from weathered PFA were recorded as a function of depth to assess mobility and migration of elements from the ash mound. Increasing concentrations with depth are indicative of continued reaction between PFA and the infiltrating porewater as a function of contact time. As pore fluids move downwards, the older porewater is located at a greater depth compared with younger porewaters and the greater contact time between PFA and porewaters results in higher solution concentrations. In addition to, the achievement of constant concentrations with depth provides evidence of equilibrium, whereas decreasing concentrations could be due to the introduction of an element from an external source, either by reaction or by dilution. Another possibility, of no change with depth, might indicate that the material or elements are inert.

Ion concentrations in the porewater of Drax PFA were found to change as a function of depth. Most of the ions present in the porewater are thought to be mainly derived internally from the reaction of PFA and only a few elements are believed to be external origin, which is derived from anthropogenic input into the Barlow ash disposal mound.

In addition to the investigation of Drax borehole samples, porewaters were also extracted from the boreholes of the Meaford ash mound to extend the age range of samples analysed, and also to compare and confirm the results obtained from the two sites. This comparison also will help to establish the general weathering behaviour of PFA.

All the analytical data were processed using the geochemical simulation software WATEQ4F (Ball and Nordstrom *et al.*, 1987), which was used to calculate the activities of individual elements, saturation indices with respect to specific minerals, and speciation of elements. For the elements showing equilibrium concentrations from the depth trends, the influence of possible solubility controlling phases was investigated using WATEQ4F.

## **3.2 Investigation of depth profiles in Drax porewater**

### **3.2.1 Introduction**

A trend of increasing concentration with depth is consistent with increased reaction of PFA as a function of contact time. Soil water movement in unsaturated zone is a layered one and new rainwater on the surface of the top soil simply pushes the old water downward (Zimmerman and Munnich *et al.*, 1966). This is believed to explain water flow in PFA disposal mounds, which are mainly composed of unconsolidated silt and sand size particles without joints or other vertical structures. Therefore, the discharge and recharge of aquifers are thought to take place by vertical seepage as downwater movement

and the depth trend investigated in the PFA from the Barlow mound is thought to show vertical variation, with little influence of lateral or partial flows in such shallow depth range investigated in this study, which is around 5 m.

	Al	Fe	SiO <sub>2</sub>	Ca	Mg	Na	K	Cl <sup>-</sup>	SO <sub>4</sub> <sup>2-</sup>	NO <sub>3</sub> <sup>-</sup>	B	Ba
Mean	0.19	0.05	0.52	516.1	168.1	89.5	143.1	200.9	2308.6	466.1	7.2	0.16
Median	0.16	0.04	0.44	559.3	137.2	55.1	129.6	132.9	2150.4	456.4	6.8	0.14
SD	0.19	0.03	0.25	187.2	117.6	86.1	96.1	239.1	1215.9	447.6	4.8	0.06
Min.	0.01	0.00	0.15	71.8	16.8	32.2	13.0	32.7	73.5	39.8	0.9	0.10
Max.	0.90	0.09	1.11	937.5	474.0	592.4	446.7	1219.2	4616.6	2601.6	19.7	0.30
n=	56	20	20	56	56	56	56	41	41	40	20	20
	Ni*	Pb*	Zn*	Cd*	Cu*	Cr*	As*	Se*	Mo	Li	Sr	V
Mean	54.0	161.1	17.1	13.9	14.4	169.0	48.0	28.4	2.04	1.36	2.59	0.12
Median	14.9	106.0	20.0	0.5	11.5	160.0	42.0	25.2	2.35	1.52	2.58	0.13
SD	56.9	171.4	11.7	18.8	12.4	99.8	23.2	18.2	0.95	0.57	0.34	0.04
Min.	0.0	0.0	0.0	0.0	0.0	9.4	21.5	11.6	0.30	0.30	2.00	0.00
Max.	170.0	590.0	50.9	50.0	50.5	366.7	110.0	94.0	3.20	2.20	3.60	0.20
n=	56	56	56	56	56	35	20	20	20	20	20	20

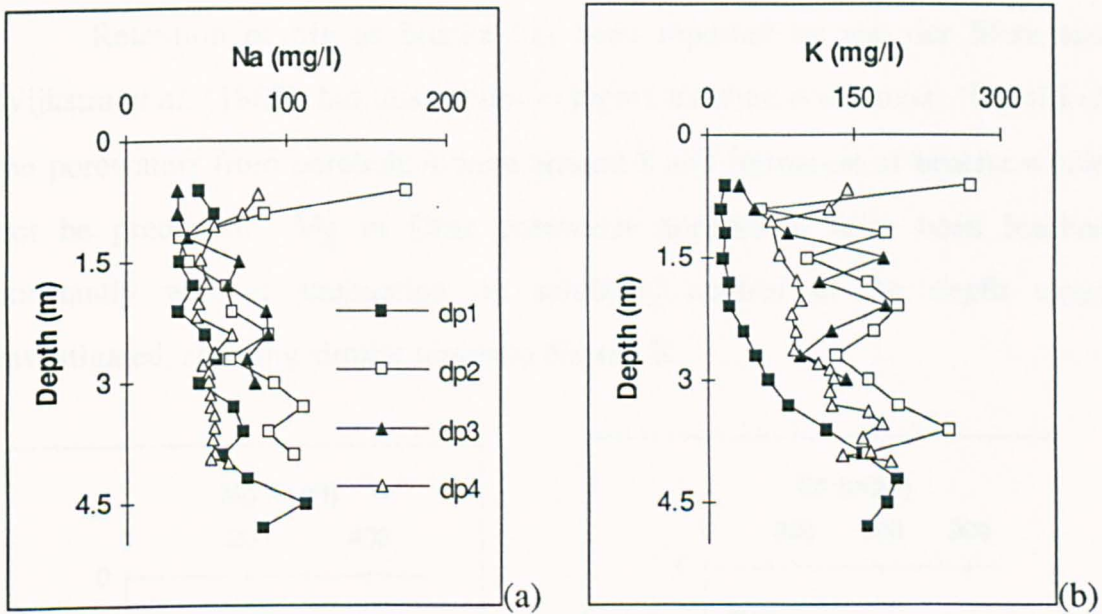
**Table 3.1 Chemical composition of whole pore water samples from the Barlow PFA mound, Drax. (unit: mg/l unless marked by \*, \*=µg/l)**

Table 3.1 shows analytical results of Drax porewater. Full analytical results are shown in Appendix C. Average Eh and pH values of the porewater from the Barlow mound were 403 mV and 8.0 respectively. Although the values were measured from the extracted porewater in the laboratory instead of directly in the field, it does suggest that the porewater system is slightly alkaline in pH and at least not in a reducing state. The Eh and pH values of Drax porewater are similar with the values measured in porewater samples collected from fly ash test cells used for artificial leaching by Fruchter and Rai *et al.* (1988), who obtained values ranging between 300 and 537 mV in Eh and 6.7 and 9.5 in pH respectively.

### 3.2.2 Depth profiles of major elements

#### 3.2.2.1 Na and K

The Na depth profiles of porewaters of all borehole samples from Drax are shown on Figure 3.1 (a). Concentrations of Na in porewater show higher values for several of the shallowest samples. This might be due either to the influence of leachate water from top soil or evapotranspiration. Except for these shallowest samples Na concentrations increase with depth, on the whole, indicating the reaction of PFA with porewater.



**Figure 3.1** Depth profiles of Na (a) and K (b) of porewater from boreholes in Drax PFA (symbols in (b) are the same as (a))

As shown in Figure 3.1 (b), concentrations of K in all four boreholes generally increase with depth, showing a similar trend to that of Na, indicating release of K. Boreholes 2 and 3 show more scatter compared with borehole 1. Concentrations of K in boreholes 2 and 4 show higher concentrations for some of the shallowest samples. No evidence has been found for the presence of solubility controlling phases or processes such as adsorption/desorption in the

depth trends of Na and K. The increasing depth trends for Na and K are interpreted as indicating continued reaction between downwards infiltrating porewaters and PFA, without attenuation within the ash mound.

### 3.2.2.2 Mg and Ca

Concentrations of Mg show similar trends to those of Na and K, increasing with depth, also indicating reaction and migration without attenuation in the ash mound (Figure 3.2 (a)). Although borehole 1 shows a maximum concentration at 3-3.5 m depth, concentrations of Mg generally increase constantly with few anomalies in the depth range investigated.

Retention of Mg as brucite has been reported by van der Sloot and Wijkstra *et al.* (1982), but this occurs in highly alkaline conditions. The pH of the porewaters from borehole 4 were around 8 and formation of brucite would not be predicted. Mg in Drax porewater appears to have been leached constantly without attenuation by solubility control in the depth range investigated, showing similar trends to Na and K.

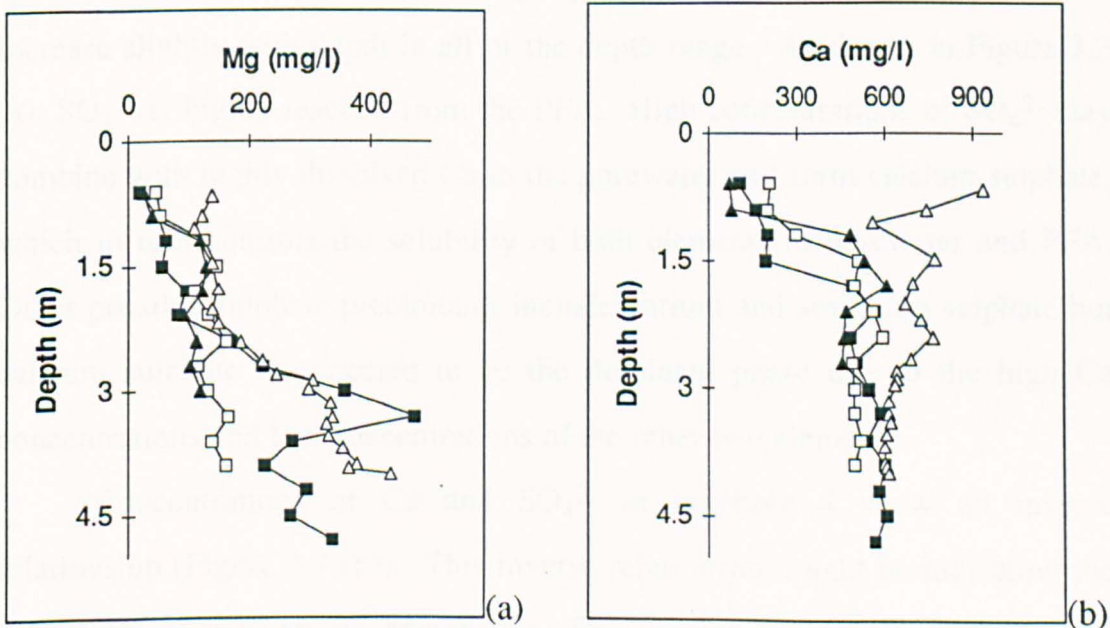


**Figure 3.2** Depth profiles of Mg (a) and Ca (b) in Drax porewater (Symbols are the same as those shown in Figure 3.1)

The depth trend of Ca for borehole 4 is different when compared with that of the other three boreholes, namely having higher values in the shallower samples (Figure 3.2 (b)). The Ca concentrations of porewater in boreholes 1, 2 and 3 increase with depth until they reach a constant level at around 2 m depth. Although borehole 4 shows a different trend between the surface and 2 m, Ca concentrations in borehole 4 also reach a nearly constant level, as with the other three boreholes. The depth trend of Ca concentration seems to imply the achievement of equilibrium concentrations, which would be controlled by thermodynamically stable phases.

### 3.2.2.3 $SO_4^{2-}$

Concentrations of  $SO_4^{2-}$  in Drax PFA porewater increase with depth, as shown in Figure 3.3 (a). Concentrations in Drax borehole 4 are higher compared with the values in the two other boreholes. The concentrations in boreholes 2 and 3 appear to achieve a relatively constant level at around 2m depth, after rapid increases from the surface. Compared with these two boreholes, the depth trend of borehole 4 seems to be slightly different, in that the concentrations increase slightly with depth in all of the depth range. As shown in Figure 3.3 (a),  $SO_4^{2-}$  is highly leached from the PFA. High concentrations of  $SO_4^{2-}$  may combine with highly dissolved Ca in the porewater and form calcium sulphate, which in turn controls the solubility of both elements in porewater and PFA. Other possible sulphate precipitates include barium and strontium sulphate but calcium sulphate is expected to be the dominant phase due to the high Ca concentrations and low concentrations of the other two elements.

Concentrations of Ca and  $SO_4^{2-}$  in borehole 4 show an inverse relationship (Figure 3.3 (b)). This inverse relationship might be indicating the formation of gypsum or anhydrite. The inverse relationship arises from differences in the rates of release of Ca and  $SO_4^{2-}$  from the PFA into the porewater. If the concentration of one species increases, then the amount of

calcium sulphate precipitate will be increased and this in turn will reduce the activity of the other species. In Figure 3.3 (b), some samples from boreholes 2 and 3 fall in a much lower range in the figure. These samples were collected from shallow depth where both Ca and  $\text{SO}_4^{2-}$  had not reached equilibrium concentration, in that depth range leaching of the PFA is the dominant process.

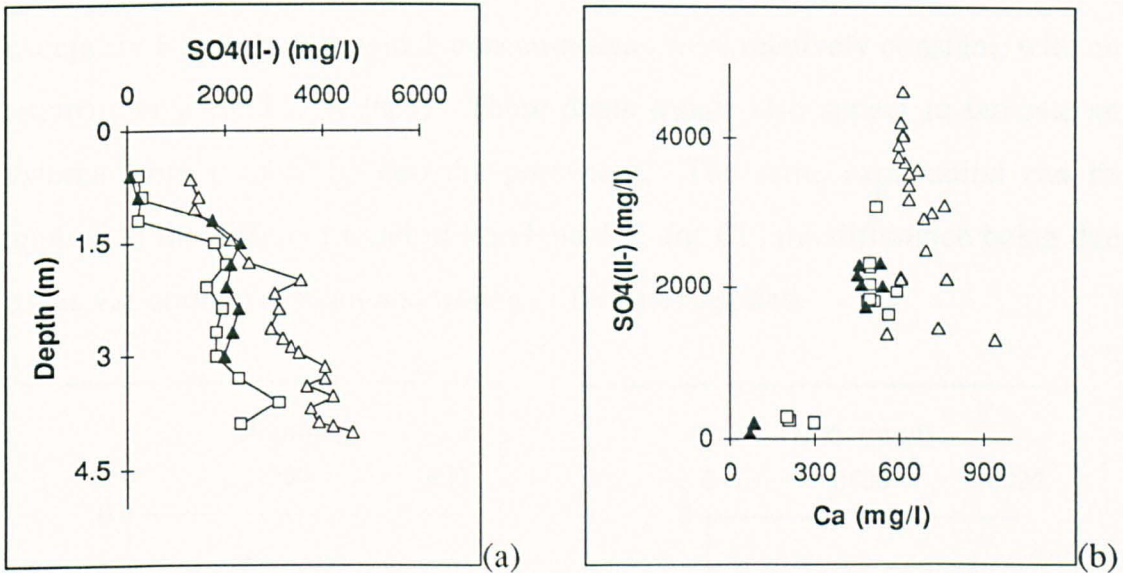


**Figure 3.3** Depth profiles of  $\text{SO}_4(\text{II}-)$  (a) comparison with Ca (b) in Drax porewater (symbols in (a) are the same as in those in Figure 3.1)

#### 2.2.2.4 $\text{Cl}^-$ and $\text{NO}_3^-$

Depth variations of  $\text{Cl}^-$  in boreholes 2, 3 and 4 show similar trends in all three boreholes, with a decrease in concentration with depth. The rate of decrease is especially high between the surface and around 2 m. Thereafter the concentrations reach a relatively constant value. Such a decreasing depth trend would appear to indicate an external source for the  $\text{Cl}^-$ . Rainwater contains  $\text{Cl}^-$ , which will contribute the  $\text{Cl}^-$  in the porewater. However, even considering evapotranspiration, the concentrations in Drax porewaters are too high to attribute the whole of the  $\text{Cl}^-$  concentrations in the porewater entirely to

rainwater. Fertiliser is thought to be a likely external source for the  $\text{Cl}^-$  in the porewater.

There are some differences in the  $\text{Cl}^-$  concentrations among the three boreholes. This could be due either to variation in the original background amounts in the ash mound or to variations in the amount of fertiliser applied.

Concentrations of  $\text{NO}_3^-$  in Drax porewater also decrease with depth except for borehole 3, in which concentrations were relatively constant, with an anomaly at around 2 m depth. These depth trends also appear to indicate an external source of  $\text{NO}_3^-$  into the porewater. The same explanation can be applied to the different trend of borehole 3 as for  $\text{Cl}^-$ , the difference being due to the variation in amount and timing of fertiliser applied.

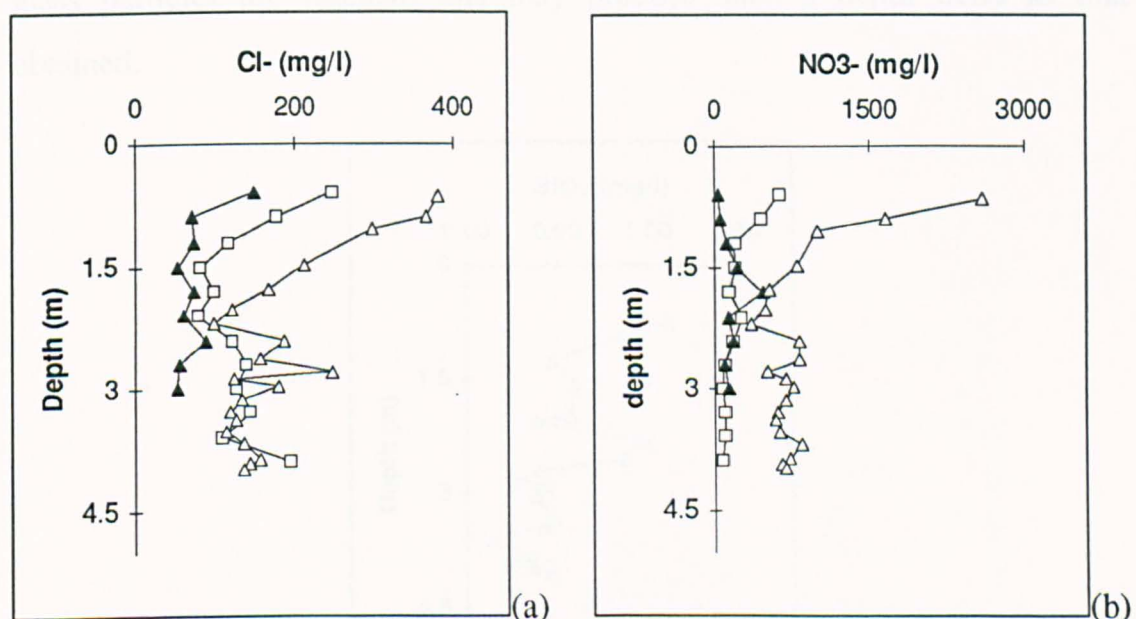


**Figure 3.4** Depth profiles of  $\text{Cl}^-$  (a) and  $\text{NO}_3^-$  (b) in Drax porewater (symbols are the same as those in Figure 3.1)

#### 2.2.2.5 Si

In Figure 3.5,  $\text{SiO}_2$  concentrations of porewater from Drax borehole 4 decrease with depth, approaching a constant value. Such a depth trend is indicative of an external origin for the silicon, but the concentrations of  $\text{SiO}_2$  in rainwater is

negligible and this can not properly explain the concentrations of  $\text{SiO}_2$  in the porewater. Relatively constant concentrations below around 2.5 m depth seem to suggest the presence of  $\text{SiO}_2$  solubility controlling solid phases.

The depth trend could possibly be explained by an understanding of the elemental associations and locations within PFA. The elements in PFA is either enriched on the surface of particles, that are readily available on contact with water or entrapped within PFA glass particles, which are more insoluble (Hulett and Weinberger, 1980; Mattigod, 1982; Dudas and Warren, 1988).  $\text{SiO}_2$  is the main component of the PFA aluminosilicate glass matrix, along with  $\text{Al}_2\text{O}_3$  and minor amounts of Na, K, Ca and Mg (Hulett and Weinberger, 1980; Mattigod, 1982; Dudas and Warren, 1988). If such Si-rich exteriors of glass particles are leached, this may produce such a depth trend as that obtained.

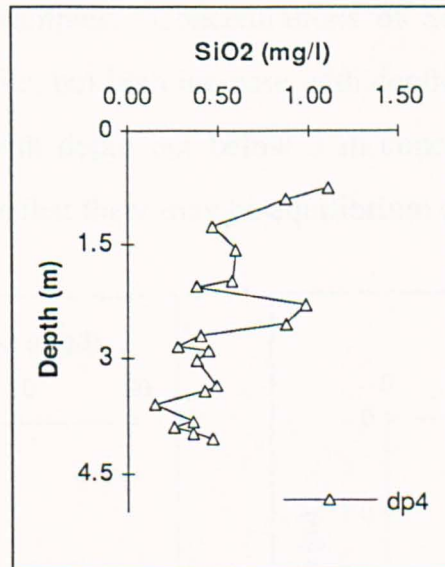


**Figure 3.5** Depth profile of Si in Drax porewater, borehole 4

### 3.2.3 Depth profiles of minor elements

Nearly all minor elements show depth-related trends in Drax PFA porewater. Concentrations of B, Cr, Li, Mo, Ni, Pb, As and Se in the porewater of Drax

borehole 4 show increases with depth, whereas Zn and Cu appear to decrease with depth. Concentrations of Ba and Sr show relatively constant concentration, except for higher values in the three shallowest samples.

### 3.2.3.1 Trace elements showing increasing depth trends: B, Cr, Li, Mo, Pb, Ni, Se and As

The depth trends of these ions are shown in Figure 3.6. Concentrations of B, Cr, Li, Mo, Ni, As, Se and Pb in porewaters increase with depth, showing evidence of reaction of PFA with infiltrating porewater. The trend for boron is particularly noteworthy. The overall concentration increase is 19.7 mg/l, which exceeds that of the other trace elements in the porewaters. Concentrations of Cr, Li and Mo also increase with depth, but compared with B the rate of increase is smaller, particularly below 3 m depth. Concentrations of Pb and Ni increase with depth but as for Na and K, higher concentrations were recorded in the shallowest two samples. Concentrations of Se and As show greater scatter in the depth profile, but both increase with depth. Concentrations of Cr, Li and Mo increases with depth but below 3 m concentrations remain more constant, which suggests that there may be equilibrium control of these

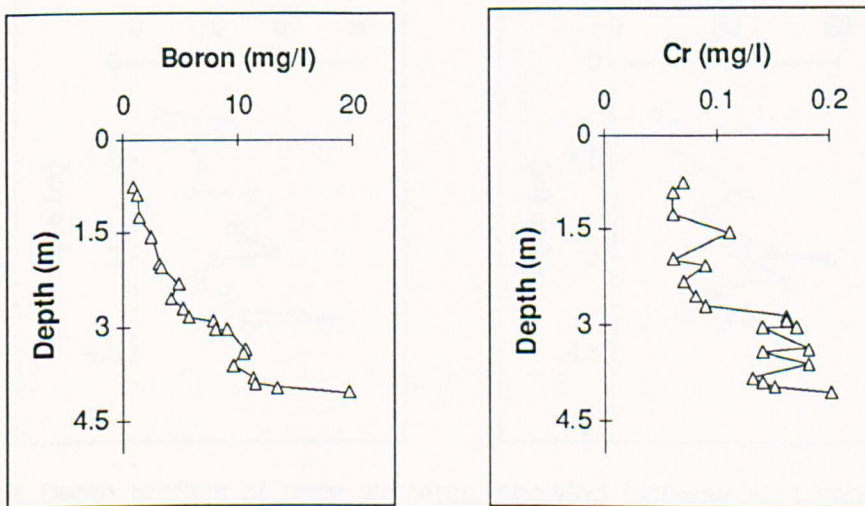


**Figure 3.6** Depth profiles of trace elements, showing increase with depth, in Drax porewater, borehole 4 (Continued-)

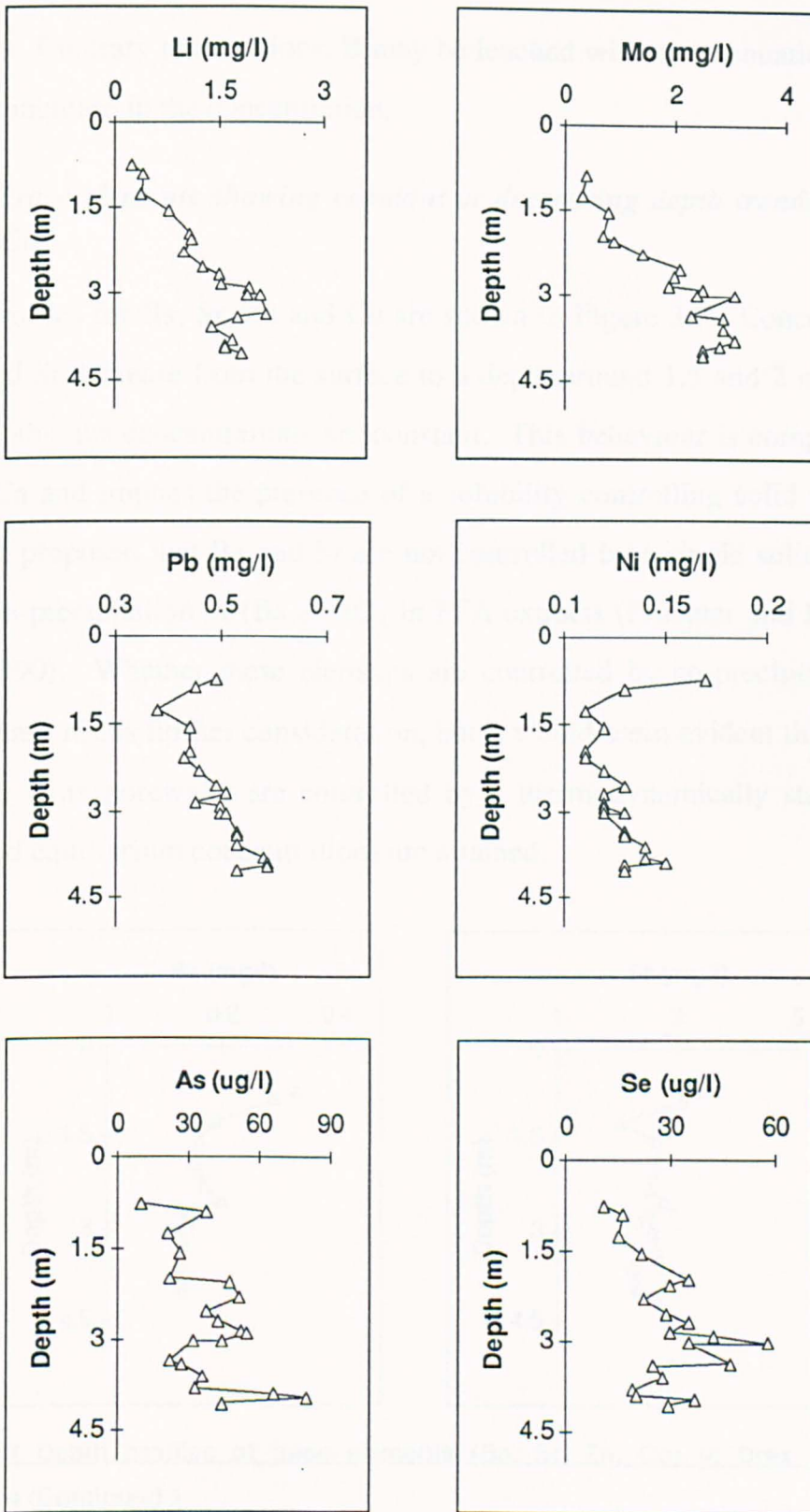


**Figure 3.6** Depth profiles of trace elements, showing increase with depth, in Drax porewater, borehole 4

elements. Contrary to these ions, B may be leached without attenuation, with a constant increase in the concentration.

### 3.2.3.2 Trace elements showing constant or decreasing depth trends: Ba, Sr, Zn and Cu

Depth profiles for Ba, Sr, Zn and Cu are shown in Figure 3.7. Concentrations of Ba and Sr decrease from the surface to a depth around 1.5 and 2 m. Below these depths, the concentrations are constant. This behaviour is comparable to that of Ca and implies the presence of a solubility controlling solid phase. It has been proposed that Ba and Sr are not controlled by a single solid solution but by co-precipitation of  $(\text{Ba,Sr})\text{SO}_4$  in PFA extracts (Fruchter and Rai *et al.*, 1988, 1990). Whether these elements are controlled by co-precipitates or a single phase needs further consideration, but it would seem evident that Ba and Sr in the Drax porewater are controlled by a thermodynamically stable solid phase and equilibrium concentrations are attained.

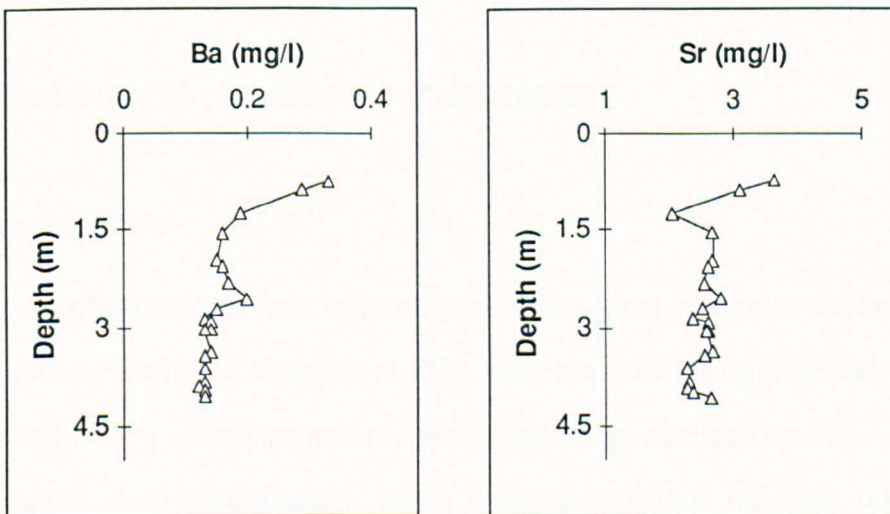


**Figure 3.7** Depth profiles of trace elements (Ba, Sr, Zn, Cu) in Drax porewater, borehole 4 (Continued-)

As to the depth trends of Zn and Cu, the trends are not clearly defined due to scatter in data. Despite the scatter, they do not seem to increase with

depth, at least. The concentrations of Zn and Cu appear to be relatively constant with depth, indicating the presence of solubility-controlling mechanisms.

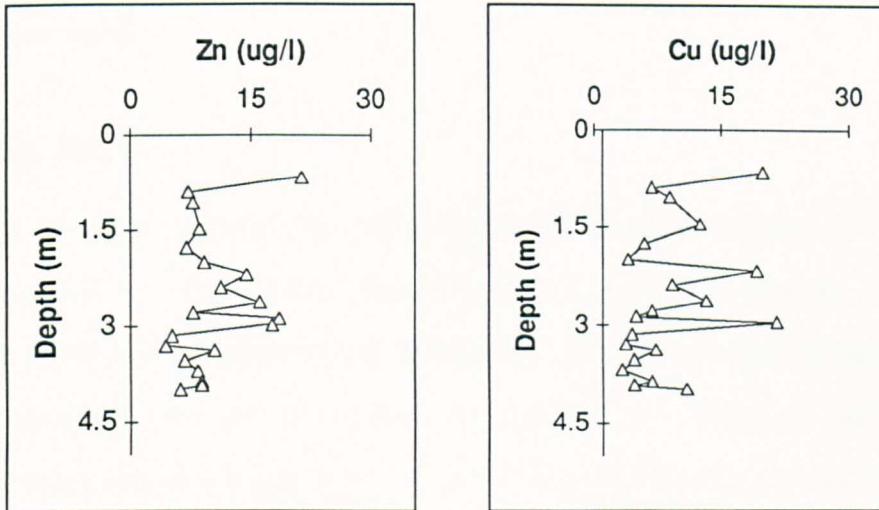


Figure 3.7 Depth profiles of trace elements (Ba, Sr, Zn, Cu) in Drax porewater, borehole 4

### 3.3 Geochemical reactions in porewater

#### 3.3.1 Introduction

From the depth trends of ions in Drax porewater, most elements are believed to have originated from the reaction of PFA with the infiltrating porewater, except for  $\text{Cl}^-$  and  $\text{NO}_3^-$ , which are mainly attributed to an external source. Amongst the internally derived elements, some show a constant increase with depth whereas others achieve more constant concentrations. The former depth variation suggests leaching and migration of the ions without control by solid phases or attenuation mechanisms within the ash mounds whereas the latter indicates the presence of some thermodynamic constraints accounting for the retention of ions.

In this section an attempt was made to define the mechanisms controlling the elements derived from the weathering of PFA, as indicated by the depth trends of porewater concentrations.

### 3.3.2 Major Ions

#### 3.3.2.1 Ca, $SO_4^{2-}$

Activities of Ca are plotted against activities of  $SO_4^{2-}$  in Figure 3.8 (a) along with calculated activities in equilibrium with gypsum and anhydrite. The  $Ca^{2+}$  activities show inverse relationship with  $SO_4^{2-}$ , this is an expected relationship if Ca concentrations are controlled by gypsum or anhydrite through the chemical reactions of Ca and  $SO_4^{2-}$ ;  $Ca^{2+} + SO_4^{2-} = CaSO_4$ : anhydrite,  $Ca^{2+} + SO_4^{2-} + 2H_2O = CaSO_4 \cdot 2H_2O$ : gypsum (from Lindsay, 1979, p89). The activities of  $Ca^{2+}$  in Figure 3.8 (a) plot nearly on the line of the calculated Ca activity in equilibrium with gypsum. Saturation indices with respect to gypsum in the Drax porewater of borehole 4 were also plotted with depth. The indices show that the porewater maintains an equilibrium relationship with respect to gypsum, except for several of the shallowest porewater samples (Figure 3.8 (b)).

Ca and  $SO_4^{2-}$  are the two main species in PFA porewater and their concentrations are controlled by the formation of gypsum. This result from geochemical modelling supports interpretation of depth trends of Ca and the relationship of Ca with  $SO_4^{2-}$ , shown previously in Figure 3.2 (b) and 3.3. (b), which was explained as indicating the achievement of equilibrium concentrations for Ca with respect to some thermodynamically stable phases. Gypsum and anhydrite were identified in many previous studies including Simons and Jeffery (1960), Roy and Griffin (1984), Warren and Dudas (1985), Rai and Ainsworth *et al.* (1987), Rai and Eary *et al.* (1987), Fruchter and Rai *et al.* (1988, 1990).

Other possible solubility controlling phases of Ca concentration in PFA are  $\text{CaCO}_3$  or  $\text{Ca(OH)}_2$  (Roy and Griffin, 1984; Rai and Ainsworth *et al.*, 1987). Among these phases,  $\text{Ca(OH)}_2$  is expected to occur in highly alkaline conditions ( $\text{pH} > 12$ ) whereas  $\text{CaCO}_3$  is strongly pH-dependent. These two compounds are not considered as possible solubility controlling phases in the Drax porewater.

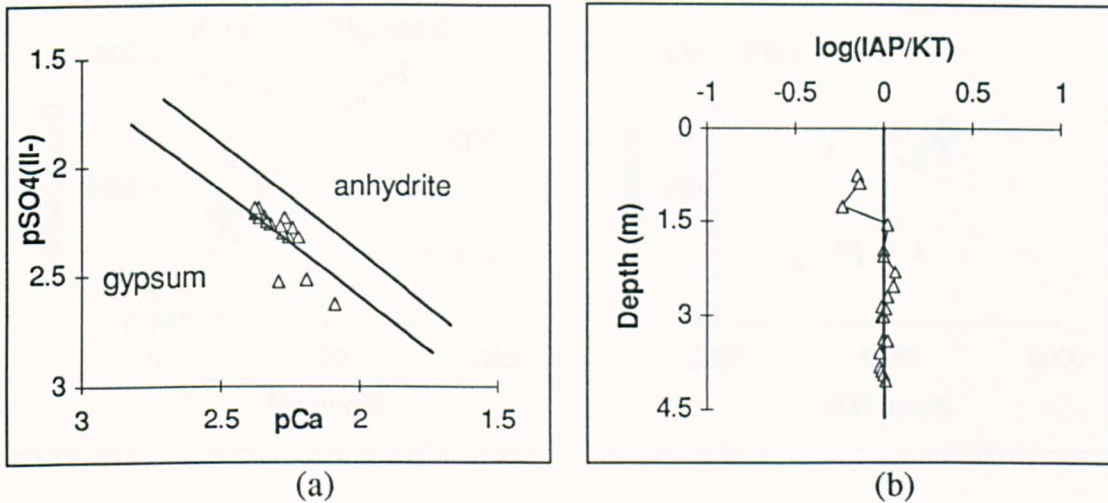


**Figure 3.8** Plot of Ca and  $\text{SO}_4(\text{II-})$  activities in Drax porewater along with the calculated activities in equilibrium with gypsum and anhydrite (a). Saturation indices with respect to gypsum (b)

### 3.3.2.2 Mg

The depth trend of Mg indicated the absence of solubility controlling solid phases. Chemical speciation of Mg shows free Mg ion,  $\text{Mg}^{2+}$  is the dominant aquatic species at shallower depths, but  $\text{MgSO}_4(\text{aq})$  is the prevailing aquatic species in the porewater below 2 m depth in borehole 4.

Concentrations of  $\text{SO}_4^{2-}$  and Mg in Drax porewater show a significant correlation ( $\sigma = 0.79$ ) with a linear relationship, indicating a common origin for the two elements in the porewater. Sulphur was reported to be exclusively present on the surface of PFA particles (van der Sloot and Wijkstra *et al.*,

1982). The relationship between Mg and  $\text{SO}_4^{2-}$  seems to indicate that the Mg leached in the porewater is from the surface associated fraction rather than from the less soluble glass matrix, because of the correlative relationship with  $\text{SO}_4^{2-}$ . Comparison of Mg with total dissolved ion concentration in the porewater of Drax borehole 4, shown in Figure 3.9 (b) indicates that dissolved Mg in the porewater is exclusively derived from within the ash mound.

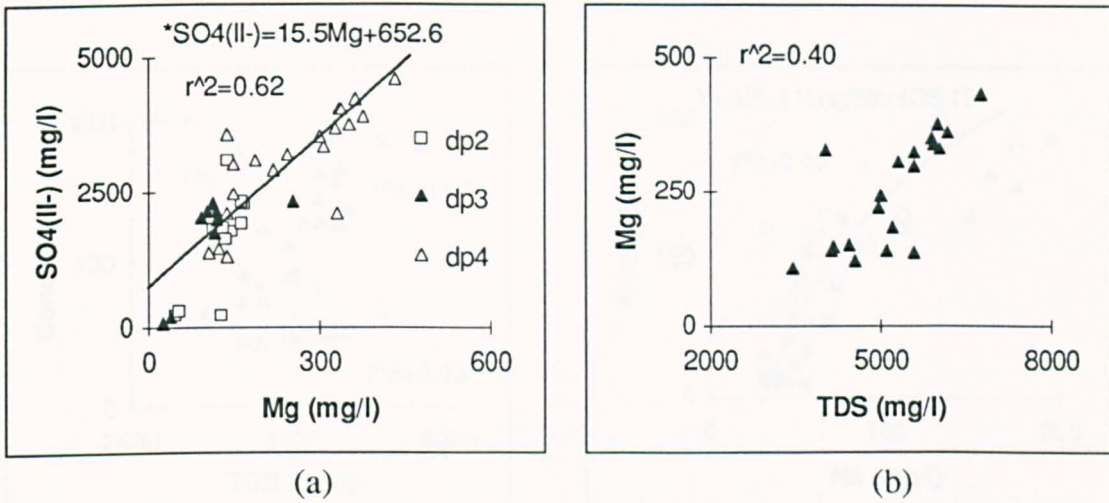


**Figure 3.9 Relationship between Mg and  $\text{SO}_4(\text{II}-)$  (\* Equation is for borehole 4 only) (a), and Mg vs. TDS (b)**

### 3.3.2.3 Na, K

No evidence of the achievement of equilibrium concentrations were found for Na and K in the depth trends. Na and K predominantly exist as free ions for all porewater samples of Drax borehole 4. Na in the porewater increases with increasing concentrations of total dissolved ions, also suggesting an internal origin for the Na in the porewater.

Concentrations of K show a correlative relationship with Na (Figure 3.10). Their relationships is a logarithmic one, which indicates a different rate of leaching. Concentrations of K decrease more rapidly than those of Na on leaching and the extrapolation using the correlation equation would seem to

pass through on the axis of Na. This suggests leaching of Na occurs in the same location as K, which might be the exterior of the PFA glass.

Concentrations of Na and K show constant increases with depth (Figure 3.1 (a), (b)), suggesting an absence of solubility controlling phases. Free ionic forms are the predominant aquatic species of Na and K in the porewater, whereas  $MgSO_4$  becomes the dominant aquatic species over free Mg ion with depth.

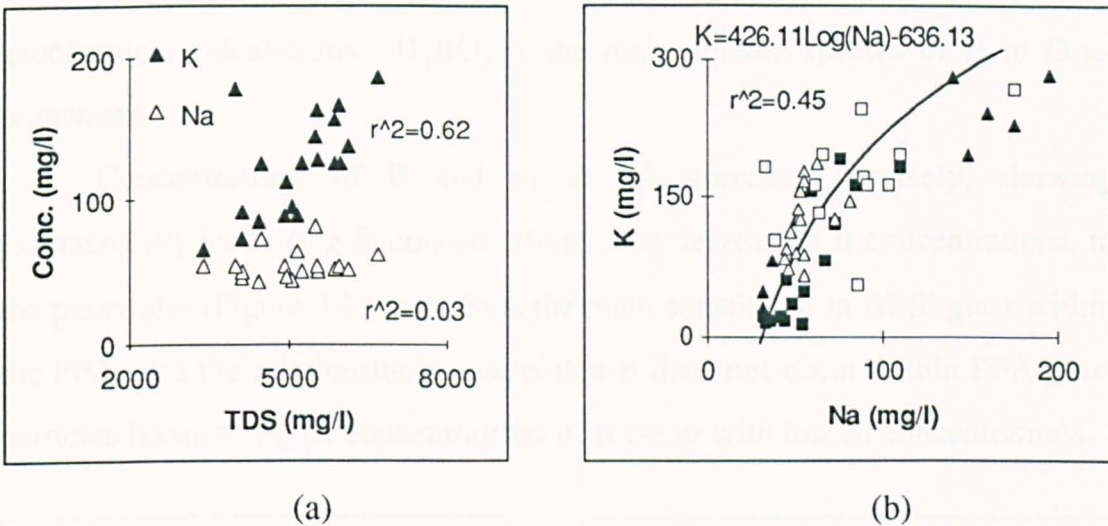


**Figure 3.10 Relationship of Na, K vs. TDS (a) and Na vs. K (b) (Symbols in (b) are the same as in Figure 3.1)**

### 3.3.3 Minor ions

B is one of the most mobile constituents of PFA, and is readily leached without showing any evidence of attenuation during infiltration in PFA column leaching tubes (Warren and Dudas, 1986). Two different types of B species were reported; one highly leachable species and the other basically insoluble (Cox and Lundquist *et al.*, 1978; James and Graham *et al.*, 1982). The former is predicted to be mainly a readily soluble admixture of salts such as borate or boric acids. These chemical forms are known to be predominant in nature, and the leachability of B in PFA was greatly varied, in as range between 17 and 74

% (James and Graham *et al.*, 1982). Hollis and Keren (1988) reported that the leachability of B from alkaline PFA is pH-dependent and at pH=9, about 35 % of B was removed by 24 hours extraction whereas at pH=6, 85 % of B was removed by the same extraction procedure.

B is highly leached from Drax PFA, 19.7 mg/l being the highest value in the porewater. Such a high leachability of B seems to indicate it is leached from the borate compounds of high solubility in the ash. No evidence of solubility controlling process were found for B, from either the depth trend or geochemical calculations.  $H_3BO_3$  is the main aquatic species of B in Drax porewater.

Concentrations of B and Si in ash correlate inversely, showing exponentially increasing Si concentrations with decreasing B concentrations, in the porewater (Figure 3.11 (a)). Si is the main constituent in Al-Si glass within the PFA, and the relationship suggests that B does not occur within PFA glass particles because higher concentrations of B occur with low Si concentrations.

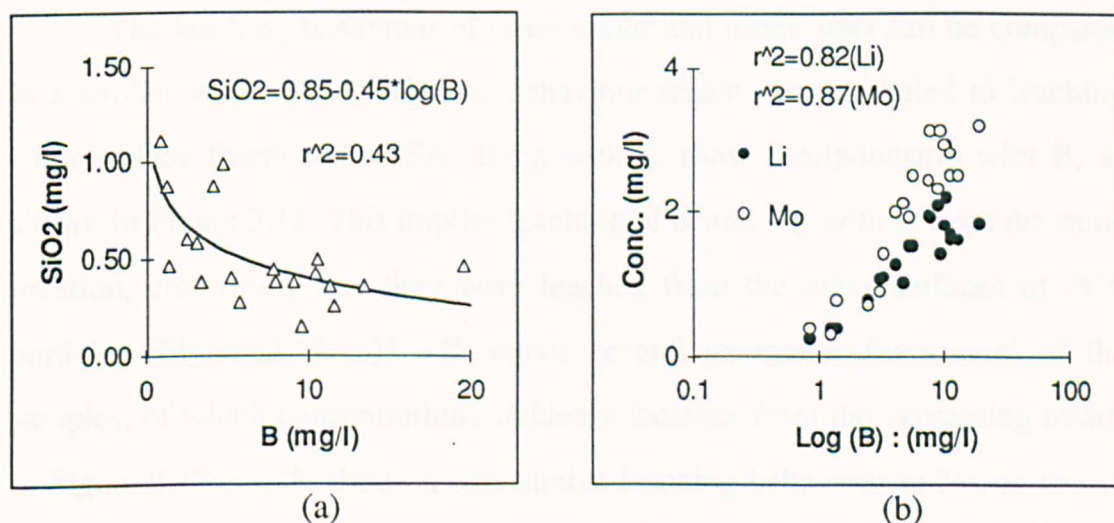


**Figure 3.11 Relationship between SiO<sub>2</sub> vs. B (a) and B vs. Li and Mo (b) (Note the logarithmic scale of B in (b))**

Concentrations of B in PFA pore water are highly correlative with Mo and Li, showing positive relationships (Figure 3.11 (a), (b)). The relationships

are exponential and this seems to indicate a different rate of leaching of the elements. Namely, B is more readily dissolved compared with Li and Mo, in the early leaching stage. These highly correlative relationships also indicate a common source for the B, Li and Mo, which thought to be a soluble admixture of the elements on the surfaces of PFA particles.

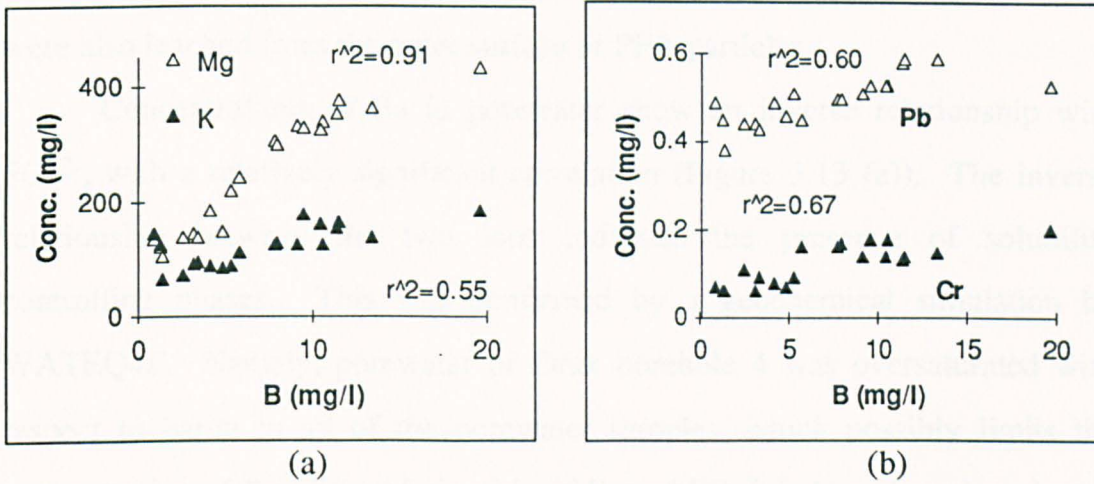


**Figure 3.12 Relationships between B vs. K and Mg (a) and B vs. Ni and Pb (b)**

The leaching behaviour of other major and minor ions can be compared in a similar way. K and Mg, the behaviour which was attributed to leaching from surface fractions of PFA, along with S, show a relationship with B, as shown in Figure 3.12. This implies leaching of K and Mg with B from the same location, confirming that they were leached from the outer surfaces of PFA particles (Figure 3.12 (a)). K shows several anomalies for several of the samples, of which concentrations suddenly increase from the decreasing trends in Figure 3.12 (a). K shows a comparable leaching behaviour to Na, as shown in Figure 3.10, and the K and Na is thought to have been dissolved from the soluble salts on the surfaces of PFA particles. The anomalies shown in Figure 3.12 (a), however, would seem to indicate leaching of K from the exterior of Al-Si glass after dissolution of the surface enriched fractions of PFA particles.

It might be the K from the ash matrix which unexpectedly raised the concentrations of K in this range of B concentrations.

Other minor ions showing strong correlation with B, include Pb and Cr (Figure 3.12 (b)). A similar explanation can be applied for the Pb and Cr as was applied to the relationships of B with Li and Mo. B would seem to be more readily soluble than other minor ions including Li, Mo, Cr and Pb, which were also leached from the outer surface of PFA particles.

Concentrations of Ba in porewater show an inverse relationship with  $\text{SO}_4^{2-}$ , with a relatively significant correlation (Figure 3.13 (a)). The inverse relationship between the two ions indicates the presence of solubility controlling phases. This was confirmed by a geochemical simulation by WATEQ4F. Namely, porewater of Drax borehole 4 was oversaturated with respect to barite in all of the porewater samples, which possibly limits the concentration of Ba. The relationship of Sr and  $\text{SO}_4^{2-}$  is less clear than that of Ba with  $\text{SO}_4^{2-}$ . If the two \* marked points in Figure 3.13(b) are excluded, Sr appears to be nearly independent of  $\text{SO}_4^{2-}$ .

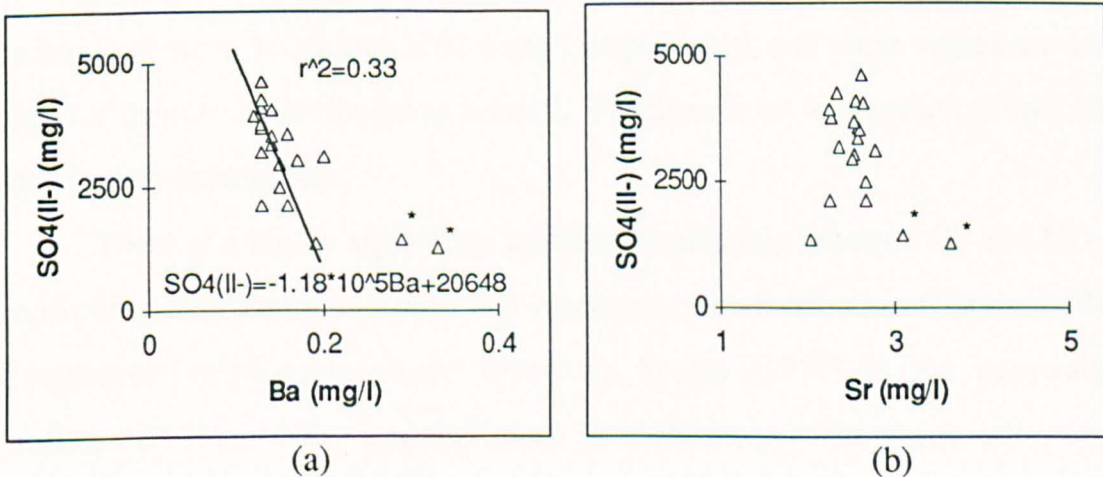


**Figure 3.13 Relationship between Ba vs.  $\text{SO}_4(\text{II}-)$  (a) and Sr vs.  $\text{SO}_4(\text{II}-)$  (b) (equation in diagram (a) was obtained after excluding \* marked data)**

It has been suggested that the solubility controlling for Ba and Sr is not due to a single phase, but is the result of co-precipitation of Ba and Sr as a

sulphate solid (Fruchter and Rai *et al.*, 1988, 1990). A recent study of the solubility of (Ba, Sr)SO<sub>4</sub> precipitates by Felmy and Rai *et al.* (1993) suggests that a single solid-solution phase does not control both the aqueous Ba and Sr, instead barite is formed initially, due to its high solubility, and then small amounts of Sr are substituted into the barite. The results of geochemical calculations on Drax porewater, agree well with those acquired by Fruchter and Rai *et al.* (1988, 1990), with the porewater showing oversaturation with respect to barite (BaSO<sub>4</sub>) and undersaturation with respect to celestite (SrSO<sub>4</sub>). This result implies that Ba and Sr are not controlled by a single phase, either barite or celestite, but that the Ba and Sr are more likely to be controlled by (Ba, Sr)SO<sub>4</sub>, with varying mole fractions of Ba and Sr.

### 3.4 Elements with an external origin

Both Cl<sup>-</sup> and NO<sub>3</sub><sup>-</sup> concentrations in Drax porewater from borehole 4 decrease with depth (Figure 3.4). These depth trends seem to indicate an external origin. Rainwater contains Cl<sup>-</sup> and NO<sub>3</sub><sup>-</sup> and can contribute to soil water. However, the highest concentrations of Cl<sup>-</sup> and NO<sub>3</sub><sup>-</sup>, in near-surface porewater of Drax borehole 4, were 380.9 and 2601.6 mg/l respectively, and these values are too high for them to be attributed to rainfall. Fertiliser is an appropriate source for such high concentrations.

There is a highly significant positive relationship between Cl<sup>-</sup> and NO<sub>3</sub><sup>-</sup> confirming their common origin and mechanism of distribution (Figure 3.14). Comparable relationships were found by Spears (1979) in the porewater profiles of Cl<sup>-</sup> and NO<sub>3</sub><sup>-</sup> concentrations in chalk areas. The relationship was explained by input from an external source, namely fertiliser. The positive relationship in Figure 3.14 indicates that the decrease of NO<sub>3</sub><sup>-</sup> is not due to denitrification, because NO<sub>3</sub><sup>-</sup> concentrations decrease along with those of Cl<sup>-</sup>. The change in concentrations of both NO<sub>3</sub><sup>-</sup> and Cl<sup>-</sup> with depth can be attributed to variations in the rate of supply, followed by dilution, due to differential flow

between soil and PFA, or dispersion by lateral flow. The regression equation for the  $\text{Cl}^-$ - $\text{NO}_3^-$  data does not pass through the origin, which indicates changes in the  $\text{Cl}/\text{NO}_3$  ratio. There was a significant difference at the 95% confidence level between the ratios for the upper half section (mean = 4.29) and the lower half section of the borehole (mean = 4.97). According to work by Spears (1979), such changes in ratio with depth are due to by a change with time, or denitrification with depth. However, the variation could be explained as variation in the input, with the ratio decreasing as fertiliser  $\text{NO}_3^-$  and  $\text{Cl}^-$  input increase relative to rainwater  $\text{Cl}^-$ .

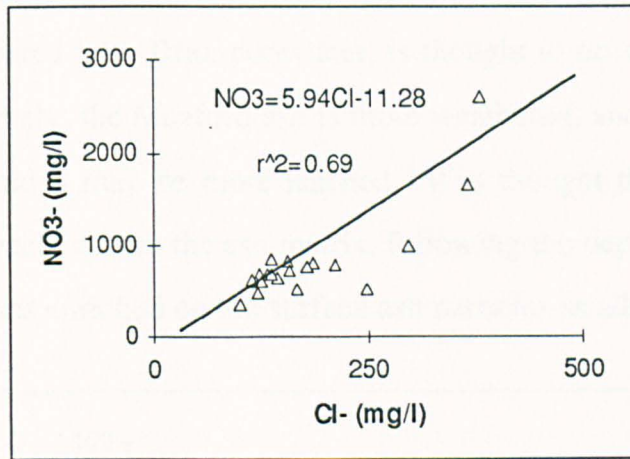


**Figure 3.14 Relationship between  $\text{NO}_3^-$  and  $\text{Cl}^-$  in porewater of borehole 4**

### 3.5 Chemistry of Meaford porewater

As was described in Chapter 2, the Meaford PFA disposal site was investigated to extend the age of PFA investigated and to confirm the results from the Drax ash mound. The composition of Meaford and Drax porewater were compared to determine the change in porewater composition with more weathering. Depth profiles were also investigated to assess the mobility and migration of elements from the ash into porewater, as was conducted on the Drax porewater. Generally the results from the investigation of Meaford porewater agree well

with those acquired from the study of the Drax ash mound, and confirm those conclusions established in the study of Drax pore water.

### 3.5.1 Chemical composition of Meaford porewater

Average concentrations of Meaford porewater are shown in Table 3.2. The main components for both Drax and Meaford porewater are compared in Figure 3.15. The ionic concentrations of Drax porewater are higher than those of Meaford porewater except for Al and Si, which are higher in the Meaford porewater. The concentration of K and  $\text{SO}_4^{2-}$  are especially low in Meaford porewater, compared with other cations. The depletion of K and S in Meaford porewater, compared with Drax porewater, is thought to do with the degree of weathering. Namely, the Meaford ash is more weathered, and surface-enriched fractions of K and S may be more leached. It is thought that K in Meaford porewater was leached from the ash matrix, following the depletion of more the soluble K fractions enriched on the surface ash particles as admixture of salts.

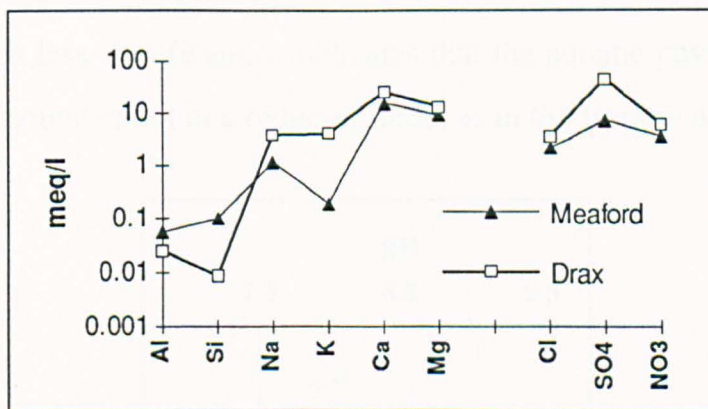


**Figure 3.15 Comparison of average concentrations of the major ions in Meaford and Drax porewater**

The average ratio of Na/K in Meaford porewater is 3.56, which is much higher than the value of 0.63 in Drax porewater. However, the ratios of Na/K in solid PFA are 0.30 for the former and 0.26 for the latter, so the values are similar in both sites. The higher ratio of Na/K in the Meaford porewater,

compared with Drax porewater, would seem to suggest either higher dissolution of Na or less leaching of K in the Meaford porewater than in the Drax porewater. Meaford ash is more weathered than the Drax ash and lower concentrations of Na are expected, since the concentration is expected to generally decrease with the degree of weathering. The ratios indicate lower dissolution of K in Meaford porewater, which is thought to be the result of the dissolution of PFA glass.

The higher concentrations of Al and Si in Meaford porewater is also thought to be the result of Al-Si glass. The concentrations of Al in Barlow porewater were very low and did not show any specific depth trend.

The pH of Meaford porewater was measured in the laboratory and it was slightly more alkaline than Drax porewater, ranging between 8.1 and 9.0. The pH values increase with depth (Figure 3.16) from neutral to alkaline. Much of the alkalinity is thought to be contributed by the dissolution of  $\text{SO}_4^{2-}$ , Ca and Mg. Eh was also measured and the average value recorded was 440 mV. Although this was not measured in the field but in the laboratory, which make the value much less significant, it indicates that the aquatic environment in the Meaford ash mound is not in a reducing state, as in the Barlow ash mound.

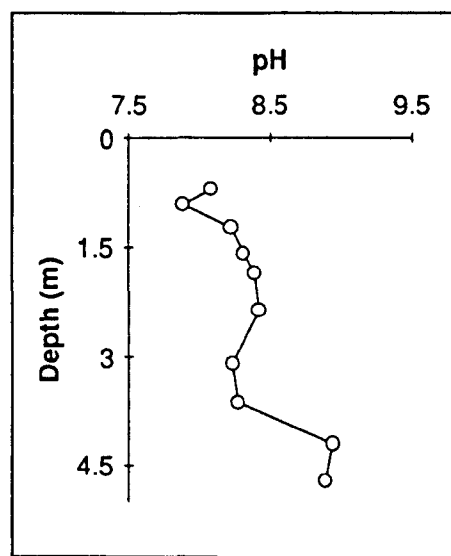


**Figure 3.16 Variation of pH in Meaford porewater with depth**

Depth (m)	pH	Ca	Mg	Na	K	Fe	Al	B	Ba	Co	Cr	Cu	Li	Ni	Pb	Si	Sr	As*	Se*	Mo	Cl <sup>-</sup>	NO <sub>3</sub> <sup>-</sup>	SO <sub>4</sub> <sup>2-</sup>
0.7	8.1	160.3	31.0	19.2	8.8	0.02	0.13	0.84	0.18	0.04	0.02	0.01	0.01	0.01	0.19	4.31	1.20	25	18.7	0.1	46.6	198.4	299.1
0.9	7.9	216.7	67.8	22.9	7.3	0.04	0.20	1.46	0.24	0.05	0.03	0.02	0.14	0.10	0.22	3.74	2.06	27	15.8	0.2	69.1	213.9	372.6
1.2	8.2	311.8	104.6	18.7	6.8	0.04	0.02	2.47	0.32	0.05	0.04	0.01	0.32	0.07	0.27	3.79	2.26	37	10.0	0.4	85.5	393.7	467.7
1.6	8.3	150.9	156.2	22.2	5.7	0.02	0.11	5.15	0.27	0.04	0.07	0.01	0.42	0.06	0.21	3.31	1.70	41	10.0	0.5	80.5	349.0	530.2
1.8	8.4	87.8	157.8	24.1	4.8	0.20	0.50	7.03	0.21	0.03	0.13	0.01	0.36	0.04	0.18	3.08	0.96	63	11.3	0.6	130.1	264.0	872.2
2.4	8.4	96.5	124.7	23.5	4.6	0.07	0.32	7.58	0.27	0.04	0.10	0.01	0.33	0.04	0.15	2.98	1.14	59	10.0	0.6	80.8	153.0	608.1
3.1	8.3	158.3	89.7	30.3	6.5	0.05	0.29	14.00	0.19	0.04	0.18	0.03	0.28	0.08	0.19	3.36	1.43	45	16.2	0.7	53.2	109.8	768.3
3.6	8.3	455.3	202.6	33.1	7.4	0.09	0.38	24.72	0.19	0.08	0.12	0.02	0.27	0.11	0.43	1.78	2.79	39	13.9	1.1	55.2	132.8	4016.0
4.2	9.0	738.7	95.9	33.7	10.3	0.29	1.30	11.81	0.27	0.10	0.11	0.02	0.41	0.17	0.57	1.45	4.31	32	10.0	1.9	55.2	150.7	4230.8
4.7	8.9	820.2	75.3	39.4	12.4	0.11	1.55	7.60	0.27	0.10	0.12	0.01	0.43	0.16	0.69	1.06	4.75	22	26.7	1.8	47.3	152.3	3954.7
Avg.	8.4	319.7	111.6	26.7	7.5	0.09	0.48	8.30	0.24	0.02	0.06	0.02	0.30	0.09	0.31	2.90	2.30	39	14.0	0.8	70.4	211.8	1612.0

**Table 3.2 Chemical composition of Meaford porewater (Unit: mg/l except for \*, \*=µg/l)**

### 3.5.2 Depth profiles of Meaford porewater

The ionic concentrations of Meaford pore water show depth-related variation for nearly all elements, as shown in Figures 3.17–20. The depth trends of Meaford porewater are very similar to those of Barlow porewater.

#### 3.5.2.1 Ca, Mg, Na and K

The concentrations of Ca, Na and K in Meaford porewater increase with depth (Figure 3.17). The concentrations of Mg initially increases with depth, up to 2 m in depth, but decreases with depth thereafter. The depth variation of Na and K is similar to that of Drax porewater, whereas Ca and Mg are different. The concentration of Ca in Meaford porewater increases constantly with depth and does not appear to achieve equilibrium concentration. The concentration of Mg, which showed constantly increasing depth variation in Drax porewater, also show a somewhat different trend in Meaford porewater, with the concentration not constantly increasing, but decreasing after a certain depth.

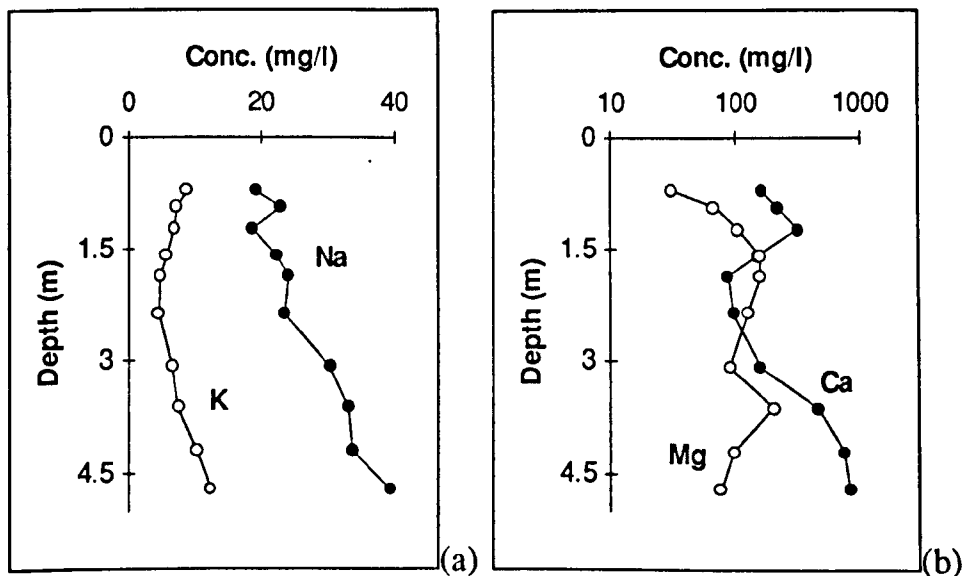


**Figure 3.17** Depth profiles of major elements (Na, K, CA, Mg) in Meaford porewater

### 3.5.2.2 Si and Al

The concentration of  $\text{SiO}_2$  constantly decreases with depth, whereas Al increases with depth (Figure 3.18). The two elements appear to show inverse relationship. Compared with Drax porewater, higher concentrations of Al and Si are dissolved in Meaford porewater. The main source of both Si and Al leaching from PFA is Al-Si rich glass or mullite. For  $\text{SiO}_2$ , it would appear that higher concentrations at shallower depths are due to a greater amount of Si being made available from PFA as vertical seepage of porewater strip off the outer surface of ash particles as explained for the depth trend of  $\text{SiO}_2$  concentrations in Drax porewater. The inverse relationship seems to imply the presence of Al-Si precipitates, which may control the solubility of the Al and Si in PFA porewater.

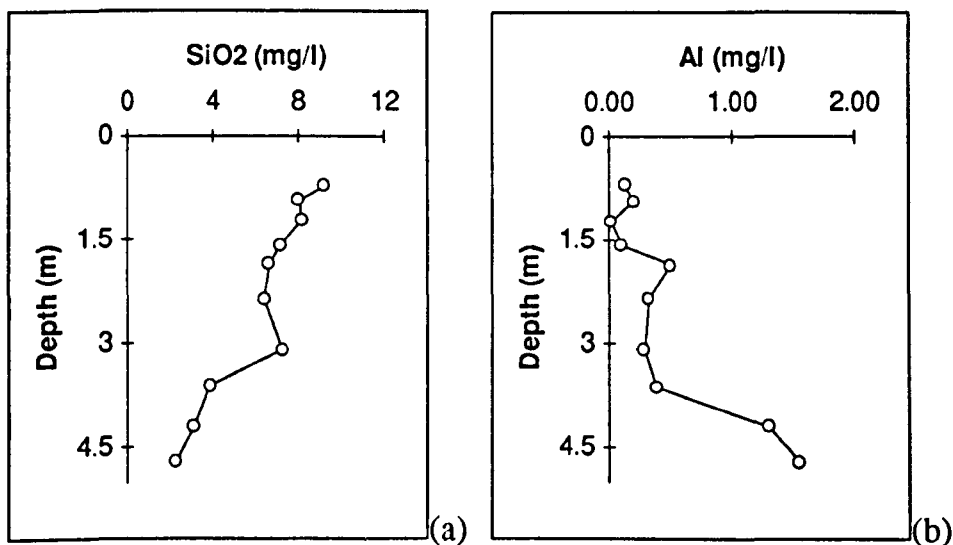


**Figure 3.18** Depth profiles of  $\text{SiO}_2$  (a) and Al (b) in Meaford porewater

### 3.5.2.3 Anions

The depth profiles of anion concentrations in Meaford porewater are shown on Figure 3.19. All anions including  $\text{Cl}^-$ ,  $\text{NO}_3^-$  and  $\text{SO}_4^{2-}$  in Meaford porewater show the same trends as those in Drax porewater. A similar explanation can be

applied. Namely, the decrease with depth for of  $\text{Cl}^-$  and  $\text{NO}_3^-$  indicates an external origin, possibly fertiliser, whereas the depth trend of  $\text{SO}_4^{2-}$ , an increase with depth, implies derivation from PFA.

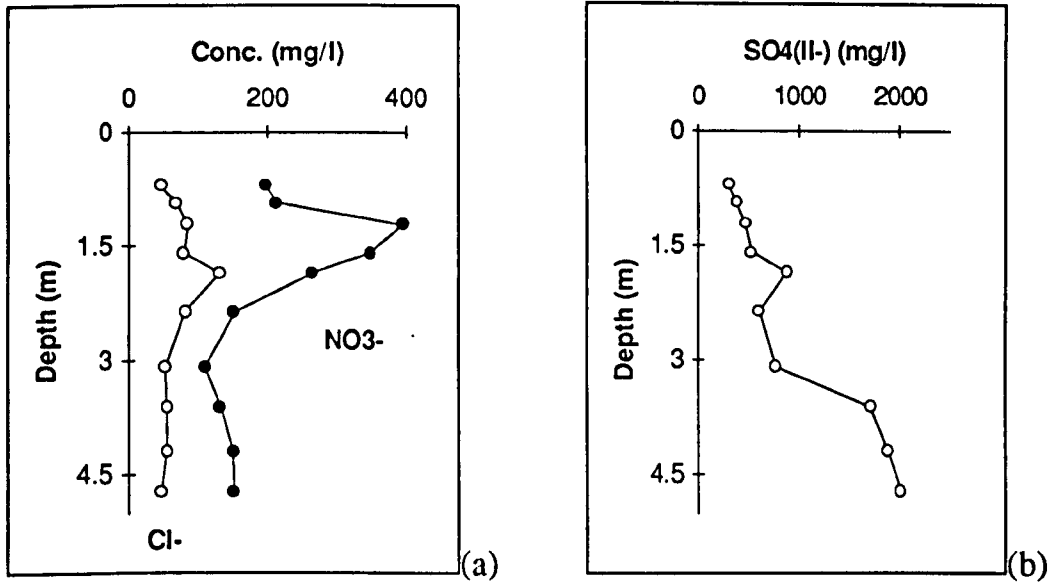


**Figure 3.19** Depth profile of anions in Meaford porewater

$\text{NO}_3^-$  and  $\text{Cl}^-$  show similar peaks at about 1.5 m depth. These similar depth trends and peaks in Meaford porewater are thought to indicate the timing of the fertiliser application.

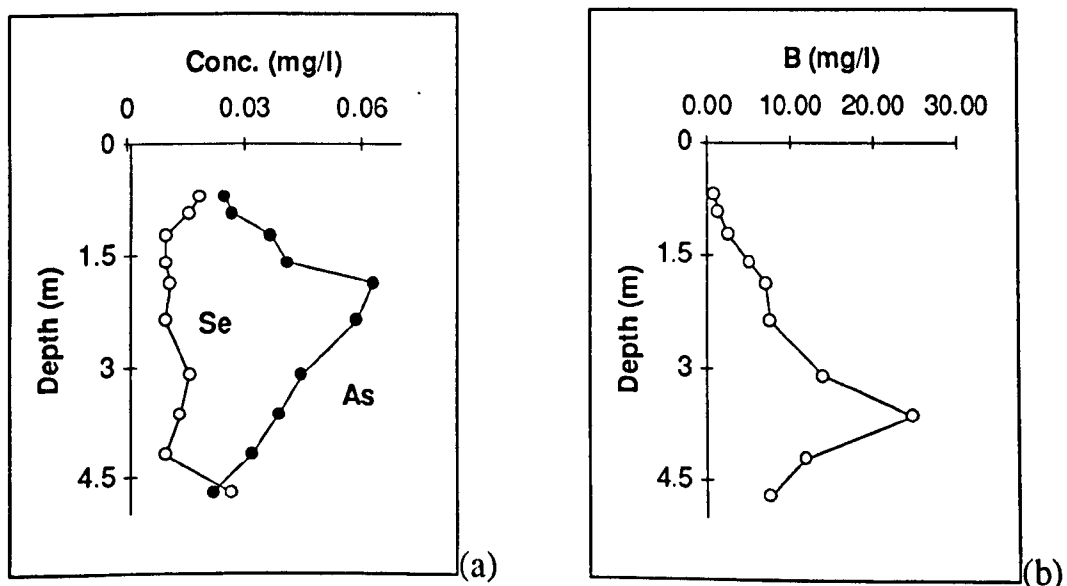


**Figure 3.20** Depth profiles of minor ions in Meaford porewater (Continued-)

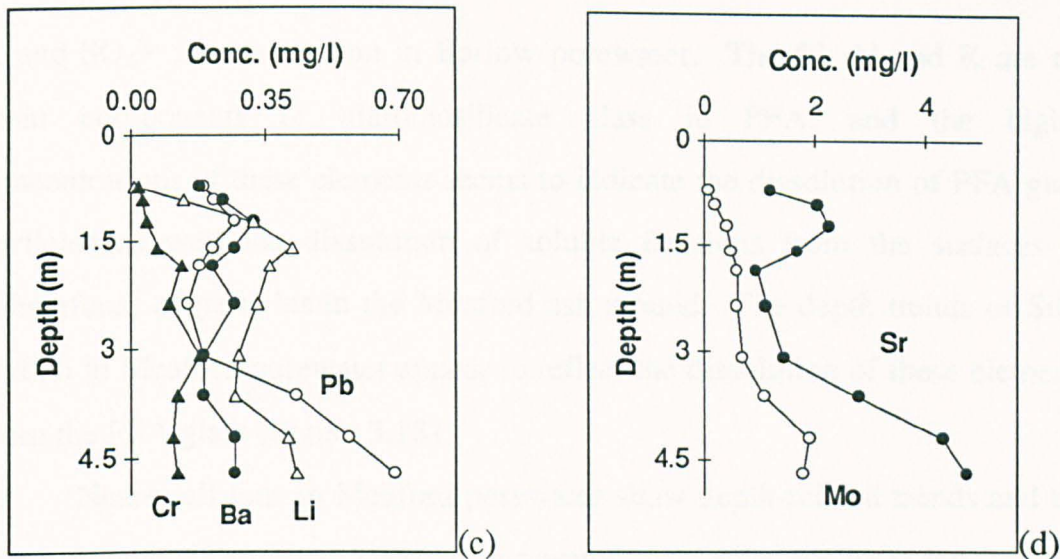


**Figure 3.20** Depth profiles of various minor ions in Meaford pore water

### 3.5.2.4 Trace cations

Concentrations of B, Li, Mo, Sr and Pb increase with depth, indicating dissolution of these elements. The concentration of B, however, decreases, after increasing up to a depth of about 4 m. Concentrations of Cr and Ba are relatively constant through all depth ranges, indicating the presence of solubility controlling phases. The concentrations of As follows a similar pattern to that of B but it reaches a maximum value at a shallower depth, at a depth of about 2 m.

## 3.6 Geochemistry of porewater and its long-term influence on groundwater

### 3.6.1 Comparison of Drax and Meaford porewater

#### 3.6.1.1 Dissolution of glass particles

There is a slight difference in the composition of Drax and Meaford porewater, as shown in Figure 3.15. In Meaford porewater Si and Al are higher, whereas

K and  $\text{SO}_4^{2-}$  are lower than in Barlow porewater. The Si, Al and K are the main components of aluminosilicate glass in PFA, and the higher concentrations of these elements seems to indicate the dissolution of PFA glass particles as well the dissolution of soluble fractions from the surfaces or subsurfaces of particles in the Meaford ash mound. The depth trends of  $\text{SiO}_2$  and Al in Meaford porewater appear to reflect the dissolution of these elements from the PFA glass (Figure 3.18).

Nearly all ions in Meaford porewater show depth-related trends and the depth trends of Drax and Meaford porewater are similar for most ions. Some elements show more distinct trends in the Meaford depth profiles. This appears to be attributable to a longer contact time in the more weathered ash. The depth trends of Meaford porewater would seem to confirm the depth trends of Drax porewater.

### *3.6.1.2 Concentrations of trace elements in Barlow and Meaford porewater*

It is noteworthy that the levels of trace elements in Meaford and Drax porewater are very similar to each other, except for Li. The concentration of Li was much higher in the Meaford porewater. The similar concentrations of trace elements in both porewaters imply two things, firstly, more easily soluble, surface enriched trace elements, were dissolved in both porewaters, except for Li, secondly, trace elements are not that rapidly leached under natural weathering conditions as was expected except for some trace elements such as Li, B

Hulett and Weinberger (1980) suggested that surface enrichment of trace elements occurs by a diffusion mechanism as well as by volatilisation and condensation on surfaces during combustion. A diffusion mechanism explains why trace elements are not only condensed on PFA surfaces but also concentrated into glass phases outside of PFA particles. The solubility of metals is strongly pH dependent because most of their reactions with solutions

involve the  $H^+$  ion. Consequently, their solubility is much greater in acidic environment. The pH of Barlow and Meaford porewater is neutral to slightly acidic and such solutions are not expected to scavenge as much metal from PFA as in laboratory experiment using strong agent. It is presumed that although many trace elements are known to be enriched on the surface, and readily available for leaching on contact with water, many of the trace elements are released more slowly under natural weathering condition. In addition to the weathering condition, the association of trace elements within the exterior shell of PFA particles is thought to control the slow but longer, constant release of the trace elements from the weathered PFA. B and Li seem to be more readily soluble than the other trace elements.

### 3.6.2 Evolution of porewater and implications for groundwater pollution

The concentration of many elements increase as a function of depth, both in the Barlow mound and Meaford site. The concentrations could be extrapolated to become far greater, provided that equilibrium calculations signified undersaturation. The chemical evolution of the infiltrating porewater will continue until it discharges as leachate from the ash mound.

Ca	Mg	Ni	K	Fe	Al	Si	B	Ba	Ca
608	363	52	137	0.09	0.03	0.2	13	0.1	0.05
Co	Cr	Cu	Li	Mn	Ni	Pb	Sr	Zn	
0.10	0.15	0.01	1.6	0.00	0.13	0.59	2.4	0.02	
Mo	As*	Se*	Hg*	Cl	NO <sub>3</sub>	SO <sub>4</sub>	pH	Eh(mV)	
2.5	80	37	<5.0	145	634	4023	8.26	409	

**TABLE 3.3 Porewater analyses from PFA emplaced in 1975 and subjected to natural weathering in the PFA disposal mound. The analysis shown is for a sample at a depth of 4.0 m within the PFA mound. (Element concentrations: mg/l and \* $\mu$ g/l)**

Table 3.3 shows the porewater composition collected at a depth of 4 m in Barlow borehole 4. This is the final composition of porewater which has been subjected to weathering reactions for at least 10 years, considering the infiltration rate. These analyses provide an indication of the likely contribution to groundwater of a thin blanket of older PFA.

### 3.7 Conclusion

(1) Nearly all cations and anions in porewaters from the Barlow mound show depth-related trends. Concentrations mainly increase with depth, which indicates that the PFA is reactive and elements in the PFA are leached on contact with water.

(2)  $\text{Ca}^{2+}$  and  $\text{SO}_4^{2-}$  are the two main species in the Drax and Meaford porewaters, and for most samples equilibrium calculations indicate saturation with respect to gypsum. Evidence of equilibrium in the porewater is provided by the attainment of constant concentrations in depth profiles.

(3) The decreases in porewater concentrations of  $\text{Cl}^-$  and  $\text{NO}_3^-$  with depth are very similar and a common external source is indicated. The concentrations of the  $\text{Cl}^-$  and  $\text{NO}_3^-$  from the shallowest samples are too high to be attributed to a natural source, such as rainwater, and fertilisers are probably responsible.

(4) The time difference between the oldest and youngest PFA in the Barlow ash mound was 3 years, but the concentrations and depth profiles of boreholes in the Barlow ash mound were relatively similar each other. It is thought that the infiltration rate is fast enough not to result in detectable differences over such a short time period.

(5) Meaford porewater, which was extracted from more weathered PFA than Drax PFA, had higher concentrations of Al and Si compared with Drax porewater whereas the concentration of  $\text{Al}_2\text{O}_3$  and  $\text{SiO}_2$  in the original PFA is

higher in the Drax ash than the Meaford ash. This trend appears to indicate more dissolution of PFA glass-forming elements in more weathered PFA. The depth trend of Al of the Meaford PFA also indicates reaction during weathering of the PFA glass-forming elements, which form the PFA matrix.

(6) When Drax porewater is compared with Meaford porewater, more soluble-surface enriched fractions appear to be involved with the dissolution of Drax PFA, whereas the elements from the Meaford ash are mainly from glass and mineral phases. B, one of the most mobile elements in PFA, seems to represent this trend. Depth trends in the porewaters of both sites are similar to each other and, the depth variation of the Meaford confirms the trend of the Barlow ash mound.

(7) Porewater in the PFA mounds show chemical evolution during weathering and its composition appears to keep changing as a function of time and depth. The concentrations of many elements, including some toxic trace elements, increase and this is likely to influence on groundwater composition, ultimately, as leachate is liberated from the ash mounds.

## Chapter 4

### Chemistry and Mineralogy of PFA and their changes during weathering

#### **4.1 Introduction**

The mineralogy and chemistry of Drax and Meaford PFA were determined primarily to characterise the mineralogical and chemical properties of these ashes and to compare the results with the composition of PFA described in previous studies. The samples studied include fresh and weathered Drax PFA and weathered Meaford PFA. In addition to this basic purpose, the PFA has been investigated for two important reasons: firstly, if changes in the porewater composition occur, as was demonstrated in Chapter 3, a suitable source, within the PFA, should be demonstrated; and secondly, solution from the PFA will cause detectable changes in solid PFA over a long period of time, which will be consistent with the changes in corresponding porewater composition. Solid, borehole, PFA samples were analysed to detect any such depth related trends and to compare with the depth profiles of the porewater. Porewater chemistry should reveal present day reactions whereas solid PFA will indicate the long term effects of the reactions.

In addition to the chemical changes, mineralogical changes may occur in solid PFA during weathering. PFA is largely composed of unstable aluminosilicate glass particles, and some proto-type clay minerals, such as allophane, may have formed. Allophane was reported by Warren and Dudas (1985), in weathered PFA subjected to artificial weathering in the laboratory. The clay minerals, if present, are of interest because they would provide information about the extent of particle weathering, and would also be

indicators of porewater composition, through a knowledge of the clay stability fields.

The location of the elements within PFA is the main factor controlling their leaching behaviour. Namely, surface-enriched fractions are readily available on contact with water, and will be more easily dissolved into solution than those trapped within the matrices of PFA particles. The inter-elemental relationships of weathered PFA may reveal information about elemental geochemical associations and the relationships of elements within the PFA.

The mineralogy of fresh and weathered Drax PFA, and Meaford PFA, was identified by X-ray diffraction and SEM, whereas the chemical composition of the PFA samples was determined by XRF. For some selected weathered PFA samples, clay size particles under 2  $\mu\text{m}$  were fractionated, to enhance the possibility of secondary clay minerals being detected. In addition to the investigation of PFA particle morphology using SEM, semi-quantitative analysis of selected weathered Drax PFA samples was conducted, using an energy dispersive X-ray system to compare the variation of composition of the particles as well as to detect any secondary mineral phases.

## **4.2 Mineralogy and chemistry of fresh PFA**

### **4.2.1 Mineralogy of fresh Drax PFA**

According to Simons and Jeffery (1960), British PFA contains between 50 and 90% glass and also minerals consisting of quartz (1-6.5%), mullite (9-35%) and magnetite/hematite (up to 5%). In the X-ray diffraction traces of the PFA samples from Barlow the minerals recorded are: quartz, mullite, magnetite, and hematite. No significant differences were marked between weathered and fresh Drax PFA (Figure 4.1). The predominance of an amorphous glass phase in PFA is shown by the characteristic amorphous bulge between  $10^\circ$  and  $40^\circ 2\theta$ .

In addition to the spherical glass particles, big irregular amorphous components were also identified by SEM (Plate 4.2).

#### ***4.2.1.1 Quartz***

Quartz mainly occurs as discrete grains, the morphology of which suggests partial melting during combustion (Plate 4.2(c)). Quartz also occurs as large particles within PFA glass spheres, which were observed after removing the glass fractions surrounding the particles (Hulett and Weinberger, 1980).

#### ***4.2.1.2 Iron oxides***

Iron oxides, such as magnetite and hematite, were identified from XRD traces, as shown in Figure 4.1. In the SEM, iron-rich phases appear as dendritic structures on the surfaces of PFA particles (Plate 4.2 (d)).

#### ***4.2.1.3 Mullite***

Although mullite was identified by XRD, no direct observation was made by SEM. Mullite was only observed after dissolving the silica-rich exterior surfaces of PFA particles using HF, and the mullite within the particles mainly occurred in an aggregate or acicular form (Hulett *et al.*, 1980; Mattigod, 1982).

#### ***4.2.1.4 The amorphous components***

Glassy spheres are volumetrically predominant among all PFA solid phases. The glass spheres show a wide size range, from sub-micron to as much as 1 mm. The particle morphology is typically solid spheres but some glass spheres are entrapped within big particles (plerospheres) and some particles show hollows on their surfaces (cenosphere) (Plate 4.2 (a), (b)). Amorphous glass particles are largely divided into two different phases, namely: an Al-Si-rich

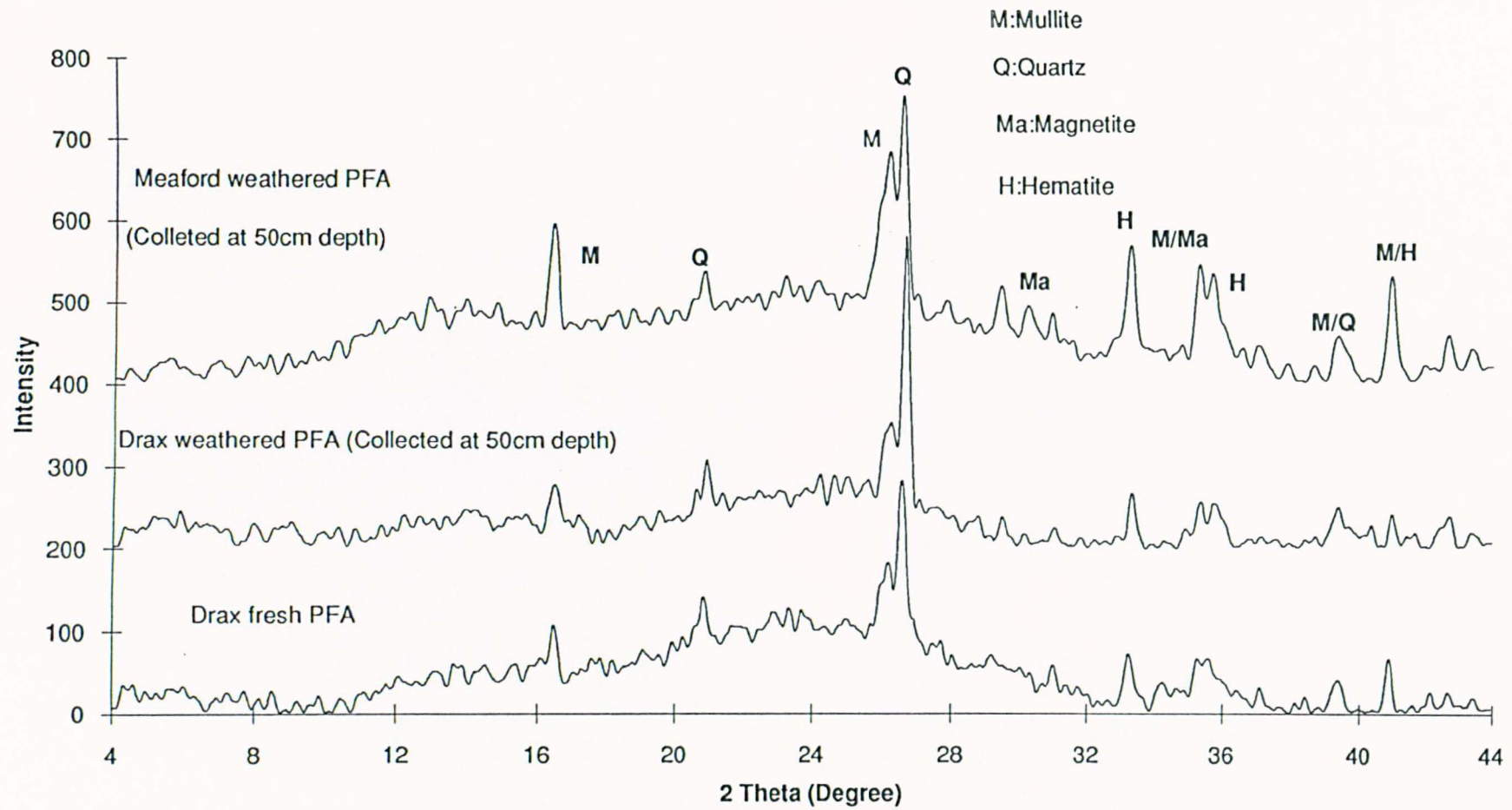
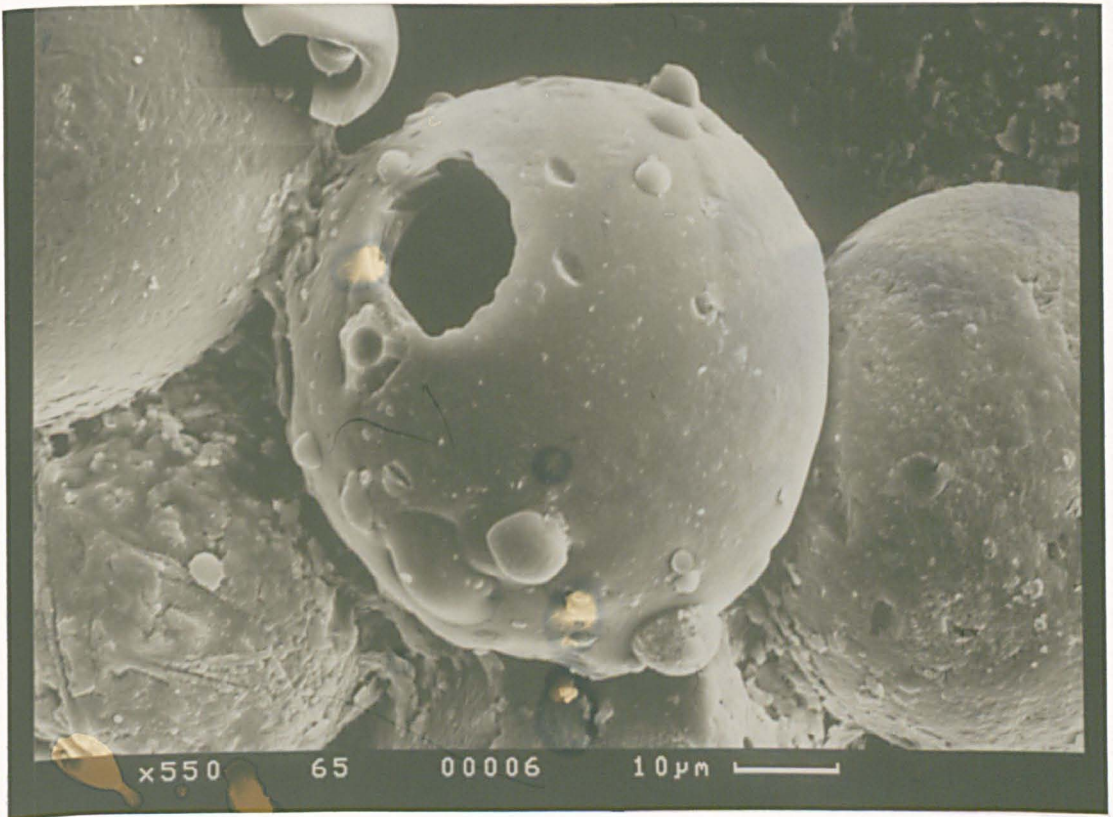
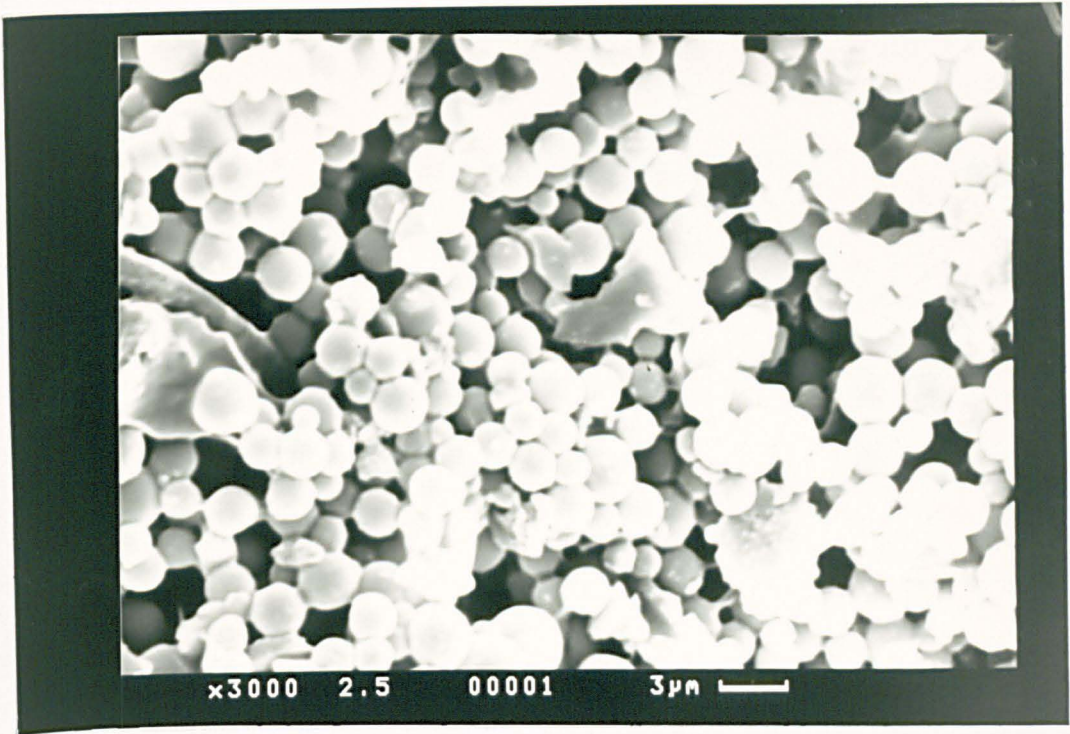


**Figure 4.1 X-ray diffractogram of whole Drax and Meaford PFA**

**(a) Typical morphology of fresh PFA particles: characteristically composed of spherical particles.**

**(b) Typical morphology of large fresh PFA particle: some large PFA particles show hollows on their surfaces (cenospheres). Sometimes the particles are filled with smaller PFA particles (plerospheres) and often smaller particles are attached on the surface of the large PFA particles**

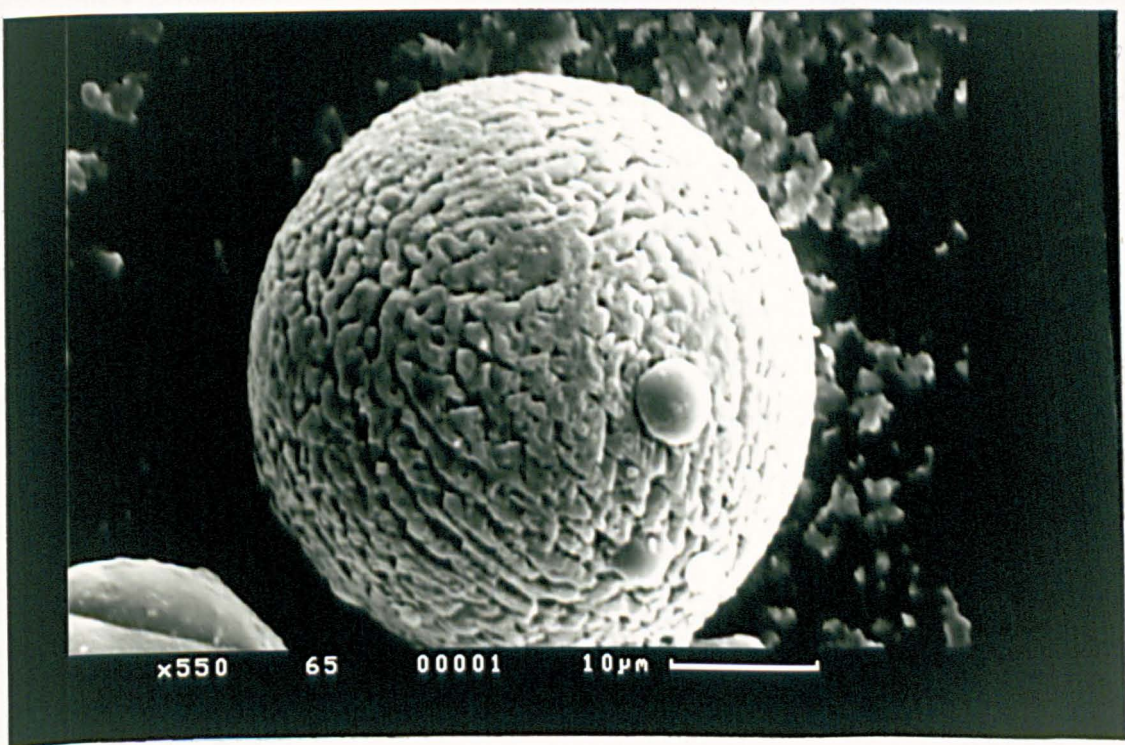
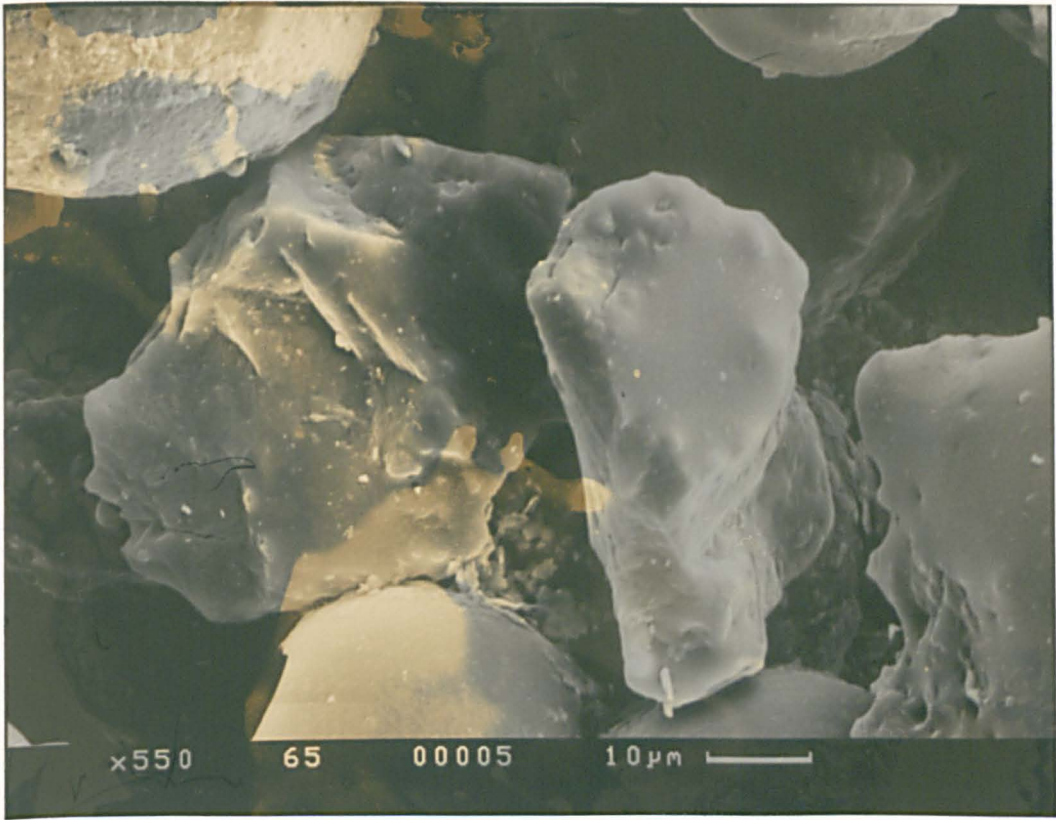


**(c) Partially melted quartz, a result of high temperature combustion**

**(d) Iron-rich phases showing characteristic dendritic textures on their surfaces**

**Plate 4.2 SEM photographs of fresh Drax PFA**

plant  
the  
4.2  
Chloro  
faint  
faint  
faint  
faint  
faint  
faint



phase and an iron-rich phase. The iron-rich phase has dendritic structures on the surfaces of particles.

#### 4.2.2 Chemistry of fresh Drax PFA

Chemical analyses of fresh Drax PFA samples are shown in Table 4.1. The feed coal burnt in Drax Power Station is supplied by a local colliery. Although only three samples were analysed, they show little variation between the samples, in spite of the time gap between collections, which the samples have been collected over two years, from the temporary PFA yard. The composition of PFA from Drax Power Station is similar to the average chemical composition of PFA from other UK coal-fired stations, with slightly lower contents of  $\text{Fe}_2\text{O}_3$ , and higher  $\text{SiO}_2$  (Data from National Power). According to the classification scheme of Roy and Griffin (1982), all the samples, including fresh and weathered Drax PFA and Meaford weathered PFA, fall in the alkaline modic group (Figure 4.3). This classification is mainly based on the major element chemistry and pH. The modic group is defined as PFA that is predominantly composed of  $\text{SiO}_2 + \text{Al}_2\text{O}_3 + \text{TiO}_2$ , with smaller proportions of iron, sulphur, and alkalis, including Ca, Mg, Na and K.

Table 4.1 shows the average chemical composition of fresh and weathered Drax PFA. In fresh Drax PFA, the proportion of  $\text{Al}_2\text{O}_3$  and  $\text{SiO}_2$  accounts more than 70% of the whole. Fresh Drax PFA is alkaline, with pH values between 9.5 and 10.0. The proportion of  $\text{K}_2\text{O}$  is relatively high and this suggests that the parent clay mineral was illite rather than kaolinite. Iron is mainly in an oxidised form,  $\text{Fe}_2\text{O}_3$ , with only a small proportion of FeO being present. This is probably due to the oxidation of iron during combustion. The chemical composition of Drax fresh PFA was compared with the average composition of crust material. PFA is enriched for most of the trace elements, including V, Cr, Ni, Cu, Zn, Ba and Pb.

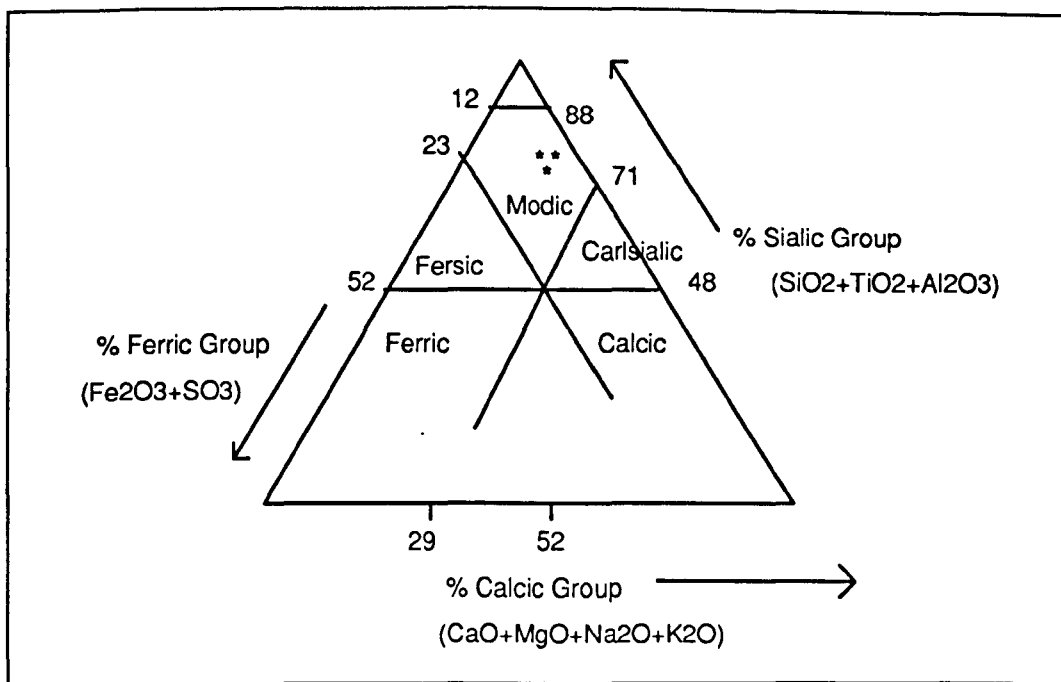


**Figure 4.3 Classification of PFA used in this study, after the scheme of Roy and Griffin (1982) (\* Drax fresh PFA)**

#### 4.2.3 Comparison between fresh and weathered Drax PFA

There are no substantial differences in chemical composition between the fresh and weathered PFA despite the fact that the latter has been subjected to weathering for 16 years. Comparison with the composition of fresh PFA could be misleading, if there had been changes in the supply of coal to Drax in the period covered. Major changes have not taken place and this is also borne out by the overall similarity between the composition of fresh and weathered PFA.

However, this is not to say that there are no minor changes due to weathering. The concentrations of CaO, MgO, Na<sub>2</sub>O and SO<sub>3</sub> are lower in weathered PFA compared with fresh PFA, whereas K<sub>2</sub>O and Al<sub>2</sub>O<sub>3</sub> show similar values in the two ashes. FeO is expected to have been oxidised during weathering and to occur predominantly as the oxidised form, Fe<sub>2</sub>O<sub>3</sub>, in weathered ash. However, the change in the chemical form of iron, due to weathering, was smaller than expected. The ratio of FeO to total Fe<sub>2</sub>O<sub>3</sub>

[FeO/(FeO+Fe<sub>2</sub>O<sub>3</sub>)] was 0.342 and 0.326 in fresh and weathered ash respectively, a difference of about 5 %. The oldest ash investigated in this study was deposited 16 years ago, yet little oxidation of iron has occurred in this time.

%	SiO <sub>2</sub>	TiO <sub>2</sub>	Al <sub>2</sub> O <sub>3</sub>	FeO	Fe <sub>2</sub> O <sub>3</sub>	MgO	CaO	Na <sub>2</sub> O	K <sub>2</sub> O	P <sub>2</sub> O <sub>5</sub>	SO <sub>3</sub>	L.O.I	pH
	<i>Fresh PFA</i> (No. of samples=3)												
Mean	53.43	0.95	25.89	1.09	4.98	1.73	1.90	1.56	3.75	0.21	0.35	2.26	9.8
SD	0.64	0.006	0.66	0.07	0.20	0.09	0.19	0.16	0.17	0.024	0.11	1.17	0.4
	<i>Weathered PFA</i>												
Mean	50.74	0.89	25.90	1.31	6.74	1.48	1.39	1.02	3.71	0.19	0.18	4.70	8.0
SD	1.11	0.02	0.53	0.07	0.31	0.15	0.17	0.13	0.07	0.002	0.14	1.12	0.2
No.	55	55	55	15	15	55	55	55	55	55	55	55	15
Crust*	59.3	0.9	15.8	4.4	2.6	0.2	4.0	7.2	3.0	2.4	0.35		
ppm	V	Cr	Mn	Ni	Cu	Zn	Rb	Sr	Y	Zr	Nb	Ba	Pb
	<i>Fresh PFA</i> (No. of samples=3)												
Mean	255	137	504	113	142	116	165	293	50	195	20	1063	75
SD	14.6	10.2	27.0	11.5	16.9	6.0	13.9	19.6	2.3	4.4	0.1	154.4	9.7
	<i>Weathered PFA</i>												
Mean	276	140	465	114	176	112	165	248	54	185	17	763	77
SD	20.4	7.9	36.7	7.9	22.9	21.0	4.4	15.8	2.7	6.5	1.5	30.5	13.4
No.	55	55	55	55	55	55	55	55	55	55	55	55	55
Crust*	135	100	950	75	55	70	90	375	33	165	20	425	13

**Table 4.1** Chemical composition of fresh Drax PFA, compared to: weathered PFA and average crustal composition (\* adapted from Mason and Moore (1982), pH: no unit)

## 4.3 Chemical changes in Drax PFA during weathering

### 4.3.1 Depth profiles of major elements

Depth profiles of elemental composition of Drax PFA were investigated to detect any depth-related trends. Depth variations of the major elements in borehole samples of PFA are shown in Figure 4.4. However, the proportionate

amount of individual elements leached from PFA during weathering is very small, and therefore the depth variation in PFA induced by weathering was not that clearly detected.

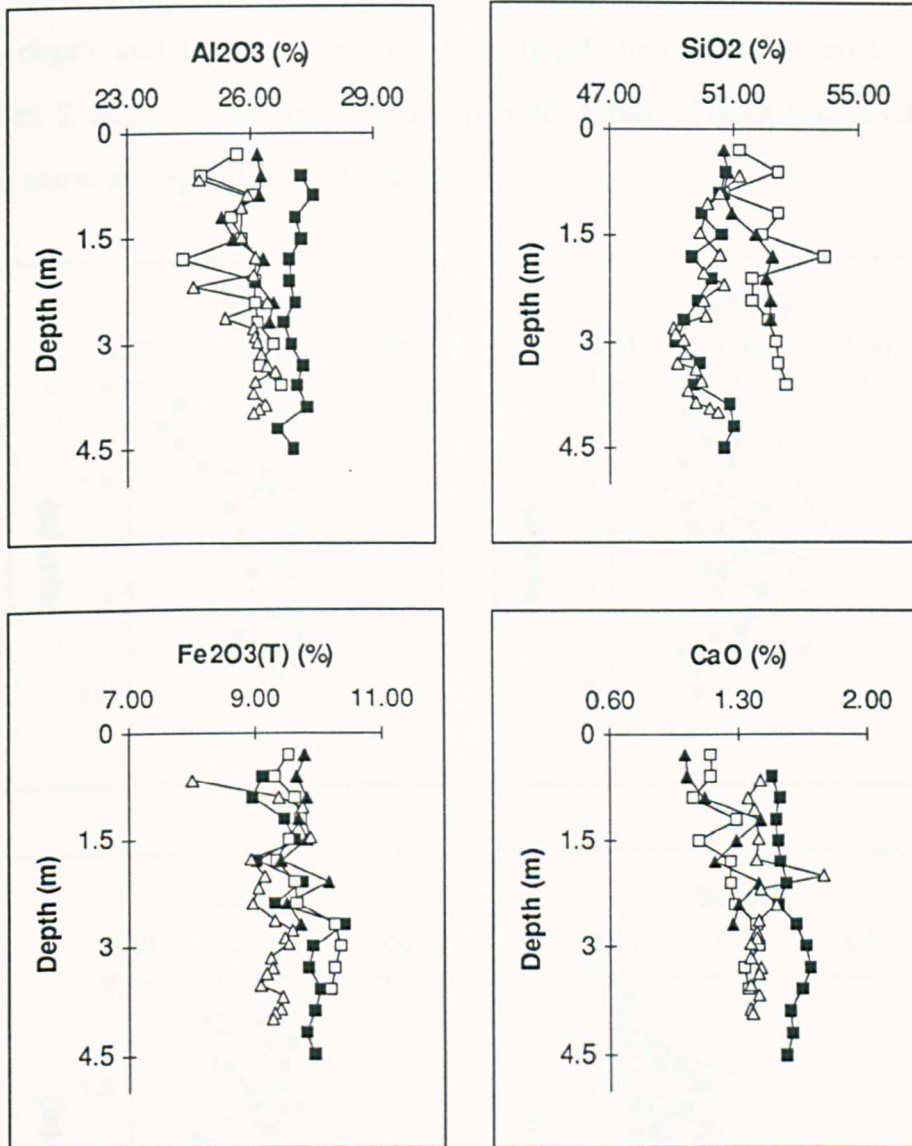


**Figure 4.4** Depth profiles of major elements in weathered PFA, Barlow (■: borehole 1, □: borehole 2, black triangle : borehole 3, open triangle: borehole 4) (continued-)

The concentrations of Al<sub>2</sub>O<sub>3</sub>, Fe<sub>2</sub>O<sub>3</sub>, MgO and SO<sub>3</sub> would generally appear to increase with depth. The concentration of SO<sub>3</sub> shows the most distinctive trend of all, along with the concentration of MgO in borehole 1. Sulphur is known to be located predominantly on the surfaces of PFA particles

(Hansen and Fisher, 1980), and this makes it readily leachable on contact with water. The concentration of CaO also appears to increase with depth in boreholes 2 and 3, whereas in boreholes 1 and 4 CaO seems to be constant with depth. The concentration of SiO<sub>2</sub> in boreholes 1 and 4 shows a decrease to a certain depth and then an increase with depth thereafter, whereas SiO<sub>2</sub> in boreholes 2 and 3 is relatively constant with depth. Na<sub>2</sub>O and K<sub>2</sub>O do not seem to show any specific depth trends.

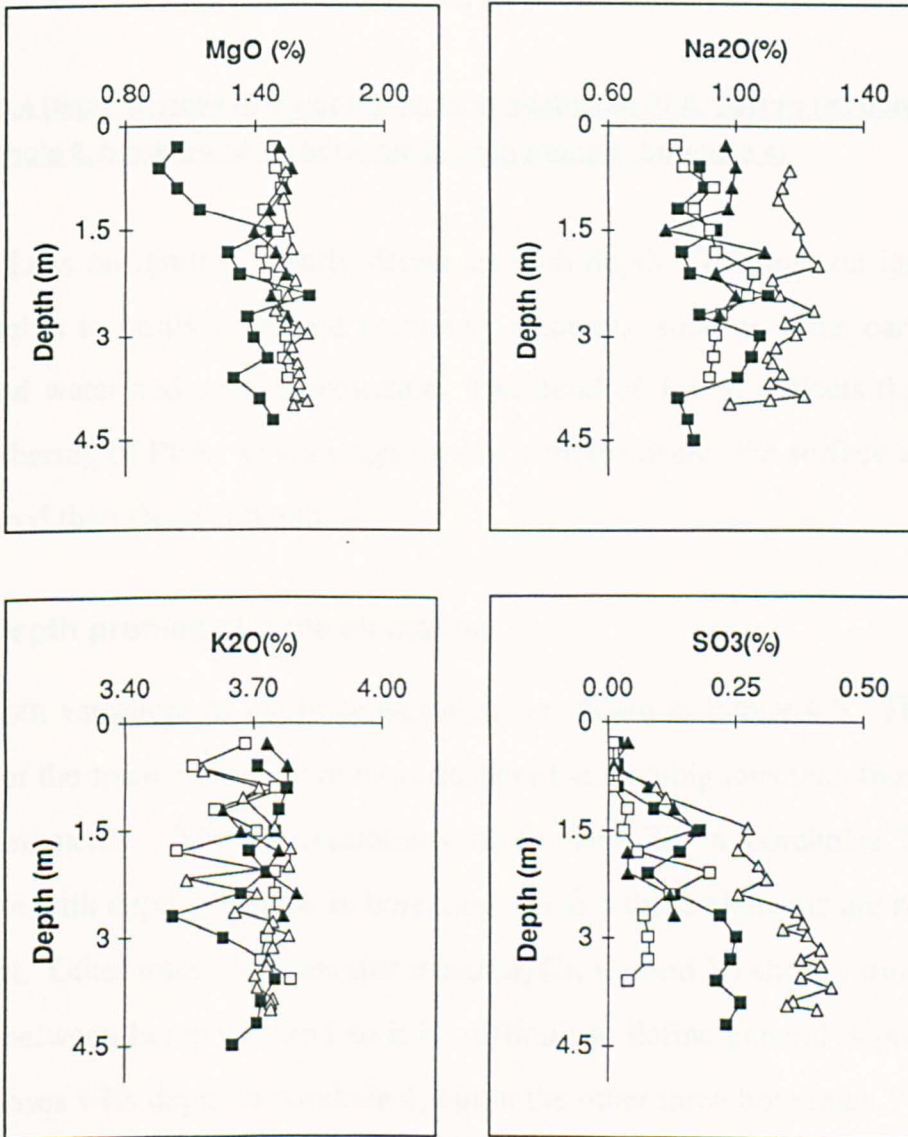


**Figure 4.4** Depth profiles of major elements in weathered PFA, Barlow (■: borehole 1, □: borehole 2, black triangle : borehole 3, open triangle: borehole 4) (continued-)

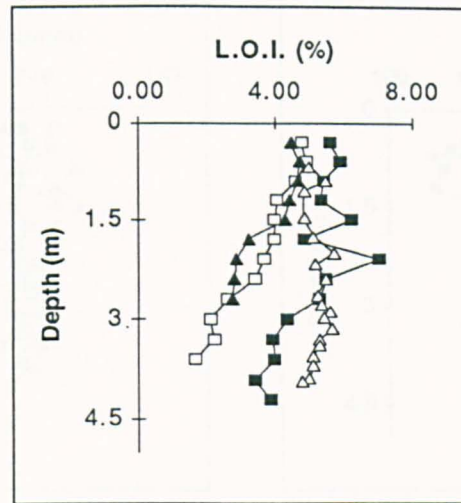


**Figure 4.4** Depth profiles of major elements in weathered PFA, Barlow (■: borehole 1, □: borehole 2, black triangle : borehole 3, open triangle: borehole 4)

'Loss on ignition' clearly decreases with depth. The loss on ignition is attributable to easily dissolved secondary minerals, such as some carbonates, absorbed water and organic materials. The trend of 'L.O.I.' reflects the degree of weathering of PFA, which suggests that samples nearer the surface are more weathered than those at depth.

#### 4.3.2 Depth profiles of trace elements

The depth variations of the trace elements are shown in Figure 4.5. The depth trends of the trace elements are more scattered and ambiguous than those of the major elements. The concentrations of Pb and Zn in boreholes 2 and 3 decrease with depth, whereas in boreholes 1 and 4 these elements are relatively constant. Other trace elements (for instance, Cr, Cu and V) show various depth trends between boreholes, and so it is difficult to define general depth trends. V increases with depth in borehole 4, but in the other three boreholes V appears to decrease with depth. The concentrations of Ba, Sr and Ni seem to be rather constant, in general.

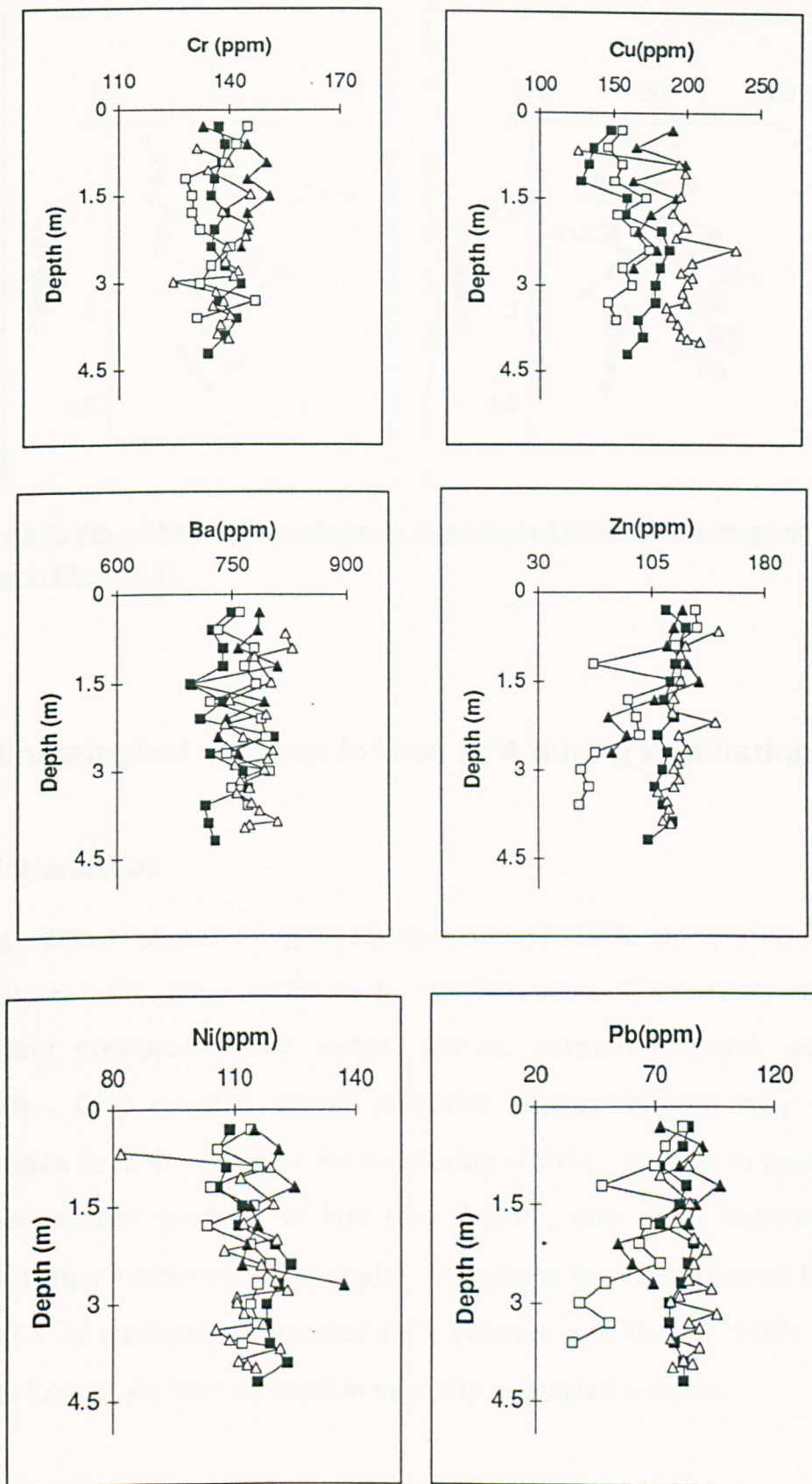


**Figure 4.5** Depth profiles of trace elements in weathered PFA, Barlow (Symbols are the same as in Figure 4.4 (Continued-))

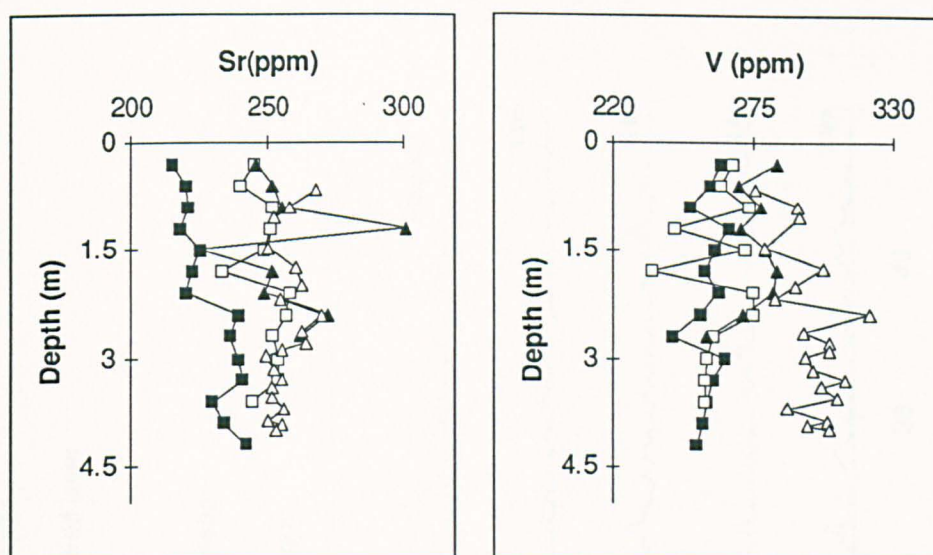


**Figure 4.5** Depth profiles of trace elements in weathered PFA, Barlow (Symbols are the same as in Figure 4.4)

## 4.4 Mineralogical changes in Drax PFA during weathering

### 4.4.1 Introduction

During weathering, mineralogical changes occur in PFA, along with chemical changes, and this may be shown by the formation of secondary minerals. Secondary precipitates may include calcite, calcium sulphate, and clay minerals. Clay minerals are of particular interest, because they provide information as to the extent of the weathering of PFA. In order to concentrate possible reaction products of less than  $2\ \mu\text{m}$ , clay sized fractions were obtained from weathered PFA samples. Allophane has been detected by XRD and DTA in artificially weathered PFA (Warren and Dudas, 1985) but the mineral has not yet been reported in naturally weathered samples.

### 4.4.2 XRD investigation of clay fractionated samples

A number of clay minerals were detected, which would not be anticipated if these were reaction products. Clay fractions were separated from top soil, and

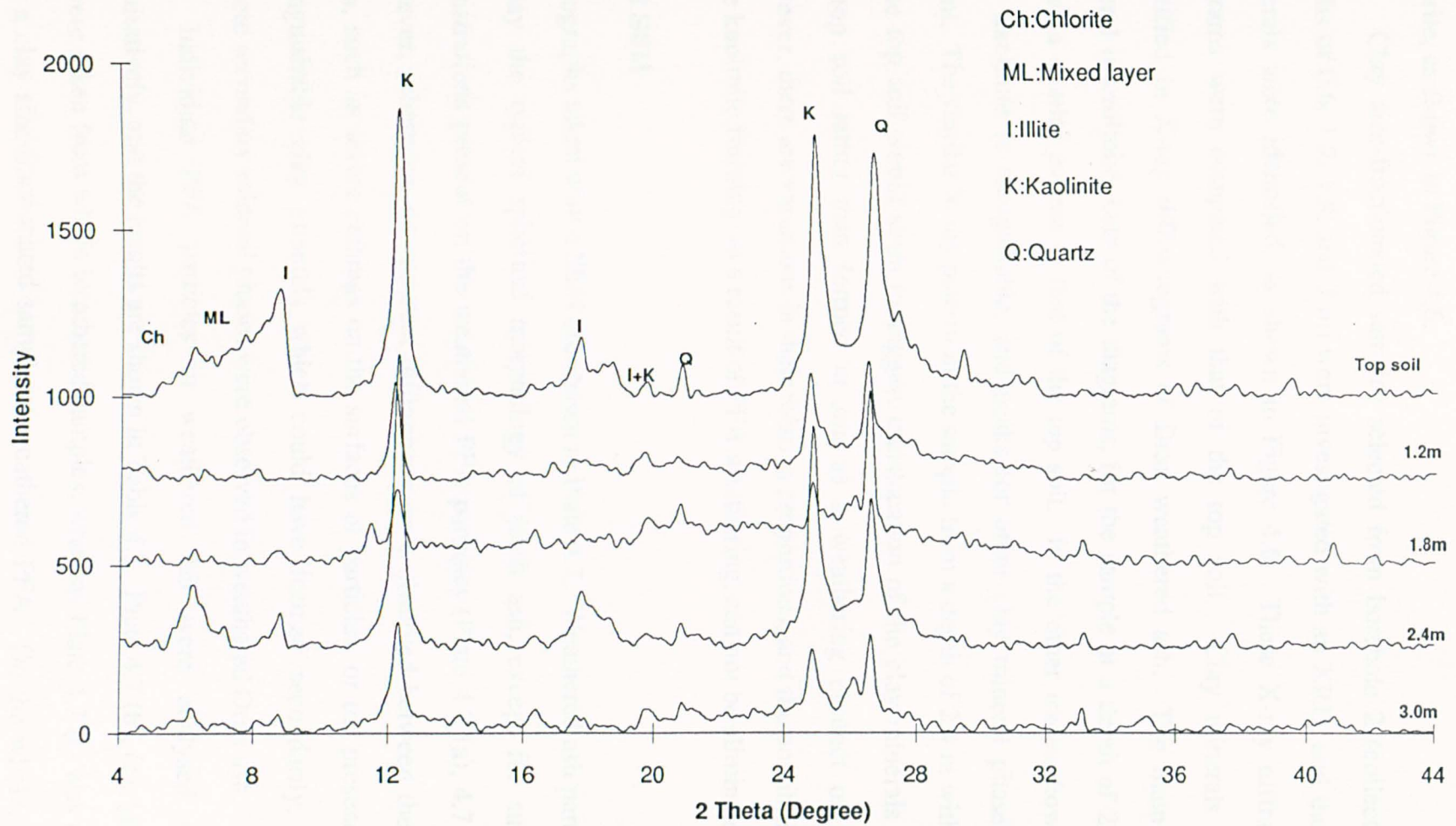


**Figure 4.6 X-ray diffractogram of clay-fractionated samples from Drax borehole 2**

the minerals identified were: quartz, kaolinite, illite, mixed-layer clay and chlorite, as shown in Figure 4.6.

Clay size-fractionated samples selected from borehole 2 (collected at depths of 0.6, 1.2, 1.8, and 3 m) were investigated with an XRD, and the clay minerals were identified, as shown in Figure 4.6. These X-ray diffraction diagrams were compared with that of the top soil. Clay minerals were identified in X-ray diffractograms of Drax weathered ash. The main clay mineral is kaolinite. One of the diagrams, for the sample at a depth of 2.4 m, shows a similar pattern to that of the top soil. In the other traces, however, only kaolinite is recognisable, and peaks for other clay mineral phases are absent. The similar X-ray pattern in the sample from a depth of 2.4 m with that of the top soil would seem to suggest translocation of the clay minerals from the top soil rather than formed *in situ* as a weathering product of PFA. However, there are variations in their relative proportions, and the possibility of some kaolinite forming, as a result of PFA weathering, can not be eliminated.

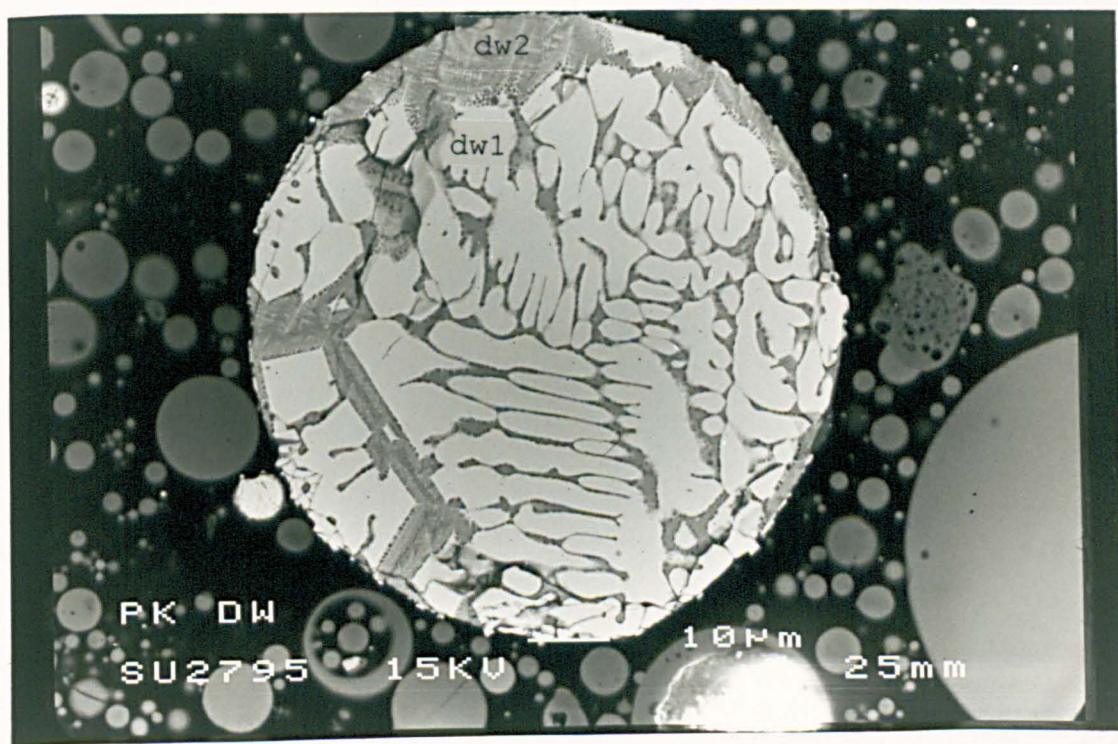
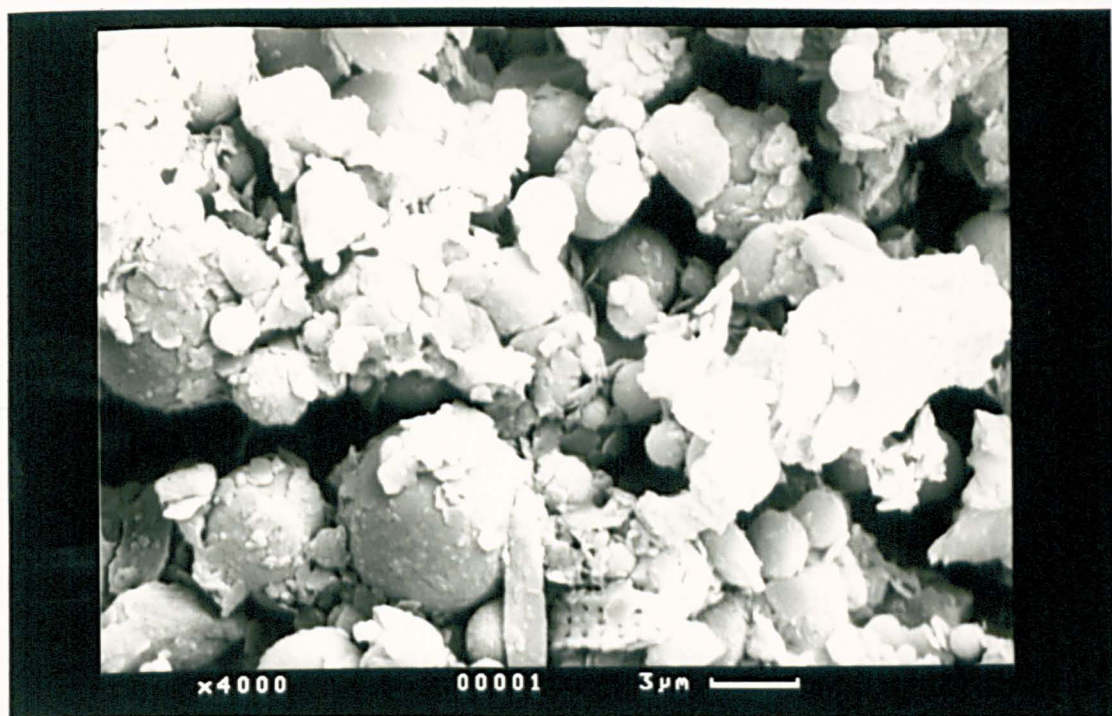
#### 4.4.3 SEM

Photographs taken with a SEM are shown in Plate 4.7. Weathered ash particles display the typical spherical morphology of fresh ash, except for surface encrustations present on the weathered PFA particles (Plate 4.2 (a), 4.7 (a)). However, otherwise, no apparent differences were observed between the two ashes, such as severe etchings on the surfaces of particles, or the presence of distinguishable clay minerals which could have formed secondarily. No discrete secondary mineral phases were observed in weathered Drax ash.

Individual PFA particles in weathered ash were analysed semi-quantitatively, and the results are shown in Table 4.2. Plate 4.7 (b), (c), (d) and (e) were taken from whole weathered samples, whereas Plate 4.7 (f) was taken from a clay size-fractionated sample of weathered PFA. On the whole, there are two different types of particle: one is Si-rich and the other is iron-rich.

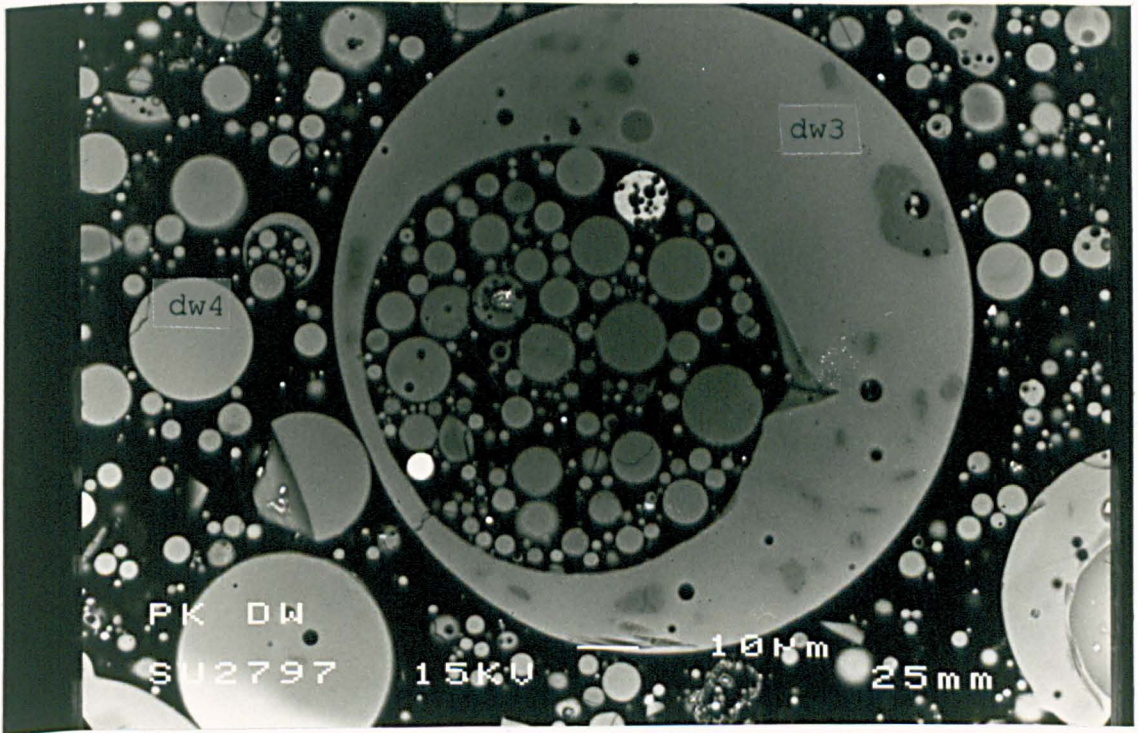
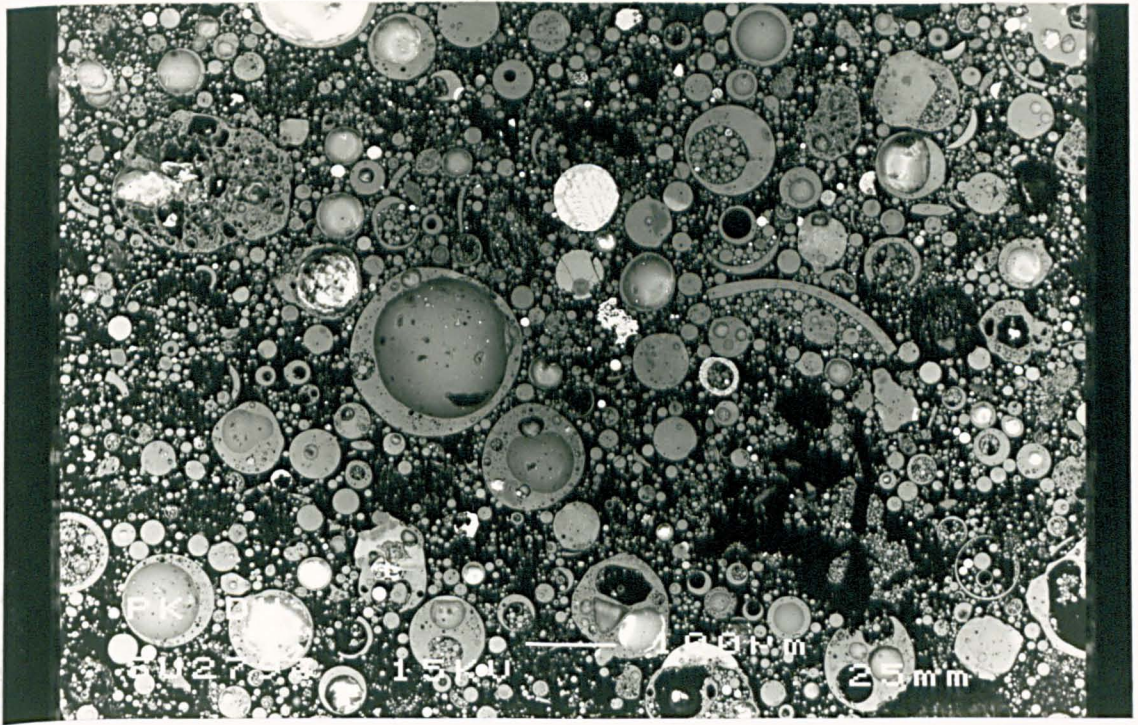
**(a) General morphology of weathered PFA : encrusted and porous weathering products occur on the surface of weathered PFA particles**

**(b) Iron-rich particle showing dendritic structures. The darker area is Si-rich (dw2), whereas the brighter area represents an iron-rich phase (dw1)**



**(c) Back scatter image of weathered Drax PFA showing typical spherical morphology**

**(d) Back scattered image of a large PFA glass particle (plerosphere), which contain smaller particles inside**



**(e) Weathered PFA particles showing SiO<sub>2</sub>-rich reaction rims**

**(f) Secondary image of clay-fractionated particles from weathered PFA**

**Plate 4.7 SEM photographs of weathered Drax PFA**

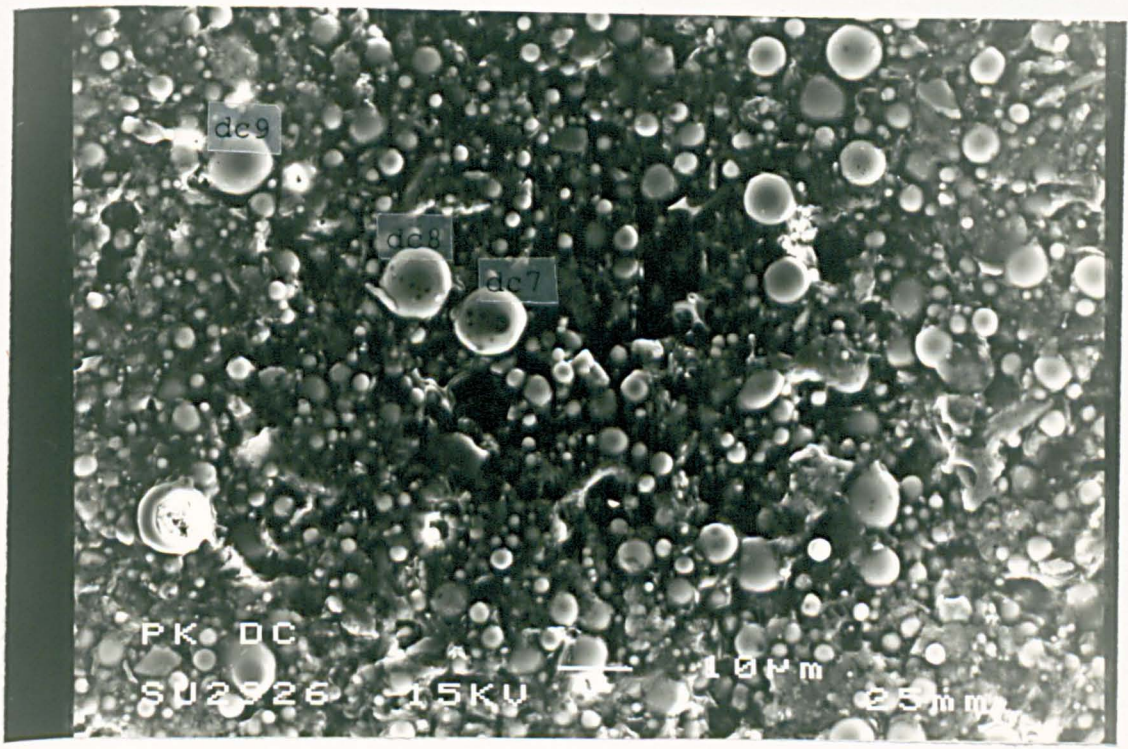
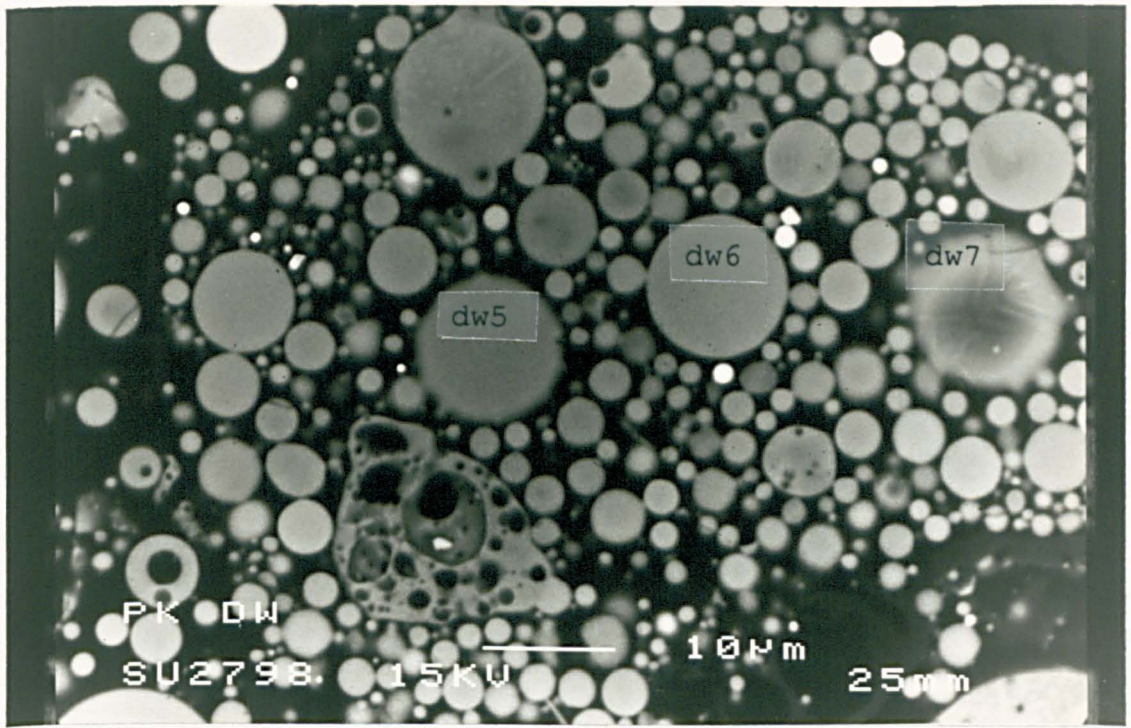


Plate 4.7 (b) shows typical iron-rich particles, interlaced with darker, Si-rich phases. The brighter areas are entirely composed of iron oxide, as indicated in Table 4.2. Iron oxide is discriminated by its brightness in back scatter images. In Plate 4.7 (c), (d) and aluminosilicate PFA glass particles show typical spherical form. Particles may be solid, hollow, or contain entrapped smaller particles. The average composition of weathered PFA glass particles is similar to that of PFA as a whole, but with less CaO. In Plate 4.7 (e), the analysed particle has a high concentration of SiO<sub>2</sub> in the outer rim. This may be a silicon gel, which resulted from the reaction of the particle with porewater. The structure within the sphere is thought to be mullite, embedded in aluminosilicate glass. The mullite could only be observed as a result of the partial dissolution of the Si-rich exterior shell of the particle, using HF (Hulett and Weinberger, 1980; Hulett and Weinberger *et al.*, 1980).

Sample	SiO <sub>2</sub>	TiO <sub>2</sub>	Al <sub>2</sub> O <sub>3</sub>	Fe <sub>2</sub> O <sub>3</sub> (T)	MgO	CaO	Na <sub>2</sub> O	K <sub>2</sub> O	total
dw1	0.19	-	2.25	99.27	0.27	-	-	-	99.27
dw2	30.77	0.77	5.93	55.43	0.23	0.37	-	0.38	93.86
dw3	48.42	1.28	26.07	5.50	1.06	0.33	0.95	4.18	87.77
dw4	44.62	1.24	28.11	8.00	1.00	0.27	0.49	3.13	86.87
dw5	46.66	0.73	25.52	4.90	1.24	0.37	1.04	4.24	84.69
dw6	46.69	1.29	23.19	7.01	2.41	2.23	0.46	3.32	86.60
dw7	87.74	-	1.11	0.23	-	0.10	-	0.45	89.64
dc7	53.07	1.01	34.53	4.16	1.44	0.31	0.42	5.06	100.00
dc8	52.88	1.09	34.94	4.24	1.49	0.55	0.59	4.23	100.00
dc9	53.58	1.34	25.49	10.11	1.79	1.63	0.52	4.49	100.00

**Table 4.2 Semi-quantitative analyses of weathered Drax PFA particles**

The chemistry of the particles in the clay-fractionated samples is similar to that of particles on the whole, weathered PFA samples, and no secondary clays were identified (Plate 4.7 (f)).

## 4.5 Weathered Meaford PFA

### 4.5.1 Introduction

Weathered Meaford PFA is older than weathered Drax PFA, and is thought to be more weathered than weathered Drax PFA. The weathered PFA at Meaford Power Station was deposited at least 20 years ago, and possibly as long ago as 40 years. Compared to the weathered Drax ash, weathered Meaford ash is lower in SiO<sub>2</sub> but higher in Fe<sub>2</sub>O<sub>3</sub>. The concentration of trace elements in PFA is generally higher in the weathered Meaford ash, especially Mn, Zn, Ba and Pb (Table 4.3). These differences between the weathered Drax and Meaford ashes are thought to reflect differences in the feed coal composition, as well as secondary changes during weathering.

%	SiO <sub>2</sub>	TiO <sub>2</sub>	Al <sub>2</sub> O <sub>3</sub>	Fe <sub>2</sub> O <sub>3</sub>	MgO	CaO	Na <sub>2</sub> O	K <sub>2</sub> O	P <sub>2</sub> O <sub>5</sub>	SO <sub>3</sub>	L.O.I	
Mean	42.91	0.81	24.93	13.14	1.42	3.13	0.67	2.12	0.36	0.24	9.89	
SD	1.37	0.01	0.55	0.66	0.06	0.14	0.05	0.07	0.07	0.10	1.36	
No.	8	8	8	8	8	8	8	8	8	8	8	
Drax	50.74	0.89	25.90	9.67	1.48	1.39	1.02	3.71	0.19	0.18	4.70	
ppm	V	Cr	Mn	Ni	Cu	Zn	Rb	Sr	Y	Zr	Ba	Pb
Mean	273	115	969	143	199	959	101	360	56	168	1245	239
SD	8.3	5.6	60.4	12.1	18.8	60.8	6.1	37.9	4.8	2.1	222.8	36.4
No.	8	8	8	8	8	8	8	8	8	8	8	8
Drax	276	140	465	114	176	112	165	248	54	185	763	77

**Table 4.3 Average chemical analysis of weathered Meaford PFA and comparison with weathered Drax PFA**

Current, unweathered Meaford ash samples are unavailable, so depth profiles were investigated using a borehole through ash of a constant age, to detect chemical changes during weathering. The depth trends of solid PFA are also compared to the corresponding porewater composition to deduce the

nature of the weathering reactions caused by infiltrating porewater. It was expected that the Meaford ash would be more weathered, and would show further changes in mineralogy and chemistry. The formation of secondary mineral phases is more likely in older ash.

#### 4.5.2 Depth profiles of Major elements in Meaford PFA

The depth profiles of weathered Meaford PFA were investigated to evaluate the changes in composition of more weathered PFA, and thereby to extend the results obtained from Drax PFA (Figure 4.8). Several elements show a depth-related variation, and the depth trends of Meaford PFA appear to be more distinct than those of weathered Drax PFA.

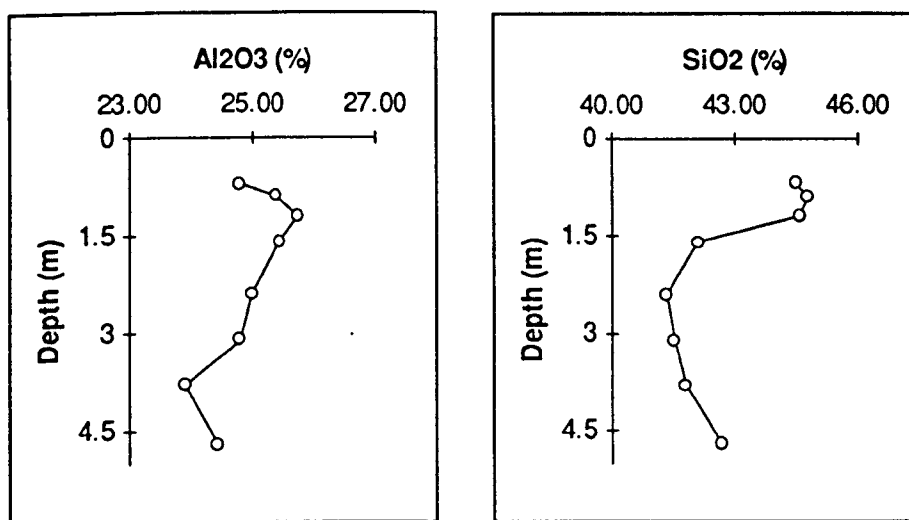


Figure 4.8 Depth profiles of the major elements in weathered Meaford PFA (Continued-  
1)

The major elements CaO, MgO, Fe<sub>2</sub>O<sub>3</sub> and SO<sub>3</sub> are depleted at shallow depths, but their concentrations increase with depth. Al<sub>2</sub>O<sub>3</sub> is depleted near to the surface, but its concentration decreases with depth, after attaining a maximum value at a depth of about 2 m. The concentrations of Na<sub>2</sub>O and K<sub>2</sub>O appear to decrease with depth, in general, but the concentrations become more constant at greater depths.

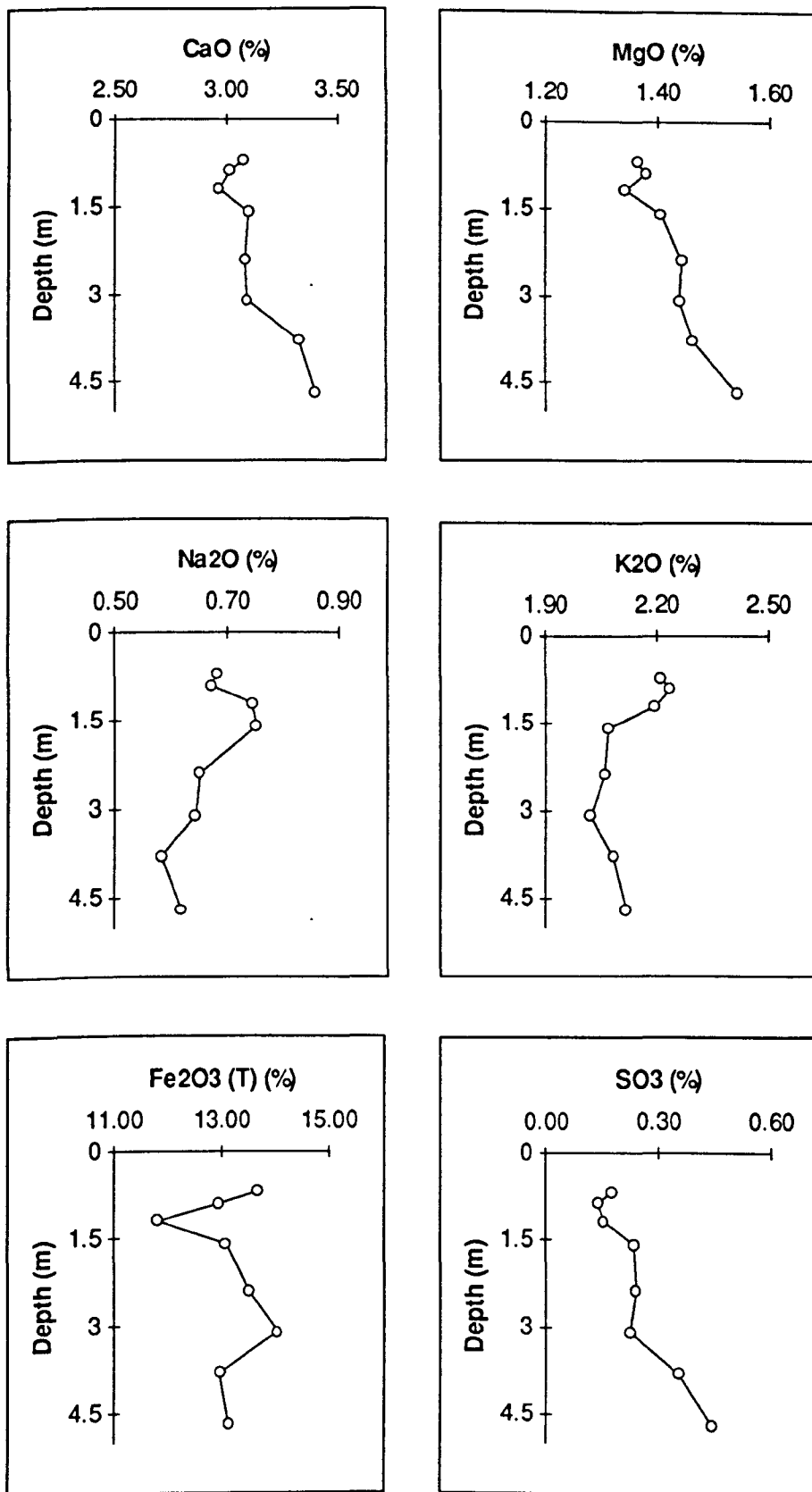
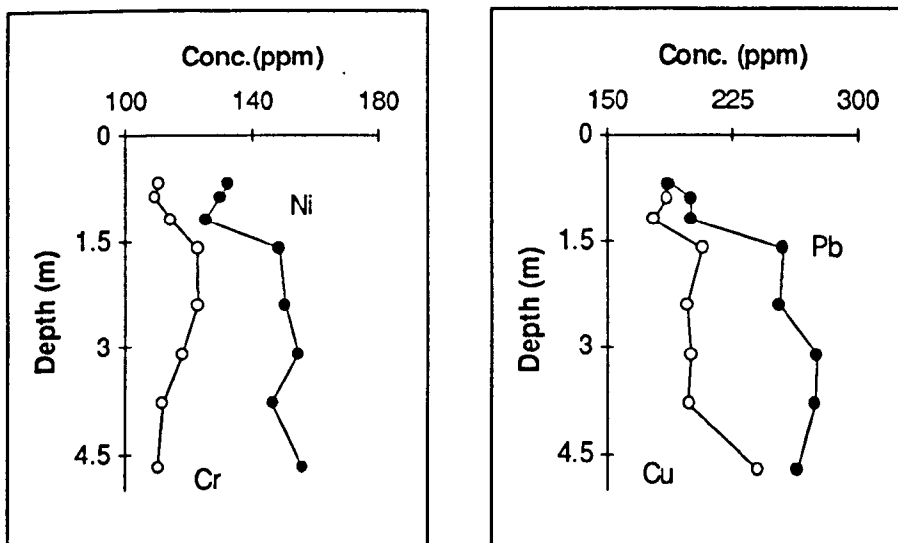


Figure 4.8 Depth profiles of the major elements in weathered Meaford PFA

The depth profiles of the major elements would seem to indicate loss of the elements from PFA during weathering. The depth profiles of CaO, MgO and SO<sub>3</sub> clearly illustrate this. Fe<sub>2</sub>O<sub>3</sub> also shows such a trend, except for some higher values for the two shallowest samples. The depth trend of Al<sub>2</sub>O<sub>3</sub> is similar to that of Na<sub>2</sub>O, whereas the trends of SiO<sub>2</sub> and K<sub>2</sub>O appear to be similar to each other.

#### 4.5.3 Depth profiles of trace elements in Meaford PFA

Nearly all the trace elements in weathered Meaford PFA show depth-related trends (Figure 4.9). The concentrations of Cu, Ni, Mn, Pb and Zn increase with depth, whereas the concentration of Cr decreases after attaining a maximum value at a depth of about 2 m. In the case of Mn, the highest values are shown by the two shallowest samples. The concentration of Ba also increases with depth and reaches a maximum value at a depth of about 3 m, and then decreases with further depth.



**Figure 4.9** Depth profiles of trace elements in weathered Meaford PFA (Continued-)

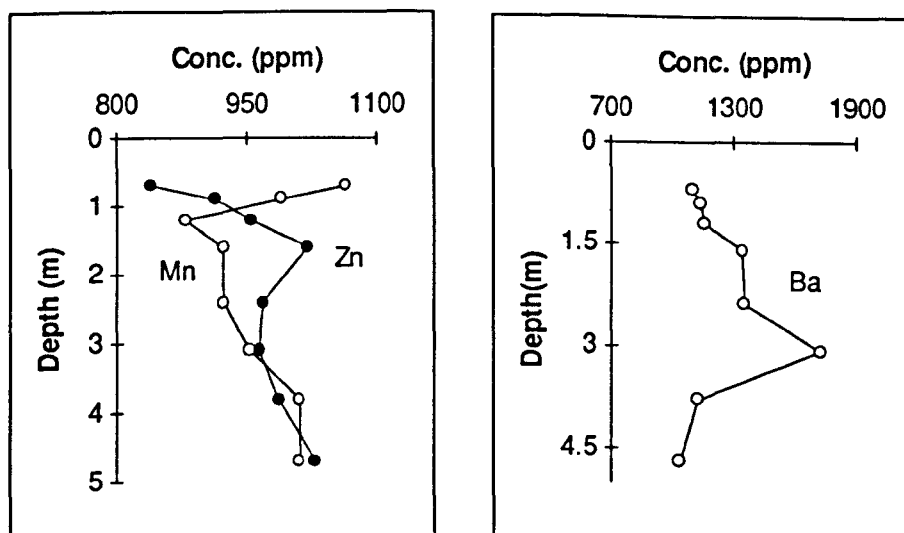


**Figure 4.9** Depth profiles of trace elements in weathered Meaford PFA

These depth trends indicate depletion reaction of the elements from PFA, which is more distinct in the samples of shallower depth. The depth trends of the trace elements in Meaford ash are more distinct compared those of Drax ash, which are thought as a result of more weathering during longer disposal.

#### 4.5.4 Mineralogy of Meaford PFA

##### 4.5.4.1 XRD

Weathered Meaford PFA samples taken from different depths in the borehole were compared to each other to detect mineralogical changes with various degrees of weathering. The X-ray diffractograms of weathered Meaford PFA samples were also compared with that of the top soil which covered the PFA (Figure 4.10).

Quartz, mullite and iron oxides are the main mineral phases in weathered Meaford PFA, and is therefore very similar to the mineralogy of weathered Drax PFA, as shown in Plate 4.2. The variation in the X-ray patterns of weathered Meaford PFA samples, with depth, is very small. The sample

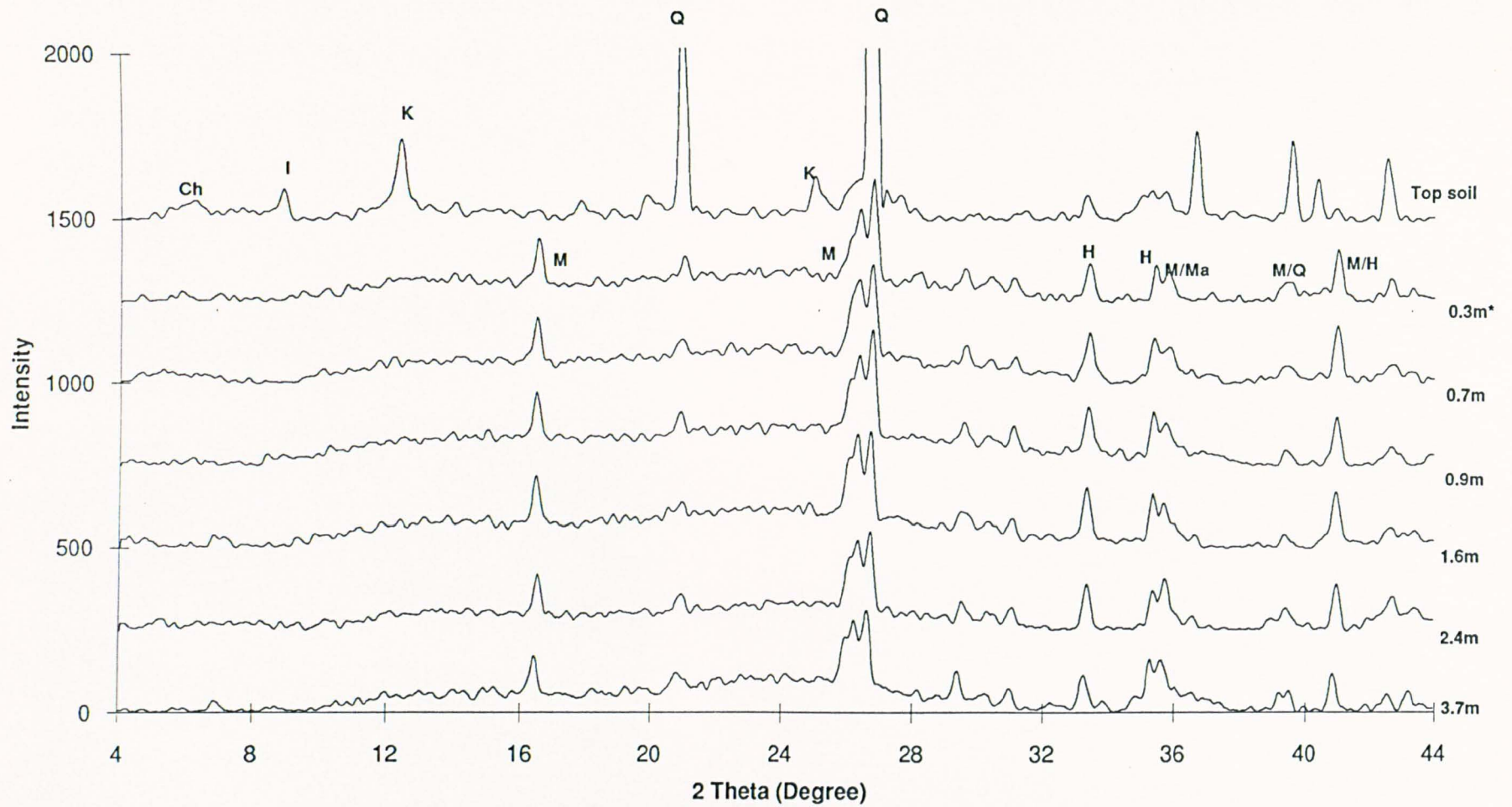
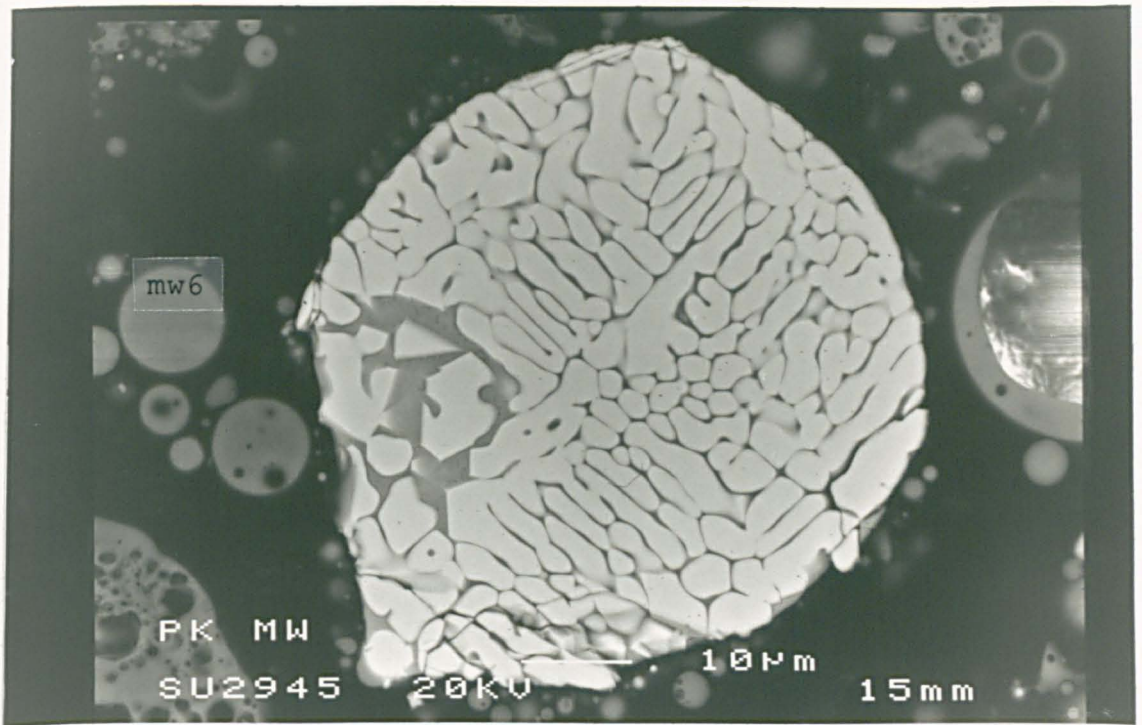


Figure 4.10 X-ray diffractogram of weathered Meaford PFA samples, collected at various depths (\*: clay fractionated sample)

**(a) Typical morphology of Meaford weathered PFA particles**

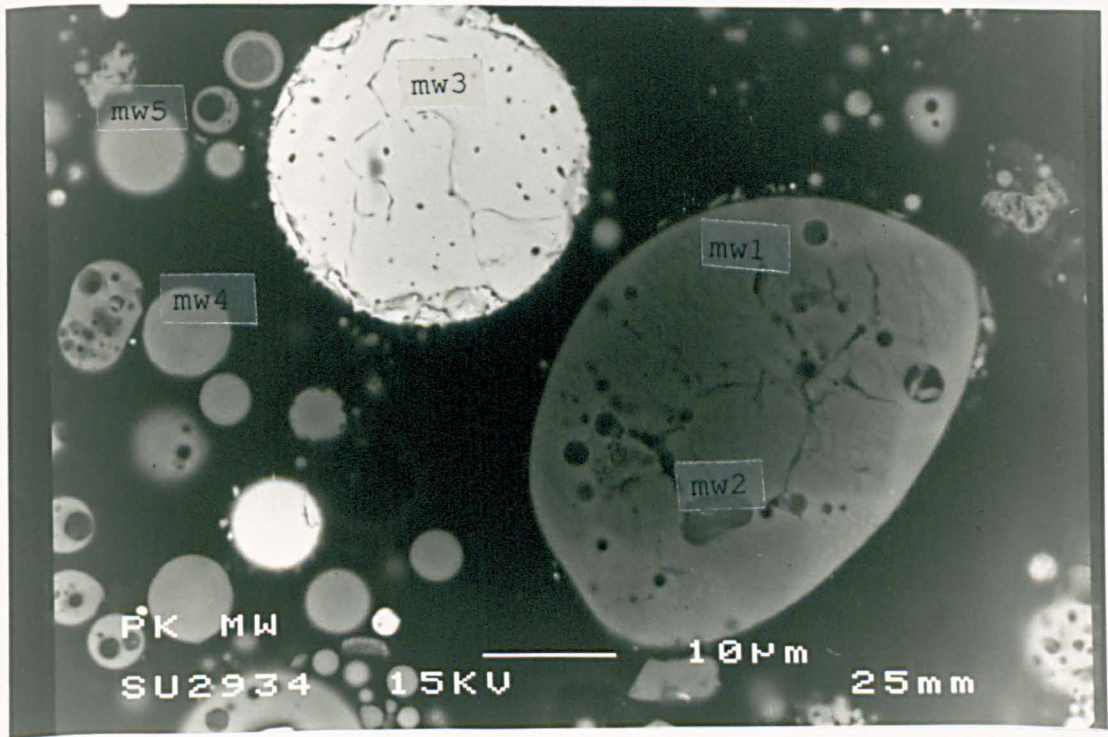
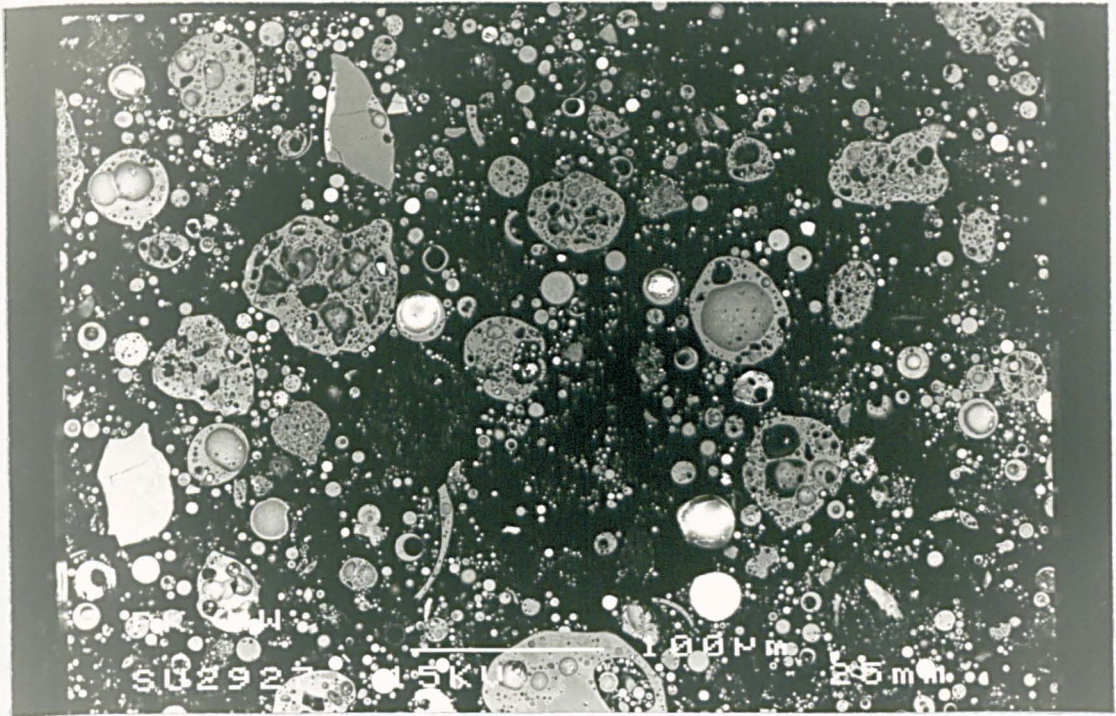
**(b) Spherical PFA particles in Meaford PFA: the darker is Si-rich and the brighter is iron-rich phase by semi-quantitative SEM analysis using JEOL JSM 6400**



**(c) Iron-rich particle, showing a dendritic structure**

**(d) Big particle of Meaford weathered PFA, containing various phases inside of the particle**

**Plate 4.11 SEM photographs of weathered Meaford PFA**



from a depth of 0.3 m is clay size-fractionated, but it does not show a different pattern to that of the unfractionated samples.

No evidence of the presence of secondary clay minerals was found from the X-ray diffractograms. The clay-fractionated sample collected from a depth of 0.3m did not give a different pattern, when compared to the other, unfractionated samples collected from a greater depth. In addition to this there is no sign of the clays present in the top soil being present.

#### 4.6.3.2 SEM

Meaford PFA appears to be generally less homogenous in morphology than Drax PFA, and contains a greater proportion of irregularly shaped, large particles. These irregularly shaped, large particles show vesicles within them (Plate 4.11).

Sample	SiO <sub>2</sub>	TiO <sub>2</sub>	Al <sub>2</sub> O <sub>3</sub>	Fe <sub>2</sub> O <sub>3</sub> (T)	MgO	CaO	Na <sub>2</sub> O	K <sub>2</sub> O	SO <sub>3</sub>	total
mw1	98.90	.	0.26	0.46	.	.	.	.	0.20	99.74
mw2	78.60	0.32	15.21	2.14	0.60	.	0.27	2.76	.	99.85
mw3	3.79	0.18	0.61	94.77	0.37	0.14	.	.	.	99.85
mw4	53.40	2.38	29.40	7.59	1.41	0.90	0.73	4.10	.	99.91
mw5	54.73	1.13	29.12	7.01	1.37	0.35	0.49	5.70	.	99.90
mw6	59.57	1.10	20.91	3.77	0.94	10.74	0.60	2.25	.	99.88

**Table 4.4 Semi-quantitative analyses of weathered Meaford PFA particles**

Chemical analyses of Meaford PFA particles, by SEM-EDX, are shown in Table 4.4. Mw 1 is thought to be an analysis of quartz. Mw 4, 5 and 6 are analyses of typical PFA particles, and they are similar to the composition of whole Meaford ash. Mw 3 is an analysis of an iron-rich, magnetic phase. The morphology of particles in Drax and Meaford ashes differ, but the chemical composition of typical PFA particles is relatively similar. No discrete secondary mineral phases were observed in the weathered Meaford PFA.

## 4.6 Geochemistry of PFA and its relationship to porewater composition

### 4.6.1 Geochemical associations in PFA

Certain elements are concentrated together with other elements within PFA glass or other specific locations within PFA. These geochemical associations influence the composition of the leachate that results from the weathering of the ash by infiltrating porewater.

As was mentioned earlier, PFA largely consists of aluminosilicate glass, minerals and sublimates. The aluminosilicate glass can be divided into two sub-parts: a Si-rich exterior glass and an interior, quartz-mullite phase (Hulett and Weinberger *et al.*, 1980; Dudas and Warren, 1987).

#### 4.6.1.1 $Al_2O_3$ vs. $K_2O$

$Al_2O_3$  and  $K_2O$  are strongly correlated ( $\sigma=0.85$ ), with a low intercept value (Figure 4.12). This relationship would seem to indicate a close association in one source. The major phase containing the  $Al_2O_3$  and  $K_2O$  is aluminosilicate. During the formation of PFA glass clay minerals are partially melted, fluxed by K, to produce an Al-Si glass (Hubbard and McGill *et al.*, 1984).

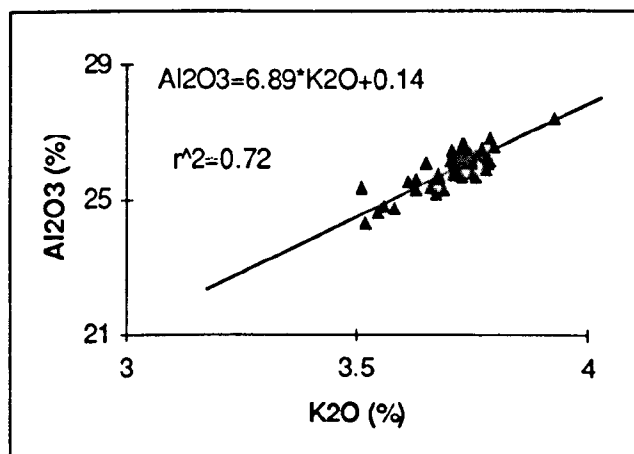
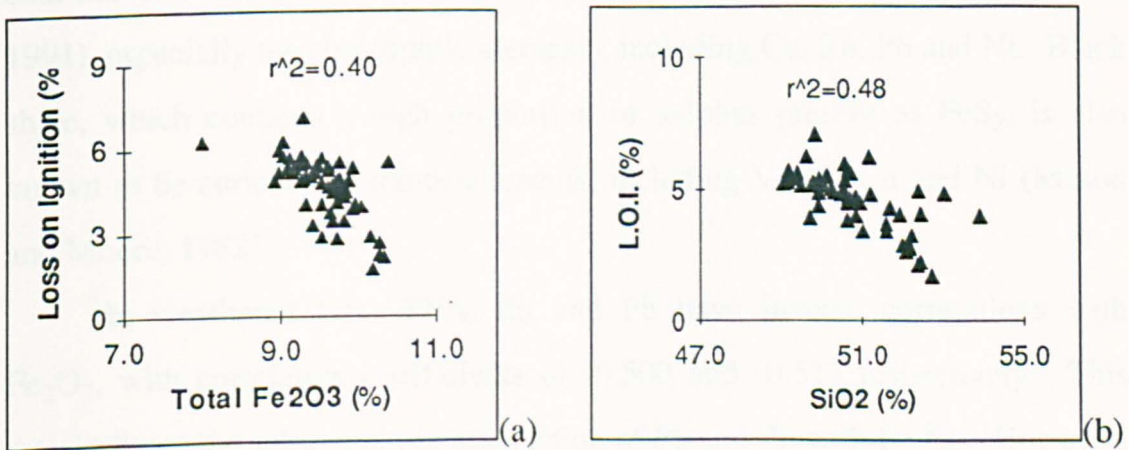


Figure 4.12  $Al_2O_3$  vs.  $K_2O$  in weathered Drax PFA

Investigation of the aluminosilicate glass, by etching the Si-rich exterior of the PFA particles with HF, revealed an interior structure to the PFA glass particles. This consisted of aggregates of acicular crystals of mullite, with an Si matrix (Hulett and Weinberger, 1980; Mattigod, 1982; Dudas and Warren, 1987). K is also associated with glass particle surfaces as well as the matrix, whereas Al is predominantly distributed in the quartz-mullite phase of the PFA glass (Hulett and Weinberger *et al.*, 1980). The strong association of the K with Al in the diagram indicates the K in the weathered ash is predominantly from the matrix with the Al in the weathered PFA. This relationship appears to indicate either the depletion of the surface associated K fraction or original variation of the surface enriched K in the PFA.

#### 4.6.1.2 $Fe_2O_3$ and $SiO_2$ vs. L.O.I.

$Fe_2O_3$  and  $SiO_2$  in Drax PFA boreholes showed increase with depth whereas 'loss on ignition' decrease with depth (Figure 4.4) and consequently the concentrations of the total  $Fe_2O_3$  and  $SiO_2$  respectively show a relatively strong inverse correlation with the L.O.I (Figure 4.13).



**Figure 4.13 Relationships between  $Fe_2O_3$  and  $SiO_2$  vs. L.O.I. in weathered Drax PFA**

An easily breakable secondary mineral, the organic material contained in PFA and adsorbed water are thought as the major contributor to L.O.I. The

content of organic material in the PFA mound is believed to be higher in the depth of near-surface because of a biological activity. The secondary weathering product is also believed to be higher in shallow depth, where more amounts of the elements in PFA were leached. The inverse relationships of  $\text{Fe}_2\text{O}_3$  and  $\text{SiO}_2$  with L.O.I. appear to indicate that the  $\text{Fe}_2\text{O}_3$  and  $\text{SiO}_2$  leached from the PFA glass are one of the main contributors to the easily breakable secondary products in weathered PFA.

#### 4.6.1.3 $\text{Fe}_2\text{O}_3$ and trace elements

PFA can be classified into three main phases: glass, mullite and iron-rich magnetic spinel; of these three phases, the iron-rich spinel is known to be enriched in many trace elements (Hulett and Weinberger *et al.*, 1980; Norton and Markuszewski *et al.*, 1986). The first row transition elements, Cr, Mn, Co, Ni, Zn and Cu have been reported to be more concentrated in the magnetic component of PFA, possibly in the form of magnetic spinels,  $\text{Fe}_{3-x}\text{M}_x\text{O}_4$  (Hulett and Weinberger *et al.*, 1980; Hulett and Weinberger, 1980). Pyrite is thought to be the main source for the iron and sulphur of PFA. Pyrite within coal has been recognised as a source of many trace elements in PFA (Spears, 1991), especially the chalcophile elements, including Cu, Zn, Pb and Ni. Black shale, which contains a high proportion of sulphur present as  $\text{FeS}_2$ , is also known to be enriched in minor elements, including V, As, Cu and Ni (Mason and Moore, 1982).

In weathered Drax PFA, Zn and Pb have inverse correlations with  $\text{Fe}_2\text{O}_3$ , with correlation coefficients of -0.500 and -0.517 respectively. This may indicate the solid-solution association of Pb and Zn with  $\text{Fe}_2\text{O}_3$ . However, no significant correlative relationships were found for the other trace elements. Trace elements are not associated specifically with one phase but are distributed between several phases in various proportions (Hansen and Fisher, 1980; Hulett and Weinberger *et al.*, 1980), therefore the relationship of those

elements located in more than one phase with other elements will be complicated.

#### 4.6.1.4 Pb vs. Zn

Pb and Zn have a correlative relationship to each other, as shown in Figure 4.14; this indicates that they have a close association in some common phase in Drax PFA. These two elements also decrease in concentration with depth, contrary to the general depth trend of other elements in Drax PFA, which increase with depth. Zn and Pb have negative correlations with  $\text{SiO}_2$ . The correlation coefficient values are -0.478 and -0.588 respectively.

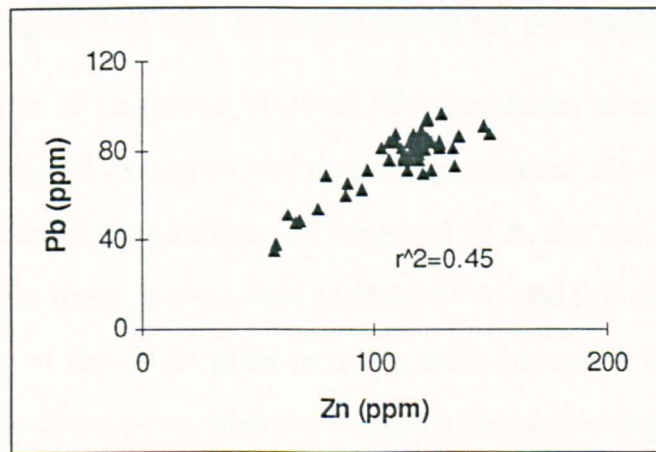


**Figure 4.14 Relationship between Zn and Pb in weathered Drax PFA**

They also show significant positive correlations with 'loss on ignition' (Figure 4.15). The negative correlations with  $\text{SiO}_2$  and positive correlations with L.O.I. would seem to indicate the relative increase of Pb and Zn as weathering progresses. These elements are known to be very immobile in nature and therefore their proportions in weathered PFA increase with respect to other more mobile elements as weathering progresses and the more mobile elements are leached away. Hence, at shallow depth, where weathering has been most intense, Pb and Zn have become enriched by virtue of the depletion of the other elements.

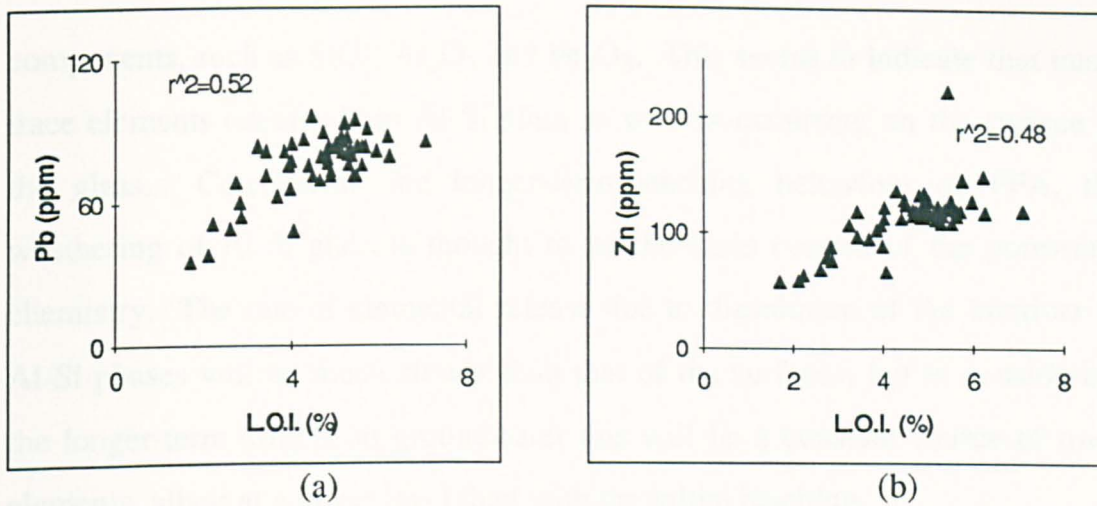


**Figure 4.15 Relationships of Zn and Pb with L.O.I. in weathered Drax PFA**

#### 4.6.2 Weathering of PFA and its implications for porewater chemistry

The depth profiles of Drax and Meaford PFA boreholes revealed the chemical changes that occurred during weathering and confirmed the reactions deduced from the porewater depth profiles. In Meaford PFA, the changes in Al and Si concentrations are more distinct than in Drax PFA, and this seems to be due to greater leaching of the Al-Si glass portions with increased weathering. Such depth trends also correspond with the Meaford porewater depth profiles of Al and Si.

Weathering products, including clays, were not detected in the ashes of either site. SEM observations showed no severe etching or evidence of dissolution of PFA glass surfaces, and the formation of clays could be a longer-term phenomenon than expected. In Drax PFA, some migrated clay fractions were observed, which are thought to have originated from the top soil. The depth range investigated in this study has a maximum of only 5 m, from the surface. Within this depth range it is thought that leaching processes dominate, and this may account for the lack of formation of secondary minerals.

The depth profiles of trace elements in Drax PFA are not clear, but are more distinct in Meaford PFA, along with the other main PFA glass

components, such as  $\text{SiO}_2$ ,  $\text{Al}_2\text{O}_3$  and  $\text{Fe}_2\text{O}_3$ . This seems to indicate that many trace elements occur within Al-Si glass as well as occurring on the surface of the glass. Considering the longer-term leaching behaviour of PFA, the weathering of Al-Si glass is thought to be the main control of the porewater chemistry. The rate of elemental release due to dissolution of the interiors of Al-Si phases will be much slower than that of the surfaces, but in considering the longer-term effects on groundwater this will be a constant source of trace elements, albeit at a lower level than with the initial leaching.

#### 4.7. Conclusion

(1) Drax and Meaford PFA are classified as belonging to the alkaline modic group by the classification scheme of Roy and Griffin (1982). Glassy phases are predominant, with the other main mineral phases in both ashes comprising minor amounts of quartz, mullite and hematite/magnetite.

(2) There are only a minor difference in the chemical composition between the fresh and weathered Drax PFA on the whole. It was difficult to compare the fresh and weathered ash directly due to the uncertainty of the chemistry of the feed coal for the both ashes. The difference in the  $\text{FeO}/\text{Fe}_2\text{O}_3$  ratio in the fresh and weathered Drax ash was about 10 % and this indicates little oxidation has occurred in the weathered ash for the period of weathering, 16 years, and therefore it is expected that no substantial changes occurred between the fresh and weathered PFA chemistry during weathering.

(3) Nevertheless the result from the (2) of whole PFA in , some elements in solid, weathered PFA of both Drax and Meaford sites show depth-related trends. The trends are comparable to those of the corresponding porewater and therefore the changes in solid PFA composition appear to confirm the depth variations found in the porewater chemistry.

(4) The depth profiles are more distinct in the Meaford ash, especially for the major elements,  $\text{Al}_2\text{O}_3$ ,  $\text{SiO}_2$  and  $\text{Fe}_2\text{O}_3$ , which are the main components of PFA glass particles and the trace elements, Ni, Pb, Zn and Ba. This difference reflects increased dissolution of unstable PFA glass in the Meaford ash, which is more weathered than the Drax ash, as weathering progresses.

(5) Some clay minerals, including kaolinite and illite, were identified in weathered PFA collected at various depths in the Barlow mound. However, these clays were also detected in the imported top soil covering the PFA. Although migration of clay minerals from the surface is believed to have taken place, some *in situ* formation of kaolinite within the PFA can not be precluded. SEM analysis showed no substantial changes in the surfaces of weathered PFA particles, when compared to fresh PFA, except for the removal of sub-micron particles and the formation of surface encrustations.

(6) Loss on ignition is higher in the depth of near surface, indicating the higher content of the organic material and some easily breakable secondary weathering products. The depletion of the major elements at shallow depth, where a leaching process is more active, would seem to be a main contributor to the secondary weathering products.

The porewater investigation (Chapter 3) demonstrated that the release of many trace elements associated with the aluminosilicate PFA glass, are controlled by weathering of the glass. The geochemical associations of the elements within both PFA demonstrates the relationship between the release of the trace elements and the dissolution of the aluminosilicate glass.

## Chapter 5

### Chemistry of effluents from the Barlow ash mound

#### **5.1 Introduction**

The Barlow ash mound, at Drax Power Station, is well-engineered, with leachate water generated within the site being prevented from migrating into underlying soil layers by an effluent drainage system installed within the ash mound. Effluent samples were collected from two different places, one directly from outlet drainage pipes and the other from the ditch running around the site, which collects all of the effluent from the pipes. Effluent samples collected directly from the outlet drainage are defined as leachate water, whereas the term ditch water is used to refer to samples collected from the ditch, which is also fed by surface run-off and rainwater.

It is leachate water that affects groundwater composition where there is no proper protection in the disposal site. As a consequence, the leachate water composition can be directly compared with several standards of water quality to assess the extent of the hazard presented by the leachate water. A comparison of the chemical composition of leachate water with that of porewater is expected to provide information about the reaction path of porewater within the ash mound. The composition of the leachate is regarded as the final composition of the porewater, since the leachate has been affected by reactions during migration through the entire thickness of the mound, unlike the porewater of the depth range investigated.

The aim of the analysis of leachate water chemistry is to investigate the level of elemental concentration attained in water which has interacted with an ash mound which was deposited 16 years ago. The porewater is compared with

the leachate water to see how the chemistry of porewater is related to leachate water chemistry.

## 5.2 Chemistry of effluents from the Barlow mound

### 5.2.1 Leachate water

#### 5.2.1.1 Samples

Chemical analyses of leachate water collected directly from the outlet drainage pipes in the Barlow ash mound are shown in Table 5.1. The samples were collected in sequence from the northern side of the mound, where new ash is currently being deposited. No. 8 was collected from where the oldest ash was deposited, whereas No. 1 is from the youngest ash deposit (Figure 2.1). There is not, however, any specific relationship between the composition of collected leachate water and the age of ash deposited. The measured flow rate of the leachate from the Barlow mound at the time of collecting, which was May, 1992, was approximately 25 tonnes per day.

#### 5.2.1.2 Chemical composition of leachate water

The pH of the leachate is neutral to slightly alkaline, ranging between 7.5 and 8.4. The leachate water was in an oxidising environment, having an average Eh value of 440 mV.

The concentrations of major ions in eight different Drax leachate water samples were plotted, for comparison with each other, in Figure 5.1. Among the eight samples, only No. 1 shows a slightly different pattern compared with the other samples, having lower Na and K, but the Drax leachate waters of different outlet drainage appear to be generally uniform in composition. Ca, Mg, Na and K are the major cations, with  $\text{SO}_4^{2-}$  being the most important

anion. The concentrations of Si were low, and it is not a significant ion in the leachate water. This pattern seems to represent the characteristic nature of PFA, in which all of these four elements are typically enriched and readily leachable.

Among the trace elements B and Li have significant concentrations, recording maximum values of 22.3 and 24.8 mg/l respectively. The concentration of As in L5, 16.9 mg/l, is particularly high.

Some of the leachate water concentrations are variable in relation to each other. Na and K of the major ions and B, Cr, Li, Mn, As and Se of the trace elements have variable concentrations. Meanwhile some elements are much less variable among the different samples. These are Ca, Mg, Ba, Cd, Co, Cu, Ni and Cl<sup>-</sup> along with pH and Eh values.

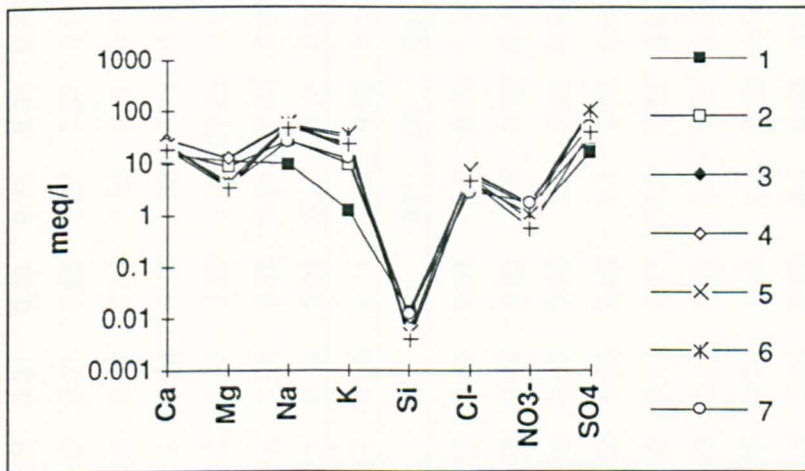


**Figure 5.1** The major ionic compositions of Drax leachate water samples

### 5.2.2 Chemistry of ditch water

Chemical analyses of ditch water are shown in Table 5.2. The average composition of the leachate water is shown in Table 5.1 together with data from National Power, presented for comparison. The concentrations of elements in

Sample	Ca	Mg	Na	K	Fe	Al	Si	B	Ba	Cd	Co	Cr	Cu	Li	Mn	Ni
L 1	292.5	138.4	234.8	50.1	0.03	0.05	0.91	2.48	0.22	0.02	0.05	0.03	0.01	0.71	1.84	0.09
L 2	350.4	107.7	637.7	401.6	0.01	0.01	0.73	5.92	0.17	0.02	0.06	0.04	0.01	10.07	2.62	0.08
L 3	576.0	151.9	1286.7	741.8	0.01	0.06	0.67	7.37	0.14	0.03	0.07	0.05	0.02	6.64	6.64	0.11
L 4	566.7	152.9	1386.9	828.4	0.08	0.35	0.69	8.21	0.14	0.04	0.08	0.05	0.02	20.14	5.00	0.10
L 5	446.4	46.8	1262.5	1245.2	0.08	0.14	0.33	6.74	0.13	0.04	0.06	0.98	0.04	24.64	0.80	0.11
L 6	455.5	56.0	1302.2	1403.9	0.07	0.29	0.23	22.29	0.10	0.04	0.06	0.11	0.03	24.76	0.00	0.10
L 7	476.7	48.4	613.7	481.2	0.05	0.00	0.81	8.35	0.09	0.03	0.06	0.04	0.01	10.53	0.01	0.09
L 8	377.4	43.0	1151.4	957.1	0.04	0.01	0.27	15.66	0.09	0.03	0.05	0.04	0.01	14.71	0.94	0.08
AVG	442.7	93.1	984.5	763.7	0.05	0.11	0.58	9.63	0.14	0.03	0.06	0.17	0.02	15.67	2.23	0.10
	pH	Eh(mv)	Pb	Sr	V	Zn	As	Se	Hg	Mo	Cl-	NO <sub>2</sub> -	NO <sub>3</sub> -	SO <sub>4</sub> (II-)	Br	HCO <sub>3</sub> - *
L 1	8.0	439	0.26	1.11	0.03	0.04	2.0	0.00	1.57	0.7	205	2.56	52.9	831	2.9	829.6
L 2	8.1	443	0.31	1.48	0.03	0.03	0.6	0.00	0.29	0.6	210	-	95.8	1512	5.3	1643.2
L 3	8.3	442	0.43	1.70	0.05	0.09	0.3	0.00	0.20	0.6	240	0.66	107.5	4458	11.2	1092.6
L 4	8.0	441	0.43	1.72	0.06	0.06	0.1	0.01	0.40	0.7	243	1.94	110.9	5259	12.3	621.7
L 5	7.8	442	0.40	1.88	0.11	0.17	16.9	0.11	0.00	1.9	266	-	105.4	4634	29.1	640.2
L 6	7.5	439	0.42	2.03	0.07	0.11	5.3	0.01	0.00	1.4	160	0.32	68.0	5130	8.7	672.8
L 7	8.2	438	0.37	1.55	0.03	0.03	0.6	0.00	0.02	0.7	105	0.81	116.4	2619	7.7	537.3
L 8	8.4	440	0.35	1.83	0.03	0.12	6.4	0.00	0.00	1.5	173	1.44	37.0	2000	18.6	3167.7
AVG	7.4	440	0.37	1.66	0.05	0.08	4.0	0.01	0.30	1.0	200	1.30	86.7	3305	12.0	1150.6

Table 5.1 Chemical composition of Barlow leachate water collected in May, 1992. Unit: mg/l unless indicated, except for pH. (\* calculated)

	Ca	Mg	Na	K	Fe*	Al	Cr*	Cu*	Mn	Ni	Zn*	Cl-	NO <sub>2</sub> -	NO <sub>3</sub> -	SO <sub>4</sub> (II-)
D 1	244.8	53.6	367.5	230.0		0.1	8.0			0.01					
D 2	224.2	57.6	315.0	173.0		0.1	12.0			0.01					
D 3	157.2	40.7	118.0	16.0		0.0	20.0			0.01					
D 4	424.9	46.0	141.0	151.0		0.0	340.0			0.00					
D 5	354.6	41.1	1320.0	560.0		0.0	0.0			0.00					
D.6	392.0	43.6	350.6	222.5	32.9		395.4	6.7	0.12	1.50	80.2	307	0.40	10.5	4400
D 7	403.5	50.8	464.8	217.5	11.1		450.5	5.6	0.01	0.40	8.4	337	0.36	24.5	4750
D 8	411.0	62.8	370.5	232.6	9.8		113.4	5.1	0.01	0.00	7.0	176	0.14	12.2	4611
D 9	418.0	39.1	202.3	115.9	8.0		0.3	0.4	0.04	0.50	6.0	130		7.4	3256
AVG	336.7	48.4	405.5	213.2	15.5	0.04	148.8	4.5	0.05	0.27	25.4	238	0.30	13.7	4254
AVG1	442.7	93.1	984.5	763.7	50.0	0.11	170.0	20.0	2.23	0.10	80.0	200	1.30	86.7	3305
AVG2	189.8	56.4	221.4	24.2	30.0	0.00	0.00	40.0	0.02	0.01	70.0	314	0.00	21.5	664

**Table 5.2 Chemical composition of ditch water, Barlow ash mound (Unit: mg/l \* µg/l)**

ditch water is generally lower than in leachate water because the ditch water is fed by surface run-off and rainwater, which dilute the leachate water. The concentrations of Mg, Na, K,  $\text{NO}_2^-$  and  $\text{NO}_3^-$  in the ditch water are about half the levels seen in the leachate water, whereas there are much smaller differences between the ditch and leachate water concentrations of Ca and  $\text{SO}_4^{2-}$ . All of the trace ions are lower in concentration in ditch water than in leachate water.

Ca and  $\text{SO}_4^{2-}$  concentrations are controlled by calcium sulphate present in the porewater, therefore the similar concentrations of the Ca and  $\text{SO}_4^{2-}$  in ditch and leachate water is attributed to the achievement of fast equilibrium in both waters.

### 5.2.3 Geochemical associations

The elemental concentrations in leachate water were plotted against the concentrations of total dissolved solids (TDS) in Figure 5.2. The concentrations of Na, K, Ca and  $\text{SO}_4^{2-}$  in the leachate increase with the amount of TDS while those of Mg,  $\text{Cl}^-$  and  $\text{NO}_3^-$  do not increase but show irregular patterns. The patterns for Na, K, Ca and  $\text{SO}_4^{2-}$  indicate their common source, whereas the trends for Mg,  $\text{Cl}^-$  and  $\text{NO}_3^-$  indicate either an external source or the achievement of equilibrium concentration.  $\text{Cl}^-$  and  $\text{NO}_3^-$  were demonstrated to have an external source, namely fertiliser, in Chapter 3. The Mg in leachate water seems to have achieved equilibrium concentrations and magnesite might be a possible solubility controlling phase.

Of the trace elements, the concentrations of Li and Pb increase with TDS. B also shows a similar trend, with a few exceptions. The concentration of Ba appears to be independent of TDS, being relatively constant with changes in TDS. Ba was demonstrated to have achieved equilibrium concentration in porewater. Geochemical calculations also indicates that the leachate water is oversaturated with respect to barite. The rate of increase in Pb concentration in

leachate water with increases in TDS is in decline, such that Pb is approaching a relatively constant concentration against TDS. This appears to indicate the achievement of equilibrium concentration for Pb, and this is supported by geochemical calculations for the leachate water, which indicate near-equilibrium conditions with respect to cerrusite.

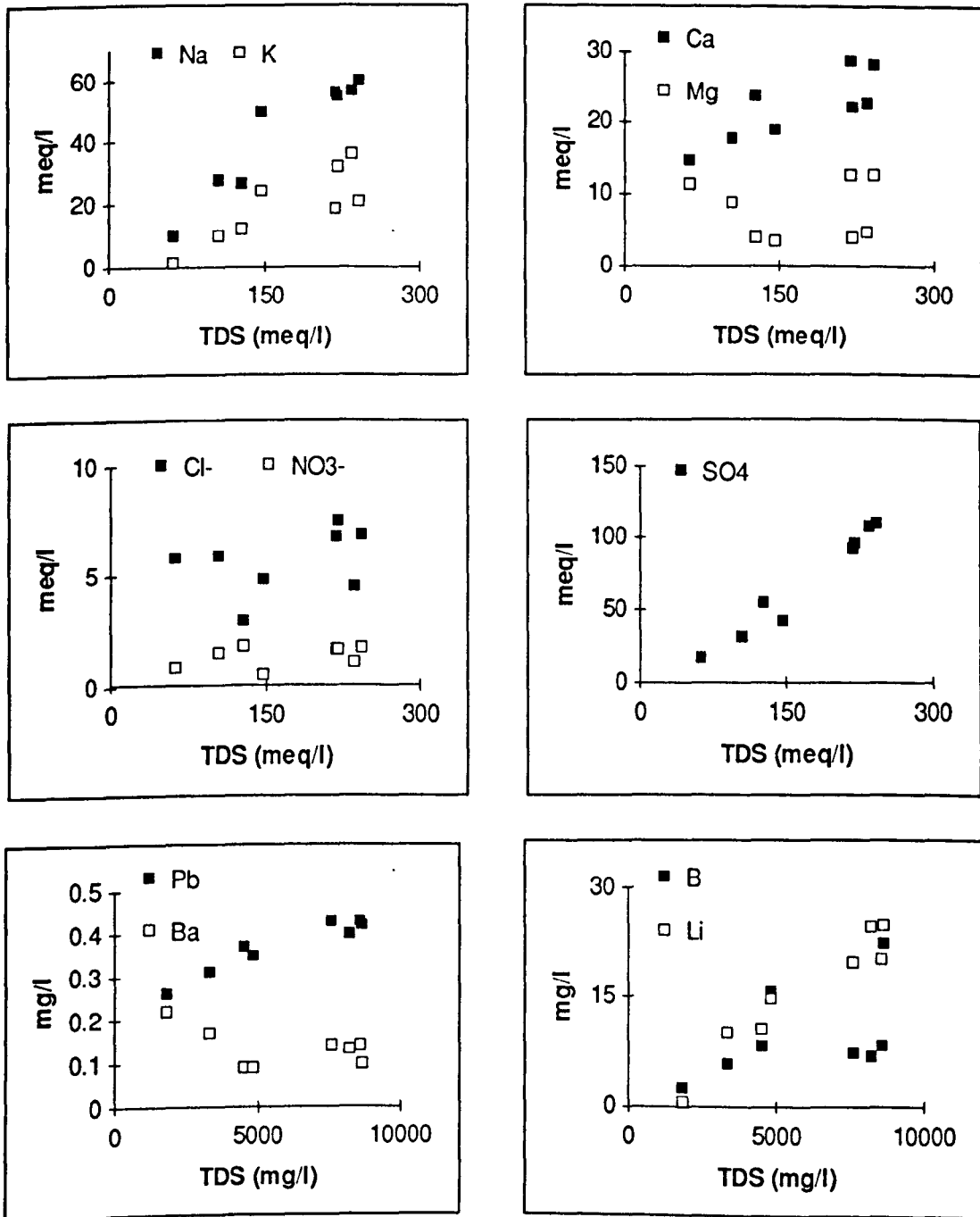


Figure 5.2 Ionic concentration vs. TDS in Barlow leachate water

Comparison of concentrations with TDS indicates that nearly all the elements are derived internally, as was indicated from the porewater analysis. Anions such as  $\text{Cl}^-$  and  $\text{NO}_3^-$  are thought to have come from an external source. The intercept on the TDS axis shown by Li does not occur with any other trace elements. This is most likely to be due to original variations or to be induced by other specific attenuation mechanisms.

#### 5.4 Rate of infiltration of porewater in the Barlow ash mound

In the Barlow ash mound, the amount of specific elements removed from solid PFA can be estimated from whole PFA analyses. The time period of weathering is known, and the volume of water required to give the observed compositional changes is calculated from porewater analyses. So the rate of infiltration of porewater in the Barlow PFA mound was calculated from chemical data from porewater and solid PFA. Details of this method are explained by Spears and Reeves (1975), who successfully applied the method to the calculation of the percolation rate of porewater in Quaternary sediments. This concept is shown in Figure 5.3. The less weathered PFA samples were collected from the bottom of Drax PFA boreholes. The relative difference in composition was used to calculate the percolation rate, because the PFA shows a small degree of weathering at depth.

Among the elemental variations with depth in solid PFA,  $\text{SO}_3$  in borehole 4 from the Barlow ash mound shows the most distinctive result of leaching from solid PFA (Figure 4.4 in Chapter 4). Concentrations of  $\text{SO}_3$  decreased up to 3 m in depth and then the concentration is constant below that depth. The average bulk density of PFA in the previous literature ranges between 1.01 and 1.43 (Mattigod and Rai *et al.*, 1990) and a value of 1.2 was used in calculating the amount of  $\text{SO}_3$  removed from PFA during weathering. The percolation rate in the Barlow ash mound was calculated as follows:

Average concentration of S lost from PFA : 0.112 %

Average bulk density of PFA : 1.2, Depth of weathered PFA : 3m

Average concentration of  $\text{SO}_4^{2-}$  porewater less background: 1800  $\mu\text{g/ml}$   
(S=600  $\mu\text{g/ml}$ )

$\text{SO}_3$  removed from PFA in mg:  $0.112 \% \times 1.2 \times 300 \text{ cm} \times 10^6 / 100 =$   
 $4032 \times 10^2 \mu\text{g} \text{----- (1)}$

Amount of porewater required to remove (1):  $4032 \times 10^2 \text{ mg} + 600$   
 $\mu\text{g/ml} = 6.72 \times 10^2 \text{ ml} \text{----- (2)}$

Hence, rate of infiltration is  $6.72 \times 10^2 \text{ cm} + 16 \text{ years} = 42 \text{ cm/year}$

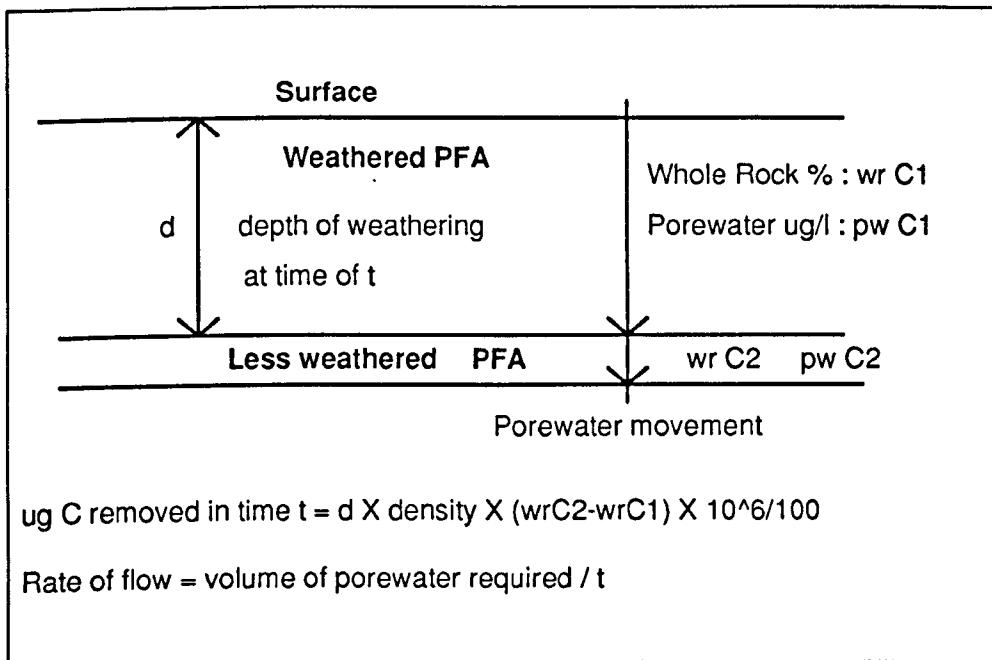


**Figure 5.3 Schematic diagram for the calculation of percolation rate in ash disposal mound (Adapted and modified from Spears and Reeves (1975))**

The calculated infiltration rate should be compared with meteorological data. The average annual rainfall at the Beal Weir Station (Nat. Grid Ref. SE 534255), the nearest gauging station to the Barlow ash mound, between 1958~1990 is 980 mm (Marsh and Lees *et al.*, 1993). Base on the S values in the Barlow PFA and porewaters, approximately 50 % of the rainfall infiltrates into

the PFA mound. This volume is somewhat larger than the 20-30 % estimated of Brown and Ray *et al.* (1976).

### 5.5 Comparison of leachate water with porewater

The ionic concentrations of leachate water and porewater are compared in Table 5.3. The porewater shown in the Table was collected at a depth of 4 m, from borehole 4. The concentrations of the leachate water would be much higher for several elements if the values for L1 were omitted (Table 5.1).

	Ca	Mg	Na	K	Fe	Al	Si	B	Ba
PW	608	363	52	137	0.09	0.03	0.36	13.4	0.10
Leach.	443	93	985	764	0.05	0.11	0.58	9.6	0.14
	Cd	Co	Cr	Cu	Li	Mn	Ni	Pb	Sr
PW	0.05	0.10	0.15	0.01	1.6	0.00	0.13	0.59	2.4
Leach.	0.03	0.06	0.17	0.02	15.7	2.23	0.10	0.37	1.7
	Zn	As	Se	Hg	Cl <sup>-</sup>	NO <sub>3</sub> <sup>-</sup>	SO <sub>4</sub> (II <sup>-</sup> )	pH*	Eh(mv)
PW	0.02	0.080	0.04	<0.005	145	634	4023	8.3	409
Leach.	0.08	0.004	0.01	0.30	200	87	3305	8.0	440

**Table 5.3 Comparison of the porewater composition collected at 4 m depth and average leachate water composition (unit : mg/l. \* no unit)**

Higher concentrations are observed for Na, K, Li and Mn in leachate water when compared with porewater, whereas the concentrations of Mg and NO<sub>3</sub><sup>-</sup> are higher in the porewater. The concentrations of other elements, including Fe, Al, Si, B, Ba, Cd, Co, Cr, Ni, Pb, Sr, Zn, Cl<sup>-</sup> and SO<sub>4</sub><sup>2-</sup> are similar in the two types of water sample.

The depth trends and geochemical calculations obtained for the porewater indicated that a few elements had achieved equilibrium concentration. These included Ca, SO<sub>4</sub><sup>2-</sup>, Ba and Sr, and possibly Zn and Cu - with a little uncertainty due to their low concentrations in the porewater. The

concentrations of elements which show equilibrium concentrations in the porewater show comparable concentrations in leachate water. These elements appear to be controlled by solubility controlling solid phases both in the porewater and the leachate water.

The concentrations of Na, K, Li and Mn, however, are too high to relate them to porewater. Such high concentrations are more likely to result from the initial leaching of PFA, during which stage the readily leachable surface-enriched fractions are rapidly dissolved. The calculated percolation rate of porewater within the ash mound was estimated to be around 30-40 cm/year. This infiltration rate suggests that porewater starting at one point in the mound might have migrated around 6m, at best, during the 16 years since deposition began. It is presumed that the Barlow ash mound was subjected to rainfall from the start of the disposal. Leachate from the initial stage of weathering, with high ionic concentrations, will still be being discharged, because of the height of the ash mound, namely 36 m. The Na, K, Li and Mn are all typical surface-associated elements and the high concentrations of these specific elements in both surface-enriched fractions and the leachate clearly supports this explanation.

Other possible explanation is the effect of a lateral flow within the Barlow ash mound. The porewater generated near the surface is believed to be subjected to the lateral flow as the porewater migrates downwards due to the slope of the ash mound as shown in Figure 5.4. This lateral flow effect will lead the porewater migration along the slope, delaying the discharge of the porewater generated in the centre of the mound. Consequently, the porewater from the centre of the mound may still represent the characteristics of the initial leaching stage.

There are also big variations among the leachate samples (Table 5.2). This can be explained as being due to mixing and diluting of the leachate water

with rainwater or surface run-off, which infiltrate the slope of the ash mound as shown in Figure 5.4.

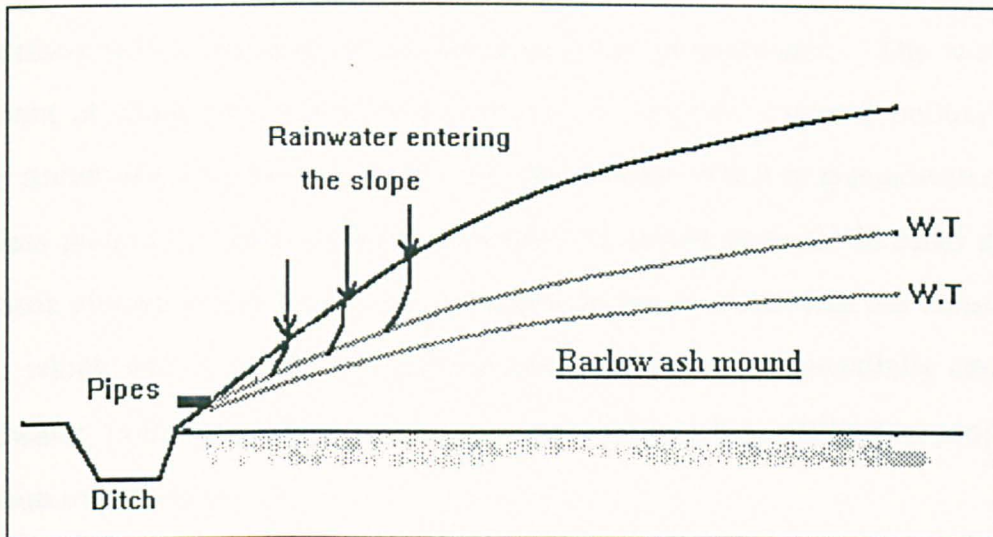


**Figure 5.4** Schematic diagram for the infiltration of rainwater on the slope of the ash mound

## 5.6 Comparison of the chemistry of leachate water with water quality standards

The average concentrations of leachate water from the Barlow mound was compared with two different water quality standards, the EC landfill directive and the Barlow discharge consent, given by the National River Authority.

The concentrations of  $\text{SO}_4^{2-}$ , As, B, Cd, Cr and Pb exceed, or nearly exceed, one of the standards, those given by the NRA (National River Authority). Other elements, including  $\text{Cl}^-$ , Cu, Zn, Hg and Ni, do not exceed the standards. Among the elements exceeding the standard levels, As, Cd, Cr and Pb are very toxic, and can cause serious illness, even in small amounts, in drinking water (Alloway, 1990; Ferguson, 1992). Special treatment will be necessary to reduce their concentrations in discharging leachate.

When applying such water standards to the effect of the leachate on groundwater, totally different concepts should be applied. Elements that have migrated from the ash mound may be diluted when the leachate is discharged into surface water but this needs not apply for groundwater. The water movement of groundwater is generally very slow and the external pollutants may be accumulated in the aquifer because the dilution effect in groundwater is much less than in the surface water. Therefore, it should be borne in mind that even those elements with lower concentrations in the leachate than the consent levels, which do not exceed the water quality standards can potentially cause groundwater pollution, when discharged into the aquifer without a proper protection or treatment.

	Barlow Leach.	EC Landfill Directive <sup>1</sup>	Barlow Consent (NRA)		Barlow Leach.	EC Landfill Directive <sup>1</sup>	Barlow Consent (NRA)
Cl-	200		1200-6000	Cr	<u>0.2</u>	0.1-0.5	0.1
SO <sub>4</sub> (II-)	<u>1150</u>		200-1000	Hg	0.003	0.02-0.1	
Cu	0.02	2-10	0.1	Ni	0.1	0.4-2.0	0.5
Zn	0.08	2-10	1.0	Pb	<u>0.4</u>	0.4-2.0	0.5
As	<u>0.08</u>	0.2-1.0	0.01	B	<u>9.6</u>		5.0
Cd	<u>0.03</u>	0.1-0.5	0.005	pH	8.0	4-13	6-9

Table 5. 4 Comparison of average PFA leachate with standards for drinking water and landfill leachate discharge (Unit : mg/l except for pH). <sup>1</sup> EC official journal No.C 190/1, July, 1991

## 5.7 Conclusion

(1) Ionic concentrations of some elements in the leachate water of the Barlow mound are generally much higher than in the porewater. Those elements showing elevated levels are Na, K, Li and Mn, the concentrations of which, in the porewater, did not show any evidence of the achievement of

equilibrium concentrations. The leachate water discharged currently appears to contain high amounts of dissolved solids from the initial stage of leaching. Disposal at the Barlow site started 16 years ago, but contrary to expectation the surface-enriched inorganics in the ash mound are still contributing greatly to the leachate.

(2) The concentrations of Ca,  $\text{SO}_4^{2-}$ , Ba and Sr show relatively little variation among leachate water, ditch water and porewater. These elements are thought to have achieved equilibrium concentrations rapidly, and their concentrations are controlled by solubility controlling solids. The concentrations of Mg and Pb appear to be in equilibrium concentration in the leachate. Their concentrations in porewater increased with depth, without showing evidence for the presence of solubility controlling phases in the depth range investigated. Therefore, equilibrium must have been attained by further reactions within the ash mound beyond the depth range drilled.

(3) Most elements in the leachate were derived internally from the reaction of PFA with infiltrating water.  $\text{NO}_3^-$  and  $\text{Cl}^-$  are exceptions which are thought to have an external origin, namely fertiliser.

(4) The infiltration rate calculated based on the chemical composition of PFA and porewater showed a value of 30-40 cm/year. Comparison of this value with the meteorological data suggests about 50% of the rainfall infiltrates into the Barlow ash mound, which is larger than the previous observation in the field lysimeter.

(5) The concentrations of As, Cd,  $\text{SO}_4^{2-}$ , Cr, Pb and B exceed the discharging limits set either by the EC landfill directive or the NRA's Barlow water consent. Barlow leachate water should therefore be discharged after suitable treatment has reduced the concentrations of these elements to below the critical levels. However, consideration should also be given to the reduction of the levels of those elements which are just under their limits, in view of the possibility that the leachate samples were diluted by surface water.

## Chapter 6

### Batch leaching Tests

#### **6.1 Introduction**

Batch leaching test using deionised water was undertaken as a feedback base, primarily to confirm the field investigation, along with the column leaching test (Chapter 7). The results from the batch leaching test: (a) allow a comparison with previous work on the leaching of fresh PFA; (b) extend the data base for weathered PFA, which should also provide confirmation of the leaching behaviour of fresh PFA; (c) provide laboratory information on weathering to compare with the field studies being undertaken at Drax and Meaford Power Stations; and (d) enable assessment of the hazard presented by the PFA investigated, due to leaching, by direct comparison with the EEC directive for drinking water abstracted from surface water (75/440/EEC, June 1975), and the Landfill Directive (EC official journal No. C 190/1, July 1991).

The concentrations of elements in solutions and PFA both before and after successive leaches were compared and the changes were recorded to see if there were any significant reactions and the extent of such reactions. The leaching behaviours of individual elements were compared to establish general trends and to investigate the geochemical associations of elements. The analytical data were also analysed thermochemically, using the geochemical simulation computer program WATEQ4F to identify reaction mechanisms and the composition of the phases controlling elemental retention in PFA and thereby concentration in the eluate. This will be discussed in Chapter 8 together with the data from the column leaching tests.

In addition to the aims to supplement the field study, the batch leaching test was also undertaken using PFA and synthetic leachates, which were made to

simulate the composition of industrial land-fill leachate. As was demonstrated in the field investigation, the weathering of PFA produces insoluble reaction products and the mobility of elements could be reduced by reaction with the secondary products. If such reactions are significant, PFA could provide some amelioration of the toxicity of eluates generated by other waste materials. Two experimental procedures were adopted: firstly, batch leaching, described in this chapter, and secondly, column leaching, described in the next chapter (Chapter 7). Standard leaching experiments examine the loss of elements from PFA into solution, whereas in this work the interest is extended to the loss from solution.

## 6.2 Experiments

### 6.2.1 Material

#### *6.2.1.1 PFA samples*

Three different sample types were used, namely fresh Drax PFA, weathered Drax PFA and Meaford PFA. The weathered PFA samples used in this investigation were obtained from the Barlow disposal mound (Grid. ref. SE 655 277) at Drax Power Station, and from the decommissioned power station at Meaford (Grid. ref. SJ 896 373). The weathered PFA from the Barlow mound at Drax Power Station was emplaced in 1975 and samples were obtained from a shallow pit at depths of 0.5 to 0.8 m from the surface. Fresh PFA was also collected from Drax to compare the leaching behaviour of the fresh and weathered PFA. Weathered Meaford samples were also collected from a shallow pit located on the PFA plateau at depths of between 0.5 and 0.8 m. The weathered Meaford samples are older. It is thought that the ash was deposited more than 20 years ago (but is not more than 40 years old), and presumably is more weathered than the samples

obtained from the Barlow mound. Meaford was selected for additional sampling in order to extend the age range of the material examined.

All of the PFA samples were oven dried at 105°C overnight before using in the experiments. No further treatments such as sieving or crushing were done.

### 6.2.1.2 Composition of synthetic leachate

To simulate the leachate from waste materials, an artificial leachate solution was prepared, similar in composition to that of leachate resulting from the codisposal of domestic and industrial waste, with the exception of the heavy metals, which are approximately ten times higher than normally encountered (Table 6.1). A synthetic leachate of similar composition was used in the work of Newman and Ross (1985). In addition to the elements Cd, Ca, Cr, Cu, Fe, Mn, Hg, Na, K, Ni, Zn and Li, the solution contained Cl, acetic acid (5000 mg/l), propionic acid (3000 mg/l), butyric acid (2000 mg/l), and phenol (20 mg/l). The solution was adjusted to pH 4.5 with NH<sub>4</sub>OH.

pH	Ca	Na	K	Mg	Fe	Al	B	Ba	Cd
4.55	615	1032	735	87	123	(0.12)	(0.23)	0.04	121
Cr	Cu	Li	Mn	Ni	Pb	Si	Sr	Ti	V
80	118	19	(0.18)	109	0.22	(0.81)	(0.16)	(0.05)	(0.11)
Zn	As	Hg	Se	Mo	Cl <sup>-</sup>	NO <sub>3</sub> <sup>-</sup>	SO <sub>4</sub> <sup>2-</sup>		
108	(0.27)	13.8	(0.33)	(0.68)	1973	21	419		

**Table 6.1 Composition of the synthetic leachate used in the batch leaching test (analysis by ICP. Unit: mg/l unless indicated.) Those elements whose concentrations are shown in brackets originate as impurities in the standard chemicals**

The composition of the synthetic leachate changed after preparation due to some precipitation. The solution was filtered to remove precipitates and then analysed to check the change in the composition. The concentrations of Pb and Cr changed substantially. The concentration of Pb and Cr in the synthetic leachate decreased to 99 % and 50 % of the initial level in the synthetic leachate.

## 6.2.2 Experimental procedures

The batch leaching was based on Standard Method DIN 38414-84 (1984), the German standard. This procedure was developed for the determination of the leachability of waste material, particularly sludge and sediments, by water.

### 6.2.2.1. *Procedures of batch leaching tests*

#### Procedures using synthetic leachate

50 g of the three PFA samples (fresh Drax, weathered Drax, and weathered Meaford) were placed in 1 litre polypropylene bottles and 500 ml of synthetic leachate solution were added to each bottle. The bottles were then shaken for 24-hours in an end-over-end shaker at room temperature and the elute filtered through a 0.45  $\mu\text{m}$  micropore membrane filter under vacuum. The Eh, pH and conductivity were measured, and the solutions used for cation analysis were acidified to 1 %  $\text{HNO}_3$ . The procedure was repeated but with the synthetic leachate replaced by deionised water. This procedure was repeated a further three times.

#### Procedures using deionised water

The above procedure is to determine the loss of elements from solution and thus the gain onto the solid PFA, but there will also be some elements which are leached from the PFA. This contribution to solution was determined with the same three samples, using deionised water instead of the synthetic leachate solution, followed by further additions of deionised water, as in the above procedure. Six samples were run in each 24-hour shaking and this was repeated four times producing a total of 24 samples.

### 6.2.2.2 Analysis

Both solutions and the solid PFA were analysed. Cations (Ca, Mg, Na, K, Al, Si, B, Ba, Cd, Co, Cr, Cu, Li, Mn, Ni, Sr, Ti, V and Zn) in the water samples were determined using ICP-AES in two laboratories, primarily to extend the number of elements analysed, but also as a check on the quality of the analyses for those elements determined in duplicate. Elements were detected down to a concentration of 0.01 mg/l, which is appropriate for those elements in the synthetic leachate and a number of other elements released in significant concentrations by the leaching of PFA. A number of trace elements will be released into solution from PFA in concentrations lower than 0.01 mg/l and for their determination either ICP-MS or furnace AAS would have been employed if the experimental work had not been essentially concerned with the possible interaction between synthetic leachate and PFA. As, Hg, Se and Mo were also determined by Perkin Elmer M2100 AAS using hydride generation. Anions ( $\text{Cl}^-$ ,  $\text{NO}_3^-$  and  $\text{SO}_4^{2-}$ ) in the water samples, were measured using Dionex 2000i Ion chromatography.

The composition of the solid PFA was also determined before and after the leaching by synthetic leachate and deionised water. The samples were analysed by Phillips 1400 X-ray fluorescence spectrometry using lanthanum borate fused discs for the determination of major and trace elements.

## 6.3 Batch leaching with deionised water

### 6.3.1 Introduction

A number of authors have investigated the leaching behaviour of PFA using the batch leaching technique (Brown and Ray *et al.*, 1976; Theis and Westric *et al.*, 1978; Talbot and Anderson *et al.*, 1978; van der Sloot and Wijkstra *et al.*, 1982;

Wadge and Hutton *et al.*, 1986 ; Grisafe and Angino *et al.*, 1988; Hjelmar, 1990) and demonstrated high concentrations of the major ions Ca, Mg, Na, K,  $\text{SO}_4^{2-}$  and Cl, and the trace elements As, Cr, Mo, Se, V and B in the initial eluate. The results generated in the present study using deionised water should be similar to those of previous studies in the case of fresh PFA, but not necessarily in the case of weathered PFA. In previous studies the effect of weathering has been investigated either in the laboratory or, to a lesser extent, in field trials, but for a shorter time period weathering than the weathered PFA used in the present project.

### 6.3.2 Leaching behaviour of PFA with deionised water

#### 6.3.2.1 Batch leaching of fresh Drax PFA with deionised water

The batch leaching concentrations of the eluates from fresh Drax PFA, using deionised water, are shown in Table 6.2 (Samples Dfd1-4 are successive eluates). The readily leached major elements from the fresh PFA are Ca, Na and K, in order of concentration, and S (as  $\text{SO}_4^{2-}$ ). Al and Si are major components of the ash and are present in the eluates, but only at concentrations of a few mg/l. Other elements are present in solution at comparable to the Si and Al concentrations, but these are trace elements in the ash, and therefore a significantly higher proportion of these elements is released by leaching. Notable in this group of elements are B and Mo.

In successive eluates (Dfd2-4 Table 6.2) the elements most readily leached from the ash in the first treatment are present at much lower concentrations. Approximately 80 % of the total amount of the water soluble Ca, Na, K and S (as  $\text{SO}_4^{2-}$ ) is liberated in the first treatment. Other elements which clearly exhibit this pattern are B, Cr, Cu, Li, Ni, Hg, Mo and Cl<sup>-</sup>, indicating that these elements are concentrated on the surfaces of PFA particles, as indicated by previous work (Theis and Wirth, 1977; Hansen and Fisher, 1980, Clarke and Sloss, 1992). There

are, however, elements which differ markedly in behaviour and comparable amounts are dissolved with each leaching. Falling into this group are Mg, Al, Ba, Si, V, As and Se. The implication is that these elements are present in less readily soluble components of the ash and presumably this is essentially the glass. Elements intermediate in leaching behaviour are: Fe, Co, Pb, Sr, Zn and Zr.

#### *6.3.2.2 Batch leaching of weathered Drax PFA with distilled water*

Weathered Drax PFA was deposited near to the surface of the Barlow mound seventeen years ago, and throughout the subsequent period has been subjected to weathering due to infiltrating porewater. Loss of the readily soluble elements from weathered Drax PFA would therefore be anticipated to have occurred. The results shown in Table 6.2 (Dwd1) show that this is indeed the case. The concentrations of Ca, Na, K,  $\text{SO}_4^{2-}$ , B, Cr, Cu, Li, Ni, Hg and Mo are all much lower, with some of the trace elements below the detection limits. One element which is present at a higher concentration in weathered PFA is N (as  $\text{NO}_3^-$ ) and the most likely explanation is derivation from fertilisers applied at the surface.

Many trace elements in the weathered ash were released in relatively uniform amounts in successive eluates, using deionised water. The concentrations are broadly comparable to those levels in the final eluate of the fresh ash which was treated once by the synthetic leachate and three times by deionised water. This seems to indicate that weathering of PFA liberates much of the surface-associated soluble fractions at an early stage, and this is followed by a more constant release of matrix associated elements at a slower rate.

#### *6.4.2.3 Batch leaching of weathered Meaford PFA with distilled water*

The results obtained from the material from Meaford (Mwd 1-4, Table 6.2) are similar to those obtained from the weathered PFA from Drax, in terms of the leaching trends and concentrations. Although the total amount dissolved the

	pH	Pe	C mS	Ca	Na	K	Mg	Fe	Al	B	Ba	Cd	Co	Cr	Cu
dfd1	9.34	8.39	1130.0	173.1	42.1	21.3	0.99	0.25	3.67	2.77	0.30	0.00	0.05	0.30	0.10
dfd2	9.97	7.87	150.8	19.3	4.9	2.8	1.5	0.04	1.37	0.93	0.29	0.00	0.02	0.06	0.02
dfd3	7.12	7.92	242.0	35.3	2.9	1.9	2.12	0.04	0.07	0.52	0.89	0.00	0.02	0.04	0.01
dfd4	8.80	7.20	70.0	10	1.5	0.4	1.4	0.10	1.72	0.24	0.25	0.00	0.02	0.03	0.01
dwd1	7.26	8.42	215.0	26.6	4.3	2.4	1.98	0.02	0.60	0.18	0.54	0.05	0.00	0.01	0.00
dwd2	7.60	7.98	102.4	10.5	2.6	0.5	0.78	0.02	0.79	0.08	0.40	0.00	0.00	0.00	0.00
dwd3	7.67	7.47	61.0	9.4	1.8	0.3	0.57	0.01	0.80	0.06	0.24	0.00	0.00	0.00	0.00
dwd4	8.10	7.23	102.9	8.6	1.1	0.1	0.47	0.01	1.07	0.03	0.17	0.00	0.00	0.00	0.00
mwd1	7.08	8.69	193.0	21.1	3.6	3.6	1.27	0.14	0.37	0.18	0.28	0.16	0.00	0.06	0.05
mwd2	7.40	7.94	111.5	10.3	4.2	0.4	0.71	0.03	0.28	0.15	0.72	0.01	0.00	0.00	0.00
mwd3	7.26	7.46	60.5	9.4	2.1	0.7	0.62	0.08	0.75	0.08	0.23	0.01	0.00	0.00	0.00
mwd4	7.73	7.17	65.3	8.8	3.1	0.2	0.55	0.06	0.74	0.08	0.45	0.00	0.00	0.35	0.00
	Li	Ni	Pb	Si	Sr	V	Zn	Zr	As	Hg	Se	Mo	Cl-	NO <sub>3</sub> -	SO <sub>4</sub>
dfd1	0.74	0.18	0.15	1.55	0.48	0.36	0.18	0.26	0.14	0.22	0.15	1.12	6.10	0.75	492.43
dfd2	0.10	0.02	0.10	1.86	0.10	0.26	0.02	0.12	0.12	0.03	0.15	0.23	2.30	0.73	34.64
dfd3	0.06	0.00	0.05	3.38	0.17	0.21	0.15	0.09	0.49	0.03	0.11	0.09	0.46	7.23	22.1
dfd4	0.02	0.02	0.05	1.56	0.05	0.24	0.02	0.07	0.34	0.14	0.14	0.04	0.34	2.59	19.7
dwd1	0.03	0.00	0.00	1.25	0.14	0.11	0.06	0.01	0.31	0.01	0.05	0.00	7.31	24.29	17.52
dwd2	0.01	0.00	0.00	1.08	0.06	0.12	0.06	0.00	0.29	0.00	0.00	0.00	5.21	1.22	3.99
dwd3	0.01	0.00	0.00	1.16	0.04	0.11	0.03	0.00	0.30	0.01	0.00	0.00	1.65	1.57	1.50
dwd4	0.00	0.00	0.00	1.15	0.04	0.09	0.01	0.00	0.22	0.00	0.01	0.00	0.54	0.57	1.26
mwd1	0.02	0.03	0.00	1.55	0.17	0.07	0.12	0.01	0.18	0.01	0.07	0.00	3.20	2.37	21.08
mwd2	0.00	0.00	0.00	1.78	0.09	0.09	0.05	0.00	0.17	0.03	0.06	0.00	3.61	0.52	4.90
mwd3	0.00	0.00	0.00	1.69	0.07	0.09	0.04	0.00	0.18	0.00	0.08	0.00	1.50	0.59	2.30
mwd4	0.00	0.00	1.41	1.26	0.07	0.07	0.02	0.00	0.18	0.00	0.04	0.03	2.90	1.30	1.41

**Table 6.2 Analytical results of the eluate from the batch leaching test with deionised water (Concentrations in mg/l unless indicated).**

weathered ash was much reduced compared with the fresh PFA still some trace elements were being released from weathered PFA which has been weathered for more than 20 years. This was noticeable for As, Se and B.

The Meaford sample is believed to be older than that from Drax but there is no obvious evidence in the eluates that the Meaford ash is more weathered than the Drax ash. After depletion of the surface associated elements, matrix associated elements would be expected to be released from the weathered ash. In this case, for weathered ash, it is not the kinetic rate of dissolution of the surface-enriched fractions but rather the weathering of aluminosilicate PFA glass that will control the dissolution of the elements from the ash.

### **6.3.3 Mobility of elements and leaching behaviour - data from the batch leaching tests with deionised water**

#### ***6.3.3.1 Major elements***

The major elements that are readily leachable from fresh PFA are S (as  $\text{SO}_4^{2-}$ ), Ca, Na and K, in order of descending concentration (Table 6.2).

Ca in fresh PFA is very mobile and 13.0 % of total Ca was dissolved in the first eluate. Ca in weathered ash, however, was less mobile, with only 0.9 and 2.9 % of Ca being removed from weathered Meaford and Drax ashes, respectively, in the first eluates. This difference in mobility between fresh and weathered ash indicates that the elements being leached are dissolved from different locations. In the fresh ash, more soluble, surface-associated Ca oxides are being dissolved, whereas matrix-associated Ca, that is much less soluble, is probably contributing to the weathered ash eluate. Aquatic speciation of Ca shows  $\text{Ca}^{2+}$  free ion is the dominant species in the initial weathered Drax and Meaford PFA eluates, whereas  $\text{CaSO}_4$  is also an important species in the fresh ash eluate (Table 6.3).

S (as  $\text{SO}_4^{2-}$ ) is readily soluble both in fresh and weathered ashes. More than half of the total amount of S leached in the weathered ash, using deionised water, are present in the first eluates (Table 6.2). For the fresh PFA, more than 80 % of the total S is dissolved from the ash into the first eluate.

Na and K in fresh ash were relatively mobile, with 6.7 and 1.4 % of the initial contents respectively being present in the first eluates using deionised water. In both weathered ashes, these two elements were immobile, and only about 1.0 % or less were leached in the first eluate. The concentrations of Na and K do not decrease with successive eluates after the first eluate, both in fresh and weathered ash. The low mobility of Na and K from weathered ash is also attributable to the nature of their distribution within PFA, in the case of weathered PFA dissolution occurs from the PFA matrix, since much of the more soluble oxides initially present on the surfaces of PFA particles in fresh PFA have been removed.

	mwd1	mwd2	mwd3	mwd4	dwd1	dwd2	dwd3	dwd4	dfd1	dfd2	dfd3	dfd4
$\text{Ca}^{2+}$	89.5	96.1	97.2	97.9	91.3	95.9	97.6	96.8	46.7	71.5	93.3	91.1
$\text{CaSO}_4$	8.2	2.4	1.1	0.7	6.6	1.9	0.7	0.6	48.1	10.9	2.6	1.2
$\text{CaHCO}_3$	2.1	1.3	1.5	1.0	2.0	1.7	1.4	1.5	0.4	0.3	3.7	1.6
$\text{CaCO}_3$	0.1	0.2	0.2	0.3	0.2	0.5	0.4	1.1	4.8	17.3	0.3	6.1

**Table 6.3 Variations in aqueous Ca species distribution in the eluates using deionised water (Unit: %, the legend is the same as that in Table 6.2)**

$\text{Cl}^-$  and Mg are leached from the PFA, but concentrations are low in the first eluate, which suggests these elements are not associated with the enriched surface layers of the PFA. Furthermore the concentrations do not decrease with successive leaching, nor are the concentrations different to those of the eluate of weathered ash. In the case of Mg, however, this was leached in appreciable amounts by synthetic leachate. The concentration of Mg in solution is pH-dependent and in a highly alkaline environment Mg is retained by PFA as

$\text{Mg}(\text{OH})_2$  (van der Sloot and Wijkstra *et al.*,1982). The leaching behaviour of Mg may indicate the presence of a solubility controlling phase.

Al, Fe and Si are virtually immobile in both fresh and weathered PFA, and only small amounts were leached. The concentrations of Al, Fe and Si in both weathered and fresh ash are similar and do not decrease in successive eluates as do Cl and Mg. This leaching behaviour also indicates that Al and Si are not concentrated in the easily soluble, surface-enriched fractions of PFA. Speciation calculations for Fe in the eluates indicate that free Fe ion was exclusively present in the oxidised form:  $\text{Fe}^{3+}$ , and Fe-hydroxides including  $\text{Fe}(\text{OH})_2$ ,  $\text{Fe}(\text{OH})_3$  and  $\text{Fe}(\text{OH})_4$  were the main aquatic species in the eluate (Table 6.4).

	mwd1	mwd2	mwd3	mwd4	dwd1	dwd2	dwd3	dwd4	dfd1	dfd2	dfd3	dfd4
$\text{Fe}(\text{OH})_2^+$	36.2	21.4	26.7	10.6	27.2	12.3	11.9	4.5	0.1	0.0	34.4	0.5
$\text{Fe}(\text{OH})_3$	62.9	76.6	71.9	84.5	71.4	83.4	83.9	83.8	27.5	8.8	64.7	58.9
$\text{Fe}(\text{OH})_4^-$	0.8	2.19	1.4	4.9	1.5	4.4	4.2	11.7	72.4	91.2	0.0	40.6

**Table 6.4 Variation of aquatic Fe species in the eluates obtained by deionised water (Unit: %, the legend is the same as in Table 6.2)**

Observation of the leaching behaviour of the major elements indicate that the admixtures of soluble salts on the surfaces of PFA particles (the surface-enriched fractions) appear to be readily soluble in fresh PFA, releasing the S, Ca, Na and K which are present in these salts.

### 6.3.3.2 Trace elements

Cr, Mo and B all show marked decreases with successive eluates from fresh PFA, with lower values recorded for the two weathered PFA samples, which suggests surface enrichment of these elements. Even though the concentration of Cr decreases markedly, the total amount of Cr leached from solid PFA is small, only 3.5 % in the fresh ash and below 1 % in the weathered ashes. This

implies that less soluble Cr fractions could exist in a solid solution form within the Si-rich crusts of glass particles, as well as occurring within the more soluble surface associated fraction, as was suggested by Hulett and Weinberger (1980). B is known to exist in two different species; one is readily soluble and the other insoluble (Cox *et al.*, 1978). He reported that about 50% of B was water leachable and the other was essentially insoluble. In the leaching of weathered ash, the concentration of B in the eluate was very low and had a constant value in successive eluates, whereas it was more soluble in the fresh ash. This suggests that B species in the weathered ash are less soluble than those in the fresh ash. B is known to be volatile and predominantly located on the surfaces of PFA particles (Clarke and Sloss, 1992), and this evidence of a different solubility for B species in weathered and fresh ash seems to agree with previous research, such as that by Cox *et al.* (1978).

V decreases, but not markedly so, with successive eluates, whereas As and Se remain more constant. The latter behaviour would be anticipated from elements present in particulate material, possibly in a relatively unstable glass, rather than an element with a surface association.

Other trace elements that the present study suggests are readily leached include Sr, Cu, Li, Zn, Hg and Zr, and possibly Cd, Ni and Co. The uncertainty arises because the concentrations were close to the detection limits. Fe could be grouped with V as elements which are leached only marginally more readily from the fresh ash in the initial extraction than in subsequent extractions, whereas Ba and NO<sub>3</sub> behave like As and Se in that the amount extracted in successive leaches is more uniform. The proportions of elements extracted from fresh PFA is much larger than that from weathered ash, especially for B, Hg and S. Some elements, such as As and Pb, showed greater discharge from

weathered ash, this is thought to be due to an increase in acidity as weathering progresses.

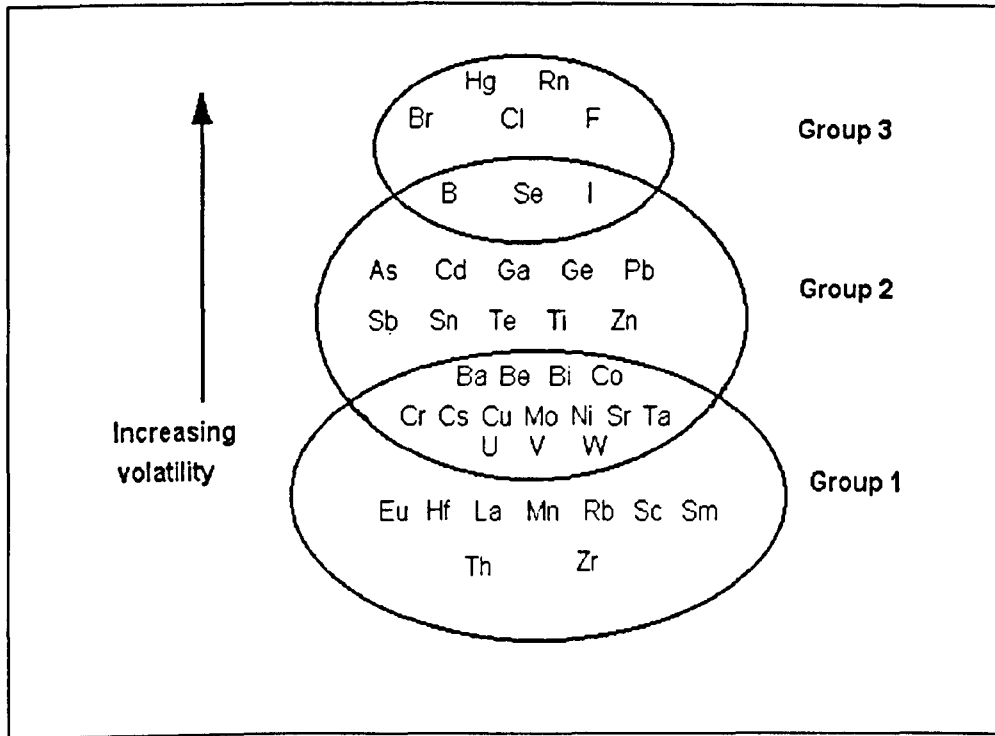


**Figure 6.1 Classification of trace elements by their behaviour during combustion and gasification (after Clarke and Sloss, 1992)**

The behaviour of these elements broadly conforms with the behaviour determined by other authors, although there are differences, probably reflecting overall differences in ash composition and the distribution of elements in the ash, which is related to combustion conditions. Hjelmars (1990) noted that the only trace elements leached in appreciable amounts were those forming anionic species (Cr, Mo, As, Se and V). The solution concentrations recorded were certainly higher for Cr and Mo (maximum 16 and 41 mg/l respectively) than in the present work (Table 6.2). Without question, solubility is an important factor controlling solution concentrations, but how much of an element may be leached from PFA is also a function of the location of the element within the PFA. The higher the volatility of an element during combustion the more likely

it is that the element is surface associated and hence accessible to leaching. The compilation of trace element behaviour during combustion produced by Clarke and Sloss (1992) arranges the elements according to volatility in three overlapping groups (Figure 6.1).

#### **6.3.4 Comparison of the eluates from deionised water with water quality standards**

The Standard Method DIN 38414-84 (October, 1984), which was adopted in this study, was designed to assess the leachability of sediment and slurry. The analytical result of PFA extracts using deionised water are compared with: the water quality standard of the EEC (Table 6.5), which is the Council directive for surface water intended for the abstraction of drinking water (75/440/EEC, June 1975); and the Landfill directive (EEC official journal No C190/1, July 1990). Among the several standards for surface water used for the abstraction of drinking water, two standards were adapted. Category A1 is the guideline for water which needs simple physical treatment and disinfection, and Category A3 covers water which needs intensive and extended physical and chemical treatment, such as disinfection by chlorination up to the break-point, coagulation, flocculation, decantation, filtration, and adsorption using activated carbon.

In fresh PFA eluate, Cd, Cr, Hg, Ni and  $\text{SO}_4^{2-}$  are in the hazardous range as classified by the EEC Landfill Directive, and in weathered ash only As falls in this range. Comparison of the weathered Drax and Meaford ash eluates with the Surface water directive shows that the levels of As, Cd and Hg in all the ash eluates exceed the mandatory guide of category A3, and Zn exceeds the guide level of category A1. The concentrations of Cr and Cu in fresh Drax and weathered Meaford ash eluate also exceed the guide level of category A1.  $\text{SO}_4^{2-}$  and B in the fresh ash eluate exceed the Surface water directive

guideline. When compared with the limits for drinking water, almost all elements in the eluate exceed the limit.

This comparison with the EEC guidelines suggests that eluate from the PFA disposal site needs special care before discharge and could affect the quality of drinking water.

	pH	As	Cd	Cr	Cu	Pb	Hg	Ni	Zn	Cl <sup>-</sup>	SO <sub>4</sub> <sup>2-</sup>	B
<b>*Landfill Directive</b>	4-13	0.2- 1.0	0.1- 0.5	0.1- 0.5	2-10	0.4- 2.0	0.02- 0.1	0.4- 2.0	2-10	1200 - 6000	200- 1000	-
<b>**Surface water(A3)</b>	-	0.10	0.005	0.05	-	0.05	0.001	-	5.0	-	250	-
<b>↑surface water(A1)</b>	6.5- 8.5	0.01	0.001	-	0.02	-	0.0005	-	0.5	200	150	1.0
<b>Drinking water↓</b>	<9.5	0.05	0.005	0.05	0.10	0.05	0.001	0.05	0.1	25	25	1.0
<b>Drax Fresh</b>	9.4	0.14	0.12	0.30	0.10	0.01	0.22	0.13	0.18	6.1	492	2.8
<b>Drax Weath.</b>	7.3	0.31	0.01	0.01	0.01	0.02	0.01	0.00	0.05	7.1	18	0.2
<b>Meaford</b>	7.1	0.18	0.07	0.06	0.06	0.01	0.01	0.06	0.12	3.2	21	0.2

**Table 6.5 Comparison of eluates from fresh and weathered PFA with the EEC Landfill Directive (Unit: mg/l except for pH)**

#### 6.4 Electrical conductivity and relationship with eluate quality

Electrical conductivity (EC) was measured and this value decreases rapidly as the concentration of elements decrease. Electrical conductivity is the reciprocal of electrical resistivity and EC has higher values with higher concentrations of ions in water, and so it may be used as a measure of the amount of elements dissolved in the eluate.

Regression analysis of EC and total ion concentrations in the eluate reveal a straight line relationship with a highly significant correlation coefficient ( $r=0.99$ ) (Figure 6.2 (a)). EC is known to reflect the total concentrations of dissolved ions in the solution, and these two parameters are quantitatively related (U.S. Salinity Lab, 1954). Elsewi and Page *et al.* (1980) measured the electrical conductivity in various solutions, including water extracts, 0.01N NaCl extracts, and 0.1N NaCl with pH 3 extracts, and reported that conventional estimates of total ion concentrations in solution, expressed as meq/L, obtained by multiplying EC by 10 gave overestimates. In this

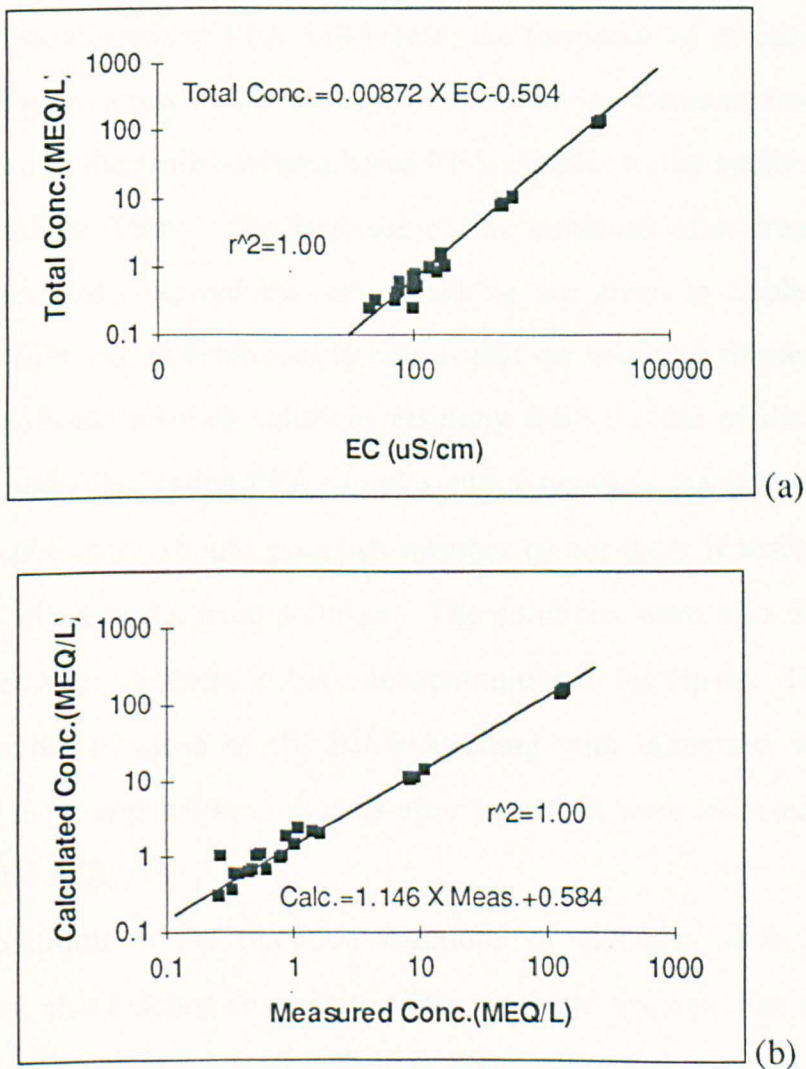


**Figure 6.2 Correlation between total ion concentration and electrical conductivity in the ash eluate**

experiment, however, the linear relationship between measured EC and the total ion concentration show a highly significant correlation coefficient ( $r=0.99$ ) and a good agreement between the measured total ion concentrations and the ones estimated from EC (Figure 6.2(b)). Thus measured EC can be used as a rough and quick measure of the total sum of dissolved solids in the PFA eluate.

## 6.5 Reaction of PFA with synthetic leachate

### 6.5.1 Introduction

The natural weathering of PFA will lead to the formation of reaction products, including clay minerals which are capable of removing elements from solution. The response of the fresh and weathered PFA samples to the synthetic leachate should therefore differ. The analyses of the solutions after treatment with synthetic leachate followed by water leaching are given in Table 6.6. One important difference in behaviour to note is that the resulting solutions are acid compared with the alkaline solutions resulting from the use of distilled water (Table 6.6 and 6.2). Using PFA samples and a synthetic leachate in the batch leaching experiments should establish whether or not there is reaction leading to the loss of elements from solution. The solutions were also analysed for other elements only present in trace concentrations in the eluate. These results are comparable to those of the batch leaching with deionised water. The changes in the composition of eluates after treatment were assessed as well as those of solid PFA.

In addition to the retention reactions of elements with PFA, some elements are also leached from PFA. The synthetic leachate has a pH of 4.5 and contains organic acids and there is a greater loss into solution than is the case with deionised water. the solubilities of Si, Al, Fe, Ca and Mg from the common silicate minerals are higher in organic acids than in water (Huang and

Keller, 1970). This is well illustrated by Si, Al, Sr, Mn and B, and also applies to a number of other elements (Table 6.6), but the synthetic leachate is not an ideal solution to study PFA dissolution of the elements in low concentrations because blank concentrations are high. Differential dissolution, nevertheless, does provide information about element reactions in the ash, providing that the experimental conditions are designed for dissolution and not, as in the present case, for investigating elemental loss from solution.

## 6.5.2 Batch leaching of fresh Drax PFA with synthetic leachate

### 6.5.2.1 Changes in solution

The first eluate from fresh Drax ash using the synthetic leachate (Dfs1, Table 6.6) yielded high solution concentrations of Ca, Na, K and S (as  $\text{SO}_4^{2-}$ ), which exceeded the concentrations of the synthetic leachate (Figure 6.3). Much Cl<sup>-</sup> was retained in the ash, contrary to the other elements. The differences are broadly comparable with the behaviour of the ash with distilled water (Table 6.2). The eluate does, however, contain organic acids, and this could account for the enhanced dissolution of Ca. The same explanation applies to Mg, which is present in the synthetic leachate but has a higher concentration after reaction. The concentrations of Na and K do not show large changes after treatment.

One element which does decrease significantly after reaction is Fe. The solution concentration of the Fe is reduced by approximately 50 %.

Figure 6.4 shows retention of trace elements from synthetic leachate, within PFA, after batch leaching tests. The negative sign in the diagram indicates the amount of loss from the synthetic leachate. The other elements present in the eluate as major components are Cd, Cr, Li, Ni, Zn and Hg. In all cases, concentrations after reaction are comparable to the starting composition, with possibly Cu decreasing, suggesting reaction with the PFA.

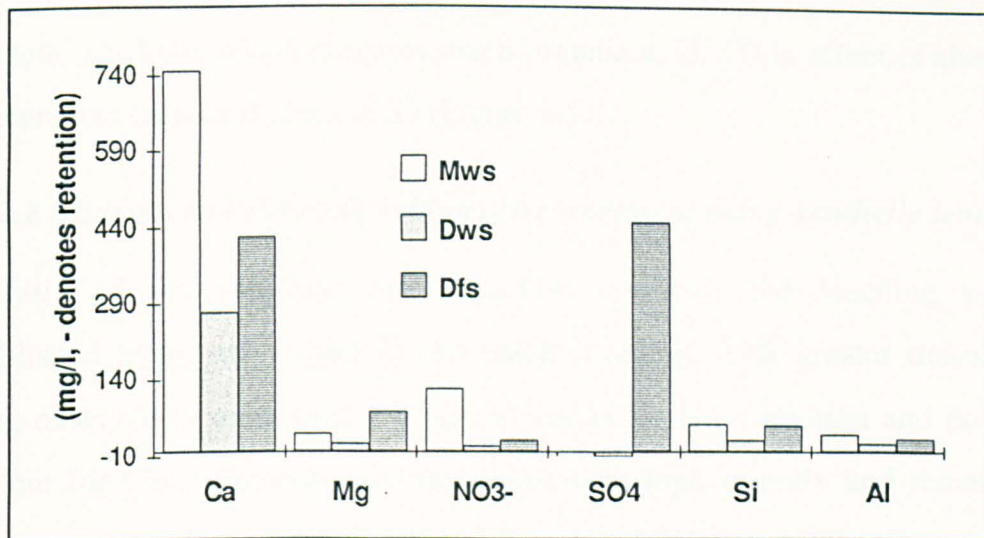


**Figure 6.3** Change of concentration of the major elements in the first eluates of Drax and Meaford ashes after treatment with synthetic leachate. (Positive value indicates amount leached from PFA and negative value indicates the amount retained by PFA)

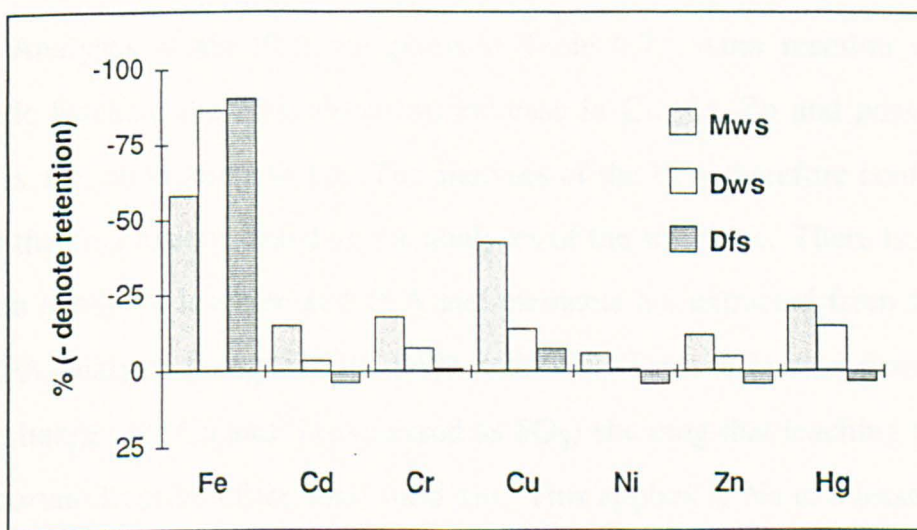


**Figure 6.4** Changes in the percentage of trace elements (Fe, Cd, Cr, Cu, Ni, Zn, Hg) in eluates after treatment with synthetic leachate (A negative sign indicates the % retained in the ash)

Si and Al are present only in trace concentrations in the synthetic leachate but after reaction solution concentrations are greatly in excess of amounts liberated with distilled water (Figure 6.3). As for the greater dissolution of Mg this is attributed to the more aggressive nature of the

synthetic leachate, which contains much organic acid. This effect is also seen for elements such as B, As and Se (Figure 6.5).

### **6.5.2.2 Changes in PFA composition after treatment using synthetic leachate**

Analysis of the solutions after reaction confirms the leaching pattern established using only water in the batch leaching, with greater dissolution being observed in most cases. There is loss of Fe from solution and possibly Cu, but for other elements concentrations were high initially and remain so. The experimental conditions had a high ratio of solution (500 ml) to sample (50g) and significant reaction with the PFA might not be detected in the solution analysis. This difficulty can be resolved by analysis of the PFA before and after the reactions.

Analyses of the PFA are given in Table 6.7. After reaction with the synthetic leachate the PFA shows an increase in Cu, Cr, Zn and possibly Ni. There is also an increase in Fe. The analyses of the PFA therefore confirm and extend the conclusions based on the analyses of the solutions. There is reaction between synthetic leachate and PFA and elements are extracted from solution. The PFA analysis (samples DF, DFD and DFS, Table 6.7) also demonstrate major changes for Ca and S (expressed as  $\text{SO}_3$ ) showing that leaching removes an important fraction of the total solid ash. This applies to Na to a lesser extent but not to K.

### **6.5.3 Batch leaching of weathered Drax PFA with synthetic leachate**

A comparison of weathered and fresh Drax PFA after deionised water leaching demonstrated a greater loss into solution from the fresh ash (Table 6.2, 6). The same relationship holds when comparing the performance of the two materials with synthetic leachate, (Dws 1 and Dfs 1 Table 6.6, Figure 6.3). Only in the case of Ca, however, is the amount leached significantly greater than the initial concentration in the eluate. Na, K and S (as  $\text{SO}_4^{2-}$ ) are all present at

concentrations close to those of the eluate. For the elements Mg, Al, B, Ba, Si and Sr, which are either absent or low in concentration in the eluate, the loss from the ash into solution is greater than for deionised water. The same relationship was noted for the fresh ash. This behaviour is due to the acidity of the synthetic leachate, as was discussed earlier.

The elements Fe, Cr, Cu, and possibly Zn and Hg, show a decrease in concentration in solution, after treatment of the weathered PFA (Figure 6.4). In order to substantiate the conclusions regarding reaction and loss from solution, the analyses of weathered Drax PFA after treatment with deionised water and eluate are compared (samples Dwd and Dws in Table 6.2, 6). There are increases in Cr, Cu and Zn in the ash after reaction with the synthetic leachate. The gain in Fe by the PFA noted in the solution analyses is not apparent in the PFA analyses (Table 6.7). This is because Fe is a major component of the ash and the gain is proportionately small. Nevertheless, in general, the analyses of the PFA and of the solutions after reaction do demonstrate reactions leading to loss of elements from solution.

#### **6.5.4 Batch leaching of weathered Meaford PFA with synthetic leachate**

Analyses of the solutions obtained from the Meaford sample are shown in Table 6.6 (Mws 1 - Mws 4). There is close agreement with the results obtained from the weathered Drax sample. There is major dissolution of Ca, but Na, K and S (as  $\text{SO}_4^{2-}$ ) are close to their initial eluate concentrations. As noted in previous sections the low pH eluate produces greater dissolution than water. Elements not present in the synthetic leachate, or present only in trace amounts, are observed after the batch leaching in high concentrations. In this category are Mg, Al and Si.

A key observation in this work is the reduction in concentrations of Fe, Cd, Cr, Cu, Ni, Zn and Hg in the eluate after reaction with the weathered Meaford PFA (Mws1 Table 6.6). Compared with the weathered Drax PFA

there is a greater fall in concentrations and two additional elements show significant decreases, namely Cd and Ni. These findings are confirmed by analyses of the weathered Meaford PFA, which is higher in Fe, Cr, Ni, Cu and Zn after treatment with the eluate (sample MWS compared with MW, Table 6.7). Evidence of reaction is therefore obtained for these elements, both by gain onto PFA and loss from solution. The magnitude of the changes for these elements is:

weathered Meaford PFA > weathered Drax PFA > fresh Drax PFA.

This corresponds to the age, and presumably the extent, of weathering and formation of secondary minerals.

#### **6.5.5 Trace elements retention from synthetic leachate**

Trace elements in the synthetic leachate are either retained in PFA or the synthetic leachate dissolve elements from the PFA during the batch leaching tests. The leaching behaviour of the trace elements using the synthetic leachate is here compiled according to the type of result obtained from the batch leaching tests. Largely element behaviour can be divided into three different categories, retention, limited retention and dissolution. However, only Cu and Fe showed large retention in general.

##### ***6.5.5.1 Group 1: Significantly retained in the ash (Cu and Fe)***

Cu is similar in behaviour to Fe in that all three samples show a decrease in concentration after treatment with synthetic leachate, but the relative changes differ, and only the relative changes of Cu and Fe in the weathered Meaford sample are comparable. More than 40 % of Cu in the synthetic leachate was retained in weathered Meaford ash, whereas 12.2 % and 6.8 % were retained in weathered and fresh Drax ash respectively (Figure 6.4).

	pH	Pe	C (mS)	Ca	Na	K	Mg	Fe	Al	B	Ba	Cd	Cr	Cu	Li
Syn. Lea.	4.55	9.10	3550	615.9	1032.2	734.6	86.99	122.96	0.12	0.23	0.04	121.18	79.78	117.57	19.44
dfs1	4.80	10.48	15530	1038.3	1046.9	745.9	165.69	64.54	24.79	6.00	0.22	125.86	79.04	109.54	18.99
dfs2	5.31	8.98	1060	71.3	69.4	34.4	12.19	0.36	0.72	0.67	2.08	4.80	1.80	3.16	0.99
dfs3	5.92	7.78	98	9.3	5.6	3.5	1.33	0.00	0.04	0.19	0.76	0.38	0.40	0.24	0.06
dfs4	6.74	7.25	36	3.1	1.3	0.7	0.54	0.02	0.03	0.06	0.47	0.04	0.23	0.02	0.01
dws1	4.75	10.55	14400	888.3	1034.8	731.2	102.46	65.93	16.65	0.65	0.72	117.18	74.23	103.23	19.45
dws2	5.15	8.99	1123	65.8	79.6	42	9.38	0.90	0.98	0.25	1.24	5.71	2.17	3.61	1.20
dws3	5.94	7.80	105	7.5	5.6	3.8	1.4	0.12	0.02	0.13	0.74	0.56	0.39	0.30	0.10
dws4	6.81	7.23	31	2.1	1.4	0.8	0.6	0.07	0.00	0.08	0.26	0.09	0.14	0.03	0.03
mws1	5.00	10.49	15720	1363.9	1023.9	727.7	121.14	51.31	33.60	0.83	0.48	103.10	65.57	67.57	18.89
mws2	5.51	8.91	1490	128.6	85.8	58.4	16.59	1.35	0.24	0.22	0.99	3.95	1.86	1.33	1.32
mws3	6.20	7.87	210	18.9	9.8	8.7	2.93	0.21	0.00	0.16	0.73	0.48	0.53	0.15	0.14
mws4	6.78	7.43	68	6.0	2.7	2.6	1.26	0.28	0.00	0.11	1.30	0.10	0.30	0.03	0.03
	Mn	Ni	Pb	Si	Sr	Ti	V	Zn	As	Hg	Se	Mo	Cl-	NO3-	SO4
Syn. Lea.	0.18	109.40	0.22	0.81	0.16	0.05	0.11	107.60	0.27	13.85	0.33	0.68	1973.49	20.67	419.25
dfs1	2.96	114.18	0.35	51.84	1.46	0.14	0.28	112.17	0.65	14.32	0.50	1.00	1005.95	43.30	869.68
dfs2	0.81	4.48	0.00	5.05	0.22	0.01	0.02	5.52	0.03	0.49	0.05	0.01	74.78	3.31	38.89
dfs3	0.12	0.23	0.01	2.28	0.08	0.00	0.01	0.71	0.01	0.01	0.04	0.00	4.22	0.79	6.08
dfs4	0.03	0.03	0.01	1.51	0.05	0.01	0.02	0.13	0.01	0.01	0.02	0.12	2.47	2.73	5.28
dws1	1.40	108.54	0.16	23.32	1.32	0.08	0.16	102.78	0.59	12.06	0.43	0.75	1065.44	31.42	408.30
dws2	0.48	5.76	0.00	6.57	0.18	0.00	0.02	6.85	0.02	0.58	0.05	0.01	78.06	1.93	21.00
dws3	0.08	0.51	0.00	2.85	0.09	0.00	0.01	0.88	0.03	0.01	0.04	0.00	5.77	0.46	5.05
dws4	0.02	0.07	0.00	2.23	0.02	0.00	0.01	0.21	0.01	0.01	0.06	0.00	0.88	0.87	3.25
mws1	3.56	102.97	0.23	54.89	5.05	0.13	0.15	94.60	0.56	10.89	0.50	0.70	1208.92	143.27	387.50
mws2	0.78	6.15	0.00	11.62	0.52	0.01	0.02	6.16	0.05	0.37	0.01	0.01	83.02	0.91	24.36
mws3	0.17	0.74	0.00	8.91	0.17	0.00	0.01	0.95	0.00	0.03	0.05	0.00	7.87	0.89	11.29
mws4	0.05	0.15	0.00	7.35	0.07	0.00	0.01	0.30	0.02	0.01	0.07	0.00	1.41	0.61	8.11

**Table 6.6 Analytical results of the eluate from the batch leaching test with synthetic leachate (Concentrations in mg/l unless indicated. df = Drax fresh PFA, dw = weathered Drax PFA, mw = Meaford weathered PFA. 1 indicates treatment with eluate. 2, 3 and 4 are successive treatments with synthetic leachate)**

	L.O.I.%	SiO <sub>2</sub> %	TiO <sub>2</sub> %	Al <sub>2</sub> O <sub>3</sub> %	Fe <sub>2</sub> O <sub>3</sub> (T) %	MnO <sub>2</sub> %	MgO%	CaO%	Na <sub>2</sub> O%	K <sub>2</sub> O%	P <sub>2</sub> O <sub>5</sub> %	SO <sub>3</sub> %	Mn
DF	0.92	53.01	0.95	26.58	7.39	0.06	1.69	1.86	1.70	3.89	0.24	0.48	498
DFD	2.55	52.92	0.94	26.63	6.95	0.06	1.70	1.43	1.53	3.85	0.24	0.06	467
DFS	2.49	53.70	0.97	26.79	7.61	0.06	1.58	1.10	1.56	3.96	0.23	0.03	476
DW	5.11	51.42	0.89	25.50	9.01	0.06	1.48	1.30	1.33	3.64	0.20	0.08	443
DWD	4.95	50.55	0.91	26.61	8.89	0.06	1.52	1.25	1.33	3.78	0.19	0.14	461
DWS	5.31	49.94	0.94	26.65	8.59	0.06	1.50	0.81	1.27	3.72	0.23	0.01	419
MW	8.31	43.81	0.80	24.18	14.04	0.14	1.41	3.19	0.78	2.14	0.30	0.18	1071
MWD	8.26	44.93	0.82	25.03	13.03	0.13	1.39	2.95	0.74	2.20	0.32	0.19	975
MWS	7.64	45.53	0.85	25.41	13.32	0.13	1.29	1.53	0.83	2.25	0.33	0.09	987
	NI	Cu	Zn	Rb	Sr	Y	Zr	Nb	Ba	Pb	V	Cr	Total
DF	109	162	110	180	314	48	190	20	1134	67	249	125	99.42
DFD	103	151	112	175	301	47	190	14	1158	68	252	129	100.14
DFS	112	269	134	178	296	49	194	18	1100	68	235	174	99.35
DW	113	179	113	167	251	46	179	18	771	84	272	129	100.09
DWD	133	194	125	173	271	56	183	17	856	95	285	146	100.29
DWS	133	401	157	178	262	50	182	17	865	98	296	212	99.11
MW	143	173	800	107	323	53	168	13	1071	175	244	105	98.87
MWD	142	176	808	109	322	49	166	14	1030	183	249	106	98.64
MWS	224	731	1039	115	296	54	175	14	1105	220	264	250	100.16

**Table 6.7 Composition of PFA before and after treatment with distilled water (d) and synthetic leachate (s). Concentrations of major elements are percentages and trace elements are parts per million. PFA samples indicated as follows: DF = Drax fresh, DW = Drax weathered, MW = Meaford weathered. The suffixes D and S indicates composition after treatment with deionised water (D) and synthetic leachate (S).**

### 6.3.5.2 Group 2: Limited retention reaction (Cd, Cr, Ni, Zn and Hg)

Other elements, namely Cd, Cr, Ni, Zn and Hg, show only limited retention, and then only in the Meaford sample with any certainty. In Drax PFA, the amount retained is greater in the weathered ash than in the fresh ash, as is shown in Figure 6.4. Among these elements, Cd, Ni and Zn were reported to be controlled by adsorption/desorption processes in the investigation of mobility to the groundwater aquifer (Talbot *et al.*, 1978), but the experimental condition of the batch leaching test does not appear to be favourable to this process.

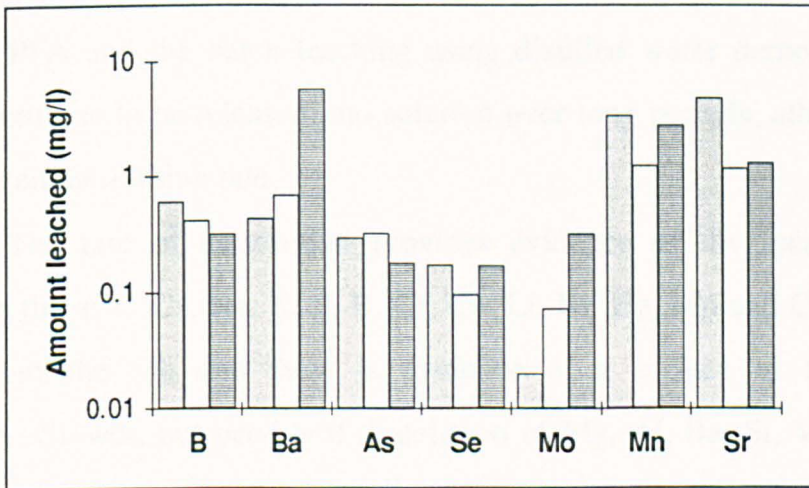


**Figure 6.5** Changes in the concentrations of trace elements (B, Ba, As, Se, Mo, Mn, Sr) in eluates after treatment with synthetic leachate (Symbols for the sample are the same as in Figure 6.3 and 4)

### 6.5.5.3 Group 3: Leached from the ash (Sr, Mn, As, B, Ba, Se, Mo and V)

Sr and Mn were released from PFA into solution and the order of amount released is similar to the amount of Al and Si released. About 4.2 to 15.2% of Sr was leached from PFA, and the amount of Mn released was about 2.8 to 5.6%, according to the type of ash. Mo and B were more leached from fresh PFA but the other elements (Ba, As and Se) do not show any dependence on the type of PFA (Figure 6.5).

## 6.6 Conclusion

The batch leaching experiments were conducted with the three types of PFA sample using distilled water as well as synthetic leachate, including fresh, weathered Drax ash and weathered Meaford ash. There were reactions between the PFA and the synthetic leachate and some of the element concentrations in the solution were reduced.

(1) Batch leaching of fresh PFA with distilled water confirms the results of other workers. However, little work has been undertaken previously on weathered PFA and the batch leaching using distilled water demonstrates that elements continue to be released into solution over long periods, albeit at a very much reduced dissolution rate.

(2) The rate of dissolution provides evidence of the location of the elements in the ash. Ca, Na, K, S, B, Cr, Cu, Li, Ni, Hg, Mo and Cl are readily leached from the ash and there is evidence of a surface or fine particle association. Slower, but persistent dissolution of Mg, Al, Ba, Si, V, As and Se are apparently present in less readily soluble components of the ash and presumably this is essentially the glass. Fe, Co, Pb, Sr, Zn and Zr exhibit intermediate behaviour.

(3) Comparing the concentration of elements in the eluate with the EEC directives for Landfill, and secondly, Surface water for the abstraction of drinking water, indicates that many trace element are in the hazardous range, which indicates that this eluate needs special treatment before discharge. Further comparison with the EEC Drinking Water Limits also show that both the Meaford and Drax PFA eluates greatly exceed the limits.

(4) Conductivity of the eluate shows a good correlative relationship with the total concentration of eluate expressed as meq/l. The calculated total concentration of PFA extracts also agrees well with measured concentration and

therefore the conductivity can be used as a quick reference for estimating the total dissolved quantity in the PFA eluate.

(5) In batch leaching experiments using a simulated land-fill leachate and weathered PFA, elements are removed from solution. Decreases in solution concentrations (measured by ICP) have been recorded for Fe, Cd, Cr, Cu, Ni, Zn and Hg. Confirmation of the increases on the PFA has been obtained by analyses of the PFA (Cd and Hg were not included in the XRF analyses).

(6) The order of metal retention by the three samples is: Meaford > weathered Drax > fresh Drax, which corresponds with the degree of weathering of the material. It is concluded that more weathered the sample is the more effective it is at removing elements from solution.

(7) The synthetic leachate contains organic acids with a pH of 4.5. Compared with the distilled water there is evidence of greater dissolution of a number of elements from the PFA. These are elements not present in the synthetic leachate.

## Chapter 7

### Column leaching Tests

#### **7.1 Introduction**

In the previous chapter (Chapter 6), the results of batch leaching tests were described, with the aim of confirming the field investigation and assessing the possible ameliorating ability of PFA during weathering reactions with landfill leachate from industry. Column leaching tests were also undertaken with the similar aims, primarily to extend the results obtained from the batch leaching tests, particularly the period of reactions. Compared with the batch leaching test, the column leaching test, which passes input solution continuously through the reacting column of PFA, is thought to yield longer-term data, which more closely model natural weathering conditions. The column leaching test also: allows a comparison with previous work on the leaching of fresh ash, provide laboratory information of weathering to compare with the field investigation. The experiments are inter-related, however, in term of the specific factors controlling the solubility of elements. The column and batch leaching experiments are complementary to each other, and also to field observations.

During the column leaching tests, six columns were run in total, filled with three different PFA samples (fresh Drax, weathered Drax, and weathered Meaford), and using two different input solutions, namely synthetic leachate and deionised water. The total period for completing the column leaching tests was 33 days, which is a short period compared with other long-term experiments, which have been conducted over several years, such as those by Jones and Lewis (1960), Brown and Ray *et al.* (1976), Dudas (1981), Fruchter and Rai *et al.* (1990), Hjelmar (1990).

## 7.2 Experimental Method

### 7.2.1 Samples with synthetic leachate

The same types of sample of PFA were used in the column leaching tests as were used in the batch leaching tests, namely fresh PFA from Drax, weathered PFA from the Barlow disposal mound (Grid Ref. SE 655277) and weathered PFA from the decommissioned power station at Meaford (Grid Ref. SS 896373).

*pH	Ca	Na	K	Mg	Fe	Al	B	Ba	Cd
4.55	764	1983	1007	97	100	nd	(0.28)	0.03	121
Co	Cr	Cu	Li	Mn	Ni	Pb	Si	Sr	Tl
(0.16)	76	111	22	(0.19)	106	(0.39)	(0.88)	(0.15)	(0.07)
V	Zn	As	Hg	Se	Mo	*Cl <sup>-</sup>	*NO <sub>3</sub> <sup>-</sup>	*SO <sub>4</sub> <sup>2-</sup>	
nd	109	(0.15)	6.7	nd	(0.27)	1973	21	419	

**Table 7.1 Composition of the synthetic leachate used in the column leaching tests (analysis by ICP. Unit: mg/l unless indicated. Those elements whose concentrations are shown in brackets originated as impurities in the standard chemicals)**

The solution used in the batch leaching tests was also used in the column leaching tests, but the synthetic leachate was analysed again to check any changes during the storage. Ca, Na, K, Fe and Hg show considerable changes, whereas the changes in the other elements were small. The composition of the simulated leachate is shown in Table 7.1.

### 7.2.2 Design of columns and experimental procedure

Six columns were constructed from acrylic plastic tubes, as shown in Figure 7.1, which is a modification of the column designed by Brown and Ray *et al* (1976). The PFA samples, in their natural moisture condition, were lightly packed into the columns to achieve a uniform density, comparable to those recorded in the literature (Dry bulk density: 1.01 mg/m<sup>3</sup> - 1.43 mg/m<sup>3</sup>,

Mattigod and Rai *et al.*, 1990). The dimensions of the column and the bulk densities are given in Table 7.2.

Test Code	Materials (samples and solutions used)	D X H (cm)	Weight (g)*	Moisture content(%)	Flow rate (mm/day)	Bulk density *
DFS	Drax fresh sample with synthetic solution.	5 X 40	1000	2.17	25	1.25
DFD	Drax fresh sample with deionised water.	5 X 40	940	2.17	25	1.17
DWS	Drax weathered sample with synthetic leachate.	5 X 40	1000	4.99	25	1.21
DWD	Drax fresh sample with synthetic leachate.	5 X 40	970	4.99	25	1.17
MWS	Meaford fresh sample with synthetic leachate.	5 X 40	1000	11.36	25	1.13
MWD	Meaford weathered sample with deionised water.	5 X 40	990	11.36	25	1.12

**Table 7.2 Test conditions for column leaching tests (\* Dry basis)**

1000 ml of solution, either deionised water or synthetic leachate, were passed through each column at a flow rate of 25 mm/day. The eluates collected from the column was sampled at intervals of 50 ml. Each collected sample was divided into two aliquots, one untreated, for the anion determinations by ion chromatography (Dionex 2000i), and the other acidified to 1 % in HNO<sub>3</sub> for the cation determination by ICP-AES. The results are given in Tables 7.3 and 7.5, for the deionised water and the synthetic leachate respectively. Difficulties were met in the column containing the weathered Meaford sample. A peristaltic pump was used to supply solution to the columns at a constant rate, but the pump could only be connected to up to four tubes at a time, so injection tubes were used for the two Meaford ash columns. As a result it was difficult to control the flow rate, and only the first 150 ml of the synthetic leachate solution passing through the column of weathered Meaford ash was collected.

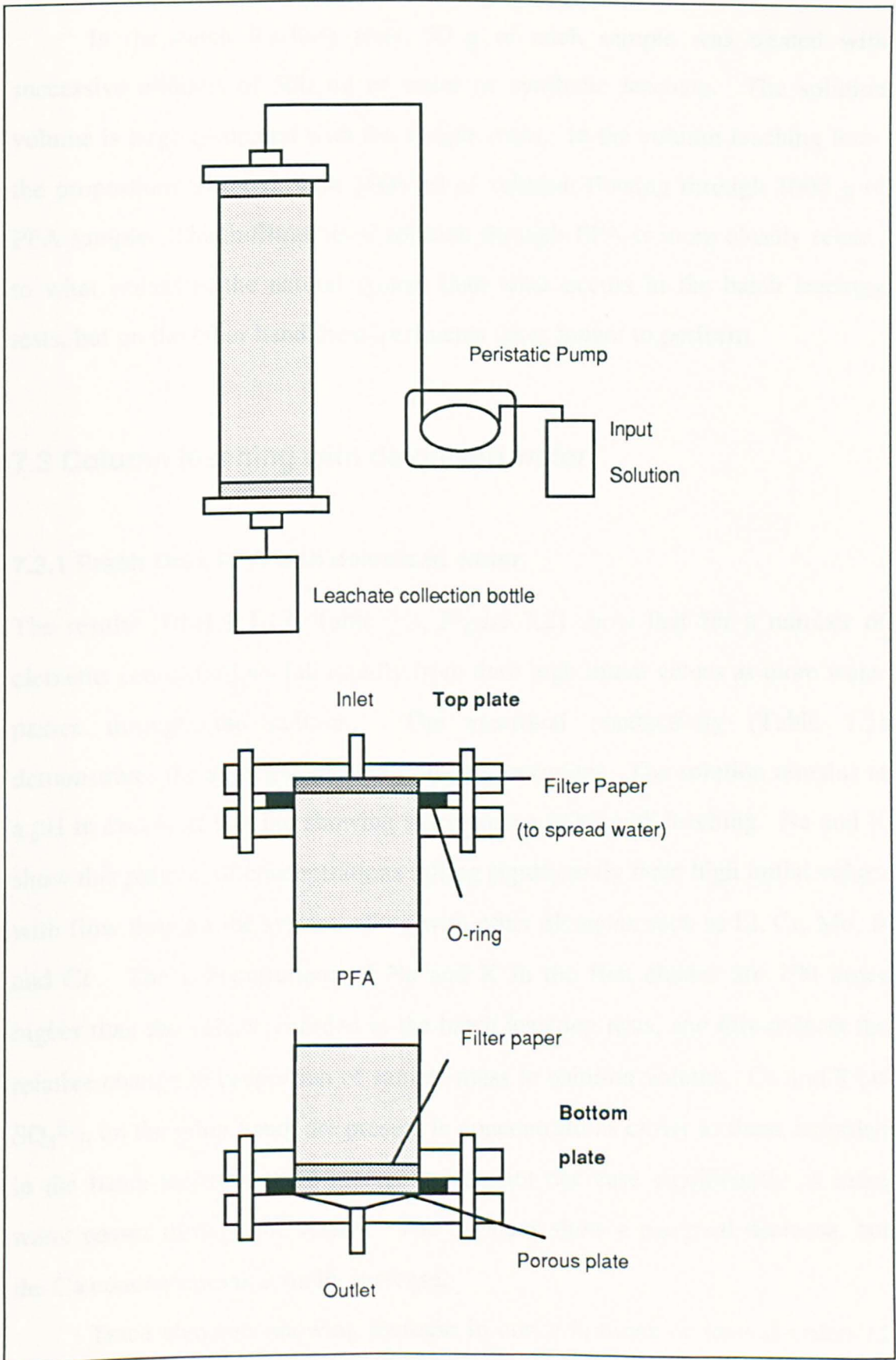


**Figure 7.1 Set-up for column leaching tests in down flow configuration**

In the batch leaching tests, 50 g of each sample was treated with successive aliquots of 500 ml of water or synthetic leachate. The solution volume is large compared with the sample mass. In the column leaching tests, the proportions differed, with 1000 ml of solution flowing through 1000 g of PFA sample. This infiltration of solution through PFA is more closely related to what occurs in the natural system than what occurs in the batch leaching tests, but on the other hand the experiments takes longer to perform.

## 7.3 Column leaching with deionised water

### 7.3.1 Fresh Drax PFA with deionised water

The results (Dfd1.1-1.13, Table 7.3, Figure 7.2) show that for a number of elements concentrations fall rapidly from their high initial values as more water passes through the column. The electrical conductivity (Table 7.3) demonstrates the aggregate decrease in concentrations. The solution remains at a pH in excess of 9.0, but showing a decreasing trend with leaching. Na and K show this pattern, of concentrations falling significantly from high initial values with flow through the system, along with other elements such as Li, Cr, Mo, B and Cl<sup>-</sup>. The concentrations of Na and K in the first eluates are 100 times higher than the values recorded in the batch leaching tests, and this reflects the relative change in proportion of sample mass to solution volume. Ca and S (as SO<sub>4</sub><sup>2-</sup>), on the other hand, are present in concentrations closer to those recorded in the batch leaching experiments, and do not decrease significantly as more water passes through the system. The S values show a marginal decrease, but the Ca concentrations actually increase.

Trace elements showing increase in concentrations of several orders of magnitude in the column leaching tests as compared to the batch leaching tests

	pH	C( $\mu$ S/cm)	Ca	Mg	Na	K	Fe	Al	B	Ba	Cd	Co	Cr	Cu
dfd1-1	9.35	22300	353.4	36.7	5760.5	2113.5	0.17	0.99	72.21	0.08	0.05	0.05	23.95	0.14
1-2	9.39	3430	350.7	22.5	1571.4	804.6	0.17	0.27	45.03	0.06	0.01	0.02	5.16	0.03
1-3	9.49	1630	430.9	20.9	471.0	433.0	0.31	0.24	33.07	0.06	0.01	0.02	1.66	0.01
1-4	9.46	1030	499.8	21.7	179.4	282.9	0.17	0.26	29.23	0.05	0.01	0.00	0.86	0.01
1-5	9.29	899	499.9	22.3	86.6	194.1	0.19	0.30	26.91	0.05	0.01	0.00	0.51	0.01
1-6	9.42	821	548.5	23.7	53.3	156.4	0.16	0.30	27.16	0.05	0.01	0.01	0.34	0.00
1-7	9.44	793	565.2	22.4	35.8	117.3	0.41	0.32	25.14	0.04	0.23	nd	0.50	0.43
1-8	9.20	759	587.1	22.0	27.2	102.2	0.33	0.37	23.33	0.04	0.01	0.05	0.12	0.09
1-9	9.14	744	601.1	21.6	24.5	89.8	0.20	0.29	22.28	0.03	0.00	nd	0.16	0.01
1-10	9.12	747	595.7	20.0	21.2	81.8	0.16	0.32	20.70	0.03	nd	nd	0.13	0.02
1-11	9.13	736	590.4	18.3	17.8	73.8	0.13	0.34	19.13	0.03	nd	nd	0.10	0.03
1-12	9.01	714	582.7	17.7	17.5	65.8	0.12	0.26	17.53	0.04	nd	nd	0.12	0.03
1-13	9.11	716	588.6	15.5	15.6	59.5	0.06	0.29	16.00	0.03	nd	0.02	0.08	0.03
dwd3-1	7.49	9560	1626.2	232.5	141.8	157.1	0.21	0.21	2.10	0.33	0.02	0.03	0.20	0.04
3-2	8.10	2960	516.8	65.3	57.9	79.0	0.05	0.05	1.50	0.15	0.00	0.01	0.10	0.01
3-3	8.11	330	112.9	14.1	25.1	42.6	0.12	0.06	1.31	0.14	0.00	0.02	0.06	0.01
3-4	8.21	281	93.5	11.8	17.6	39.0	0.10	0.04	1.21	0.15	0.00	0.01	0.04	0.00
3-5	8.25	171	64.3	8.2	11.3	30.5	0.15	0.06	0.98	0.09	0.00	0.01	0.05	0.00
3-6	8.32	145	53.7	6.9	9.0	26.7	0.16	0.08	0.95	0.92	0.00	0.00	0.05	0.00
3-7	8.35	144	60.8	7.7	11.3	29.3	0.07	0.05	1.51	0.11	nd	0.02	0.05	0.01
3-8	8.32	128	54.3	6.8	9.0	27.5	0.03	nd	1.13	0.11	nd	nd	nd	0.01
3-9	8.34	123	53.3	5.5	6.4	22.4	0.00	nd	0.78	0.10	nd	nd	0.07	nd
3-10	8.43	104	47.9	6.0	8.4	24.9	0.04	nd	0.85	0.12	nd	nd	nd	0.01
3-11	8.31	109	47.9	6.0	6.6	23.1	0.00	nd	0.82	0.15	nd	nd	0.04	0.03
3-12	8.23	103	44.6	5.7	5.6	23.1	0.01	nd	0.68	0.14	nd	nd	0.00	0.03

**Table 7.3 Analytical results for eluates of column leaching tests with deionised water (unit : mg/l unless indicated) Continued-**

	Li	Mn	Ni	Pb	Mo	Sr	V	Zn	As	Hg	Se	Si	Cl <sup>-</sup>	NO <sub>3</sub> <sup>-</sup>	SO <sub>4</sub> <sup>2-</sup>
<b>dfd1-1</b>	42.97	0.02	0.05	0.20	183.21	1.79	1.53	0.06	0.82	0.08	2.21	6.83	1122.0	93.9	1609.3
<b>1-2</b>	17.29	0.01	0.02	0.05	28.38	1.41	0.76	0.01	0.23	0.03	0.41	4.50	127.6	39.0	1506.2
<b>1-3</b>	8.42	0.01	0.02	0.07	6.62	1.37	0.49	0.04	0.08	0.02	0.12	3.37	21.4	15.9	1544.6
<b>1-4</b>	5.18	0.01	0.02	0.04	2.54	1.39	0.41	0.01	0.04	0.01	0.03	2.64	27.7	33.3	1078.0
<b>1-5</b>	3.78	0.00	0.02	0.03	1.71	1.38	0.39	0.01	0.08	0.02	0.07	2.53	10.6	29.8	1772.2
<b>1-6</b>	3.07	0.00	0.00	0.02	1.38	1.47	0.39	0.01	0.08	0.01	0.07	2.55	17.1	24.6	1573.2
<b>1-7</b>	2.45	0.00	0.01	0.07	0.65	1.41	0.26	0.24	0.01	0.07	nd	2.34	15.4	16.7	1446.8
<b>1-8</b>	2.14	0.00	0.07	0.25	0.64	1.45	0.38	0.03	0.00	nd	nd	2.40	10.5	19.1	1495.5
<b>1-9</b>	1.98	0.00	nd	0.17	0.80	1.48	0.29	0.01	0.00	nd	nd	2.49	5.9	6.2	1504.2
<b>1-10</b>	1.77	0.00	0.00	0.10	0.69	1.48	0.33	nd	0.07	nd	nd	2.40	10.3	7.7	1427.4
<b>1-11</b>	1.57	0.00	0.00	0.02	0.57	1.48	0.38	nd	0.15	nd	nd	2.31	6.8	4.3	1460.2
<b>1-12</b>	1.46	0.00	0.01	0.29	1.04	1.48	0.43	0.02	0.35	nd	0.30	2.40	2.5	3.2	1413.5
<b>1-13</b>	1.28	0.00	nd	0.09	0.97	1.50	0.39	nd	0.09	nd	0.06	2.39	2.2	1.2	1423.9
<b>dwd3-1</b>	0.24	0.02	0.04	0.14	0.64	6.94	0.28	0.37	0.29	0.01	0.55	8.87	1661.7	1224.7	3213.9
<b>3-2</b>	0.15	0.00	0.00	0.02	0.62	2.02	0.23	0.17	0.24	0.01	0.22	8.66	295.4	1056.0	676.5
<b>3-3</b>	0.14	0.00	0.03	0.02	0.38	0.50	0.19	0.10	0.23	0.00	0.13	7.41	54.3	167.2	138.4
<b>3-4</b>	0.10	0.00	nd	0.05	0.24	0.44	0.20	0.09	0.25	0.01	0.10	6.70	48.0	149.0	174.4
<b>3-5</b>	0.07	0.00	0.01	0.01	0.26	0.30	0.19	0.07	0.27	0.01	0.05	5.69	3.8	nd	63.7
<b>3-6</b>	0.06	0.00	0.02	0.01	0.21	0.26	0.20	0.08	0.28	0.00	0.11	5.94	11.1	58.0	101.2
<b>3-7</b>	0.07	0.00	0.00	0.10	0.30	0.26	0.22	0.09	0.28	nd	0.03	5.84	3.5	8.5	75.5
<b>3-8</b>	0.05	nd	0.01	nd	0.27	0.24	0.07	0.07	0.18	nd	nd	5.44	4.8	6.6	61.5
<b>3-9</b>	nd	nd	nd	0.01	nd	0.26	0.12	0.05	0.17	nd	nd	5.37	6.5	8.3	57.3
<b>3-10</b>	0.05	nd	nd	0.06	0.03	0.23	0.13	0.03	0.16	nd	nd	4.98	2.2	6.4	42.5
<b>3-11</b>	0.05	nd	0.00	0.08	0.30	0.23	0.10	0.08	0.19	nd	0.07	5.13	2.4	4.4	35.7
<b>3-12</b>	0.06	nd	nd	0.17	0.23	0.21	0.13	0.04	0.13	nd	nd	5.05	1.3	4.2	27.4

**Table 7.3 Analytical results for eluates of column leaching tests with deionised water (unit : mg/L unless indicated) Continued-**

	pH	C( $\mu$ S/cm)	Ca	Mg	Na	K	Fe	Al	B	Ba	Cd	Co	Cr	Cu
mwd6-1	8.54	499	225.3	28.8	32.3	41.7	0.12	0.07	1.89	0.13	0.02	0.02	0.11	0.03
6-2	8.26	373	182.2	25.2	19.9	35.6	0.15	0.07	1.11	0.13	0.01	0.01	0.10	0.02
6-3	8.34	366	190.7	24.6	21.5	38.2	0.00	nd	0.89	0.13	0.08	0.04	0.11	0.00
6-4	8.28	279	146.2	19.1	17.3	32.0	0.03	0.03	0.83	0.11	nd	nd	0.04	0.04
6-5	8.34	210	98.8	13.0	13.7	28.4	0.04	nd	0.78	0.09	nd	0.00	0.07	0.01
6-6	8.43	177	106.5	14.1	13.8	27.1	0.04	0.05	0.72	0.12	nd	nd	0.03	0.02
6-7	8.34	154	80.6	10.7	11.7	25.8	0.03	0.05	0.78	0.11	nd	0.02	0.04	0.01
6-8	8.18	145	66.9	9.1	10.4	22.2	0.06	0.08	0.72	0.12	nd	0.01	0.02	0.00
6-9	8.26	140	62.4	8.3	9.7	23.1	0.01	0.03	0.78	0.12	nd	0.03	0.01	0.01
6-10	8.28	129	59.0	7.8	8.7	20.4	0.02	nd	0.78	0.13	nd	nd	nd	0.03
6-11	8.31	113	55.2	7.5	7.8	22.2	0.07	nd	0.71	0.12	nd	nd	0.01	0.03
6-12	8.28	100	48.5	6.3	7.4	16.0	0.04	0.00	0.56	0.11	nd	nd	nd	0.03
6-13	8.24	99	49.7	6.5	6.4	17.8	nd	nd	0.55	0.12	nd	nd	0.01	0.01

	Li	Mn	Ni	Pb	Mo	Sr	V	Zn	As	Hg	Se	Si	Cl <sup>-</sup>	NO <sub>3</sub> <sup>-</sup>	SO <sub>4</sub> <sup>2-</sup>
mwd6-1	0.05	0.01	0.03	0.04	0.23	1.65	0.11	0.29	0.10	0.02	2.22	9.34	32.2	148.3	677.7
6-2	0.03	0.00	0.03	0.03	0.21	1.39	0.10	0.15	0.06	0.01	2.45	8.18	29.0	181.3	417.7
6-3	0.06	0.00	0.07	0.02	0.27	1.36	0.13	0.19	0.13	nd	2.08	6.41	120.5	18.2	354.1
6-4	0.04	0.00	nd	0.13	0.03	1.03	0.06	0.09	0.21	nd	1.70	5.77	10.3	47.0	267.0
6-5	0.02	0.00	nd	0.05	0.13	0.71	0.06	0.05	0.09	nd	0.21	5.55	4.5	16.9	162.6
6-6	0.03	0.00	nd	0.19	0.03	0.76	0.05	0.08	0.19	nd	nd	5.32	7.5	11.3	150.3
6-7	0.03	0.00	nd	0.21	0.09	0.60	0.07	0.06	0.07	nd	nd	5.25	1.7	4.5	34.8
6-8	0.01	0.00	nd	0.25	0.03	0.50	0.04	0.07	0.18	nd	nd	4.86	0.9	6.2	73.4
6-9	0.03	0.00	0.00	nd	nd	0.49	0.08	0.06	0.06	nd	nd	4.95	3.6	2.4	61.8
6-10	0.02	0.00	nd	0.15	0.00	0.46	0.01	0.05	0.15	nd	0.45	4.97	2.2	2.6	56.5
6-11	0.01	0.00	nd	0.24	0.07	0.44	0.01	0.03	nd	nd	nd	4.70	3.8	2.0	50.2
6-12	0.04	nd	nd	0.32	0.13	0.38	0.00	0.04	0.16	nd	nd	4.02	4.0	3.7	44.0
6-13	0.01	nd	nd	0.01	0.07	0.39	0.06	0.01	0.08	nd	nd	4.08	8.0	1.9	39.2

**Table 7.3 Analytical results for eluates of column leaching tests with deionised water (unit: mg/l unless indicated)**

are: B, Cr, Li and Mo. These elements are readily leached and the anionic species for B, Cr and Mo are soluble at the pH values encountered.

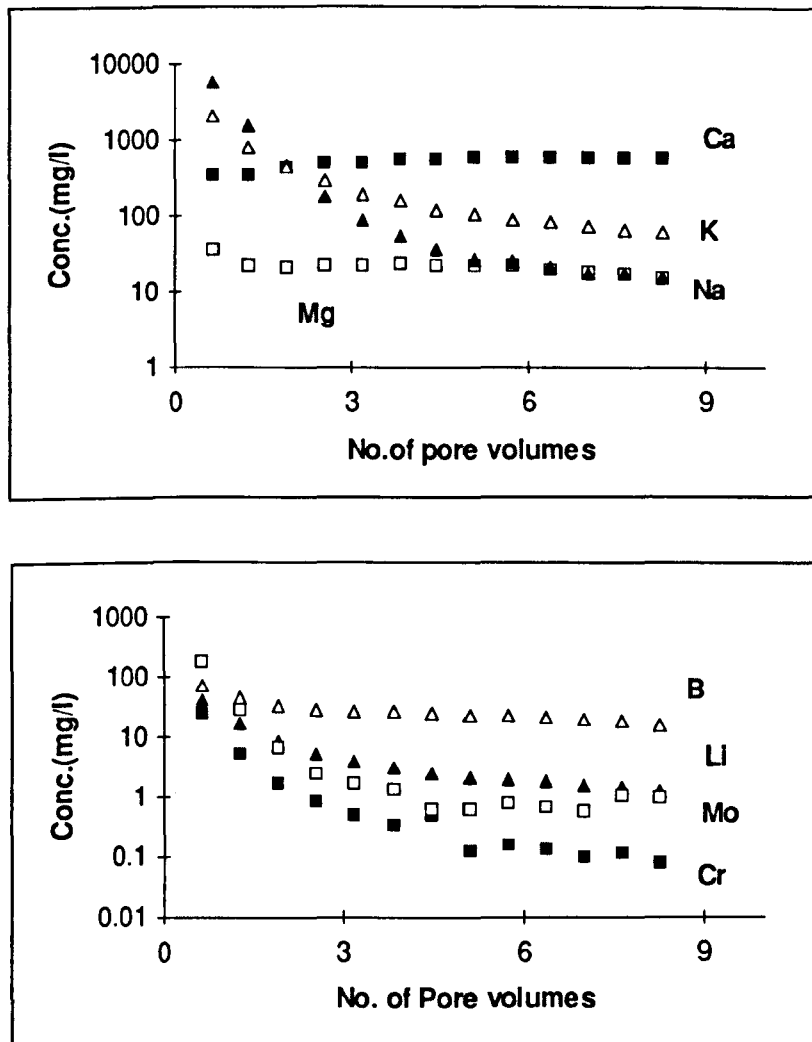


**Figure 7.2 Variations in elemental concentrations in fresh Drax PFA eluate treated with deionised water (Continued-)**

Other elements are recorded at concentration levels comparable with those of the initial batch leaching, and concentrations either decrease, but proportionally less than for elements such as Na and K, or remain approximately constant. The former include Si. In the latter category are Fe, Al, Ba and Sr and equilibrium reactions are indicated. Among the anions,  $\text{Cl}^-$  and  $\text{NO}_3^-$  were highly leachable in the initial eluate, but leachability decreased progressively. The increase in the alkalinity of the PFA eluate is thought to be

mainly due to the rapid hydrolysis and dissolution of Ca, Mg and  $\text{SO}_4^{2-}$  as was suggested by Hodgson and Dyer *et al.* (1982).

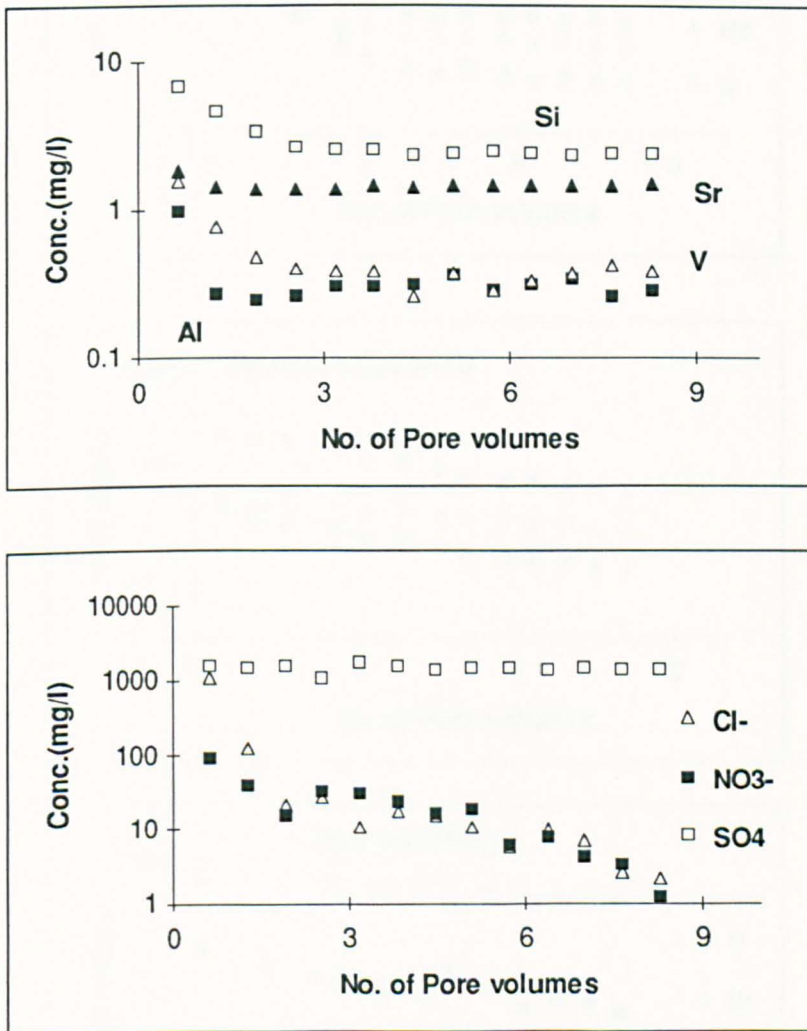


**Figure 7.2 Variations in elemental concentrations in fresh Drax PFA eluate treated with deionised water**

#### 7.4.2 Weathered Drax and Meaford PFA with deionised water

The analyses (Dwd 3.1-3.12 and Mwd 6.1-6.13, Table 7.3, Figure 7.3) showed low initial concentrations for the readily soluble elements, in general, and for Na and K in particular, which is to be expected as these are weathered samples. Na and K concentrations decreased as more water passed through the column, but K eventually achieved a near-constant concentration.

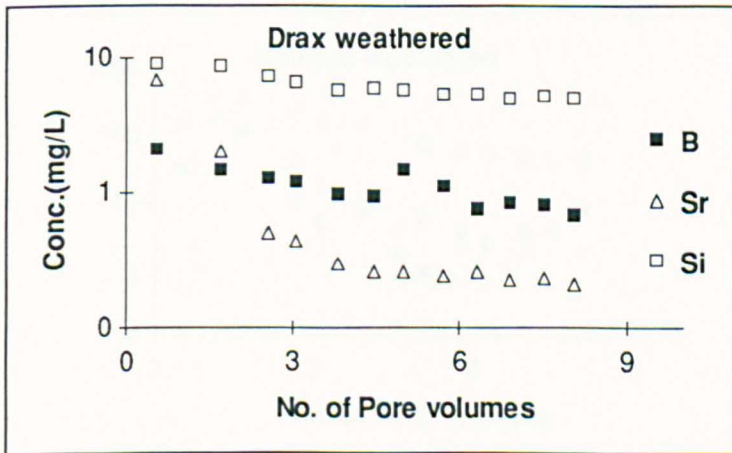
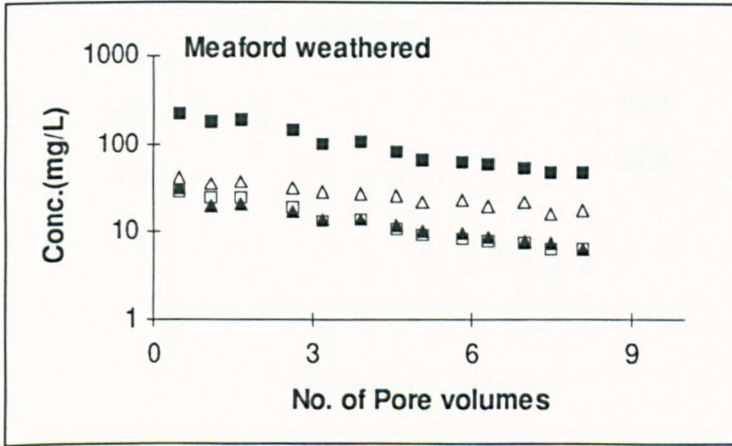
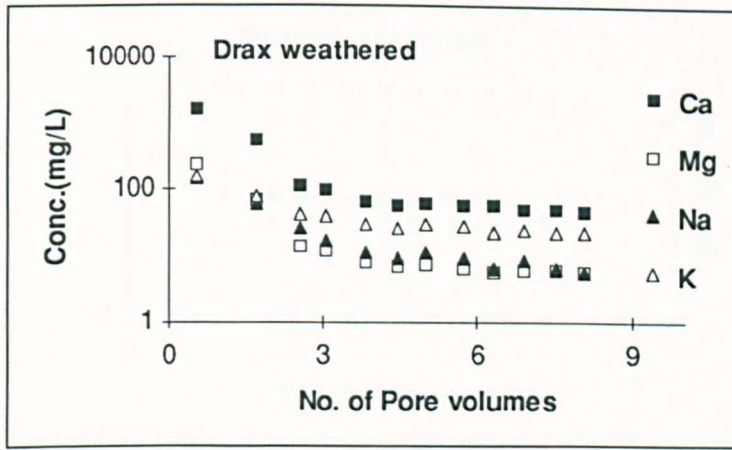


**Figure 7.3 Variations in elemental concentrations in weathered Drax and Meaford PFA eluate treated with deionised water (symbols are the same for both Drax and Meaford data) (Continued-)**

Compared with the fresh PFA, B, Cr, Li and Mo are all present in much lower concentrations in the weathered PFA. This is essentially due to the removal of the readily accessible elements from the PFA during natural

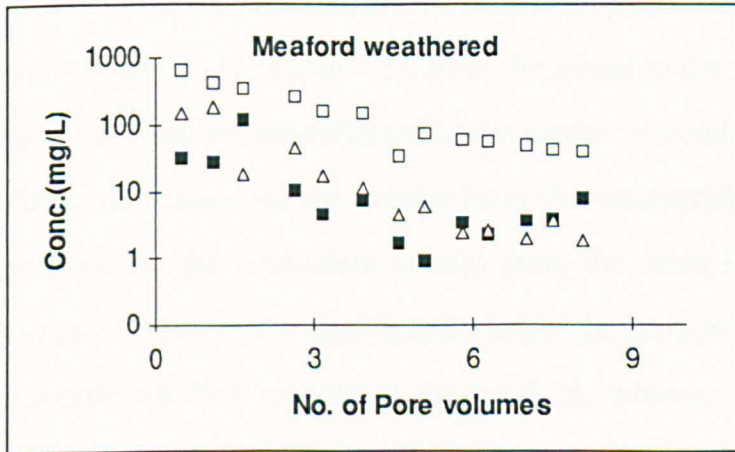
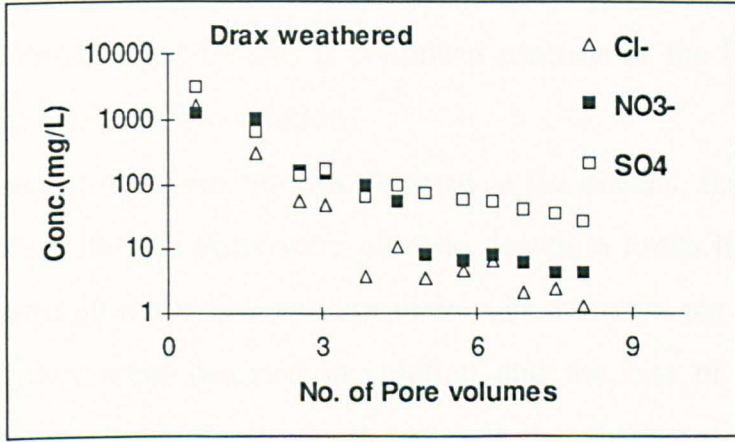
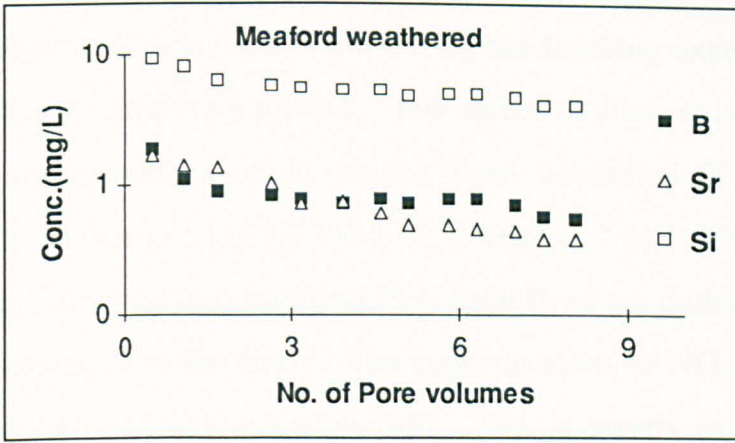


**Figure 7.3 Variations in elemental concentrations in weathered Drax and Meaford PFA eluate treated with deionised water (symbols are the same for both Drax and Meaford data)**

weathering. The PFA samples were not dried before the columns were packed so the initial concentrations recorded should be approaching those of the

natural porewaters. Concentrations fall during the leaching experiment, as the porewaters were progressively diluted. How effective dilution is, may be seen in the  $\text{NO}_3^-$  concentrations of the eluates from weathered PFA from Drax (Sample Dwd analyses 3.1-3.12 Table 7.3, Figure 7.3). The high  $\text{NO}_3^-$  concentrations compared with the fresh PFA from Drax are probably a result of external derivation, from fertilisers. The concentrations of  $\text{NO}_3^-$  in the eluate decrease by a factor of approximately 300. This is greatly in excess of the decreases noted for B, Cr, Li and Mo, which all decrease by a factor of less than 10. The explanation for this is continued reaction of the PFA, releasing these and other elements into solution.

A range of trace elements was detected in the eluates, for example Cd, Co, Cu and Hg, although these were close to detection limits in a number of cases. Concentrations are low and are mainly in the parts per billion range. Nevertheless, they were detected in solution and the rate of concentration decrease with flow through the system indicates that there was dissolution of the ash during the course of the experiment. For example, As falls from 0.29 mg/l to 0.13 mg/l (Dwd 3.1-12, Table 7.3), from the initial to the final eluate.

Solution concentrations are reflected in the electrical conductivity values (Table 7.3). All of the values for the eluates from the weathered PFA samples are lower than those for the equivalent eluates from the fresh PFA, and with few exceptions the differences are significantly large. In relation to this, the pH values for the weathered PFA samples averaged 8.26, whereas the values for the fresh PFA averaged 9.27. The solubilities of the anionic species of B, Cr and Mo will be affected by this difference in pH, but this does not account for the difference between weathered and unweathered samples, which arises because the readily leached elements in the fresh PFA were largely removed during natural weathering.

## **7.4 Leaching behaviour of elements from the column leaching tests**

### **7.4.1 Introduction**

The column leaching tests using a synthetic leachate were conducted basically as complementary experiments to the batch leaching tests. In the batch leaching tests, the leaching tests with deionised water were run mainly to monitor blank concentrations. However, the data from the batch leaching tests with deionised water were useful in another way, by providing information about the locations of elements within PFA.

However, the design and running time of column leaching tests are closer to natural conditions, and therefore the data from column leaching tests with deionised water provide more practical data, by simulating natural weathering reactions. The column leaching tests using weathered ash will also extend the degree of weathering investigated, providing an extended data base for the long-term behaviour of weathered ash.

### **7.4.2 Leaching behaviour of major elements**

Most of the major elements in fresh PFA, including Mg, Na, K, Fe, Al and Si, are matrix associated, whereas more than 70 % of Ca is associated with the acid soluble portions (Hansen and Fisher, 1980). In addition to the matrix associated portions, major elements in the fresh ash are also known to be associated with the surfaces of glass particles in oxide forms. These readily accessible surface-enriched portions will be leached with more ease than the particle interiors, and the release of such surface-associated portions will control the composition of fresh PFA eluate in the early leaching stages.

In weathered PFA, on the other hand, it is expected that much of the surface-associated inorganic salts will have been removed during natural

weathering, and it is the elements in the exterior glass shell that will be liberated into the eluate. In the leaching of weathered ash, the rate of aluminosilicate glass dissolution is expected to be the main control on the release of elements and hence the composition of the eluate.

#### 7.4.2.1 Calcium

Ca is known to be one of the most abundant elements in fossil fuel wastes (Ainsworth and Rai *et al.*, 1987), and much of this element exists in discrete phases (Hansen and Fisher, 1980). In contrast to the findings of previous workers concerning the leaching of Ca from fresh PFA, the Ca in the initial eluate was not readily leachable and did not decrease rapidly with leaching (Figure 7.2). Instead, the concentration of Ca slowly increased with leaching, and achieved a relatively constant concentration.

Dissolved  $\text{Ca}^{2+}$ , from easily accessible CaO situated on the surfaces of PFA particles, is expected to have combined with  $\text{SO}_4^{2-}$ , forming calcium sulphate. In an alkaline environment, such dissolved  $\text{Ca}^{2+}$  will form calcite, providing that atmospheric  $\text{CO}_2$  is supplied, whereas if  $\text{SO}_4^{2-}$  is high enough, gypsum will form, in an acidic environment (Ainsworth and Rai, 1987). Calcite is pH dependent, but the Ca concentrations in the eluates do not seem to be pH-dependent, instead the concentration of Ca and  $\text{SO}_4^{2-}$  seem to be controlled more probably by gypsum, as was demonstrated by the field investigations. However, the solution concentration of Ca plotted against  $\text{SO}_4^{2-}$  in Figure 7.4 do not show an inverse relationship but appears to be independent and the presence of the solubility controlling phase is not demonstrated.

In the column eluates of the weathered ashes,  $\text{Ca}^{2+}$  and  $\text{SO}_4^{2-}$  show a positive relationship. The linear relationships, with a significant correlation value, indicate a common source for the  $\text{Ca}^{2+}$  and  $\text{SO}_4^{2-}$ , possibly gypsum. The weight ratio of dissolved S/Ca in the weathered ash eluate was, however, 0.50,

which exceeds the ratio of S/Ca in anhydrite or gypsum, which is 0.80. An additional source of S, other than  $\text{CaSO}_4$ , is indicated.

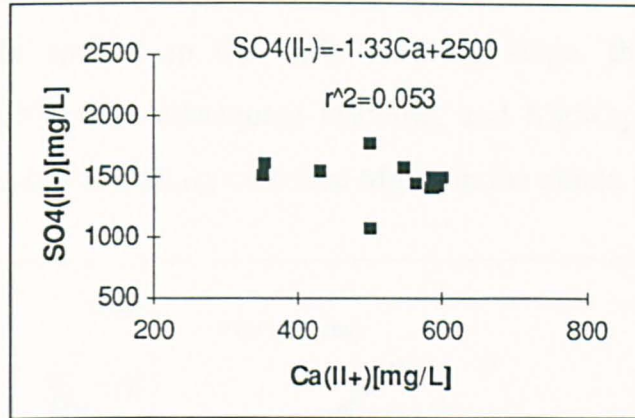


**Figure 7.4 Comparisons of solution concentrations of Ca vs. SO<sub>4</sub>(II-) in fresh ash eluate of column leaching tests**

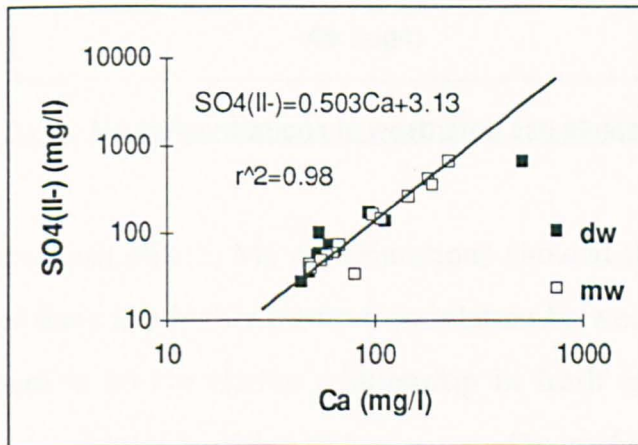


**Figure 7.5 Plot of Ca vs. SO<sub>4</sub>(II-) concentrations in weathered ash eluate**

In the weathered ash eluate a positive relationship was obtained for  $\text{Ca}^{2+}$  and  $\text{SO}_4^{2-}$ , contrary to the inverse relationship of fresh ash eluate (Figure 7.5). The concentrations of Ca and  $\text{SO}_4^{2-}$  are much lower in the weathered ash eluate, by about 10 and 20 times respectively. It is probable that the low concentrations of Ca and  $\text{SO}_4^{2-}$  in the eluate mean that the solution was undersaturated with respect to gypsum.

not volatilised during combustion and is not preferentially enriched in smaller particles (Hansen and Fisher, 1980, Grisafe and Angino *et al.*, 1980). The Mg speciation calculations made by WATEQ4F indicated that  $\text{MgCO}_3^-$  was the dominant aquatic species in the early leaching stage, this was gradually replaced by  $\text{MgSO}_4$  with subsequent leaching, and  $\text{MgSO}_4$  later became the dominant aquatic species, along with free  $\text{Mg}^{2+}$ , in the eluate from fresh ash.

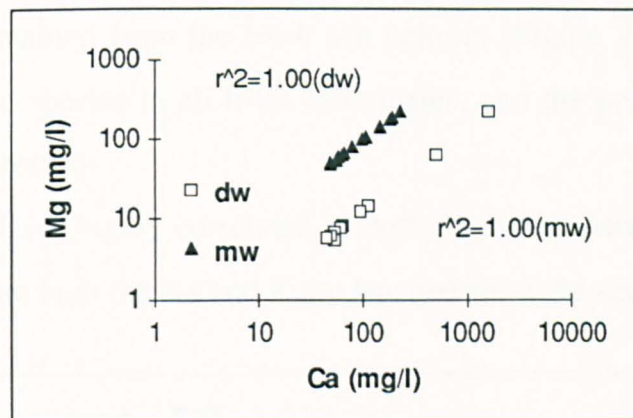


**Figure 7.6 Plot of Ca vs. Mg concentrations in weathered ash eluate**

In weathered ash eluate, Mg concentrations showed the same variation pattern as Ca, and there is a highly positive correlation between the two (Figure 7.6), whereas there is no correlative relationship in fresh ash eluate. Mg is thought to follow a similar leaching behaviour to Ca in the weathered PFA, which is dissolved from the exterior shells of Al-Si glass particles. Some anomalies in the Mg concentrations of the initial eluates are thought to be due to a mixing and dilution of porewaters in the weathered ash. Speciation calculations for weathered ash eluate indicate that initially  $\text{MgSO}_4$  was the dominant aquatic species, followed by  $\text{Mg}^{2+}$ , and with subsequent leaching  $\text{Mg}^{2+}$  is more abundant proportionately than  $\text{MgSO}_4$ .

### 7.4.2.3 Sodium and Potassium

Hansen and Fisher (1980) reported that more than 70 % of Na in PFA was associated with the aluminosilicate matrix of the ash particles, using a HF and HCl leaching experiment. In their experiment, about 20 % of Na was leached with HCl, and this was thought to represent the surface-enriched proportion. It is thought that it was this surface associated Na that was strongly leached in the initial eluates obtained from the fresh ash column (Figure 7.2).  $\text{Na}^+$  was the dominant aquatic species in all fresh ash eluates, and the proportion increased as leaching progressed.

Na and K are highly correlated in both fresh and weathered ash eluate. This indicates that both the Na and K are leached from the same source.

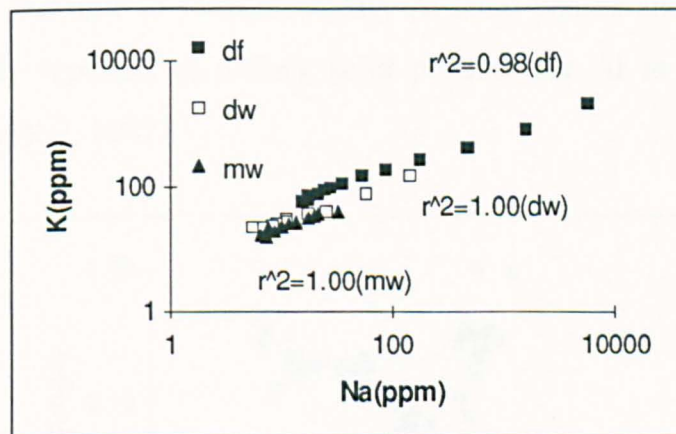


**Figure 7.7 Plot of Na vs. K in column leaching tests**

### 7.4.2.4 Al-Si and their relationship with other major elements.

Al and Si are the main components of aluminosilicate glass, along with iron, whereas iron is also strongly concentrated in iron-rich particles (Chapter 4). The concentrations of Al in fresh PFA eluate did not decrease as leaching progressed (Figure 7.2). Al is a non-volatile element, which is not enriched on the surfaces of PFA particles. Among the three major phases of PFA, namely,

progressed (Figure 7.2). Al is a non-volatile element, which is not enriched on the surfaces of PFA particles. Among the three major phases of PFA, namely, silicon-rich glass, magnetic spinel, and mullite-quartz phase, Al was reported to be mainly distributed in the mullite-quartz phase (Hulett *et al.*, 1980).

The relationships between the concentration of Al and pH, in the eluates of all PFA types, was plotted in Figure 7.8. The variation of Al with pH followed the general Al solubility trend, namely showing a minimum value in the neutral pH range. This indicates that the solubility of Al is controlled by secondary Al hydroxides rather than by its availability. The leachability of the Al in PFA is therefore a function of pH, rather than the availability of Al, on the surfaces of ash particles. The relationship of Al and pH is similar in the batch leaching tests (Chapter 6 and 8). Mullite ( $\text{Al}_6\text{Si}_2\text{O}_{16}$ ) is known to be highly soluble and able to form secondary Al solid phases and  $\text{Al}(\text{OH})_3$  is the most frequently reported secondary solid product for Al in weathered PFA (Ainsworth and Rai, 1987).

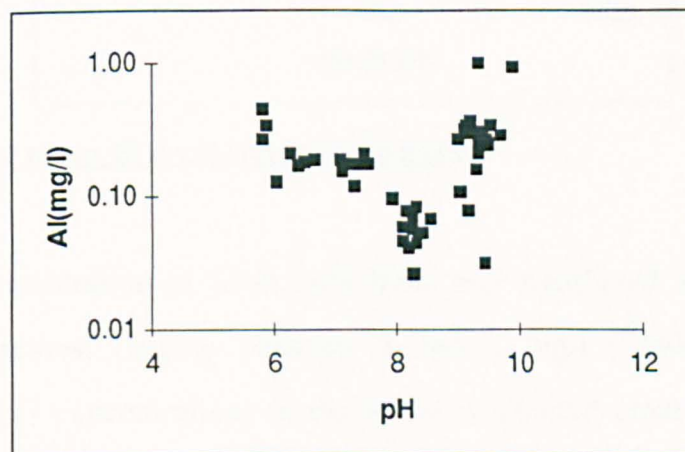


**Figure 7.8** Variation of Al concentrations with pH in the eluates from the column leaching tests

Even though Si itself is not a toxic element in the environment, solid phases of Si are important in controlling some trace elements associated with it. It is reported that As, Se, Pb, Hg, Ba and Sr are associated with the glass phase

It is reported that As, Se, Pb, Hg, Ba and Sr are associated with the glass phase and V, Cr, Mo, Fe and Ti with the quartz and mullite phases (Hulett and Weinberger *et al.*, 1980, Hulett and Weinberger, 1980). The concentrations of Si in fresh ash were significantly correlated with those of the major elements: Mg, Na and K, and the trace elements: B, Ba, Cr, Li, Mn, Mo, Sr, V and As. In weathered ash, the concentration of Si also showed significant correlation with Ca, Mg, Na and K, and also some trace elements, including B, Cr, Li (in Drax weathered ash only), Sr, Zn and Se. In the eluates from weathered ash, the concentrations of many trace elements were very low in the later eluates, which made it difficult to detect the inter-relationships in the weathered ash eluates.

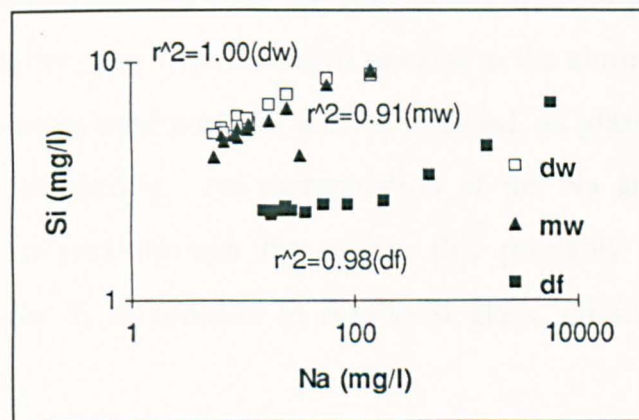


**Figure 7.9 Plot of Na vs. Si in column leaching tests**

The concentration of Si in both fresh and weathered ash decreases as leaching progresses, ranging between 9 and 2 mg/l (Table 7.3). Those somewhat higher concentrations in the initial weathered eluate are thought to be due to porewater, present within the PFA prior to the start of the experiment, mixing with the deionised water. The concentration of Si in the eluates is higher in weathered Drax and Meaford ashes than in fresh Drax ash, this is probably due to the increased dissolution of the relatively Si-rich exteriors of glass particles in the weathered ash, which followed the removal of the surface-enriched portions during natural weathering. However, the Si concentrations

secondary, solubility-controlling phases can not be excluded; this will be discussed in detail in the next chapter.

The concentrations of Na were plotted against those of Si, as shown in Figure 7.9. Both elements show low concentrations in the initial eluates, but subsequently the concentration of Si becomes constant while that of Na decreased in successive eluates. The explanation for this is that rapid dissolution of the surface-enriched portion resulted in a rapid decline in Na (which is present in this portion), whereas Si, in the eluate, is derived from Al-Si glass, which is a vast source of Si. However, in the weathered ash eluate, the concentrations of Na and Si decrease linearly, as expected. In this case, the elements are probably leached from the outer shells of Al-Si glass particles. As was described earlier, much Na is known to exist in the aluminosilicate matrix, and such matrix-associated portions will be released, as glass particles start to dissolve during weathering. An extrapolation of the Na and Si relationship does not seem to pass through the origin, this probably indicates another discrete source for Si in addition to the Al-Si glass, possibly amorphous or crystalline quartz.

The relationship of Mg with Si, in the eluates from fresh Drax PFA, are plotted in Figure 7.10. In the plot of Mg and Si, the concentration of Si is relatively constant compared with Mg, which is decreasing. Mg in the fresh ash eluate is probably derived from the surfaces of glass particles, since about 25% of Mg has been reported to be located in this portion (Hansen and Fisher, 1980); it is probably present there mainly as MgO. The solubility of Mg is known to be lower in an alkaline environment than in an acidic one, because  $\text{Mg}(\text{OH})_2$  is present as a solubility controlling solid phase for mg under highly alkaline environment (van der Sloot *et al.*, 1982).

In the eluates of Drax and Meaford weathered ash, the concentration of Ca correlates linearly with Si, passing near to the origin (Figure 7.11). This implies that Ca and Si were dissolved from a common source. In weathered

ash, as was mentioned in an earlier section, the exterior shells of Al-Si glass particles will be undergoing dissolution, liberating refractory elements, including Ca (which exists as a glass network modifier), into the eluate.

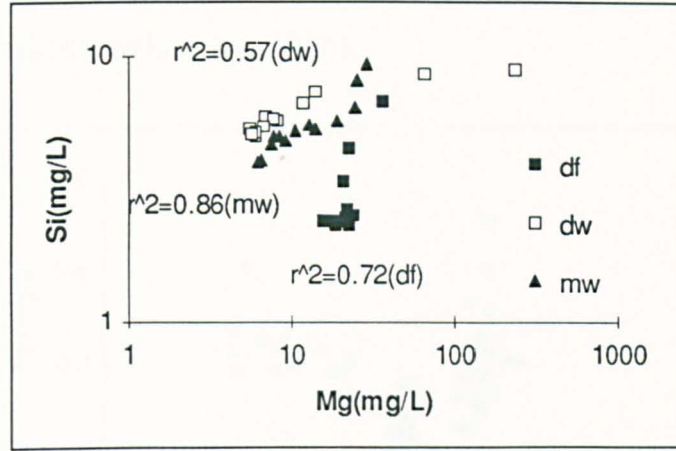


**Figure 7.10 Plot of Mg vs. Si in column leaching tests**

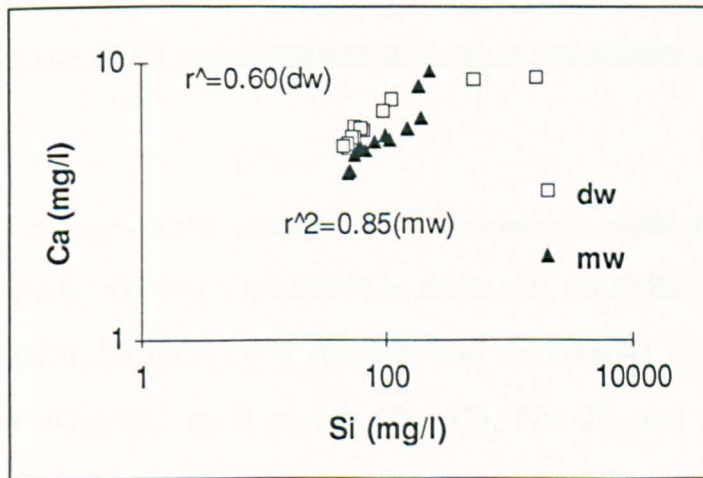


**Figure 7.11 Plot of Si vs. Ca of weathered ashes in column leaching tests**

#### 7.4.2.5 Iron

Fe is a major constituent of the PFA matrix. In addition to this matrix associated portion, several other sources of iron in PFA are known. These include discrete iron minerals, such as magnetite and hematite, which were

detected by X-ray diffraction. Some magnetic spinels, which are commonly reported as magnetite, are thought to be ferrite (Hulett and Weinberger *et al.*, 1980). Another source for the iron is iron-coated PFA particles, which are highly magnetic and contain more trace elements than Al-Si glass particles (Norton and Markuszewski *et al.*, 1986).

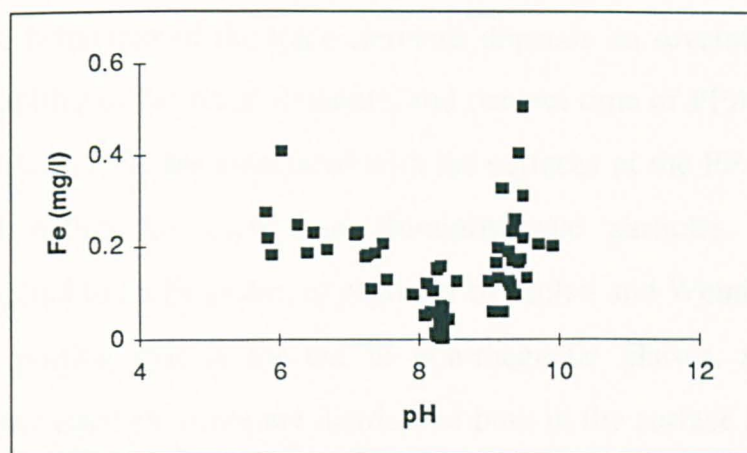


**Figure 7.12** Variation of Fe concentrations with pH in the eluates from the column leaching tests

Fe shows significant correlation relationships with other elements. These include Zn ( $\sigma=0.743$ ), Cu (0.659) in fresh ash, Al (0.873), B (0.603), Cr (0.613), Li (0.672), Ni (0.812), V (0.778), and As (0.804) in weathered ash. First transition elements, such as Cr, Mn, Co, Ni, Zn and Cu, have been reported to be associated with the magnetic phases in PFA, and such elements are thought to be located within the ash glass in a solid solution with the formula  $\text{Fe}_{3-x}\text{M}_x\text{O}_4$  (Hulett and Weinberger, 1980). Such a hypothesis may account for the elemental associations obtained in the current work.

The concentration of Fe also shows a pH-dependence, which suggests the possible influence of solubility controlling phases (Figure 7.12). However, this diagram is not sufficient to demonstrate the presence of solubility controlling solids. The equilibrium relationships indicated by the column

leaching tests will be discussed in detail in Chapter 8, together with the data from the batch leaching tests.

### 7.4.3 Leaching behaviour of trace elements

#### 7.4.3.1 General behaviour

The leaching behaviour of the trace elements depends on several factors, such as pH, availability of the trace elements, and contact time of PFA with solutes. Trace elements in PFA are associated with the surfaces of the PFA particles, or are situated within the matrix of aluminosilicate particles, or occur as substituted spinel in an Fe phase, as reported by Hulett and Weinberger (1980). Among the portion that is located in non-magnetic phases, such as glass particles, many trace elements are distributed both in the surface layers and the glass matrix. In fresh ash, it is expected that many trace elements will be leached from the surface-enriched portions, as mentioned previously, so that the concentration of the element in the eluate will decrease as leaching progresses, as the surface associated trace elements become depleted.

Several researchers have tried to categorise the specific distribution of trace elements in PFA using various methods, including leaching with various acids which attack specific crystalline phases in the PFA (Hansen and Fisher, 1980; Hulett *et al.*, 1980; Hulett and Weinberger, 1980), and column leaching tests (Warren and Dudas, 1986). From the results of laboratory column-weathering tests, using fresh alkaline PFA, Warren and Dudas (1986) grouped the trace elements in fresh PFA eluate into four categories by comparing the leaching behaviour of the trace elements with those of the major elements, which were grouped as follows; (1) Ca and Mg, (2) Si and K, (3) Al and (4) Fe.

In weathered ash, it is expected that much of the surface-enriched fraction will be depleted, and the PFA matrix-associated portions will be a more important source for the trace elements, with the amount released

dependent upon the weathering rate of the glass. In the weathering of PFA glass, pH will be the main factor controlling the trace elements release. The leaching behaviour of the trace elements in weathered ash was compared with the major elements of weathered ash eluate, and the trace elements in the fresh ash eluate. Except for Sr in weathered Drax ash eluate, few trace elements were readily leached from weathered ash. Comparison of the leaching behaviour of major and trace elements in the weathered ash reveals close affinities for B, Cr, Li, Mo, Sr, Zn and V with major elements such as Ca, Mg, Na, K and Si. In weathered ash, these elements are thought to have been released from the Al-Si glass rather than from the surface-associated fractions. With the other trace elements, including Ba, Cu, Mn, Ni, Pb, As and Se, such associations with the major elements could not be easily established, due to their low concentrations in the weathered ash eluate.

#### ***7.4.3.2 Individual leaching behaviour of the trace elements***

With the column leaching tests using deionised water, the leaching behaviour of trace elements in weathered ash was of particular interest from the standpoint of the trace elements release over a long term period. Hulett and Weinberger (1980) determined that many trace elements are enriched on the surfaces of PFA particles, not only as a result of volatilisation and condensation during the combustion but also as a result of diffusion from the interiors of particles. In addition to being located in Al-Si glass, the trace elements are associated either with an iron-rich phase or a mullite-quartz phase (Hulett and Weinberger *et al.*, 1980; Hulett and Weinberger, 1980). The leaching behaviour of trace elements in weathered Drax and Meaford ash appears to suggest that they are mainly associated with the aluminosilicate glass, either in a Si-rich glass phase or a quartz-mullite phase within the particles.

Three distinct behaviour patterns were noted for the trace elements from the column leaching tests. Cr was readily leached from the fresh ash but the

concentrations were near detection limit in the weathered ash eluate. B, Mo and Li were readily released from fresh PFA, and relatively constantly released from the weathered ash, in a similar manner to the leaching of Si, indicating an association with the Si-rich phase. Other trace elements generally show similar concentrations in the fresh and weathered ash eluates, and there is no evidence of these elements being readily leached from fresh ash. Trace elements were grouped into three categories, according to their leaching behaviour described above.

### Readily leachable only in fresh ash: Cr

Cr was strongly leached into the initial eluate, but the concentration decreased rapidly in subsequent eluates. In weathered ash, the initial concentration of Cr was 0.20 mg/l, and this decreased constantly, approaching the detection limit with progressive leaching (Table 7.3). In the column leaching tests using weathered ash, Cr showed a positive relationship with Si, indicating dissolution of the Cr simultaneously with the leaching of Si. It seems that the Cr leached from fresh ash was surface associated, and much of the surface fraction was depleted during the course of weathering. The small amounts of Cr still being released from weathered ash appear to be derived from the Si-rich glass phase (Figure 7.13).

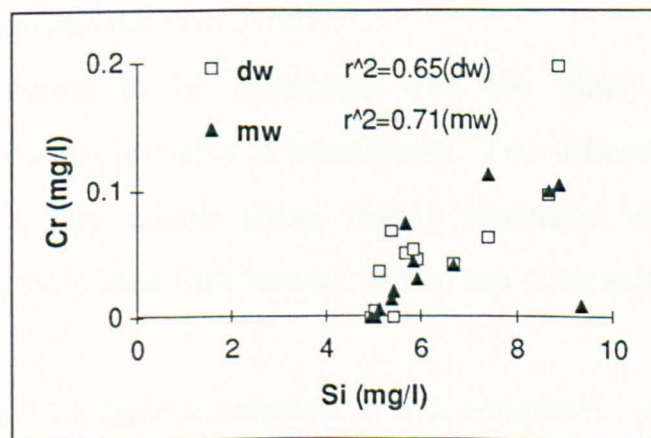


Figure 7.13 Plot of Si vs. Cr in column leaching tests

Trace elements that are readily leached from fresh ash and constantly released from weathered ash: B, Li, Mo and (Se)

These trace elements appear to be associated with both the surfaces and interiors of aluminosilicate glass particles. Se was readily dissolved in the fresh ash, but the concentrations were generally low, and were less than the detection limit for some samples.

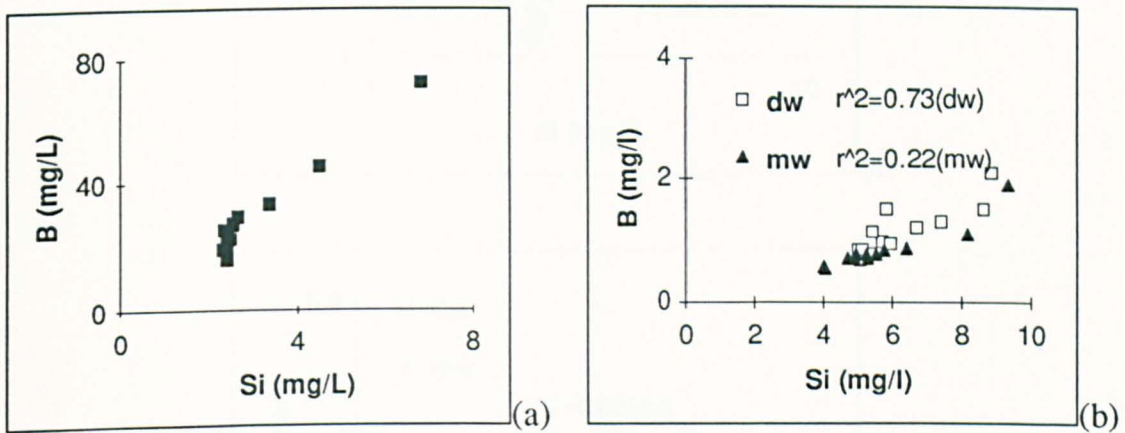


Figure 7.14 Plot of Si vs. B in column leaching tests

**Boron.** B is one of the most abundant trace elements in PFA and highly leachable in water. Most known B minerals are fairly soluble and solution concentrations of B in aqueous systems are expected to be controlled by adsorption/desorption reactions or the dissolution rate of the B-containing solid matrix (Ainsworth and Rai *et al.*, 1987).

B is reported to be associated with the glassy phase and the aluminosilicate matrix, probably as borosilicate. Two different B species have been reported: a very soluble phase, mainly associated with PFA, and an insoluble phase, associated with furnace bottom ash (Cox and Lundquist *et al.*, 1978).

In Figure 7.14, the concentration of B is compared with that of Si, both in fresh and weathered ash eluate. In the fresh ash eluate, B decreased as

leaching progressed, whereas Si kept rather constant. With the eluates of weathered ash, Si and B show a linear relationship, decreasing at a similar rate, implying an association of B with the Si-rich glass phase.

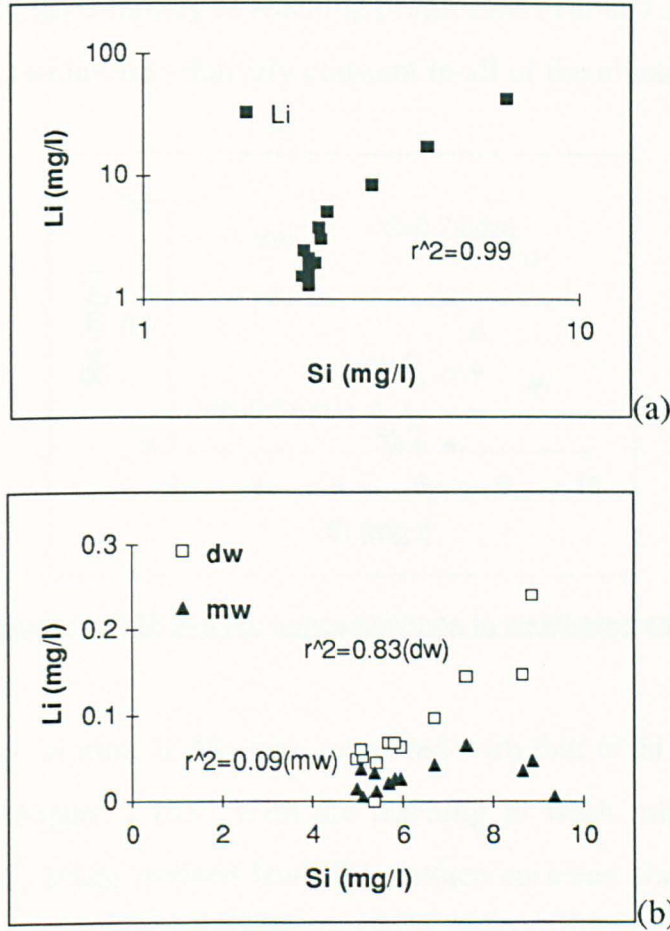


**Figure 7.15** Plot of Si vs. Li of the fresh PFA (a) and weathered PFA in column leaching tests

**Lithium.** Lithium was readily leachable from fresh ash, but its concentration dropped to under 0.2 mg/l in weathered ash eluate (Table 7.3, 5, Figure 7.2). Li seems to be mainly surface associated, with small amounts incorporated into the exteriors of glass particles. The surface-associated portions seem to be effectively dissolved during weathering.

This is confirmed by Figure 7.15, which shows the relationship between Si and Li in both fresh and weathered ash eluates. In the leaching of fresh ash,

Li decreased faster than Si, but in the weathered ash eluates they decreased at a similar rate.

**Molybdenum.** Mo was strongly leached into the initial eluate, but its concentration dropped rapidly as leaching progressed (Table 7.3). In weathered ash, the concentrations are relatively constant in all of the eluates.

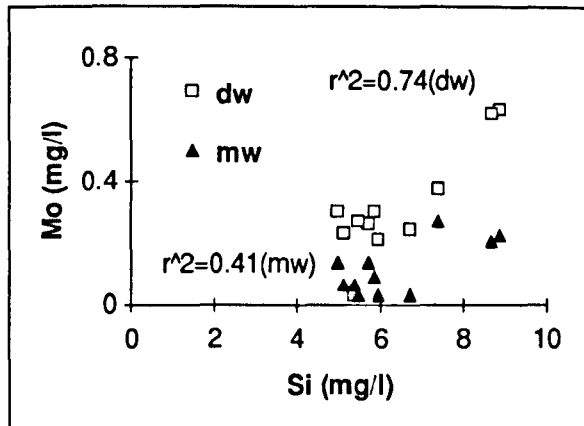


**Figure 7.16 Comparison of Si and Mo concentrations in weathered ash eluates**

The concentration of Mo was compared with that of Si in the fresh and weathered ash (Figure 7.16). With the leaching of fresh ash, Mo decreased rapidly, probably being derived from the surface-enriched fraction. No solid phases which control the solubility of Mo in PFA are known, yet  $\text{CaMoO}_4$  (powellite) has been predicted as a possible solubility controlling solid in hot-water extracts of fly ashes (Ainsworth and Rai *et al.*, 1982).  $\text{MoO}_3(\text{s})$ ,  $\text{Fe}_2(\text{MoO}_4)_3$  and  $\text{CaMoO}_4$  were predicted as possible solubility controlling phase for Mo, where  $\text{CaMoO}_4$  is controlling at  $\text{pH} > 5$  (van der Sloot and Hjelmar *et al.*, 1989). In the weathered ash eluates, the concentration of Mo generally decreased relatively constantly as leaching progressed, although some eluates contained Mo values near to, or under, the detection limit. The relationship of Mo and Si in weathered ash eluate indicates that the two elements are associated in the aluminosilicate glass. The concentration of Mo in weathered Drax ash eluates also shows significant correlation with other

matrix-associated elements, such as Ca (0.728), Mg (0.714), Na (0.776), K (0.793) and Al (0.662), which supports the idea that Mo is associated with the glass fraction of the weathered ash.

**Selenium.** Se was readily leached from fresh ash, but the concentration of Se in both fresh and weathered ash eluates was very low, near to the detection limit for many samples. Except for the first eluate from fresh ash leaching, the concentrations of Se in the eluates of fresh and weathered ash are comparable. This indicates that in fresh ash Se is incorporated within the Si-rich glass phase, as well as having a surface association. Se is one of the most volatile elements in PFA (Clarke and Sloss, 1992). In the batch leaching tests (Chapter 6), Se was not readily leachable, and was leached into later eluates in small amounts. The possible influence of a solubility controlling phase can not be excluded.

**Trace elements showing similar leaching behaviour both from fresh and weathered ash : Ba, (Cd), (Co), (Cu), (Mn), (Ni), Pb, Sr, V, Zn, As and (Hg)**

The concentrations of the trace elements in the third group do not indicate strong leachability from fresh ash. The concentrations are similar in both types of eluate, and generally their concentrations are very low. The concentrations of the trace elements shown in parentheses were near or under the detection limit for many samples. Since the concentrations, in the eluates, of the trace elements belonging to this group kept relatively constant as leaching progressed, the presence of solubility controlling phases is inferred.

**Barium.** The concentration of Ba in the eluates of weathered and fresh ash is similar, and there is no evidence of strong leachability. The concentrations do not decrease as leaching progresses, but remain relatively constant, although there is a slight decrease in Ba concentration in the fresh ash eluates (Table 7.3). The depth trend of the Ba in porewater extracted from the borehole indicated the possible presence of a phase controlling the solubility of

Ba (Chapter 3). The relatively constant Ba concentrations in the eluates would seem to support the results of the field investigation. The equilibrium relationship will be discussed in the next chapter.

**Mercury.** Hg is very volatile and therefore has a very low content in PFA. The pattern for Hg in PFA is similar to that of Mn, decreasing in concentration as leaching progressed, falling to, or under, the detection limit (Table 7.3). Hg in PFA is enriched exclusively in the glass phase (Hulett and Weinberger *et al.*, 1980). Hg belongs to the chalcophile group of elements, which are mainly present as sulphide minerals and associated with the organic fraction in coal, but because of the extreme volatility and low condensation temperature of Hg it is expected that this element will be associated with Si-glass, rather than the Fe-magnetic phase.

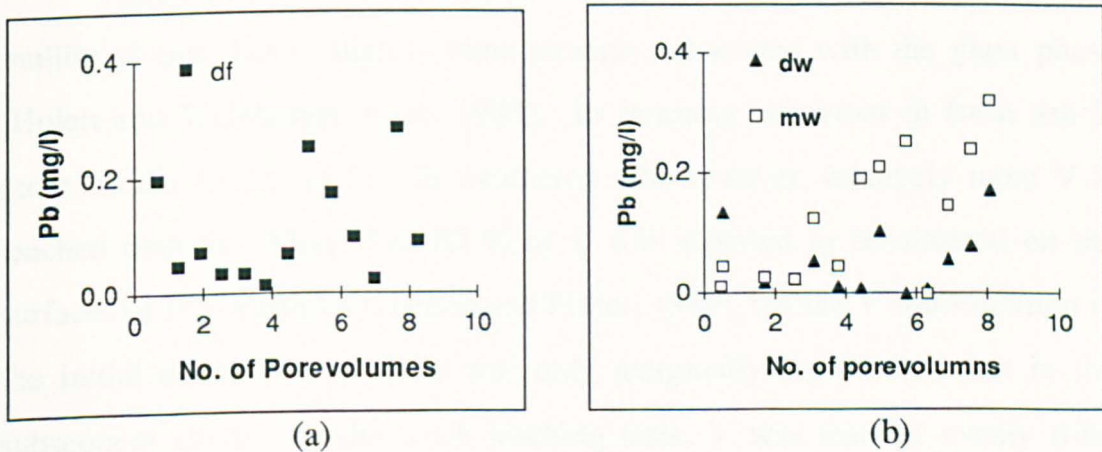


**Figure 7.17** Variation of Pb concentration in fresh (a) and weathered (b) ash eluates

**Lead.** The variation pattern of Pb concentrations in both fresh and weathered PFA eluate is not that clear, but in both cases there appears to be an overall increase of Pb concentration in the eluates as the leaching progresses (Table 7.3, Figure 7.17). In fresh ash eluate, the change was not that systematic, but the concentrations were higher in the initial eluate, compared with subsequent eluates, and there is a slight increase in concentration in the later eluates. In the case of the weathered ash eluates, Pb generally decreased

as leaching progressed, falling near to, or under, the detection limits, but again showing a slight increase in the later eluates, as with fresh ash.

**Strontium.** Strontium was relatively evenly released into the eluate of fresh ash, whereas in weathered ash the Sr concentration in the eluates decreased slightly as leaching progressed (Table 7.3, Figure 7.2, 3). The high concentrations of Sr in the initial eluates of weathered ash may be due to mixing of the added solution with porewaters originally present within the weathered ash. The variation in the concentration of Sr in the porewater samples extracted from the boreholes indicated the achievement of equilibrium concentrations, as with Ba. The relatively constant concentrations of Sr in the column leached eluates is therefore in agreement with the results of the field studies.

**Vanadium.** V is known to be associated with both glass and quartz-mullite phases, but is slightly more strongly associated with the glass phase (Hulett and Weinberger *et al.*, 1980). Its leaching behaviour in fresh ash is quite similar to that of Sr. In weathered ash, however, relatively more V is leached than Sr. More than 80 % of V was reported to be situated on the surfaces of PFA particles (Hansen and Fisher, 1980), but the V concentration in the initial eluate of this study was only marginally higher than that in the subsequent eluate. In the batch leaching tests, V was leached evenly from weathered ash, and this could support the view that the V is also incorporated into the mullite-quartz phase.

**Arsenic.** Along with Hg and Se, As is one of most volatile elements during combustion. More than 90 % of total As in PFA was found to be associated with an Fe fraction extracted by ammonium oxalate acid (Theis and Wirth, 1977). In another study, about 80 % of As was removed from PFA at the same time as nearly all Al and Si, but only 60 % of Fe, was extracted by oxalate (Warren and Dudas, 1986). From this result, they deduced that not all

As was associated with oxalate extractable Fe, but was also associated with the exterior glass of PFA particles.

In fresh ash, arsenic was not readily leachable. In weathered ash, the concentration of arsenic in the eluate decreased slightly as leaching progressed. In Figure 7.18, As is seen to deplete with decreasing Si, and the relationship with Fe indicates As is also leached from an additional, Fe-rich source. Much of the As leached by deionised water is thought to have been associated with the relatively soluble exteriors of glass particles, but it is also liberated along with oxalate extractable Fe contained within the glass.

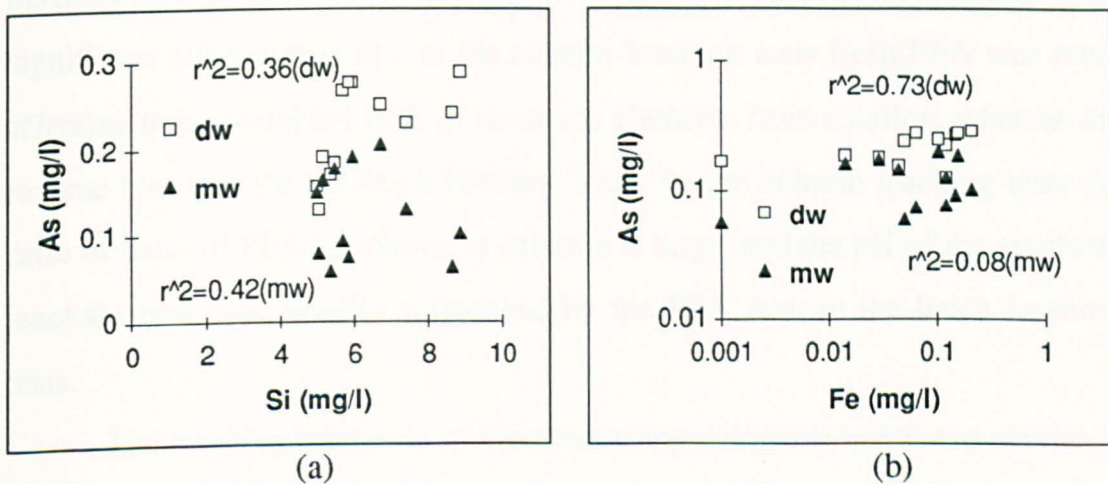


**Figure 7.18** Plots of Si vs. As (a) and Fe vs. As (b) of the weathered ash in column leaching tests

**Zn.** The concentration of Zn is generally constant in weathered and fresh ash eluates, and does not show a clear decreasing trend with progressive leaching. The initial concentrations in weathered Drax and Meaford eluates were slightly higher than in the subsequent eluates, but these are probably influenced by the porewater within the ashes. The variation pattern for Zn would seem to indicate the presence of a solubility controlling mechanism, either through adsorption or through the achievement of equilibrium concentration.

#### **7.4.4 Comparison of batch and column leaching tests**

Results from the batch and column leaching tests agree well with each other, and the column leaching tests confirm the conclusions reached by the batch leaching tests, including the important observation that elements are lost from solution by reaction with the PFA, including Fe and Cu. In the column leaching tests, however, a wider range of trace elements were retained by the PFA from the synthetic leachate, compared with the batch leaching tests. These include Cd, Cr, Hg, Ni and Zn, but these trace elements were retained partially and show breakthrough, at some stage, with subsequent leaching. One significant difference is that in the column leaching tests fresh PFA was more effective than weathered PFA in removing elements from solution, whereas the reverse was true for the batch leaching tests. In the column leaching tests the ratio of mass of PFA to volume of solution is large, and the pH of the synthetic leachate was more readily influenced by the PFA than in the batch leaching tests.

The leaching behaviour of elements using deionised water was similar in both batch and column leaching tests. Li, Mo and B were readily soluble in both the column and batch leaching tests, and the other trace elements also showed nearly the same pattern of leaching, namely, relatively constant concentration as leaching progresses.

#### **7.5 Comparison of column leaching results with water quality standards**

The column leaching tests demonstrate that there is a release of elements into solution, and therefore the leachate from PFA in landfill sites will be a potential source of contamination to the environment. The eluate collected from the column leaching tests with deionised water was compared with several water

quality standards, and is shown in Table 7.4. The values are represented as a range, and the maximum concentrations are generally from initial eluates, whereas the minimum values are from eluates collected from a late stage of leaching. The maximum value gives an indication of the worst case scenario, and the comparisons were based on these maximum concentrations. In the eluate produced from the fresh PFA, most elements exceed the recommended values, and in some cases, such as Cr, Se and B, the margin is considerable. Dilution is therefore required if all the recommended values are to be achieved. In landfill sites, leachate draining into streams and rivers will be diluted by surface run-off. Leachates passing into aquifers would also be diluted, but possibly not to the same extent. The extent of dilution would, however, be a function of the particular aquifer.

The eluate that emerged from the column of fresh PFA after a relatively long period of time provides evidence of how PFA will behave as it is progressively weathered. The volume of the flow can be related directly to rainfall and infiltration values, enabling the weathering behaviour over several years to be predicted. This assumes that the reactions in the field are duplicated in the columns, which need not be the case, because of the differing time scales. It is more realistic to consider weathered PFA, and again the initial eluate gives an indication of possible water quality. Most elements in the eluate are present at concentrations which exceed the maximum permissible concentrations but by a relatively small factor, with the exception of Se. Excessive dilution would not therefore be required to achieve drinking water standards.

Finally, in Table 7.4, quality directive concentrations for landfill leachate and the NRA consent for the Barlow disposal mound at Drax power station are presented. Elements in the eluate from the fresh Drax PFA which exceed the directive concentrations are  $\text{SO}_4^{2-}$  and Cr, whereas As and Hg are close to their limits; Cu, Zn, Cd, Ni and Pb are below their limits. Elements in

		Drinking Water quality			PFA eluate			Landfill Leachate Quality	
		CEC *	WHO*		Fresh Drax	Weathered Drax	Weathered Meaford	EC Landfill Directive	Barlow Consent (NRA)
		GL* (mg/L)	MAC* (mg/l)	GV* (mg/l)	mg/l	mg/l	mg/l	mg/l	mg/l
Calcium	(Ca <sup>2+</sup> )	100	-	-	353-589	45-1626	49-225		
Magnesium	(Mg <sup>2+</sup> )	30	50	-	16-37	6-233	7-29		
Sodium	(Na <sup>+</sup> )**	20	150	200	16-5760	6-142	6-32		
Potassium	(K <sup>+</sup> )	10	12	-	60-2113	23-157	18-42		
Chloride	(Cl <sup>-</sup> )	25	-	250	2-1120	1-1661	1-121	1200-6000	
Sulphate	(SO <sub>4</sub> <sup>2-</sup> )	25	250	400	1413-1609	27-3214	35-678	200-1000	
Aluminium	(Al <sub>3</sub> <sup>+</sup> )	0.05	0.5	0.2	0.3-1.0	nd-0.2	nd-0.1		
Nitrate	(NO <sub>3</sub> <sup>-</sup> )**	25	50	45	1-94	4-1224	2-181		
	(as N)	5.65	11.3	10					
Nitrite	(NO <sub>2</sub> <sup>-</sup> )**	-	0.1	-					
Ammonium	(NH <sub>4</sub> <sup>+</sup> )	0.05	0.5	0.2					
Iron	(Fe <sub>3</sub> <sup>+</sup> )	0.05(Fe <sub>T</sub> )	0.2(Fe <sub>T</sub> )	0.3(Fe <sub>T</sub> )	0.1-0.4	0-0.2	nd-0.2		1.0
Manganese	(Mn <sup>2+</sup> )	0.02	0.05	0.1	nd-0.02	nd-0.02	nd-0.01		

\* CEC : Council of the European Communities Directive 80/778

\* GL : Guide level, \* MAC : Maximum admissible concentration

\* WHO : World Health Organisation. Guidelines for drinking water quality. 1984, \* GV : Guide value

\*\* : Inorganic constituents of health significance (WHO, 1984). [additionally: asbestos, vanadium, beryllium, nickel, silver, - no guide value set0]

**Table 7.4 Comparison of the PFA eluate from column leaching tests with drinking water and landfill leachate quality standards (Continued-)**

		GL*	MAC*	GV*	Fresh Drax	Weathered Drax	Weathered Meaford	EC Landfill Directive	Barlow Consent (NRA)
		(µg/l)	(µg/l)	(µg/l)	(µg/l)	(µg/l)	(µg/l)	(µg/l)	(µg/l)
Copper	(Cu <sup>2+</sup> )	3000	-	1000	0-140	0-40	0-30	2000-10000	100
Zinc	(Zn <sup>2+</sup> )	5000	-	5000	0-60	30-370	0-290	2000-10000	1000
Phosphate	(HPO <sub>4</sub> <sup>2-</sup> )	400	5000	-					
Fluoride	(F <sup>-</sup> )**	8-12°C	1500	1500					
		25-30°C	700	-					
Barium	(Ba <sup>2+</sup> )	100	-	-	30-80	100-920	90-130		
Arsenic	(As)**	-	50	50	0-820	130-290	0-210	200-1000	10
Cadmium	(Cd <sup>2+</sup> )	-	5	5	0-230	0-30	0-40	100-500	5
Chromium	(Cr)**	-	50	50	80-23950	0-200	0-110	100-500	100
Mercury	(Hg)**	-	1	1	0-80	0-10	0-20	20-100	
Nickel	(Ni)	-	50	-	0-70	0-40	0-70	400-2000	500
Lead	(Pb <sup>2+</sup> )**	-	50	50	20-290	0-170	0-320	400-2000	500
Selenium	(Se)**	-	10	10	0-2210	0-550	0-2450		
Boron	(B)	1000	-	-	16000-72000	820-2100	550-1890		5000
pH	6.5-8.5	-	-	6.5-8.5	9.0-9.3	7.5-8.4	8.2-8.5	4-13	6-9
Conductivity	(µS/cm at 20°C)	400	-	-	716-22300	103-9560	99-499		

**Table 7.4 Comparison of the PFA eluate from column leaching tests with drinking water and landfill leachate quality standards**

the eluate from the weathered PFA do not exceed the directive limits, but  $\text{SO}_4^{2-}$ , Cr and Hg are close to their limits, and the other elements fall well below. The Barlow consent values are lower than the landfill directive values and are comparable with drinking water standards. The concentrations of As, Cr and possibly Cd in the eluate from weathered ash are higher than their consent values, and this suggests that leachate from the fresh ash would require significant dilution for the consent values to be achieved.

## 7.6 Column leaching tests with synthetic leachate

### 7.6.1 Fresh Drax PFA with synthetic leachate

The initial eluate has similar concentrations of Ca, Na, K and Mg (Table 7.5) to that of the fresh PFA eluate using deionised water. Na and K concentrations fall as more solution passes through the column, until the initial concentrations of the synthetic leachate are attained. Ca and Mg concentrations, on the other hand, increase as leaching progresses and exceed their initial concentrations in the synthetic leachate. Organic acids exert a considerable influence on the dissolution of common silicates and the solubilities of Si, Ca, Mg, Al and Fe are higher in organic acids than in water, whereas concentrations of Na and K are similar in organic acids as in water (Huang and Keller, 1970).

Among the trace elements, B and Mo were readily leachable from the fresh Drax ash, implying the surface association of the B and Mo in the ash. Other elements dissolved by the synthetic leachate were Si, Sr and V. These elements showed relatively higher concentration in the initial eluates, but were leached relatively constantly thereafter.

The concentration of Fe in the synthetic leachate is 100 mg/l (Table 7.1), but there was very little Fe present in the solutions that emerged from the column. Also present in the synthetic leachate, but removed in the column, are Cd, Cu, Ni, Zn and

Hg. The concentration of Cr is reduced from its value in the synthetic leachate to a lower value in the final solution. Although there is some retention of Cr, this is only partial, which is consistent with the solubility of the anionic species.

These results show that elements present in significant concentrations in the synthetic leachate are removed from solution in passing through the fresh PFA. The pH of the synthetic leachate is 4.55, whereas the emergent solution is alkaline, and this is an important factor in metal retention. Heavy metal precipitation as hydroxides, sulphides and carbonates are greatly influenced by pH, which generally lowering of pH effects a marked increase in solubility (Forstner and Wittman, 1983). Desorption of metals in aqueous solution followed a predictable pattern of decreasing release with increasing pH (Theis and Wirth, 1977). The alkalinity of PFA is believed to be from the dissolution of Ca and Mg (Hodgson and Dyer *et al.*, 1982) or oxalate extractable amorphous iron and water soluble Ca (Theis and Wirth, 1977). Al, As and Se appear to be slightly leached from the fresh ash, but the concentrations approach the concentration levels of the synthetic leachate with further leaching.

### **7.6.2 Weathered Drax and Meaford PFA with synthetic leachate**

The analyses (Table 7.5) show a similar pattern for Ca, Mg, Na and K in the weathered PFA as in the fresh PFA. The initial solution to emerge from the column is influenced by porewater concentrations within the column. Na and K concentrations tend with time and volume to approach the synthetic leachate composition, whereas Ca and Mg are enhanced by reaction between the synthetic leachate and PFA. Elements present as trace constituents in the synthetic leachate, such as B, are recorded in the emergent solution in much lower concentrations than in the fresh PFA, demonstrating the effect of weathering, but in higher concentrations than in the leaching by water, which demonstrates the greater dissolution achieved with the synthetic leachate (Table 7.3,5).

	pH	C( $\mu$ S/cm)	Ca	Na	K	Mg	Fe	Al	B	Ba	Cd	Co	Cr	Cu	Li
<b>Syn. Lea.</b>	4.55	3550	764	1983	1007	97	100	nd	0.28	0.03	121	0.16	76	111	22
<b>dfs2-1</b>	9.90	8740	830.4	6171.1	2650.7	76.6	0.20	0.92	49.46	0.12	0.04	0.05	2.98	0.58	54.05
<b>2-2</b>	9.70	5380	2362.0	2063.7	1351.1	476.9	0.21	0.29	28.54	0.30	0.04	0.06	2.98	0.01	27.31
<b>2-3</b>	9.49	5270	2567.6	1725.1	977.5	682.3	0.22	0.23	36.06	0.32	0.02	0.07	4.98	0.00	20.68
<b>2-4</b>	9.33	5110	2623.3	1644.2	867.1	767.0	0.24	0.24	56.27	0.30	0.02	0.08	14.65	0.01	18.41
<b>2-5</b>	9.37	5190	2647.9	1616.5	816.9	678.6	0.26	0.24	61.69	0.30	0.02	0.07	21.01	0.01	17.69
<b>2-6</b>	9.49	5160	3356.8	2046.9	1051.1	650.7	0.51	0.00	63.21	0.30	0.00	0.05	21.85	nd	24.62
<b>2-7</b>	9.53	5190	3307.6	1996.7	1038.6	585.1	0.13	0.34	51.15	0.29	0.00	0.00	20.45	nd	24.85
<b>2-8</b>	9.35	5130	3295.2	2034.8	1045.8	598.4	0.10	0.21	43.16	0.25	0.00	0.00	20.14	nd	25.09
<b>2-9</b>	9.32	5230	3274.3	2031.7	1029.7	593.7	0.12	0.16	40.74	0.26	0.00	0.00	19.33	nd	25.23
<b>2-10</b>	9.29	5340	3333.0	2102.9	1069.9	643.2	0.12	0.29	46.55	0.27	0.00	0.00	18.56	nd	26.46
<b>2-11</b>	9.36	5190	3234.2	2014.3	1027.9	616.2	0.10	0.29	51.51	0.26	0.00	0.10	16.18	nd	24.91
<b>2-12</b>	9.19	5240	3197.1	2022.7	1025.2	626.8	0.06	0.08	59.51	0.24	0.00	0.00	14.74	nd	24.74
<b>2-13</b>	9.06	5230	3113.2	1964.8	1016.2	648.0	0.06	0.10	66.32	0.24	0.00	0.00	13.98	nd	24.73
<b>dws4-1</b>	7.22	8020	1451.6	121.3	143.3	211.2	0.18	0.17	2.91	0.35	0.03	0.04	0.19	0.13	0.27
<b>4-2</b>	7.55	12120	2754.1	783.9	236.6	336.0	0.13	0.17	2.46	0.56	0.02	0.05	0.61	0.05	0.77
<b>4-3</b>	7.93	15700	3300.7	1563.4	606.4	216.0	0.10	0.09	2.94	0.99	0.01	0.04	10.31	0.05	13.31
<b>4-4</b>	7.32	14730	2980.2	1535.7	736.3	181.2	0.11	0.12	3.89	1.03	0.01	0.04	25.28	0.02	15.21
<b>4-5</b>	7.37	15200	3157.3	1539.6	710.6	200.4	0.18	0.17	3.70	1.03	0.02	0.05	24.30	0.03	14.74
<b>4-6</b>	6.68	5850	3088.6	1643.9	758.1	177.6	0.19	0.19	3.54	1.13	0.03	0.06	21.55	0.03	17.43
<b>4-7</b>	6.40	5030	3079.4	1727.3	796.6	178.8	0.18	0.17	3.75	1.17	0.02	0.08	25.76	0.03	18.49
<b>4-8</b>	6.49	4990	2827.3	1611.9	797.2	184.8	0.23	0.18	3.60	1.07	0.08	0.11	23.29	0.03	17.47
<b>4-9</b>	6.26	4960	2818.1	1705.7	820.3	195.6	0.25	0.21	3.45	1.17	18.78	0.16	22.07	0.03	18.49
<b>4-10</b>	6.03	5530	3194.6	1999.2	1001.7	226.7	0.41	0.13	3.75	1.23	74.58	0.12	21.24	0.00	23.27
<b>4-11</b>	5.89	4920	2994.2	1914.6	968.8	213.6	0.18	0.34	3.21	1.21	105.96	0.16	17.80	0.07	21.78
<b>4-12</b>	5.82	4800	2982.5	1908.7	968.8	212.3	0.28	0.26	3.25	1.16	117.79	0.18	16.67	0.06	22.10
<b>4-13</b>	5.83	4960	3010.0	1945.9	986.7	207.7	0.22	0.45	2.92	1.16	127.78	0.18	16.85	0.09	22.27
<b>mws5-1</b>	7.12	3320	1930.3	919.6	358.8	202.8	0.23	0.15	1.48	0.84	0.02	0.04	5.88	0.01	7.19
<b>5-2</b>	7.08	5080	2866.1	1557.3	765.2	194.4	0.22	0.19	2.20	1.05	0.01	0.07	17.61	0.02	16.38
<b>5-3</b>	7.27	4990	4015.2	2325.9	1186.9	282.1	0.18	nd	3.92	1.03	2.74	nd	20.97	0.08	26.70

**Table 7.5 Analytical results of eluates from column leaching tests with synthetic leachate (Unit : mg/l unless indicated) Continued-**

	Mn	Ni	Pb	Si	Sr	V	Zn	As	Hg	Se	Mo	Cl <sup>-</sup>	NO <sub>3</sub> <sup>-</sup>	SO <sub>4</sub> <sup>2-</sup>
Syn. Lea.	0.19	106	0.39	0.88	0.15	nd	109	0.15	6.7	nd	0.27	1973.49	20.67	419.25
dfs2-1	0.01	0.05	0.14	10.11	4.16	2.30	0.04	0.71	0.11	1.98	156.94	1882.9	86.1	44057.7
2-2	0.02	0.06	0.17	5.57	9.90	0.63	0.04	0.42	0.09	0.56	19.85	2167.8	77.5	864.7
2-3	0.02	0.07	0.15	4.67	9.82	0.54	0.04	0.48	0.08	0.50	8.74	2408.1	44.6	994.9
2-4	0.02	0.06	0.18	4.54	8.39	0.56	0.03	0.50	0.07	0.43	4.37	2298.3	24.6	518.8
2-5	0.02	0.06	0.19	4.19	7.23	0.53	0.03	0.46	0.09	0.35	2.60	2672.4	26.5	4617.8
2-6	0.01	0.00	0.26	6.24	7.07	0.47	0.07	0.02	0.00	0.11	1.69	2325.1	62.7	1410.8
2-7	0.02	0.07	0.29	5.98	6.56	0.43	0.02	0.11	0.00	0.11	1.01	2847.6	31.5	1306.7
2-8	0.02	0.00	0.39	5.91	6.44	0.42	0.01	0.31	0.00	0.49	0.97	2389.4	37.0	1282.4
2-9	0.01	0.02	0.06	5.83	6.19	0.54	0.01	0.41	0.00	0.00	1.47	2311.4	44.0	1259.2
2-10	0.02	0.05	0.38	5.97	6.32	0.48	0.01	0.39	0.00	0.52	1.54	2391.5	18.0	1358.2
2-11	0.01	0.00	0.32	5.82	6.11	0.39	0.01	0.52	0.05	0.00	1.31	3349.4	11.1	1340.3
2-12	0.01	0.00	0.11	5.39	6.12	0.38	0.01	0.28	0.00	0.15	1.44	1765.7	7.1	1302.6
2-13	0.02	0.00	0.23	5.58	6.01	0.39	0.00	0.21	0.00	0.00	1.14	3342.5	18.1	1323.1
dws4-1	0.02	0.05	0.14	12.95	6.32	0.45	1.22	0.51	0.03	0.71	0.36	1054.7	1084.0	863.7
4-2	0.02	0.05	0.18	15.05	11.43	0.57	0.40	0.72	0.05	0.68	0.40	1880.9	1796.1	794.7
4-3	0.02	0.05	0.14	13.17	14.70	0.56	0.18	0.89	0.12	0.66	0.50	2209.4	249.4	635.1
4-4	0.04	0.05	0.16	15.07	13.30	0.56	0.17	0.81	0.08	0.49	0.48	2003.6	279.2	572.3
4-5	0.07	0.13	0.16	17.65	12.40	0.62	0.19	0.84	0.08	0.55	0.32	2326.0	173.1	782.7
4-6	0.10	12.38	0.18	18.94	10.19	0.62	0.21	0.87	0.07	0.43	0.42	4324.5	65.9	555.0
4-7	0.16	52.05	0.18	20.63	9.15	0.65	0.31	0.94	0.09	0.49	0.57	2135.5	23.7	478.0
4-8	0.45	90.97	0.18	21.01	8.64	0.61	0.46	0.92	0.08	0.43	0.73	2411.5	30.0	500.4
4-9	4.64	130.21	0.21	26.71	8.55	0.62	0.56	1.03	0.10	0.47	0.91	2702.4	28.7	645.5
4-10	9.09	136.10	0.49	34.36	7.88	0.54	10.19	0.69	0.00	0.00	0.12	2459.8	22.7	588.6
4-11	11.20	130.08	0.48	34.62	6.81	0.58	45.46	0.83	0.00	0.04	0.27	3339.5	7.9	536.5
4-12	11.79	127.43	0.19	34.01	6.36	0.32	82.12	0.51	0.02	0.30	0.34	3255.2	15.5	550.7
4-13	11.65	124.69	0.23	34.58	6.25	0.47	107.55	0.53	0.00	0.09	0.57	2004.3	4.1	517.9
mws5-1	0.02	0.08	0.09	8.72	16.24	0.24	0.24	0.34	0.04	1.67	0.29	1288.7	56.1	455.9
5-2	0.03	0.07	0.17	8.72	23.96	0.30	0.08	0.47	0.07	0.46	0.29	2802.9	29.5	426.8
5-3	0.14	0.93	nd	15.35	29.91	0.50	2.80	0.02	nd	nd	nd	2678.8	41.6	404.8

Table 7.5 Analytical results of eluates from column leaching tests with synthetic leachate (Unit: mg/l unless indicated)

More Si was leached from the weathered ashes than from the fresh ash. This also seems to indicate the effect of weathering. Si is one of the main components of aluminosilicate glass and more Si will be available in the weathered ash as the surface-enriched fractions on the ash particles become depleted and the Si-rich interiors of glass particles are exposed to weathering. Ba and Sr are also leached from the weathered ash with similar patterns to those shown by fresh ash.

The Fe concentrations in the emergent solutions (Table 7.5) are uniformly low and demonstrate retention in the column. Cd, Cu, Ni, Zn and Hg are also retained, but to differing degrees. The concentrations of all these elements in the eluates are initially very low. The capacity of the column to retain all of the Cd, Ni and Zn is exceeded with time and these elements attain a "break-through", with concentrations increasing towards the synthetic leachate values. There is partial retention of Cr in the column. Although Cr appears in the emergent solution at a relatively early stage, concentrations do not increase towards the synthetic leachate value as is the case with Cd, Ni and Zn. It is thought that adsorption reactions are significant elemental retaining mechanisms in column leaching tests. Equilibrium reactions involving solubility-controlling solid phases are also important. Such partial retention of the Cr, however, appears to suggest the presence of an additional retention reaction, such as the formation of secondary precipitates.

### **7.6.3 Comparison of the leaching of fresh and weathered PFA**

Elements are lost from the synthetic leachate when passed through columns of either fresh or weathered PFA. A "break-through" was achieved for Cd, Ni and Zn in the weathered PFA, but not in the fresh PFA. The capacity of fresh PFA to extract elements from solution would therefore appear to be greater than that of the weathered PFA. pH control on precipitation could be very important as was discussed previously, with solutions emerging from the fresh PFA with pH

values in the 9.9-9.1 range, whereas in the weathered PFA from Drax the pH range was 7.9-5.8.

Fresh PFA, with readily soluble ions such as Ca, has a greater capacity to neutralise the acidic synthetic leachate than does the weathered PFA. The formation of secondary minerals in weathered PFA could be important in the metal retention, but their influence would appear to be overshadowed by changes in the pH of the system of the column leaching test. In the column leaching tests the ratio of PFA sample to solution volume is large, hence the influence of pH. In the batch leaching tests the solution volume was large, compared with the sample mass, and there was little modification of the pH of the synthetic leachate. The pH values recorded were: fresh Drax pH = 4.80, weathered Drax = 4.75, and weathered Meaford = 5.00. Under these conditions, of near constant pH, the weathered PFA demonstrated a greater potential for element extraction compared with the fresh ash.

## 7.7 Conclusion

Column leaching tests with fresh and weathered PFA using water demonstrate the difference in behaviour between elements with a surface association and those incorporated in the glass. The former are readily leached, and the latter, which are proportionally more important in the weathered ash, are released more slowly.

A solution was prepared to simulate a landfill leachate at pH 4.5, containing heavy metals. When this solution was passed through columns of both weathered and fresh PFA, elements were lost from solution. Element "breakthrough" was obtained during the column leaching. The fresh PFA had a greater capacity for element retention than did the weathered PFA.

The eluate from the fresh PFA exceeded drinking water guide-line concentrations by a considerable margin. In the eluate from the weathered PFA

many elements were lower than the guide-line concentrations, but some elements exceeded the guide-line concentrations, indicating that dilution of the leachate from the PFA mounds would be required for the target concentrations to be achieved. The conclusions from the column leaching tests can be summarised as follows:

(1) Differential dissolution occurred as the solutions passed through the columns allowing the distribution of elements in the PFA to be inferred. The weathered PFA has reduced concentrations of elements associated with soluble fine particles and surfaces, nevertheless the PFA is not inert and elements were leached into solution.

With the weathered ash eluates, trace elements incorporated into the aluminosilicate glass were released, and the concentrations were relatively constant throughout the leaching process. The weathering of the glass is an important factor in controlling the release of trace elements in weathered ash.

(2) The initial eluate concentrations generated with deionised water give an indication of porewater concentrations. The elements in the eluate from fresh PFA were considerably in excess of drinking water guide-line concentrations, as is to be expected, but the weathered PFA also generated an eluate which would require some dilution for the permissible concentrations of a number of elements to be achieved.

(3) When solutions containing heavy metals were passed through columns of PFA, metals were removed from the solutions, thus confirming the findings of the batch leaching tests.

(4) The order of element retention by the PFA is: fresh Drax PFA > weathered Drax PFA > weathered Meaford PFA. In the batch leaching tests, however, the reverse order was obtained, with the most weathered PFA (Meaford) having the greatest capacity for element retention. It is postulated that this was due to reaction of the synthetic leachate with the secondary phases

produced during weathering. In the batch leaching tests the ratio of solution volume to PFA mass was large and hence the pH remained relatively constant during the course of the experiments, whereas the change of pH in the emergent solution is greater in the column leaching test due to the large ratio between the solid and water.

(5) Batch and column leaching tests provide valuable information regarding the potential behaviour of PFA in the natural environment. Column leaching more accurately reflects the natural system, but does not eliminate the need for field based observations, particularly as there may be kinetic constraints of some of the reactions in the columns. A comparison of the results of the experimental leaching work with those of the parallel study of porewaters in the PFA disposal mounds should be of particular relevance.

## Chapter 8

### Geochemical modelling of Water/PFA interaction

#### **8.1 Introduction**

The relationship between the solution concentrations in the PFA leachate and specific chemical reactions in waste/water system has recently been examined from a fundamental thermochemical perspective by some authors, including Ainsworth and Rai (1987), Rai *et al.* (1988), Fruchter *et al.* (1988, 1990). This new approach involves the concept of waste as a mixture of discrete solid phases that control the concentrations of elements in the solution through the processes of dissolution/precipitation and adsorption/desorption (Rai *et al.*, 1988).

When fresh ash is leached, the rate of dissolution of the surface-enriched solids controls the aqueous concentration in the PFA leachate. In the case of weathered ash, however, equilibrium reactions are more important than kinetic reactions. The field investigation of the ionic concentration variations with depth showed that several elements had achieved an equilibrium concentration. Once an element has achieved an equilibrium concentration, its concentration in aqueous solution is determined by specific solubility-controlling solid phases, regardless of the location, depth and age of the sample collected. This approach will be an appropriate way of dealing with the longer-term weathering reactions of PFA, in which equilibrium reactions are a primary control. In contrast to the previous empirical approach, which did not consider thermochemically, it is expected that this new approach will enable quantitative predictions to be made regarding the aqueous concentrations of elements in the waste leachate, through the knowledge of chemical reactions between PFA and water.

The analytical data from the leaching tests were processed by the geochemical simulation computer code WATEQ4F (Ball and Nordstrom *et al.*, 1987). This calculates ionic strength, ion speciation, single and complex ion activities for aquatic species, ion activity products, and saturation indices for mineral phases. The methodology and terminology around the use of the code are described in Appendix B. The effect of solubility-controlling solid phases can be viewed either by plotting single ion activities against pH, and then comparing this plot with the solute activities maintained by a specific solid phase, or by multiplying two single ion activities to yield an ion activity product (IAP) and comparing it with the IAP calculated from known solubility data (Fruchter and Rai *et al.*, 1988). If the single ion activity or IAP from the measured analytical data agree with the one calculated from known thermochemical data (for example data from Lindsay, 1979), this implies that the solubility-controlling solid phases are present in PFA. Furthermore, the presence of these inferred solid phases can be confirmed by observations made with an SEM or an XRD.

## 8.2 Major elements

### 8.2.1 Silicon

Although Si in PFA is not of much concern, in terms of its environmental toxicity, many trace elements are associated with Si (Chapter 7), and the rate of Si release is thought to be an important factor in controlling the Si-associate trace element concentrations in the PFA leachate. Cr, B, Li and Mo in weathered Drax and Meaford ash were dissolved along with the dissolution of Si in the column leaching tests using deionised water.

The Si content of the porewater extracted from Drax and Meaford ashes in the field decrease with depth, indicating the presence of solubility

controlling phases. Ainsworth and Rai *et al.*, (1987) reported that  $\text{SiO}_2(\text{am})$  was the solubility-controlling phase at pH values  $< 10$ , in hot water extracted from PFA leachate. In the same study (Ainsworth and Rai *et al.*, 1987), it was suggested that  $\text{CaSiO}_3$  is a solubility-controlling phase at  $\text{pH} > 10$ . In the work of Fruchter and Rai *et al.* (1988, 1990), however, wairakite ( $\text{CaAl}_2\text{Si}_4\text{O}_{12} \cdot 2\text{H}_2\text{O}$ ) was suggested, instead of  $\text{SiO}_2(\text{am})$ , as a Si solubility-controlling solid phase.

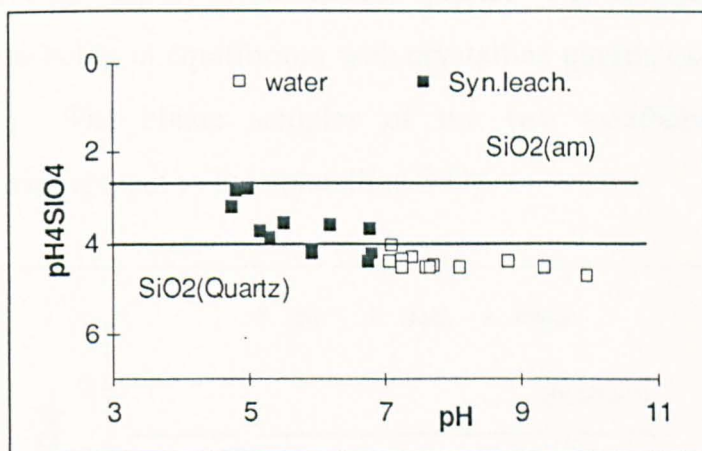


**Figure 8.1** Plot of calculated activities of  $\text{H}_4\text{SiO}_4$  v. pH from the batch leaching tests, along with calculated activities in equilibrium with  $\text{SiO}_2(\text{am})$  and  $\text{SiO}_2(\text{Quartz})$

In Figure 8.1, measured activities of  $\text{H}_4\text{SiO}_4$  from the batch leaching tests were plotted against pH, along with the line of the calculated  $\text{H}_4\text{SiO}_4$  activities in equilibrium with amorphous and crystalline  $\text{SiO}_2$ . The eluates from the batch leaching tests were slightly pH dependent in the case of some acidic samples, but the activities were generally constant, in the range of  $\text{pH} > 5$ . The concentrations of the eluates obtained from the synthetic leachate were higher than those treated with deionised water, due to the more aggressive nature of the synthetic leachate, which contained dissolving agents in the form of organic acids. Except for the three samples with the highest activities, which fall near the Si activity line in equilibrium with  $\text{SiO}_2(\text{am})$ , the activities from the batch leaching tests generally show similar values, with the activities in

equilibrium with crystalline quartz. The data from the batch leaching tests therefore seems to suggest that  $\text{SiO}_2$  is an Si solubility-controlling phase.

Figure 8.2 is a diagram using the data from the column leaching tests with deionised water. Again, measured  $\text{H}_4\text{SiO}_4$  activities were plotted against pH, along with calculated activities of  $\text{H}_4\text{SiO}_4$  in equilibrium with amorphous and crystalline  $\text{SiO}_2$ . The measured activity of  $\text{H}_4\text{SiO}_4$  shows a slight decrease with increasing pH value. The diagram shows that all eluates were undersaturated with respect to amorphous quartz. The eluates of fresh Drax ash were near to being in equilibrium with crystalline quartz, except for several initial eluates. The eluate samples of the two weathered ashes were oversaturated with respect to the crystalline  $\text{SiO}_2$ .

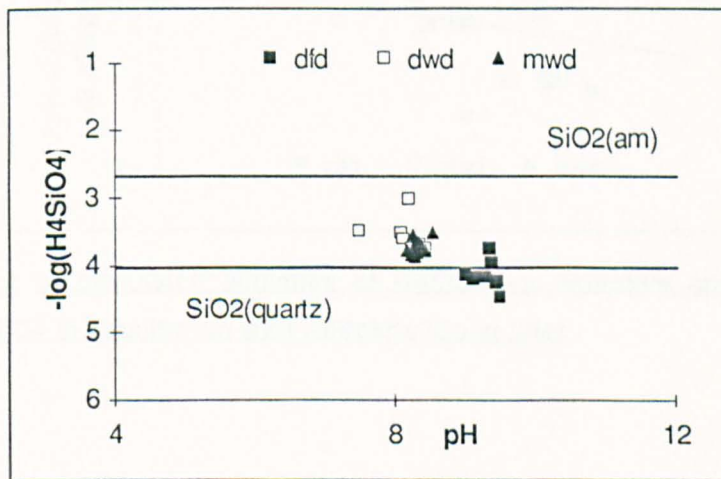


**Figure 8.2** Plot of calculated activities of  $\text{H}_4\text{SiO}_4$  vs. pH from the column leaching tests, along with calculated activities in equilibrium with  $\text{SiO}_2(\text{am})$  and  $\text{SiO}_2(\text{quartz})$

Another phase which may control the solubility of Si, wairakite ( $\text{CaAl}_2\text{Si}_4\text{O}_{12} \cdot 2\text{H}_2\text{O}$ ), was proposed by Fruchter and Rai *et al.* (1988, 1990). The calculated activity of  $\text{H}_4\text{SiO}_4$  in equilibrium with wairakite was plotted against measured activity of  $\text{H}_4\text{SiO}_4$  in Figure 8.3. Wairakite is the calcium analogue of analcite and was recorded in tuffaceous sandstones, vitric tuffs and ignimbrite which had been altered by alkaline hydrothermal fluids (Deer and

Howie *et al.*, 1992). The fresh ash eluate did not conform with the equilibrium activities line of wairakite, whereas the eluate from weathered ash did conform well with this line, and this seems to suggest that wairakite was a solubility-controlling phase during the leaching of the weathered ash.

From the relationships seen in Figures 8.1, 8.2 and 8.3, it appears that crystalline quartz is the Si solubility-controlling phase in fresh ash, whereas wairakite may be the Si solubility-controlling phase in the weathered ashes.

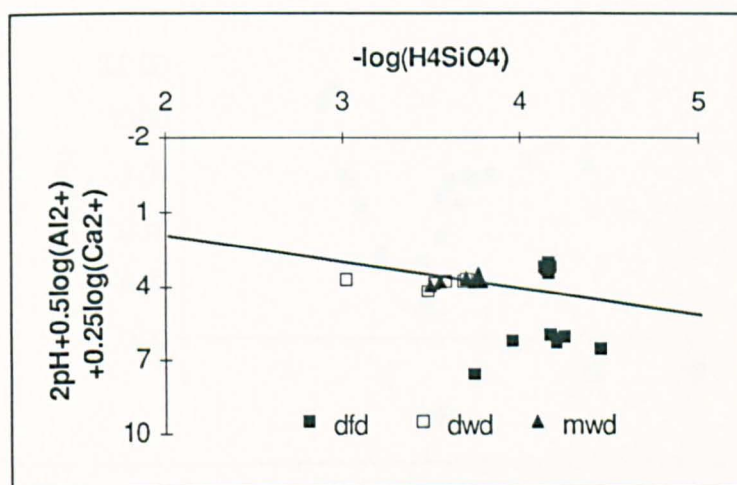


Figure 8.3 Plot of calculated activities of  $\text{H}_4\text{SiO}_4$  vs. wairakite and the predicted activity of  $\text{H}_4\text{SiO}_4$  in equilibrium with wairakite (Solid line)

### 8.2.2 Aluminium

Al is a main component of Al-Si PFA glass and the quartz-mullite phase. Mullite ( $3\text{Al}_2\text{O}_3 \cdot 2\text{SiO}_2$ ) has been reported to have an acicular form (Hu lett *et al.*, 1980, Warren and Dudas, 1984). The mullite is thought to result from the transformation of clay minerals in the feed coal at high temperatures (Hubbard and Weinberger *et al.*, 1984). At these high temperatures Al-Si oxides are less stable than  $\text{AlHSO}_4(\text{s})$  and  $\text{Al}(\text{OH})_3(\text{s})$  (Rai and Mattigod *et al.*, 1988). Several researchers (Talbot and Anderson *et al.*, 1978; Henry and

Knapp, 1980; Roy and Griffin, 1984) have predicted the presence of these secondary stable products in weathered ash.

The concentration of Al in the eluates from the batch leaching tests was strongly pH-dependent, as shown in Figure 8.4. This follows the typical solubility relationship of Al with pH, which is controlled by various Al hydroxides (Parks, 1972). This relationship seems to suggest Al is controlled by dissolution/precipitation processes involving solid phases.

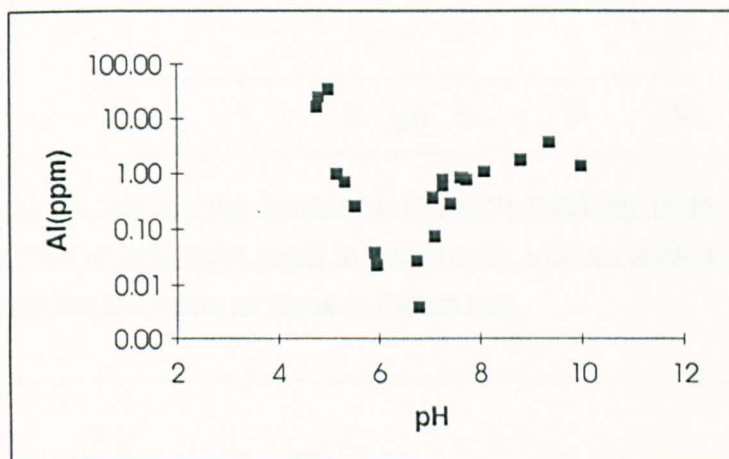


**Figure 8.4** Variation of Al concentration in the eluate from the batch leaching test as a function of pH

Measured  $\text{Al}^{3+}$  activities from the batch leaching tests were plotted against pH, along with the calculated activities in equilibrium with two different forms of  $\text{Al}(\text{OH})_3$ , as shown in Figure 8.5. Ainsworth and Rai (1987) reported that Al in PFA was controlled by  $\text{Al}(\text{OH})\text{SO}_4$  under conditions of  $\text{pH} < 6$ , by amorphous  $\text{Al}(\text{OH})_3$  at pH values between 6 and 9, and by crystalline  $\text{Al}(\text{OH})_3$  (gibbsite) at pH greater than 9. In the batch leaching tests, the range of pH values was between 4.0 and 10.0, so amorphous or crystalline  $\text{Al}(\text{OH})_3$  would appear to be the solid phase controlling the solubility of Al. The measured  $\text{Al}^{3+}$  activities show a similar trend to that of the calculated activity of  $\text{Al}(\text{OH})_3$  (am) at pH values up to 9, whereas at pH values above 9 the  $\text{Al}^{3+}$

activities fall closer to the line calculated for  $\text{Al}^{3+}$  activities in equilibrium with crystalline  $\text{Al}(\text{OH})_3$  (gibbsite).

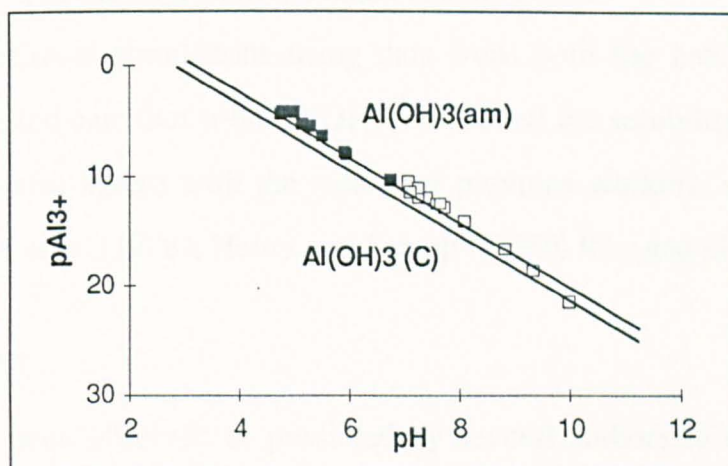


**Figure 8.5**  $\text{pAl}^{3+}$  vs. pH for the eluates from batch leaching tests, along with the calculated activities of  $\text{Al}^{3+}$  (solid lines) in equilibrium with crystalline and amorphous  $\text{Al}(\text{OH})_3$  (Symbols are the same as those in Figure 8.2)

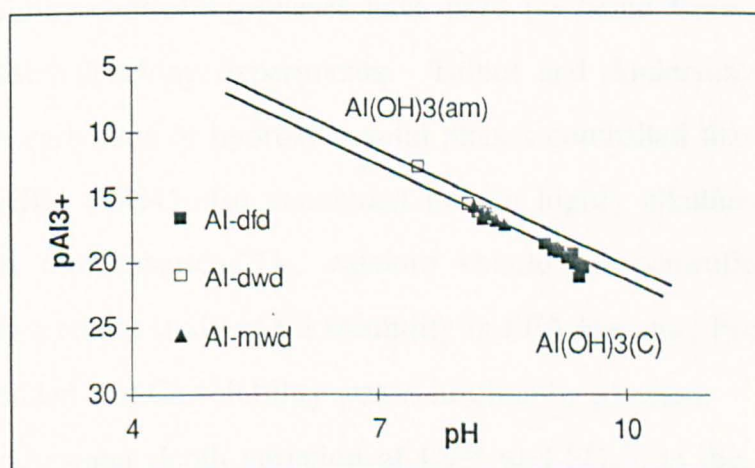


**Figure 8.6** Plot of measured activity of  $\text{Al}^{3+}$  against pH for the eluates from column leaching tests, along with the calculated activities of  $\text{Al}^{3+}$  (solid lines) in equilibrium with crystalline and amorphous  $\text{Al}(\text{OH})_3$

In Figure 8.6, the measured activities of  $\text{Al}^{3+}$  of eluates from the column leaching tests are plotted against pH, along with lines of calculated activities in equilibrium with amorphous and crystalline  $\text{Al}(\text{OH})_3$ . The eluates obtained from the columns treated with deionised water showed similar results to those

of the batch leaching tests. However, data from the column leaching tests fall mainly on the crystalline  $\text{Al}(\text{OH})_3$  line rather than on the amorphous  $\text{Al}(\text{OH})_3$  line, in contrast to the data from the batch leaching tests.

Geochemical simulations using data from both the batch and column leaching tests indicate that solid  $\text{Al}(\text{OH})_3$  controlled the solubility of Al in PFA eluate. This also agrees with the results of previous workers, such as Talbot and Anderson *et al.* (1978), Henry and Knapp (1980), Roy and Griffin (1984).

### 8.2.3 Calcium

Calcium has been observed or predicted by several authors to occur in many different minerals in fresh and weathered ashes. Solid phases that have been observed in weathered ash are: calcite and gypsum (Warren and Dudas, 1985), and ettringite (Simons and Jeffery, 1960). Apart from the observed solid phases, solubility-controlling phases have been predicted from the results of laboratory batch leaching experiments. Talbot and Anderson *et al.* (1978) reported that carbonate or hydroxide solid phases controlled the Ca solubility. Roy and Griffin (1984) also concluded that in highly alkaline solutions, in contact with atmospheric  $\text{CO}_2$ , calcium should be controlled by calcite solubility. In a recent study of Ca solubility in PFA leachate, Fruchter and Rai (1988) concluded that Ca solubility was controlled by gypsum.

The porewater depth variation of  $\text{Ca}^{2+}$  and  $\text{SO}_4^{2-}$  in the field, and the geochemical calculations using the field data, demonstrated that Ca in the PFA porewater achieved equilibrium concentration with respect to gypsum (Chapter 3). Therefore it can be stated that gypsum controls the solubility of Ca in PFA leachate.

The above conclusion is not confirmed by the experimental data. The measured activity of  $\text{Ca}^{2+}$  from the batch leaching tests was plotted against pH, along with the calculated activities of possible solubility-controlling phases, including gypsum and calcite (Figure 8.7). The measured activities of  $\text{Ca}^{2+}$  in

the eluates were undersaturated with respect to  $\text{CaCO}_3$ , except for some eluates of fresh PFA (Figure 8.7). This is also demonstrated by the saturation indices given in Table 8.1, which indicate that the eluates were undersaturated with respect to all four Ca-minerals, except for some eluates from fresh PFA, which were oversaturated with respect to calcite. As pH increased all of the eluates became oversaturated with respect to calcite but undersaturated with respect to gypsum. This diagram suggests that neither calcite nor gypsum are suitable concentration-controlling solid phases. When alkaline solution in PFA is in equilibrium with atmospheric  $\text{CO}_2$ , the concentration of Ca in the solution should be controlled by calcite solubility (Roy and Griffin, 1984), therefore it follows that the present results suggest that the eluates from the batch leaching tests were not at equilibrium with atmospheric  $\text{CO}_2$ .

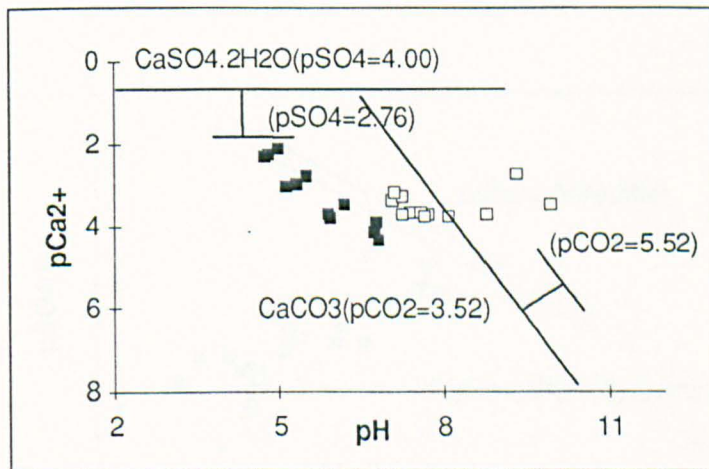


**Figure 8.7** Plot of measured  $\text{Ca}^{2+}$  activity in eluates from batch leaching tests vs. pH, along with the calculated activities in equilibrium with gypsum and calcite (The legend is the same as in Figure 8.1)

The measured activities of  $\text{Ca}^{2+}$  and  $\text{SO}_4^{2-}$  were plotted, along with the calculated activities in equilibrium with gypsum and anhydrite, in Figure 8.8. The concentrations of Ca and  $\text{SO}_4^{2-}$  in the batch leaching tests decreased as leaching progressed, with the measured activities becoming more undersaturated with respect to gypsum as leaching progressed. Figure 8.8

indicates that the Ca and  $\text{SO}_4^{2-}$  in the eluates did not achieve equilibrium concentration with respect to gypsum in the batch leaching tests.

	mws1	mws2	mws4	dws1	dws2	dws4	dfs1	dfs2	dfs4
<b>Aragonite</b>	-0.225	-1.232	-2.498	-0.632	-2.065	-3.363	-0.584	-1.913	-3.602
<b>Calcite</b>	-0.082	-1.088	-2.355	-0.448	-1.921	-3.219	-0.440	-1.769	-3.458
<b>Anhydrite</b>	-0.888	-2.323	-3.679	-0.980	-2.565	-4.476	-0.621	-2.271	-4.106
<b>Gypsum</b>	-0.686	-2.105	-3.459	-0.811	-2.347	-4.256	-0.440	-2.052	-3.886
	mwd1	mwd2	mwd4	dwd1	dwd2	dwd4	dfd1	dfd2	dfd4
<b>Aragonite</b>	-1.371	-1.556	-1.420	-1.125	-1.183	-0.896	1.233	0.722	-0.083
<b>Calcite</b>	-1.227	-1.422	-1.276	-0.981	-1.309	-0.752	1.388	0.866	0.061
<b>Anhydrite</b>	-2.081	-3.672	-4.264	-2.803	-3.763	-4.323	-0.950	-2.644	-3.977
<b>Gypsum</b>	-2.581	-3.452	-4.044	-2.583	-3.543	-4.103	-0.830	-2.444	-3.757

**Table 8.1 Saturation Indices with respect to Ca-bearing mineral phases possibly affecting the eluate**

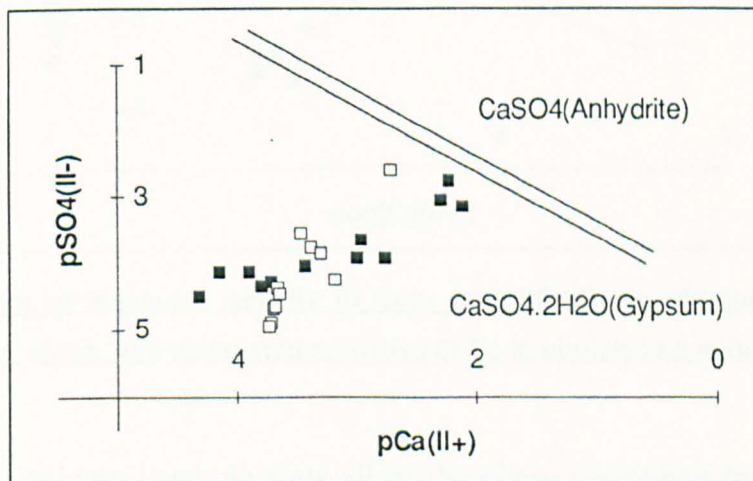


**Figure 8.8 Plot of calculated activities of  $\text{SO}_4(\text{II}^-)$  vs.  $\text{Ca}^{2+}$  in eluate from batch leaching tests, along with predicted activities of gypsum and anhydrite (solid lines)**

The column leaching tests gave similar results to the batch leaching tests. The measured activities of Ca and  $\text{SO}_4$  in all of the eluates are plotted in Figure 8.9, together with the line of activities in equilibrium with gypsum. The eluate samples from fresh Drax PFA fall on the equilibrium line for gypsum,

but the activities of the eluates from weathered ash are greatly undersaturated with respect to the gypsum. As was the case for the batch leaching tests, the concentrations of Ca and  $\text{SO}_4^{2-}$  decreased as leaching progressed, and the lowest activity values are from eluates obtained at a late stage of leaching. Therefore, the Ca concentrations of the eluates from weathered ash did not achieve equilibrium concentration during the column leaching tests. The solubility of Ca in the eluate from fresh Drax ash was initially controlled by gypsum, but as the Ca concentration in the eluate decreased, as leaching progressed, the eluate from the fresh ash also became undersaturated with respect to gypsum.

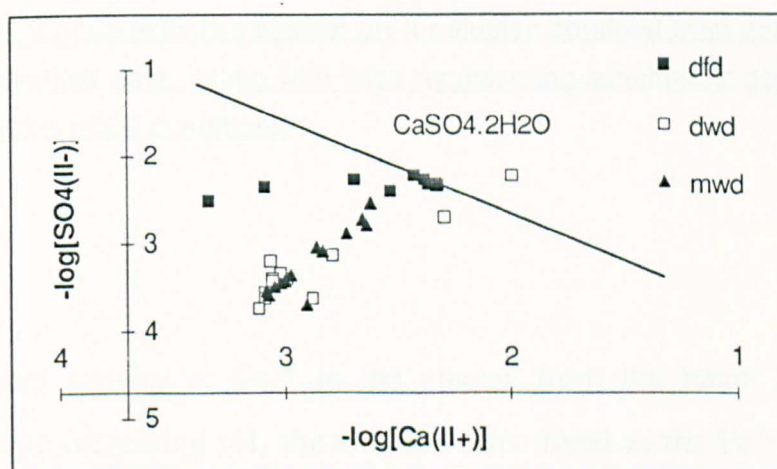


**Figure 8.9** Plot of measured activity of  $\text{Ca}^{2+}$  and  $\text{SO}_4(\text{II}-)$  in eluates from column leaching tests, along with calculated activities of Ca in equilibrium with gypsum

In the column leaching tests all of the eluates obtained by treating PFA with deionised water had pH values greater than 8, and were oversaturated with respect to calcite ( $\text{pCO}_2=3.52$ ), as shown in Figure 8.10. This suggests that there was enough time for the atmospheric  $\text{CO}_2$  to have an influence on the eluates during the column leaching tests. In an alkaline environment, Ca is thought to be controlled by the solubility of calcite, whereas gypsum is the solubility-controlling phase in a neutral to acidic environment.  $\text{Ca}(\text{OH})_2$  was

reported to exist in an extremely alkaline environment, with  $\text{pH} > 12$  (Fruchter and Rai *et al.*, 1988).

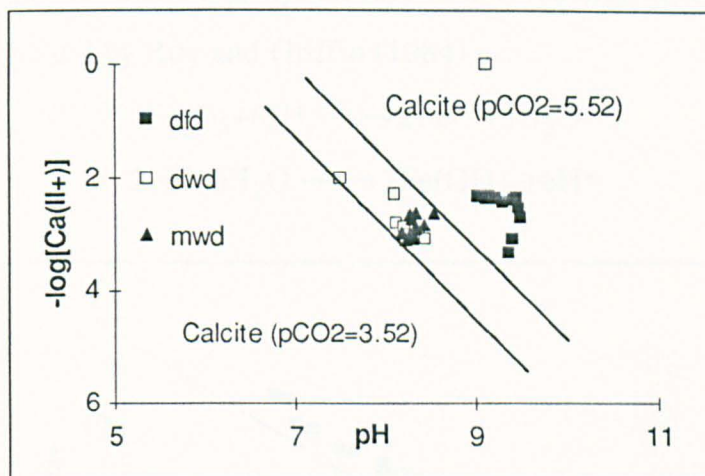


**Figure 8.10** Plot of Ca activities against pH for eluates obtained from column leaching tests using distilled water, along with lines representing activities in equilibrium with calcite at various  $\text{pCO}_2$  conditions

#### 8.2.4 Iron

The measured activity of  $\text{Fe}^{3+}$  in the eluates from the batch leaching test decreased with increasing pH, showing the same trend as the  $\text{Fe}^{3+}$  activity line representing solution in equilibrium with  $\text{Fe}(\text{OH})_3(\text{am})$ , but slightly oversaturated with respect to it, as shown in Figure 8.11. Such a discrepancy is thought to be due to the presence of some colloidal  $\text{Fe}(\text{OH})_3$ , which are not retained by  $0.45 \mu\text{m}$  filter. Colloidal metal ion precipitates such as  $\text{Fe}(\text{OH})_3(\text{s})$  or  $\text{FeOOH}(\text{s})$  may often have particle size smaller than  $0.01 \mu\text{m}$  (Stumm and Morgan, 1981). This result agrees well with the previous research of Ainsworth and Rai *et al.* (1987), Fruchter and Rai *et al.* (1988, 1990), implying that Fe concentrations in the PFA eluates were controlled by amorphous iron hydroxide precipitates.

In Figure 8.12, the activity of  $\text{Fe}^{3+}$  is plotted against pH for the eluates from the column leaching tests, along with the activity line of  $\text{Fe}^{3+}$  in

equilibrium with amorphous  $\text{Fe}(\text{OH})_3$ . The results obtained from the column leaching tests provide confirmation of the results of the batch leaching tests. The reactions of Fe-oxides and hydroxides in the reaction of PFA with water have been suggested by Roy and Griffin (1984) as:

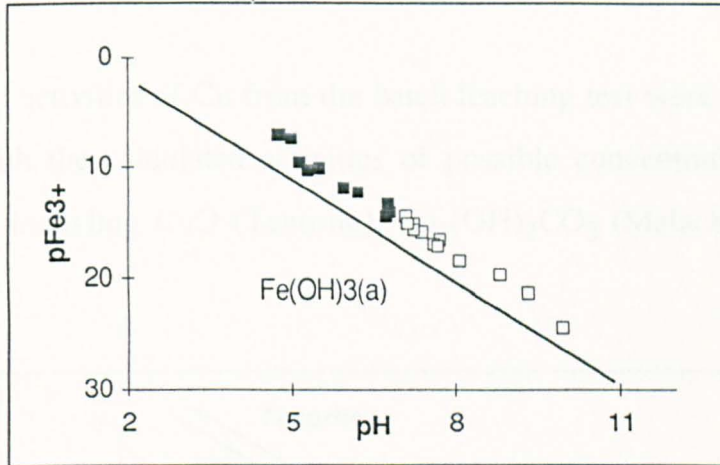
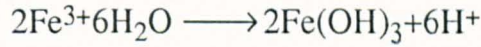


**Figure 8.11** Plot of measured  $\text{Fe}^{3+}$  activity vs. pH, along with calculated  $\text{Fe}^{3+}$  activity in equilibrium with  $\text{Fe}(\text{OH})_3$  (am) (solid line), batch leaching tests

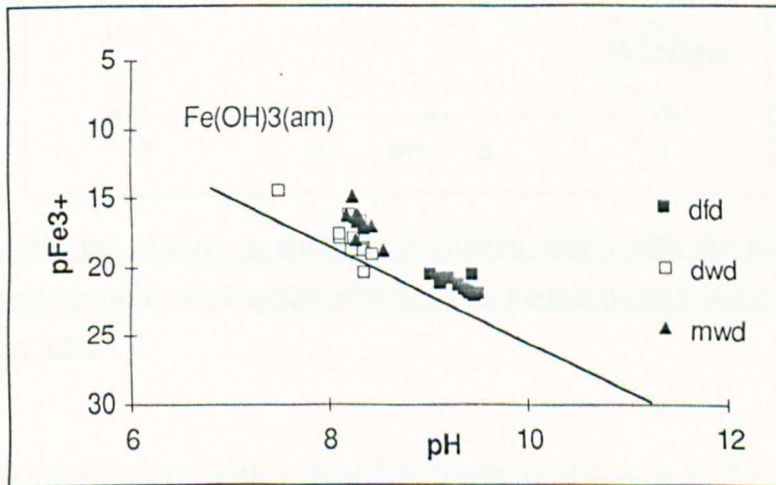


**Figure 8.12** Plot of measured activities of  $\text{Fe}^{3+}$  against pH in the eluates of column leaching tests, along with calculated  $\text{Fe}^{3+}$  activity in equilibrium with amorphous  $\text{Fe}(\text{OH})_3$ , column leaching tests

All of the data shown in the diagram show slight oversaturation with respect to  $\text{Fe}(\text{OH})_3$ . This is probably due to suspended colloidal Fe hydroxides that passed through the  $0.45 \mu\text{m}$  filter used in both types of experiment.

## 8.3 Trace elements

### 8.3.1 Copper

The measured activities of Cu from the batch leaching test were plotted against pH, along with the calculated activities of possible concentration-controlling solid phases, including CuO (Tenorite),  $\text{Cu}_2(\text{OH})_2\text{CO}_3$  (Malachite), and Soil-Cu,

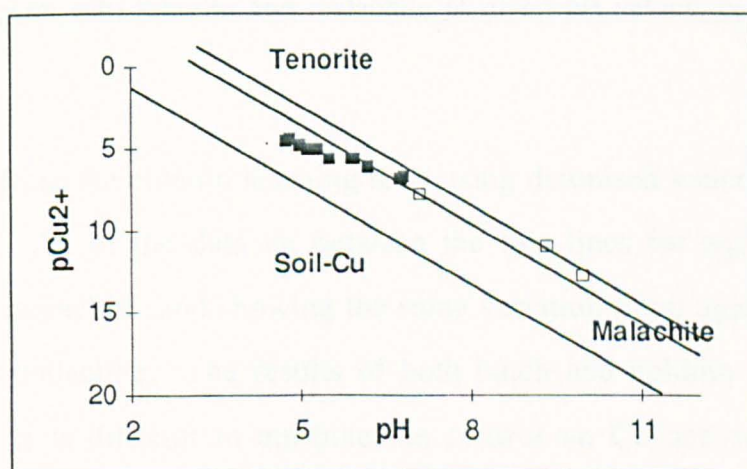


**Figure 8.13** Activities of  $\text{Cu}^{2+}$  against pH in eluates, along with the calculated  $\text{Cu}^{2+}$  activities at various pH in equilibrium with tenorite, malachite and soil-Cu (solid lines), batch leaching tests

which are in equilibrium with a solution containing Cu, at a given pH (Figure 8.13). Eluates with pH values between 2 and 6 fall on the calculated activity line for equilibrium with malachite. For pH values above 6, Cu seems to be partly controlled by tenorite. This result is slightly different from that reported by Fruchter and Rai *et al.* (1988), who reported that Cu is controlled

exclusively by CuO in the pH range 6 to 10. This difference may be due to the different chemistries of the two types of leachate used in these experiments, namely synthetic leachate and distilled water.

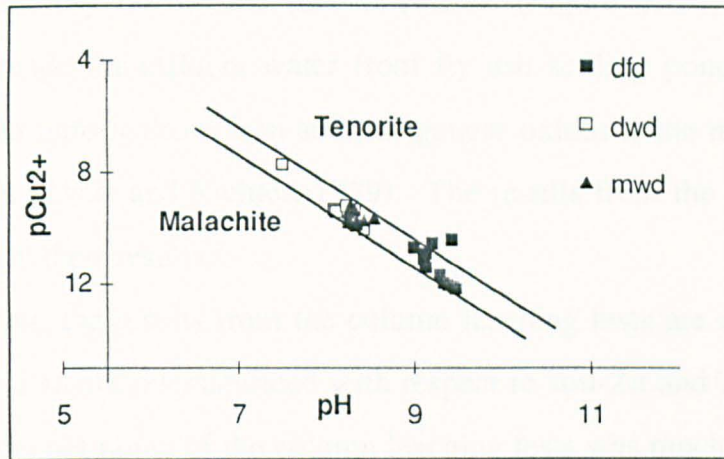


**Figure 8.14** Plot of calculated Cu<sup>2+</sup> activities vs. pH, along with predicted activities of Cu in equilibrium with tenorite and malachite at given pH values, column leaching tests

Data from the column leaching tests using deionised water are shown in Figure 8.14. All of the data lie between the two lines for equilibrium with tenorite and malachite, and showing the same variation trend against pH as the tenorite and malachite. The results of both batch and column leaching tests suggest that it is difficult to attribute the control on Cu activity to a single solubility-controlling phase. In the case of the eluate of fresh Drax ash treated with deionised water, it appears that tenorite is initially the solubility-controlling solid phase for Cu, but malachite takes over this function as the Cu activity decreases, as leaching progresses. The eluates of the weathered ashes are all undersaturated with respect to tenorite and oversaturated with respect to malachite. The results from the batch and column leaching tests would seem to suggest malachite generally controls the solubility of Cu in the interaction of PFA with water.

### 8.3.2 Zinc

The measured activities of Zn, which were plotted against pH along with the calculated activities of Zn-bearing solution in equilibrium with soil-Zn and  $\text{ZnCO}_3$ , exclusively fall on the line of soil-Zn (Figure 8.15). Geochemical calculations made for effluent water from fly ash settling ponds have shown that adsorption onto hydrous iron and manganese oxides is the major solubility control for Zn (Theis and Richter, 1979). The results from the batch leaching tests agree with their results.

However, the results from the column leaching tests are different, since nearly all the data are oversaturated with respect to soil-Zn and  $\text{ZnCO}_3$  (Figure 8.16). Also the pH range of the column leaching tests was much narrower than that of the batch leaching tests. In Figure 8.16, none of the data sets show a clear variation with pH. However, the data from the column leaching tests appear to approach the line of soil-Zn as the activity values decrease. Considering the results of both leaching tests, it is expected that Zn is ultimately controlled by soil-Zn, although the PFA eluate is initially oversaturated with respect to Zn-solids, including ZnO and  $\text{ZnCO}_3$ .

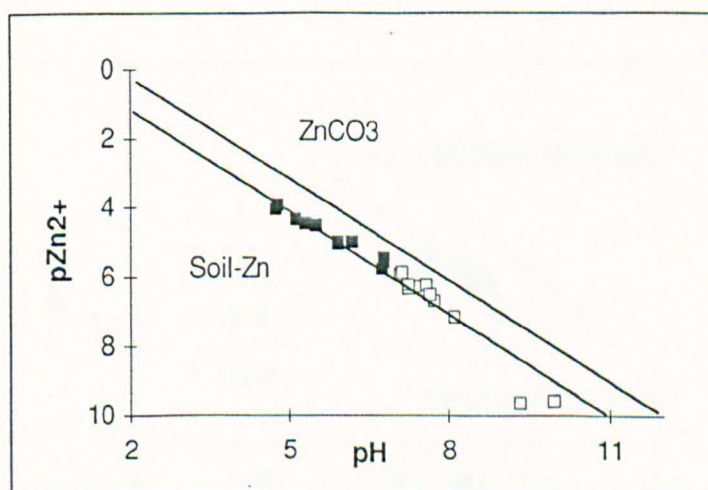


Figure 8.15 Plot of Zn activities with pH, along with calculated activities of Zn in equilibrium with Soil-Zn and  $\text{ZnCO}_3$  at given pH values (solid lines), batch leaching tests

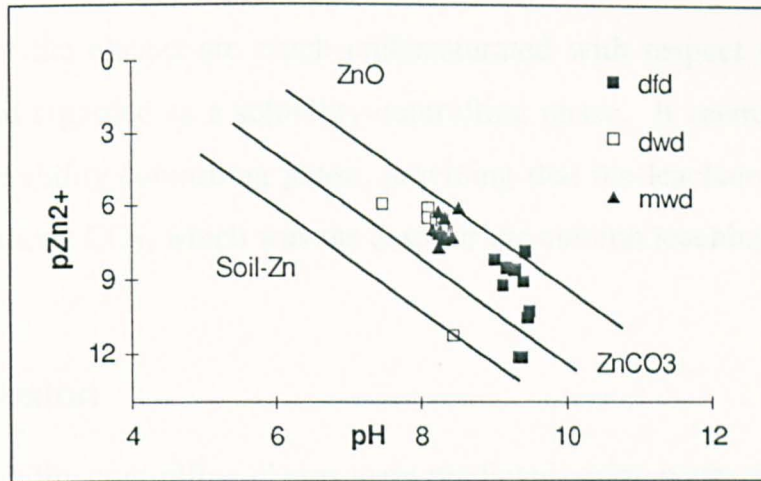


Figure 8.16 Plot of Zn activities with pH, along with calculated activities of Zn in equilibrium with Soil-Zn, ZnO and ZnCO<sub>3</sub> at given pH values(solid lines), column leaching tests

### 8.3.3 Lead

The equilibrium relationships of Pb were investigated only for the eluates of the column leaching tests, due to the low concentrations of Pb in the eluates of the batch leaching tests. In nearly all of the eluates, Pb was undersaturated with respect to PbCO<sub>3</sub>, whereas the eluate from fresh Drax ash is oversaturated with respect to these minerals in the initial leaching stage (Figure 8.17).

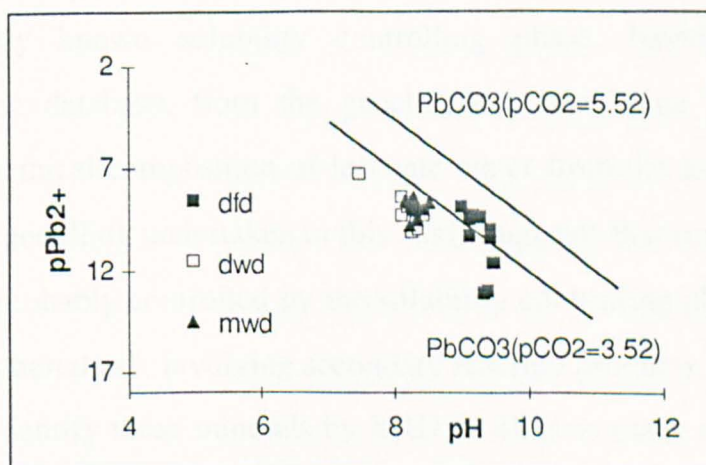


Figure 8.17 Plot of measured Pb activities with pH, along with calculated activities of Pb in equilibrium with PbCO<sub>3</sub> at given pH and pCO<sub>2</sub> values (solid lines), column leaching tests

All of the eluates are much undersaturated with respect to  $\text{PbSO}_4$ , so  $\text{PbSO}_4$  is not regarded as a solubility-controlling phase. It seems that  $\text{PbCO}_3$  may be a solubility-controlling phase, providing that the leachate is in contact with atmospheric  $\text{CO}_2$ , which was the case for the column leaching tests.

## 8.4 Conclusion

Several solubility controlling phases were predicted, using water analytical data from the leaching tests. Gypsum was identified as a concentration limiting phase for  $\text{Ca}^{2+}$  and  $\text{SO}_4^{2-}$ , both in the borehole porewater and the eluates leaching tests. Other solubility controlling solid phases identified in this study include quartz and wairakite for  $\text{SiO}_2$ ,  $\text{Al}(\text{OH})_3$  for Al,  $\text{Fe}(\text{OH})_2$  (am) for Fe, tenorite or malachite for Cu and  $\text{PbCO}_3$  for Pb. However, it should be noted that any of the predicted solubility controlling solid phase were not detected by XRD or SEM, which is crucial evidence for the geochemical modelling to be feasible in applying the natural weathering reaction of PFA. Although, it might be explained as the low concentrations for the trace elements, the solid phase involving major elements such as gypsum should be detected in the weathered PFA samples.

Precisely known solubility controlling phase, based on a sound thermodynamic database, from the geochemical calculation would help to predict the chemical composition of leachate water from the ash mound. The geochemical modelling undertaken in this study suggests that reactions of many elements are probably controlled by the solubility controlling phase both in the fresh and weathered ash, involving secondary reaction products. It is, however, necessary to identify those minerals by XRD or SEM to make the geochemical modelling a practical and feasible in understanding the reaction of PFA quantitatively and in modelling the natural weathering reaction of PFA.

## **Chapter 9**

### **Conclusions**

The potential influence of long-term PFA weathering on groundwater pollution was investigated in this study. There have been numerous studies of the environmental significance of PFA, but these have mainly focused on the leaching behaviour of fresh PFA, and over a relatively short period. Few previous studies have paid attention to the long-term leaching behaviour of weathered PFA.

The study began with direct observations of the reactions seen in weathered ash, in the field. Four boreholes of weathered PFA were taken by hand-auger drill from the Barlow ash disposal mound, which is adjacent to the Drax Power Station. The ash from the Barlow mound was up to 17 years old. In addition to the weathered ash samples from the Barlow mound, additional samples were also taken from the ash disposal mound at Meaford Power Station, to extend the age range of sample studied. The age of the oldest sample from this site is thought to be about 40 years. Porewater was extracted from the weathered PFA borehole samples, and the depth variation of the individual elements in the extracted porewater was investigated, along with the corresponding chemical and mineralogical changes in the solid PFA.

In addition to the field investigation, two different types of leaching test were conducted in the laboratory, namely batch and column leaching tests. These tests were performed using fresh and weathered Drax ash and weathered Meaford ash samples. The aims of these laboratory experiments were twofold: firstly, to simulate the natural weathering reaction of PFA in the laboratory and confirm the field work, and secondly, to investigate the ameliorating capability of PFA, particularly with respect to land-fill leachates, by trace elemental retention. The field investigation and the laboratory experiments are therefore complementary.

The field investigation of the PFA porewater from the Barlow mound revealed that nearly all of the elements in the porewater show depth-related trends.

Three different types of depth trend are generally shown: increasing concentration with depth, attainment of constant concentrations and decreasing concentration with depth. Ca and  $\text{SO}_4^{2-}$  were the two main ions derived from the weathering reactions of PFA with porewater. The concentrations of Mg, Na and K were also relatively high and B was the most mobile trace element, having a highest value of 19.7 mg/l. Li and Mo were also relatively mobile, recording maximum values of 2.2 and 3.1 mg/l respectively.  $\text{Cl}^-$  and  $\text{NO}_3^-$  decrease with depth and the origin of these two elements was attributed to an external source, namely fertiliser.

Calcium concentration attained near constant concentrations with depth in the borehole porewaters. Ca showed an inverse relationship with  $\text{SO}_4^{2-}$  in the porewater, implying the achievement of an equilibrium concentration with respect to a solid phase. This possibility was investigated using a geochemical computer code: WATEQ4F. The measured activities line of  $\text{Ca}^{2+}$  and  $\text{SO}_4^{2-}$  were compared with the calculated activities line of the  $\text{Ca}^{2+}$  and  $\text{SO}_4^{2-}$  in equilibrium with gypsum and the agreement between the two lines confirmed the gypsum as a solubility controlling solid phase. The saturation indices of porewater were also in near equilibrium with respect to gypsum in the depth range investigated, confirming the result in the above, which was obtained by comparing of single activities of  $\text{Ca}^{2+}$  and  $\text{SO}_4^{2-}$ .

Other elements with depth trends that imply the achievement of equilibrium concentration are: Ba, Sr and Si, and possibly Cu and Zn. The concentrations of Cu and Zn were low, in both cases below 30  $\mu\text{g/l}$ , so the depth trends were less reliable.

The concentrations of the major elements Na, K and Mg increase with depth and do not show evidence of having achieved equilibrium concentrations in the depth range investigated. Among the trace elements, B, Cr, Li, Mo, Pb, Ni, As and Se increase with depth. These elements do not show clear evidence of having achieved equilibrium concentration, and therefore their concentrations do not

appear to be controlled by specific solubility-controlling solids in the depth range investigated.

Geochemical modelling of the water analytical data, using the WATEQ4F computer program, yielded information on the solubility-controlling solid phase for a wide range of elements. The results of a comparison of the measured single ion activity plotted against pH with the calculated activity in equilibrium with various possible solid phases at a given pH. This is also able to be checked by an examination of the saturation indices, which are acquired by a comparison of ion activity products with the equilibrium constant. The calculation using the borehole porewater data identified gypsum as a solubility controlling phase for  $\text{Ca}^{2+}$  and  $\text{SO}_4^{2-}$ . No solubility controlling solid phases were identified for Na, K, Mg in the borehole porewater. The calculation using the data from the leaching experiments revealed  $\text{Al}(\text{OH})_3$  to be a solubility-controlling phase for Al, and  $\text{Fe}(\text{OH})_3$  for amorphous Fe.  $\text{SiO}_2$  were indicated to be solubility-controlling phases for Si in fresh ash, and wairakite ( $\text{CaAl}_2\text{Si}_4\text{O}_{12}\cdot 2\text{H}_2\text{O}$ ) for Si in weathered ash. Cu seemed to be controlled by malachite or tenorite. Zn gave varied results, the batch leaching tests indicated that soil-Zn controlled the solubility of Zn, whereas the column leaching tests suggested that  $\text{ZnCO}_3$  was the governing phase. However, the measured Zn activity in the column leaching tests decreased, as leaching progressed, towards the line of Zn activities in equilibrium with soil-Zn, so soil-Zn would seem to be the ultimate solubility-controlling phase for PFA.

The depth trends of the elements in the Drax porewater were only confirmed by the corresponding depth trends of solid weathered Drax PFA for a few elements. This is because the ratio of the amount of elements released from solid PFA to the total amount of elements in the PFA is very small, whereas the change with depth of the concentration of an element in porewater was much greater, and therefore easier to detect. Ca, Mg and S (as  $\text{SO}_3$ ) in solid PFA showed depth trends that corresponded to those of the porewater, thereby confirming the validity of the depth trends seen in the porewater. The chemical

changes during weathering could have resulted in the formation of secondary mineral products, such as clays. However, no evidence of secondary clay minerals was obtained by using an XRD and an SEM. Some clay peaks in the X-ray diffractograms obtained are thought to represent clay minerals that have been translocated from the top soil.

The depth trends of porewater and solid PFA, and the mineralogy of the Meaford weathered ash, are similar to that of the Barlow mound, at Drax Power Station. The depth trends of the Meaford porewater and solid PFA, however, are more distinct than those of the Drax ash. The Meaford ash is much older than the Drax ash, and so the extent of weathering will be greater in the Meaford ash. Because of the longer duration of weathering, greater quantities of elements have been leached from the Meaford ash than from the Drax ash. Also, more distinct depth variations were obtained for the Meaford ash, especially for the solid PFA. However, no secondary clay minerals were identified in the Meaford ash.

Leachate water samples from the Barlow ash mound were collected and analysed. The samples were collected directly collected from the outlet pipes installed at the base of the ash mound. These pipes feed a dike that surrounds the Barlow ash mound; the dike is also fed by rainfall and surface run-off. Water samples were taken from the dike. Elemental concentrations in the leachate water samples were higher than in the dike water samples, as expected, and vary greatly, depending on the location of the sampling site. Some samples show high concentrations for all elements, showing large discrepancies with the levels recorded in the porewater samples. These high values are similar to the concentrations of elements obtained in eluates from the initial stage of fresh ash leaching. This was explained as being due either to the delayed saturation of the mound, or due to lateral flow within the mound, allowing the more soluble, surface-enriched fractions of the ash particles, which are currently being leached in the inner-most part of the mound, to appear currently at the outlet pipes.

The batch and column leaching tests using deionised water revealed a different leaching behaviour for fresh and weathered ashes. More soluble, surface-associated inorganic fractions dominate the early stage of fresh PFA leaching, producing elevated concentration levels for elements such as Ca, Mg, Na, K, S (as  $\text{SO}_4^{2-}$ ), B, Li, Mo and Cr. The concentrations decreased rapidly with subsequent leaching, approaching relatively constant concentrations. When the weathered ash was leached, instead the concentrations were much lower for the elements that were readily soluble from the fresh ash were not so readily leached. Also, there were no dramatic decreases in the concentrations of the elements as the leaching progressed, unlike as in the fresh ash. The concentration levels were nearly constant throughout. The column leaching tests indicate that much of the surface-associated fractions present in fresh ash had been dissolved from the weathered ash prior to treatment, leaving the leachate to attack the more refractory aluminosilicate glass. This attack released constant levels of inorganic material, derived from within the exterior shells of the glass particles. In weathered ash, the rate of aluminosilicate glass weathering is thought to be a major factor controlling the release of the elements in PFA to the aquatic environment.

The batch and the column leaching tests of fresh and weathered PFA using the synthetic leachate demonstrated that some trace elements were removed from the synthetic leachate. Fe and Cu were the most effectively retained elements in both leaching tests, whereas Cd, Cr, Ni, Zn and Hg were retained in the column leaching tests to varying degrees. In addition to the retention reactions, the Drax and Meaford ashes showed a neutralising capacity. The neutralising capacity of PFA is attributable to the dissolution of Ca and Mg (Hodgson and Dyer *et al.*, 1982), and this could explain the results of the leaching tests.

The elemental concentrations in the porewater samples collected from the field, and the leachate samples from the laboratory experiments, including the batch and column leaching tests using deionised water, were compared with several water quality standards. The implication from the comparison is that not

only fresh ash, but also weathered ash, may yield elemental concentrations that exceed the water standards. More importantly, the release of elements from the weathered ash is constant, and decreases very slowly with time or subsequent leaching. Therefore PFA disposed of in older, less well-engineered sites, unlike the Barlow mound at Drax Power Station, which is well-engineered and monitored, may be a potential source of contamination to groundwater, even after a long period of time after its disposal.

## References

- Adriano D. C., Page, A. L., Elsewi, A.A., Chang, A.C. and Straughan, I. 1980. Utilization and disposal of fly ash and other coal residues in terrestrial ecosystem. *J. Environ. Qual.* **9**. 333-344.
- Ainsworth. C. C. and Rai, D. 1987. Chemical characterization of fossil fuel wastes. EPRI-EA-5321. Electric Power Research Institute, Palo Alto, California.
- Alberts, J. J., Newman, M. C. and Evans, D. W. 1985. Seasonal variations of trace elements in dissolved and suspended loads for coal ash ponds and pond effluents. *Water, Air, and Soil Pollution.* **26**, 111-128.
- Alberts, J. J., Weber, M. F. and Evans, D. W. 1988. The effect of pH and contact time on the concentration of As(III) and As(V) in coal ash systems. *Environmental Technology Letters.* **9**. 63-70.
- Alloway, B. J. 1990. Heavy metals in soils. Blackie & Son, Glasgow. 339pp.
- Ball, J. W., Nordstrom, D. K. and Zachmann, D. W. 1987. WATEQ4F-A personal computer FORTRAN translation of the geochemical model WATEQ2 with revised database. United Geological Survey Water Resources Investigations 87-50. United Geological Survey, Menlo Park, California.
- Bassett, R. L. and Melchior, D. C. 1990. Chemical modeling of aqueous systems. (In: Chemical modeling of aqueous systems II. edited by D. C. Melchior and R. L. Bassett, pp1-14). ACS symposium series 416. American chemical Society, Washington.
- Bauer, C. F. and Natusch, D. F. S. 1981. Identification and quantitation of carbonate compounds in coal fly ash. *Environmental Science & Technology.* **15**. 783-788.
- Brown, J., Ray, N. J. and Ball, M. 1976. The disposal of pulverised fuel ash in water supply catchment areas. *Water Research.* **10**. 1115-1121.
- Bullock, P. and Loveland, P. J. 1974. Mineralogical analyses. (In: Chapter 5. Soil survey laboratory methods. edited by B. W. Avery and C. L. Bascomb. pp57-69). Soil Survey monograph No. 6. Soil Survey, Harpenden.

- Campbell, J. A., Laul, J. C., Nielson, K. K. and Smith, R. D. 1978. Separation and chemical characterization of finely-sized fly-ash particles. *Analytical Chemistry*. **50**. 1032-1040.
- Central Statistical Office. 1992. Annual abstract of statistics. H.M.S.O.
- Cherry, D. S. and Guthrie, R. K. 1977, Toxic metals in surface waters from coal ash..*Water Res.Bull.* **13**. 1227-1236.
- Clarke, L. B. and Sloss.L. L. 1992. Trace element emissions from coal combustion and gasification (Draft). IEA coal reasearch, London.
- Cox, J. A., Lundquist, G. L., Przyjazny, A. and Schmulbach, C. D. 1978. Leaching of boron from coal ash. *Environmental Science & Technology*. **12**. 722-723.
- Deer, W. A., Howie, R. A. and Zussman, J. 1992. The rock-forming minerals (2nd edition). Longman Scientific & Technical. 696pp.
- DIN 38414, Part 4. 1984. German Standard methods for the examination of water, waste water and sludge.
- Dobie, M. and Newman, R. L. 1986. The effects and consequences of groundwater abstraction on foundation at Drax Power Station, North Yorkshire. (In: Groundwater in engineering geology. edited by F. G. Bell, M. G. Culshaw and J. C. Cripps. pp59-74) Engineering Geology Special Publication No.3, Geological Society of London, London.
- Dreesen, D. R., Gladney, E. S., Owens, J. W., Perkins, B. L., Wienke, C. L. and Wangen, L. E. 1977. Comparison of levels of trace elements extracted from fly ash and levels found in effluent waters from a coal-fired power plant. *Environmental Science & Technology*. **11**. 1017-1019.
- Drever, J. I. 1988. The geochemistry of natural water (2nd edition). Prentice-Hall Inc. 397pp
- Dudas, M. J. 1981. Long-term leachability of selected elements from fly ash. *Environmental Science & Technology*. **15**. 840-843.
- Dudas, M. J. and Warren, C. J. 1988. Submicroscopic structure and characteristics of intermediate calcium fly ashes. (In: Fly ash and coal conversion by-products: Characterization, utilization and disposal VI. edited by G. J. McCarthy, F. P. Glasser, D. M. Roy and R. T. Hemmings. pp309-316). Mat. Res. Soc. Symp. Proc. V113. Materials Research society, Pittsburg, P.A.

- Eary, L. E., Rai, D., Mattigod, S. V. and Ainsworth, C.C. 1990. Geochemical factors controlling the mobilization of inorganic constituents from fossil fuel combustion residues: II. Review of the minor elements. *J. Environ. Qual.* **19**. 202-214.
- EEC. 1975. Council Directive 75/440/EEC. *Official journal of the European communities*. No. L 194/26.
- EEC. 1980. Council Directive 80/778/EEC. *Official journal of the European communities*. No. L 229/11.
- EEC. 1991. EC Draft landfill directive. *Official journal of the European communities*. No.C 190/1.
- Edmunds, W. M. and Bath, A. H. 1976. Centrifuge extraction and chemical analysis of interstitial waters. *Environmental Science & Technology*. **10**. 467-472.
- Eggett, J. M. and Thrope, T. M. 1978. Mobilization of chromium from fly ash particulates by aqueous systems modeling natural waters. *J. Environ. Sci. Health*. **A13**. 295-318.
- Elseewi, A. A., Page, A. L. and Grimm, S. 1980. Chemical characterization of fly ash aqueous systems. *J. Environ. Qual.* **9**. 424-428.
- Förstner, U. and Wittman, G. T. W. 1986. Metal pollution in the aquatic environment (2nd edition). Springer-Verlag. 486pp.
- Felmy, A. R., Rai, D. and Moore, D. A. 1993. The solubility of (Ba,Sr)SO<sub>4</sub> precipitates: Thermodynamic equilibrium and reaction path analysis. *Geochimica et Cosmochimica Acta*. **57**. 4345-4363.
- Ferguson, J. E. 1990. The heavy elements: Chemistry, environmental impact and health effects. Pergamon Press. 614pp
- Frutcher, J. S., Rai, D. and Zachara, J.M. 1990. Identification of solubility-controlling solid phases in a large fly ash field lysimeter. *Environmental Science & Technology*. **24**. 1173-1179.
- Frutcher, J. S., Rai, D., Zachara, J. M. and Schmidt, R.L. 1988. Leachate chemistry at the Montour fly ash test cell. EPRI-EA-5922. Electric Power Research Institute, Palo Alto, California.
- Furuya, K., Miyajima, Y., Chiba, T. and Kikuchi, T. 1987. Elemental characterization of particle size-density separated coal fly ash by spectrophotometry, inductively coupled plasma emission spectrometry,

- and scanning electron microscopy-energy dispersive X-ray analysis. *Environmental Science & Technology*. **21**. 898-903.
- Gay, A. J. and Davis, P. B. 1987. Some environmental aspects of coal fly ash. (In *Coal Science and Chemistry*. edited by A. Volborth. pp 221-243). Elsevier Science Publishers B. V., Amsterdam.
- Grisafe, D. A., Angino, E. E. and Smith, S. M. 1988. Leaching characteristics of a high-calcium fly ash as a function of pH: a potential source of selenium toxicity. *Applied Geochemistry*. **3**. 601-608.
- Hansen, L. D. and Fisher, G. L. 1980. Elemental distribution in coal fly ash particles. *Environmental Science & Technology*. **14**. 1111-1117.
- Hardy, M. A. 1981. Effects of coal-fly ash disposal on water quality in and around the Indiana dunes national lake-shore, Indiana. United Geological Survey Water-Resources Investigations 81-16. United Geological Survey, Indianapolis.
- Harris, W. R. and Silberman, D. 1983. Time-dependent leaching of coal fly ash by chelating agents. *Environmental Science & Technology*. **17**. 139-144.
- Hart, A. B. 1981. The chemistry of power station emissions. (In *Energy and Chemistry*. edited by R. Thompson. pp221-251). The Royal Society of Chemistry.
- Henry, W. M. and Knapp, K. T. 1980. Compound forms of fossil fuel fly ash emissions. *Environmental Science & Technology*. **14**. 450-456.
- Hjelmar, O. 1990. Leachate from land disposal of coal fly ash. *Water Management & Research*. **8**. 429-449.
- Hockley, D. E. and Van der sloot, H. A. 1991. Long-term process in a stabilized coal-waste block exposed to seawater. *Environmental Science & Technology*. **25**. 1408-1414.
- Hodgson, L., Dyer, D. and Brown, D. A. 1982. Neutralization and dissolution of high-calcium fly ash. *J. Environ. Qual.* **11**. 93-98.
- Holcombe, L., J. Eynon, B. P. and Switzer, P. 1985. Variability of elemental concentrations in power plant ash. *Environmental Science & Technology*. **19**. 615-620.
- Hollis, J. F., Keren. R. and Gal, M. 1988. Boron release and sorption by fly ash as affected by pH and particle size. *J. Environ. Qual.* **17**. 181-184.

- Huang, W. H. and Keller, W. D. 1970. Dissolution of rock-forming silicate minerals in organic acids, simulated first stage weathering of fresh mineral surfaces. *Am. Min.* **55**. 2076-2096.
- Hubbard, F. H., McGill, R. J., Dhir, R. K., and Ellis, M. S. 1984. Clay and pyrite transformations during ignition of pulverised coal. *Mineralogical Magazine*. **48**. 251-256.
- Hubbard, F. H., Dhir, R. K. and Ellis, M. S. 1985. Pulverized-fuel ash for concrete: compositional characterisation of United Kingdom PFA. *Cement and Concrete Research*. **15**. 185-198.
- Hulett, L. D., Weinberger, A. J., Northcutt, K. J. and Ferguson, M. 1980. Chemical species in fly ash from coal-burning power plants. *Science*. **210**. 1356-1358.
- Hulett, L. D., Weinberger, A. J. 1980. Some etching studies of the microstructure and composition of large aluminosilicate particles in fly ash from coal-burning power plants. *Environmental Science & Technology*. **14**. 965-970.
- James, W. D., Graham, C. C., Glascock, M. D. and Hanna, A-S. G. 1982. Water-leachable boron from coal ashes. *Environmental Science & Technology*. **16**. 195-197.
- Jones, L. H and Lewis, A.V. 1960. Weathering of fly ash. *Nature*. **185**. 404-405.
- Kaufherr, N. and Lichman, D. 1984. Comparison of micron and submicron fly ash particles using scanning electron microscopy and X-ray elemental analysis. *Environmental Science & Technology*. **18**. 544-547.
- Kaufherr, N., Shenasa, M., and Lichtman, D. 1985. X-ray photoelectron spectroscopy studies of coal fly ashes with emphasis on depth profiling of submicrometer particle size fractions. *Environmental Science & Technology*. **19**. 609-614.
- Kopsick, D. A. and Angino, E. E. 1981. Effect of leachate solutions from fly and bottom ash on groundwater quality. *Journal of Hydrology*. **54**. 341-356.
- Lichtman, D. and Mroczkowski, S. 1985. Scanning electron microscopy and energy-dispersive X-ray spectroscopy analysis of submicrometer coal fly ash particles. *Environmental Science & Technology*. **19**. 274-277.

- Liem, H., Sandström, M., Carne, A., Wallin, S., Rydevik, U., Thurenus, B. and Moberg, P-O. 1983. Studies on the leaching and weathering processes of coal ashes. *Water Sci.Tech.* **15**. 163-191.
- Lindsay, W. L.. 1979. Chemical equilibria in soils. John Wiley and Sons. 449pp.
- Markowski, G. R. and Filby, R. 1985. Trace element concentration as a function of particle size in Fly ash from a pulverised coal utility boiler. *Environmental Science & Technology.* **19**. 796-804.
- Marsh, T. J., Lees, M. and Bryant, S. J (Editors). 1993. Hydrological data UK. Institute of Hydrology, Wallingford and British Geological Survey, Keyworth. 190pp.
- Mason, B. and Moore, C. B. 1982. Principles of geochemistry (4th edition). John Wiley & Sons. 344pp.
- Mattigod, S. V. 1982. Characterization of fly ash particles. *Scanning Electron Microscopy.* **II**. 611-617.
- Mattigod, S. V. 1983. Chemical composition of aqueous extracts of fly ash: Ionic speciation as a controlling factor. *Environmental Technology Letters.* **4**. 485-490.
- Mattigod, S. V., Rai, D., Eary, L. E. and Ainsworth, C. C. 1990. Geochemical factors controlling the mobilization of inorganic constituents from fossil fuel combustion residues: I. Review of the major elements. *J. Environ. Qual.* **19**. 188-201.
- McCarthy, G. J., Swanson, K. D., Schields, P. J. and Groenewold, G. H. 1983. Mineralogical controls on the toxic element contamination of groundwater from buried electrical utility solid wastes. North Dakota University. 59pp.
- McCarthy, G. J., Solem, J. K., Manz, O. E. and Hassett, D. J. 1990. Use of a database of chemical, mineralogical and physical properties of north American fly ash to study the nature of fly ash and its utilization as mineral admixture in concrete. (In Fly ash and coal-conversion by products: Characterization, Utilization and disposal VI, edited by R. L. Day and F. P. Glasser. pp3-33). Mat. Res. Soc. Symp. Proc. Vol. 178. Materials Research Society, Pittsburg, P.A.
- McElroy, R.M., Carr, D. S., Ensor, D. S. and Markowski, G. R. 1982. Size distribution of fine particles from coal combustion. *Science.* **215**. 13-19.

- Natusch, D. F. S., Wallace, J. R. and Evans, C. A. Jr. 1974. Toxic trace elements: Preferential concentration in respirable particles. *Science*. **183**. 202-204.
- Newman, J. R. and Ross, C. A. M. 1985. Mineralogical and geochemical controls on heavy metal pollution in monolith lysimeters. Report FLPU 85-5. Fluid process Research Group, British Geological Survey, Keyworth.
- Norton, G. A., Markuszewski, R. and Shanks, H. 1986. Morphological and chemical characterization of iron-rich fly ash fractions. *Environmental Science & Technology*. **20**. 409-413.
- Parks, G. A. 1972. Free energies of formation and aqueous solubilities of aluminum hydroxides and oxide hydroxides at 25°C. *American Mineralogist*, **50**. 1163-1189.
- Parkhurst, D. L., Thorstenson, D. C. and Plummer, L. N. 1980. PHREEQE-A computer program for geochemical calculations. United State Geological Survey Water-Resources Investigations 80-96. United States Geological Survey, Reston, Virginia.
- Phung, H. T., Lund, L. J., Page, A. L. and Bradford, G. R. 1979. Trace elements in fly ash and their release in water and treated soils. *J. Environ. Qual.* **2**. 171-175.
- Qian, J. C. and Glasser, F. P. 1988. Bulk composition of the glassy phase in some commercial PFA's. (In: Fly ash and coal conversion by-products: characterization, utilization and disposal VI. edited by G. J. McCarthy, F. P. Glasser, D. M. Roy and R. T. Hemmings. pp39-44). Mat. Res. Soc. Symp. Proc. V113. Materials Research society, Pittsburg, P. A.
- Rai, D., Ainsworth, C. C., Eary, L. E., Mattigod, S. V. and Jackson, D. R. 1987. Inorganic and organic constituents in fossil fuel combustion residues. Vol 1. A critical review. EPRI-EA-5176. Electric Power Research Institute, Palo Alto, California.
- Rai, D. Eary, L. E., Ainsworth, C. C. and Zachara, J. M. 1987. Leaching behavior of fossil fuel wastes: Mineralogy and geochemistry of calcium. (In: Fly ash and coal conversion by-products: characterization, utilization and disposal II. edited by G. J. McCarthy, F. P. Glasser and D. M. Roy. pp3-15). Mat. Res. Soc. Symp. Proc. V86. Materials Research society, Pittsburg, P.A.

- Rai, D., Mattigod, S. V., Eary, L. E. and Ainsworth, C. C. 1988. Fundamental approach for prediction pore-water composition in fossil fuel combustion wastes. (In: Fly ash and coal conversion by-products: characterization, utilization and disposal VI. edited by G. J. McCarthy, F. P. Glasser, D. M. Roy and R. T. Hemmings. pp317-324). Mat. Res. Soc. Symp. Proc. V113. Materials Research society, Pittsburg, P.A.
- Rai, D. and Szelmeczka, R. W. 1990. Aqueous behavior of chromium in coal fly ash. *J. Environ. Qual.* **19**. 378-382.
- Rehage, J. A. and Holcombe, L. J. 1990. Environmental performance assessment of coal ash site: Little Canada Structural ash fill. EPRI-EN-6532. Electric Power Research Institute, Palo Alto, California.
- Roy, W. R., Griffin, R. A., Dickerson, D. R. and Schuller, R. M. 1984. Illinois basin coal fly ashes. 1. Chemical characterization and solubility. *Environmental Science & Technology*. **18**. 734-739.
- Roy, W. R. and Griffin, R. A. 1984. Illinois basin coal fly ashes. 2. Equilibria relationships and qualitative modeling of ash-water reactions. *Environmental Science & Technology*. **18**. 739-742
- Roy, W. R., Thiery, R. G., Schuller, R. M. and Suloway, J. J. 1981. Coal fly ash: a review of the literature and proposed classification system with emphasis on environmental impacts. Environmental Geology Notes 96. Illinois Institute of Natural Resources, State Geological Survey Division, Illinois.
- Roy, W. R. and Griffin, R. A. 1982. A proposed classification system for coal fly ash in multidisciplinary research. *J. Environ. Qual.* **11**. 563-568.
- Sakata, M. 1988. Movement and neutralization of alkaline leachate at coal ash disposal. *Environmental Science & Technology*. **21**. 771-777.
- Simons, H. S. and Jeffery, J. W. 1960. an X-ray study of pulverised fuel ash. *J. appl. Chem.* **10**. 328-336.
- Simsman, G. V., Chesters, G. and Andren, A. W. 1987. Effect of ash disposal ponds in groundwater at coal-fired power plant. *Wat. Res.* **2**. 417-426.
- Smith, R. D., Campbell, J. A. and Nielson, K. K. 1979. Concentration dependence upon particle size of volatilized elements in fly ash. *Environmental Science & Technology*. **13**. 553-558.

- Spears, D. A. 1991. Pyrite in some U.K. coals. (In Processing and utilization of high-sulfur coals IV. edited by P.R. Dugan, D.R. Quigley and Y.A. Attia. pp85-93). Elsevier Science Publishers B. V., Amsterdam.
- Spears, D. A. and Reeves, M. J. 1975. The infiltration rate into an aquifer determined from the dissolution of carbonate. *Geological Magazine*. **112**. 585-591.
- Spears, D. A. 1979. Porewater composition in the unsaturated zone of the Chalk with particular reference to nitrates. *Q. Jl. Engng. Geol.* **12**. 97-105.
- Spencer, L. L and Drake, L. D. 1987. Hydrogeology of an alkaline fly ash landfill in eastern Iowa. *Groundwater*. **25**. 519-526.
- Spostigo, G and Mattigod, S. V. 1980. GEOCHEM: a computer program for the calculation of chemical equilibria in soil solutions and other natural water systems. Dept. of Soil and Environmental Sciences, University of California, Riverside.
- Starkey, H. C., Blackmon, D. D. and Hauff, D. L. 1984. The routine mineralogical analysis of clay-bearing samples. United States Geological Survey Bulletin No. 1563. United States Geological Survey.
- Stumm, W. and Morgan, J. J. 1981. Aquatic Chemistry (2nd edition). Wiley-Interscience. 780pp
- Suloway, J. J. Skelly, T. M., Dickerson, D. R., Schuller, R. M. and Griffin, R. A. 1983. Chemical and toxicological properties of coal fly ash. Environmental Geology Notes 105. Illinois State Geological Survey.
- Talbot, R. W., Anderson, M. A. and Anderson, A. W. 1978. Qualitative model of heterogeneous equilibria in a fly ash pond. *Environmental Science & Technology*. **12**. 1056-1062.
- Theis, T. L. and Wirth, J. L. 1977. Sorptive behaviour of trace metals on fly ash in aqueous systems. *Environmental Science & Technology*. **11**. 1096-1100.
- Theis, T. L. and Richter, R. O. 1979. Chemical speciation of heavy metals in power plant ash pond leachate. *Environmental Science & Technology*. **13**. 219-224.
- Theis, T. L., Westrick, J. D., Hsu, C. L. and Marley, J. J. 1978. Field investigation of trace metals in groundwater from fly ash disposal. *Journal of Water Pollution Control Federation*. **50**. 2457-2469.

- Turner, R. R. 1981. Oxidation state of arsenic in coal ash leachate. *Environmental Science & Technology*. **15**. 1062-1066.
- U.S. Salinity Laboratory Staff. 1954. Diagnosis and improvement of saline and alkali soils. USDA Handbook, No. 60.
- van der Sloot, H.A., Hjelmar, O. and de Groot, G.J. 1989. Waste/solid interaction studies-the leaching of molybdenum for pulverized coal ash. (In Flue gas and fly ash-commission of the EC. edited by Sens, P. F and Wilkinson, J. K. pp132-157). Elsevier applied Sciences, London.
- van der Sloot H. A., Wijkstra J., van Dalen, A., Das, H. A., Slanina, J., Dekkers, J. J. and Wals, G. D. 1982. Leaching of trace elements from coal solid waste. ECN-120. Netherlands Energy Research Foundation.
- Vassilev S.V. 1992. Phase mineralogy studies of solid waste products from coal burning at some Bulgarian thermoelectric power plants. *Fuel*. **71**. 625-633.
- Villaume, J. F., Bell, J. W. and Labuz, L. L. 1988. Evaluation of leachate generation at the Montour, Pennsylvania, fly ash test cell. (In: Fly ash and coal conversion by-products. Characterization, utilization and disposal VI. edited by G. J. McCarthy, F. P. Glasser, D. M. Roy and R. T. Hemmings. pp325-332). Mat. Res. Soc. Symp. Proc. V113. Materials Research Society, Pittsburg, P.A.
- Wadge, A. and Hutton, M. 1987. The leachability and chemical speciation of selected trace elements in fly ash from coal combustion and refuse incineration. *Environmental Pollution*. **48**. 85-99.
- Wadge, A., Hutton, M. and Peterson, P. J. 1986. The concentration and particle size relationships of selected trace elements in fly ashes from U.K coal-fired power plants and a refuse incinerator. *The Science of the Total Environment*. **54**. 13-27.
- Warren, C. J. and Dudas, M. J. 1984. Weathering processes in relation to leachate properties of alkaline fly ash. *J. Environ. Qual.* **13**. 530-538.
- Warren, C. J. and Dudas, M. J. 1985. Formation of secondary minerals in artificially weathered fly ash. *J. Environ. Qual.* **14**. 405-410.
- Warren, C. J. and Dudas, M. J. 1986. Mobilization and attenuation of trace elements in an artificially weathered fly ash. EPRI-EA-4747. Electric Power Research Institute, Palo Alto, California.

- Watt, J. D. and Thorne, D. J. 1965. Composition and pozzolanic properties of pulverised fuel ashes. I. Composition of fly ashes from some British power stations and properties of their component. *J. appl. Chem.* **15**. 585-594.
- White, R. E. On the measurement of soil pH. 1969. *The Journal of Australian Institute of Agricultural Science.* **35**. 3-14.
- Wolery, T. J. 1992. EQ3NR, software package for geochemical modeling of aqueous systems: Package overview and installation guide (Version 7.0). UCRL-MA-110662 PT 1. Lawrence Livermore National Laboratory, Livermore, CA.
- Wolery, T. J. and Daveler, S. A. 1992. EQ6, A computer program for reaction path modeling of aqueous geochemical systems: theoretical manual, user's guide, and related documentation (Version 7.0). UCRL-MA-110662 PT IV. Lawrence Livermore National Laboratory, Livermore, CA.
- Zimmermann, U., Munnich, K. O. and Roether, W. 1965. Tracers determine movement of soil moisture and evapotranspiration. *Science.* **152**. 346-347.

## **Appendix A. Additional experimental methods**

### **A.1 Determination of FeO/Fe<sub>2</sub>O<sub>3</sub>.**

Pratt method was used to determine the ferrous oxide in PFA.

*Reagent:* Indicator - 0.1 g of sodium diphenylamine sulphate plus 500 ml of water plus 500 ml of conc. phosphoric acid added slowly and kept cool.

50 % Sulphuric acid

40 % Hydrofluoric acid

Boric acid (Saturated solution)

Potassium dichromate 2.728 g in 2 l of water.

*Standardisation:* Analar potassium dichromate dried for 2 hours is primary standard. Concentration 1.364 g/l.

*Method:* Weigh out 0.5 g of finely ground rock powder into a 30 ml platinum dish with a well fitting lid. Moisten with 2 ml of water followed by 5 ml of 50 % sulphuric acid. Mix well then and add 10 ml of 40 % hydrofluoric acid. cover and heat cautiously but quickly to boiling point, then keep boiling for 7 minutes. Plunge the crucible and lid into 300 ml of saturated boric acid. Stir, add 10 ml of indicator solution then titrate with potassium dichromate solution until a purple end point persists for 30 seconds.

*Calculation:* 1 ml of potassium dichromate = 2.0 mg of FeO

$(\text{Vol. of titrant} \times 2 \times 100) / (\text{Wt. of sample in g.} \times 1000) = \% \text{ FeO}$

### **A. 2. Separation of clay size particles from weathered PFA.**

Clay size fractionation and separation of PFA was done following the method of Starkey and Blockman *et al.* (1984). This methods id using centrifugation to separate silt and clay size. The centrifugation is essentially an settling technique and operates according to Stoke's law.

**Procedure.** Soak 25 to 30 g of sample overnight in 100 ml of deionised water in beaker. Place the beaker contain the sample in ultrasonic bath for 5 to 15 minutes. Firstly, remove sand size particles ( $< 62\mu$ ) using 230 mesh sieve with brush. Decant the slurry solution into 250 ml bottle and add hexagonal phosphate for deflocculation. Centrifuge the solution, which sand particles were removed using the table, which is based on 600 r.p.m to separate silt and clay. Silt is presumed to have been settled in the bottom of the centrifuge tube at a depth of 1 cm after centrifuge. The supernatant is then decanted into a 1000 ml Berzelius beaker through 0.45 mm filter, using vacuum, to retain clay size particles. The last step is conducted repeatedly using the same filter when necessary.

T(°C)	16	20	21	22	23	24	25	26	27	28
*Time (min.sec)	7.30	6.50	6.42	6.34	6.25	6.17	6.09	6.02	5.55	5.48

Table A.1 Variation of time for separation of clay ( $>2\mu$ ) and silt. \* Including 30 seconds to reach 600 r. p. m. (Starkey and Blockman *et al.*, 1984)

### A. 3 Preparation of fused disc for XRF

0.750 g of ground ashed PFA samples (heated at  $450^{\circ}\text{C}$  for 4 hours to calculate 'loss on ignition') were mixed with 7.500 g of moisture-free lithium tetraborate flux (spectroflux 100) and thoroughly mixed in a Pt crucible. The mixed powder is re-weighed to ensure the loss during the mixing is within 2- mg. Using Pt-tipped furnace tongs, place the basin in the furnace and heat for 21 minutes, gently swirling at every 7 minutes. Pour the contents of the basin into the casting mould after complete dissolution of the contents in the basin and transfer the mould to the air jet cooler and leave until cold, ready for the analysis on the XRF.



Plate A. Laboratory set-up for column leaching tests

## Appendix B: Geochemical Modelling

### B.1 Thermodynamic background

**Units.** Concentrations of solutes in aqueous solutions are usually expressed as molality (m), which is moles per Kg of solvents whereas molar units (M) measure concentrations in moles per litre of solution. The molal unit is sometimes more convenient because it is not influenced by temperature, which affects on the volume of solution.

**Activities and activity coefficients.** Most chemical calculations involve activities rather than concentrations. Activity is a measure of the effective concentration of a reactant or product in a chemical reaction. Activity, which is denoted by 'a' is related with molalities by a factor called activity coefficient ( $\gamma_i$ ):

$$a_i = \gamma_i m_i$$

where, a is the activity of element *i*,  $\gamma_i$  is the activity coefficient of ion *i* and  $m_i$  is the molality of *i*, represented as mole/l.

**Ionic strength.** Ionic strength is useful concept for assessing the combined effect of the activities of several electrolytes in a solution on a given electrolyte. The ionic strength, *I*, is defined as

$$I = \frac{1}{2} \sum m_i Z_i^2,$$

where  $m_i$  the concentration in mole/l of ion *i*,  $Z_i$  is the valency of that ion and  $\sum$  denotes the product of each ion and its valency squared is summed for all ions in solution.

**Debye-Hückel equation.** The activity coefficient of solutes or individual ions can be calculated from the theoretical equations of Debye and Hückel:

$$\log \gamma_i = \frac{-Az_i^2\sqrt{I}}{1 + Ba^0\sqrt{I}}$$

up to ionic strength of about 0.1 m. for higher ionic strengths, specific-ion-interaction parameters may be added to this equation.

**Equilibrium constant.** Equilibrium constant,  $K_{\text{c}q}$ , in the chemical reaction of  $aA + bB = cC + dD$ , can be derived from the expression for chemical potential and Gibbs free energy. The Gibbs free energy per mole of reaction,  $\Delta G_R$ , is the difference between the Gibbs free energy of the products and that of the reactants:

$$\Delta G_R = G_{\text{products}} - G_{\text{reactants}}$$

which can be written, in terms of chemical potential,

$$\Delta G_R = c\mu_C + d\mu_D - a\mu_A - b\mu_B$$

Combining the result with chemical potential ( $\mu$ ),  $\mu_i = \mu_i^\circ + RT \ln a_i$  will obtain

$$\Delta G_R = \Delta G^\circ + RT \ln \left( \frac{a_C^c \cdot a_D^d}{a_A^a \cdot a_B^b} \right)$$

$\Delta G^\circ$  is the standard free energy of the reaction, that is the change in free energy when a mole of A and b mole of B, both in their standard states, are converted to c moles of C and d moles of D.

For a system at equilibrium,  $\Delta G^\circ = 0$ , and therefore can be defined as in terms of activities as:

$$RT \ln \left( \frac{a_C^c \cdot a_D^d}{a_A^a \cdot a_B^b} \right) = -\Delta G^\circ \text{ or } \frac{a_C^c \cdot a_D^d}{a_A^a \cdot a_B^b} = \exp\left(\frac{-\Delta G^\circ}{RT}\right) = K_{\text{c}q}$$

### ***Ion activity products and saturation indices.***

Saturation indices or 'degree of saturation' index is a measure of the thermodynamic state of a solution relative to equilibrium with a specified solid-phase mineral. It can be obtained by comparing ion activity product (IAP) with equilibrium constant ( $K_{\text{c}q}$ ).

Namely, if  $IAP < K_{eq}$ , dissolution will occur.

if  $IAP > K_{eq}$  precipitation will occur.

$$SI \text{ (Saturation index)} = \log \left\{ \frac{IAP}{K_{eq}} \right\}$$

SI = 0: ion product is equilibrium with respect to a given mineral phase.

SI < 0: ion product is undersaturated with respect to a given mineral phase.

SI > 0 ion product is super saturated with respect to a given mineral phase.

## **B. 2 WATEQ4F**

### ***Data input.***

Water analytical data in mg/l, pH and Eh are used in WATEQ4F. WQ4FINPT is the supplementary file of WATEQ4F for data input.

### ***Output of WATEQ4F***

#### ***Speciation***

WATEQ4F uses the input analytical data for a given sample and a set of equilibrium constants for aqueous complexation reactions within its database to calculate the concentration of single and complexed ions in mole/l.

#### ***Single ion activity coefficients and single ion activities***

Thermodynamic activity of a given solute species, which is an effective concentration, is influenced by the ionic strength of the water sample, which is calculated by WATEQ4F. WATEQ4F calculates ion activity coefficients value

for each species according to the Debye-Hückel equation and then calculates the thermodynamic activity for each species.

### ***Ion Activity Products and Saturation indices***

WATEQ4F calculates ion activity products using the single ion activities to assess whether the water sample is in equilibrium with respect to given mineral solid phases

### **B. 3 Example result of WATEQ4F calculation using the data from Barlow porewater (Drax porewater, borehole 4, collected at 4m depth)**

#### **Table B. 1 Input data**

TEMP (°C)=25.00  
PH=8.00  
EH (mv)=0.409

Ca	608.3
Mg	363.2
Na	52.1
K	137.4
Cl	86.8
SO4	2534.2
Fe Total	0.09
SiO2 Total	0.36
B Total	13.4
Al	0.03
NO3	380.4
Li	1.59
Sr	2.35
Ba	0.13
Cu	0.01
Zn	0.02
Cd	0.05
Pb	0.59
Ni	0.13
As Total	0.80
Se Total	0.37

#### **Table B.2 Charge balance**

Anal Cond= 0.0 Calc Con =5479.2

Anal EPMCAT=66.5956 Anal EPMA =61.9351 Percent difference in input cation/anion balance = 7.2560

Calc EPMCAT =44.4280 Calc EPMAN =36.7697 Percent difference in calc cation/anion  
balance = 11.0652  
Total Ionic Strength(T.I.S.) from input data=0.12104  
Effective Ionic Strength (E.I.S.) from speciation=0.07664

**Table B.3 Aquatic speciation**

Species	anal ppm	calc ppm	anal molal	Calc molal	activity	activity coefficient
Ca	608.33	401.261	1.524E-02	1.005E-02	4.239E-03	0.4216
CaSO4 aq		701.581		5.175E-03	5.267E-03	1.0178
CaCO3 aq		0.641		6.428E-06	6.543E-06	1.0178
Al	0.030	0.000	1.117E-06	2.901E-16	3.750E-17	0.1293
Al(OH)4		0.105		1.114E-06	8.874E-07	0.7976
Pb	0.590	0.054	2.860E-06	2.628E-07	1.059E-07	0.4028
PbCO3 aq		0.443		1.665E-06	1.695E-06	1.0178
PbOH		0.105		4.710E-07	3.752E-07	0.7967

**Table B.4 Saturation indices**

Phase	Log IAP/KT	Log IAP	Log KT
Anhydrite	-0.218	-4.578	-4.361
Brucite	-2.717	14.123	16.840
Celestite	-0.694	-7.326	-6.631
Gypsum	0.002	-4.579	-4.581
Quartz	-1.246	-5.227	-3.980
Tenorite	-0.740	6.880	7.620
Cerrusite	0.119	-13.440	-12.830
Wairakite	-8.674	-35.382	-26.708
Kaolinite	-1.183	6.252	7.435
dolomite	-0.300	-16.840	-16.540

## Appendix C. Data

**C-1 Porewater analyses**

**C-2 PFA analyses**

**C-3 Correlation matrix of Drax weathered PFA**

**C-4 Correlation matrix of batch leaching tests**

**C-5 Correlation matrix of the column leaching test of fresh Drax ash with deionised water**

**C-6 Correlation matrix of the column leaching of weathered Drax ash with deionised water**

**C-7 Correlation matrix of the column leaching of weathered Meaford ash with deionised water**

## Appendix C-1: Analyses of Porewater, Barlow mound, Drax

Sample: Porewater, Drax Borehole 1, Barlow mound (Unit: mg/l unless indicated, \*: ug/l)

Analysed by AAS

(m) Depth	Al	Ca	Mg	Na	K	Cr*	Ni*	Pb*	Zn*	Cd*	Cu*
0.6	0.79	103.3	19.5	44.5	18.2	9.4	10.0	200.0	10.7	0.5	44.7
0.9	0.03	159.8	47.9	54.4	13.0	17.9	10.0	200.0	50.9	0.6	31.0
1.2	0.01	202.6	63.1	35.8	18.2	204.8	4.0	0.0	14.3	0.6	0.0
1.5	0.02	195.0	54.7	32.5	16.6	253.9	4.0	100.0	12.1	0.9	0.0
1.8	0.02	489.2	93.3	41.7	22.2	366.7	8.0	100.0	0.0	0.5	0.0
2.1	0.01	563.6	82.2	32.2	22.6	342.5	25.0	0.0	1.1	0.0	1.4
2.4	0.01	481.8	166.4	48.8	36.0	319.1	5.0	0.0	0.0	0.0	0.0
2.7	0.02	500.9	221.2	55.6	49.2	236.2	3.0	0.0	0.0	0.2	0.0
3.0	0.03	545.2	359.2	45.4	61.1	241.5	13.0	200.0	26.3	0.5	7.9
3.3	0.04	585.0	474.1	67.1	81.4	305.2	17.0	100.0	20.6	0.4	2.4
3.6	0.12	538.8	272.4	73.2	121.5	316.4	10.0	100.0	25.9	0.7	19.7
3.9	0.12	601.3	224.7	59.3	157.3	260.3	4.0	0.0	7.0	0.5	11.3
4.2	0.21	581.0	293.0	75.5	192.1	266.1	0.0	0.0	0.0	0.1	0.0
4.5	0.21	603.9	268.0	110.7	181.6	249.5	3.0	0.0	9.1	0.4	0.0
4.8	0.28	568.6	336.0	85.0	161.9	267.0	14.0	0.0	17.3	1.0	19.5

Sample: Porewater, Drax Borehole 2, Barlow mound (Unit: mg/l unless indicated, \*: ug/l)

Analysed by AAS/\*\*Ion chromatography

(m) Depth	Al	Ca	Mg	Na	K	Pb*	Ni*	Cd*	Cu*	Zn*	Cl**	SO4**	NO3**
0.6	0.27	211.4	46.0	175.0	268.0	125	10.7	0.2	11.8	22.5	247.2	233.8	621.7
0.9	0.36	203.1	52.7	85.9	54.5	75	9.7	0.7	0.0	7.3	176.8	294.7	450.8
1.2	0.14	298.8	125.6	32.9	183.0	19	6.7	0.0	0.0	18.3	117.4	219.2	185.6
1.5	0.25	511.5	143.5	39.0	102.8	83	12.6	0.6	0.0	32.0	82.0	1792.7	195.0
1.8	0.33	496.5	107.5	62.0	163.0	112	14.7	0.0	11.7	11.2	98.2	2021.4	141.7
2.1	0.33	560.7	132.2	66.0	195.0	71	14.0	0.1	15.8	37.2	77.9	1632.4	257.4
2.4	0.28	591.5	160.5	88.8	171.0	96	14.2	0.4	8.5	20.3	121.9	1936.0	179.2
2.7	0.34	492.9	114.3	64.1	131.0	43	10.7	0.1	3.9	1.2	140.0	1814.1	91.7
3.0	0.30	495.0	130.4	91.7	163.0	171	15.1	0.1	9.8	18.3	126.0	1833.4	85.3
3.3	0.30	497.7	165.2	110.0	195.0	75	16.4	0.0	21.8	36.7	145.0	2276.1	99.7
3.5	0.22	518.2	137.9	88.3	247.0	100	13.4	0.3	9.3	6.6	109.8	3091.0	103.8
3.8	0.35	497.4	160.6	104.0	162.0	165	18.4	0.2	18.8	6.9	194.0	2317.4	76.2

Sample: Porewater, Borehole 3, Barlow ash mound (Unit: mg/l unless indicated, \* ug/l)

Analysed by AAS/\*\*Ion chromatography

(m) Depth	Al	Ca	Mg	Na	K	Pb*	Ni*	Cd*	Cu*	Zn*	Cl**	SO4**	NO3**
0.6	0.24	71.8	23.9	32.4	32.1	165.0	56.1	0.5	50.5	22.3	148.5	73.5	39.8
0.9	0.33	82.4	36.9	32.2	49.2	253.0	7.7	0.0	16.9	2.9	71.0	211.4	57.0
1.2	0.25	480.6	117.5	37.7	81.0	131.0	11.1	0.0	47.2	0.2	74.3	1733.2	122.0
1.5	0.18	531.0	255.1	140.0	281.0	137.0	31.9	0.0	0.0	0.3	53.7	2312.9	205.7
1.8	0.23	604.2	121.1	269.0	429.0	177.0	28.8	0.6	38.0	31.6	72.8	2126.3	461.9
2.1	0.21	467.5	92.9	195.0	283.0	76.0	10.4	0.0	25.7	30.5	61.5	2040.5	133.3
2.4	0.24	460.9	111.8	176.0	228.0	117.0	13.3	0.0	20.4	40.3	88.8	2283.6	177.7
2.7	0.23	454.7	102.3	149.0	195.0	162.0	10.2	0.0	16.4	5.2	54.8	2150.4	103.1
3.0	0.19	542.8	119.0	160.0	242.0	33.0	9.3	0.0	12.3	13.1	52.7	1998.4	134.9

Sample: Porewater, Borehole 4, Barlow mound (Unit: mg/l unless indicated)

Analysed by ICP-AES/AAS-hydride generating system/ Ion chromatography

(m) Depth	(mV)		Ca	Mg	Na	K	Fe	Al	SiO2	B	Ba	Cd	Co	Cr	
	pH	Eh													
0.7			937.5	136.7	82.1	144.5	0.00	0.08	1.11	0.86	0.33	0.04	0.08	0.07	
0.9			741.4	121.8	73.2	125.3	0.02	0.01	0.88	1.26	0.29	0.03	0.07	0.06	
1.1			557.9	106.5	54.7	65.7	0.06	0.02	0.47	1.42	0.19	0.03	0.06	0.08	
1.5	8.23	397	768.7	137.8	46.4	73.2	0.01	0.01	0.60	2.53	0.16	0.03	0.07	0.11	
1.8	7.67	395	695.7	146.7	50.4	91.5	0.00	0.09	0.58	3.15	0.15	0.03	0.07	0.06	
2.0	8.25	395	666.5	139.0	45.0	95.1	0.06	0.05	0.39	3.38	0.16	0.03	0.07	0.09	
2.2	7.53	402	720.3	149.2	43.7	84.9	0.08	0.08	0.99	4.80	0.17	0.04	0.07	0.07	
2.4	8.40	400	761.4	185.1	65.1	89.4	0.08	0.13	0.88	4.17	0.20	0.04	0.08	0.08	
2.6			691.7	219.6	54.5	88.9	0.05	0.08	0.41	5.30	0.15	0.04	0.08	0.09	
2.8	7.16	406	638.5	243.7	47.4	112.8	0.03	0.13	0.28	5.75	0.13	0.04	0.08	0.16	
2.9			639.7	305.2	51.0	126.0	0.08	0.07	0.45	7.80	0.14	0.04	0.09	0.16	
3.0			636.4	298.8	51.2	128.2	0.02	0.04	0.39	7.98	0.14	0.04	0.08	0.17	
3.2			613.8	333.1	52.3	125.8	0.03	0.01	0.39	9.14	0.13	0.04	0.08	0.14	
3.3	8.15	407	616.4	338.8	52.6	126.3	0.04	0.08	0.49	10.57	0.14	0.04	0.08	0.18	
3.4	7.75	406	623.2	326.7	54.3	163.2	0.03	0.09	0.43	10.41	0.13	0.04	0.08	0.14	
3.5			603.9	329.9	54.6	178.3	0.04	0.02	0.15	9.53	0.13	0.04	0.08	0.18	
3.7			603.0	352.9	53.1	157.2	0.08	0.07	0.36	11.36	0.13	0.04	0.09	0.13	
3.8			597.9	377.6	54.6	166.9	0.07	0.02	0.28	11.50	0.12	0.05	0.09	0.14	
3.9	8.26	409	608.3	363.2	52.1	137.4	0.09	0.03	0.36	13.40	0.13	0.05	0.10	0.15	
4.0	8.22	411	611.6	434.4	62.7	186.6	0.04	0.09	0.47	19.65	0.13	0.04	0.09	0.20	
(m) Depth	Cu	Li	Mn	Ni	Pb	Sr	Zn	V	(ug/l)		(ug/l)		(ug/l)		
									As*	Se*	Mo*	Hg*	Cl*	SO4**	NO3**
0.7	0.02	0.25	0.01	0.17	0.49	3.64	0.02	0.09	10	11	0.4	190	380.9	1291.1	2601.6
0.9	0.01	0.41	0.00	0.13	0.45	3.09	0.03	0.09	38	16	0.3	26	366.1	1451.2	1661.0
1.1	0.01	0.39	0.00	0.11	0.38	2.03	0.01	0.08	22	15	0.8	<5.0	296.8	1363.8	986.3
1.5	0.01	0.78	0.00	0.12	0.44	2.68	0.01	0.12	27	22	0.7	<5.0	212.5	2110.9	796.9
1.8	0.01	1.08	0.01	0.11	0.44	2.68	0.01	0.14	22	35	0.9	<5.0	167.5	2482.3	518.7
2.0	0.04	1.10	0.00	0.11	0.43	2.59	0.01	0.13	48	30	1.4	<5.0	120.2	3560.4	477.2
2.2	0.02	1.00	0.00	0.12	0.46	2.54	0.02	0.08	52	22	2.1	<5.0	99.5	3008.9	348.4
2.4	0.01	1.25	0.00	0.13	0.49	2.79	0.02	0.15	38	29	2.0	<5.0	186.7	3112.6	813.4
2.6	0.02	1.51	0.01	0.12	0.51	2.52	0.02	0.14	43	35	1.9	<5.0	155.9	2925.4	824.4
2.8	0.01	1.52	0.01	0.12	0.45	2.36	0.02	0.13	52	30	2.5	<5.0	248.4	3195.1	508.4
2.9	0.02	1.92	0.02	0.12	0.50	2.60	0.02	0.14	55	42	2.4	<5.0	124.1	3361.5	681.7
3.0	0.02	1.91	0.01	0.13	0.50	2.61	0.02	0.13	44	58	3.1	<5.0	179.0	3524.8	762.2
3.2	0.02	2.08	0.01	0.12	0.51	2.57	0.02	0.14	32	35	2.3	<5.0	132.9	4070.1	687.4
3.3	0.01	2.18	0.01	0.13	0.53	2.66	0.02	0.16	22	47	2.9	<5.0	119.6	4041.9	604.8
3.4	0.01	1.78	0.01	0.13	0.53	2.55	0.02	0.13	27	25	2.9	<5.0	125.5	3687.0	589.5
3.5	0.02	1.40	0.01	0.14	0.53	2.27	0.03	0.10	36	28	3.1	<5.0	114.5	2116.6	628.0
3.7	0.02	1.68	0.01	0.14	0.58	2.29	0.03	0.13	33	19	2.8	<5.0	137.4	3751.9	843.9
3.8	0.02	1.59	0.01	0.15	0.59	2.27	0.03	0.12	66	20	2.5	<5.0	157.3	3911.2	721.4
3.9	0.01	1.59	0.00	0.13	0.59	2.35	0.02	0.14	80	37	2.5	<5.0	144.7	4223.2	834.4
4.0	0.02	1.82	0.00	0.13	0.53	2.64	0.02	0.15	44	29	3.2	<5.0	137.4	4616.6	681.4

**Appendix C-2: Analyses of PFA chemistry, Barlow ash mound, Drax**

**Sample: Weathered PFA, borehole 1, Barlow mound (Unit: % unless indicated, \*: ppm)**

**Analysed by XRF (Except for L.O.I., Water content, pH, FeO and Fe2O3)**

Depth	SiO2	TiO2	Al2O3	Total Fe	FeO	Fe2O3	MnO	MgO	CaO	Na2O	K2O	P2O5	SO3	L.O.I.	pH
0.3	53.33	0.87	22.36	8.18	1.17	5.58	0.09	2.14	1.51	0.86	3.15	0.26	0.03	6.34	7.92
0.6	50.73	0.90	25.71	9.12	1.37	6.08	0.06	1.04	1.48	0.89	3.71	0.16	0.02	5.61	8.12
0.9	50.58	0.90	25.89	8.96	1.28	6.12	0.06	0.96	1.52	0.90	3.78	0.16	0.02	5.94	7.96
1.2	49.95	0.89	25.65	9.46	1.46	6.22	0.06	1.04	1.50	0.82	3.76	0.16	0.02	5.41	8.16
1.5	50.59	0.89	25.79	9.62	1.40	6.50	0.06	1.14	1.51	0.94	3.75	0.15	0.09	5.34	7.74
1.8	49.63	0.87	25.29	9.03	1.31	6.11	0.05	1.48	1.53	0.83	3.69	0.16	0.18	6.24	7.82
2.1	50.32	0.88	25.66	9.74	1.42	6.58	0.06	1.27	1.56	0.86	3.73	0.15	0.14	4.88	7.66
2.4	49.85	0.87	25.17	9.30	1.46	6.06	0.06	1.33	1.51	1.10	3.67	0.15	0.08	7.07	7.97
2.7	49.41	0.88	25.35	10.40	1.58	6.88	0.07	1.65	1.61	0.89	3.51	0.19	0.13	5.50	7.86
3.0	49.15	0.88	25.57	9.92	1.48	6.64	0.07	1.37	1.66	1.08	3.63	0.17	0.22	5.27	8.13
3.3	49.93	0.89	26.08	9.84	1.44	6.64	0.07	1.39	1.69	1.05	3.72	0.17	0.25	4.38	8.11
3.6	49.73	0.89	26.10	10.04	1.48	6.76	0.07	1.46	1.64	1.01	3.75	0.16	0.24	3.93	8.15
3.9	50.86	0.91	26.28	9.94	1.35	6.94	0.07	1.30	1.58	0.82	3.72	0.17	0.21	4.00	8.26
4.2	51.02	0.91	25.76	9.80	1.48	6.52	0.07	1.42	1.59	0.85	3.71	0.17	0.26	3.41	8.22
4.5	50.65	0.91	26.04	9.93	1.49	6.61	0.08	1.49	1.56	0.87	3.65	0.20	0.23	3.83	8.32
m	Water	V*	Cr*	Mn*	Ni*	Cu*	Zn*	Rb*	Sr*	Y*	Zr*	Nb*	Ba*	Pb*	Total
0.3	14.30	217	136	598	104	143	157	144	223	50	210	20	703	96	99.4
0.6	11.20	262	137	432	109	149	115	165	215	54	188	17	749	84	99.7
0.9	12.40	258	139	407	106	137	128	171	220	53	184	17	723	82	99.9
1.2	9.70	250	138	449	108	133	223	161	221	55	180	19	738	72	100.5
1.5	12.60	265	136	435	106	128	121	164	218	53	189	16	739	83	100.1
1.8	11.90	260	135	399	112	159	118	170	225	56	177	17	696	80	99.3
2.1	18.10	256	139	467	111	158	114	168	222	51	191	15	739	72	99.5
2.4	12.70	261	136	414	120	183	120	167	220	55	184	18	708	86	100.4
2.7	18.70	254	135	541	124	188	109	160	239	54	197	13	806	84	99.9
3.0	12.40	243	139	485	121	182	116	166	236	51	202	18	721	81	99.3
3.3	12.80	264	143	464	118	178	113	162	239	55	191	15	765	76	99.7
3.6	10.90	259	137	475	118	178	107	167	241	55	190	17	772	76	99.3
3.9	12.40	257	142	473	119	167	113	165	230	57	173	18	714	78	100.1
4.2	9.10	255	139	484	123	170	119	171	234	52	198	18	719	82	99.3
4.5	7.90	253	134	531	116	159	103	164	242	56	190	15	727	82	99.8

**Sample: Weathered PFA, Borehole 2, Barlow (Unit: % unless indicated, \*:ppm)**

**Analysed by XRF (Except for L.O.I. and pH)**

(m)														
Depth	SiO2	TiO2	Al2O3	Total Fe	MnO	MgO	CaO	Na2O	K2O	P2O5	SO3	L.O.I.	pH	V*
0.3	51.20	0.90	25.66	9.52	0.06	1.49	1.15	0.81	3.68	0.21	<.02	4.78	7.26	287
0.6	52.40	0.90	24.80	9.29	0.07	1.50	1.15	0.84	3.56	0.22	<.02	4.90	7.92	262
0.9	50.70	0.91	26.09	9.61	0.06	1.52	1.05	0.93	3.75	0.19	<.02	4.64	7.69	273
1.2	52.46	0.87	25.52	9.73	0.07	1.44	1.29	0.87	3.61	0.18	0.04	4.05	7.24	244
1.5	51.94	0.89	25.80	9.52	0.06	1.51	1.08	0.92	3.71	0.19	0.03	4.01	7.95	272
1.8	53.91	0.84	24.35	9.32	0.07	1.43	1.26	0.94	3.52	0.20	0.06	3.97	7.65	235
2.1	51.60	0.89	26.10	9.63	0.06	1.45	1.25	1.06	3.75	0.18	0.20	3.67	7.20	275
2.4	51.61	0.89	26.11	9.66	0.06	1.50	1.28	1.04	3.75	0.19	0.12	3.41	7.38	275
2.7	52.10	0.89	26.19	10.27	0.07	1.53	1.40	0.96	3.75	0.18	0.07	2.60	7.53	259
3.0	52.38	0.90	26.58	10.34	0.07	1.54	1.41	0.94	3.73	0.18	0.08	2.11	7.79	257
3.3	52.46	0.89	26.22	10.27	0.06	1.53	1.33	0.93	3.72	0.18	0.08	2.21	7.68	256
3.6	52.72	0.90	26.78	10.19	0.07	1.55	1.35	0.92	3.79	0.17	0.04	1.69	7.56	256
(m)														
Depth	Cr*	Mn*	Ni*	Cu*	Zn*	Rb*	Sr*	Y*	Zr*	Nb*	Ba*	Pb*	Total	
0.3	145	474	114	156	134	160	245	53	195	18	761	82	99.7	
0.6	142	501	106	146	135	158	240	54	186	16	733	74	99.9	
0.9	139	446	116	156	121	165	252	56	181	18	780	70	99.7	
1.2	128	514	104	151	66	162	251	50	186	15	766	48	100.4	
1.5	130	419	115	172	123	162	249	54	180	17	782	85	99.9	
1.8	130	487	103	153	89	153	233	50	188	19	721	66	100.1	
2.1	132	426	114	165	95	165	258	55	173	19	788	63	100.1	
2.4	140	432	119	174	97	164	257	55	199	15	795	72	99.9	
2.7	135	491	116	156	68	165	252	55	192	16	743	49	100.3	
3.0	132	494	114	162	58	163	254	51	188	17	799	38	100.5	
3.3	147	474	116	146	63	163	254	52	190	15	750	51	100.1	
3.6	131	479	112	152	57	161	244	52	188	17	772	35	100.4	

**Sample: Weathered PFA, Borehole 3, Barlow (Unit: % unless indicated, \*:ppm)**

**Analysed by XRF (Except for L.O.I. and pH)**

(m)														
Depth	SiO2	TiO2	Al2O3	Total Fe	MnO	MgO	CaO	Na2O	K2O	P2O5	SO3	L.O.I.	pH	V*
0.3	50.65	0.88	26.18	9.79	0.07	1.51	1.01	0.97	3.73	0.18	0.04	4.48	8.08	284
0.6	50.84	0.90	26.27	9.66	0.06	1.57	1.02	1.00	3.78	0.19	<.02	4.71	8.09	269
0.9	50.67	0.90	26.23	9.80	0.06	1.54	1.11	0.99	3.78	0.19	0.08	4.65	7.65	278
1.2	50.96	0.88	25.31	9.67	0.07	1.47	1.42	0.98	3.63	0.28	0.13	4.45	7.66	270
1.5	51.70	0.80	25.59	9.81	0.07	1.39	1.29	0.78	3.67	0.26	0.17	4.27	7.29	280
1.8	52.22	0.92	26.30	9.40	0.07	1.50	1.17	1.09	3.78	0.20	0.04	3.23	7.69	284
2.1	52.01	0.89	26.11	10.16	0.08	1.54	1.41	0.94	3.73	0.18	0.04	2.85	8.08	283
2.4	52.17	0.93	26.56	9.51	0.06	1.48	1.30	1.00	3.80	0.18	0.12	2.82	7.65	271
2.7	52.18	0.90	26.47	9.72	0.06	1.55	1.27	0.95	3.77	0.18	0.13	2.73	7.95	257
Depth	Cr*	Mn*	Ni*	Cu*	Zn*	Rb*	Sr*	Y*	Zr*	Nb*	Ba*	Pb*	Total	
0.3	133	435	115	190	125	165	246	59	182	17	786	72	99.8	
0.6	145	425	121	166	120	164	252	57	182	19	785	90	100.3	
0.9	150	443	119	199	116	166	255	54	181	15	758	80	100.3	
1.2	145	479	125	163	129	161	301	55	186	17	811	97	99.5	
1.5	151	531	114	193	137	171	225	44	192	16	697	87	100.1	
1.8	145	447	116	175	107	175	252	49	182	16	793	84	100.2	
2.1	145	536	113	167	76	162	249	54	179	16	744	54	100.2	
2.4	143	475	112	180	88	160	272	58	189	20	732	60	100.2	
2.7	181	477	137	163	79	166	262	58	183	17	759	69	100.2	

Sample: Weathered PFA, Borehole 4, Barlow (Unit: % unless indicated, \*:ppm)

Analysed by XRF (Except for L.O.I. and Water content)

(m)													Water		
Depth	SiO2	TiO2	Al2O3	Total Fe	MnO	MgO	CaO	Na2O	K2O	P2O5	SO3	L.O.I	Content	V*	
0.7	51.18	0.89	24.74	8.00	0.08	1.54	1.66	1.17	3.58	0.24	0.01	6.20	14.80	276	
0.9	50.55	0.88	25.95	9.38	0.07	1.52	1.42	1.15	3.71	0.22	0.10	4.99	10.00	293	
1.1	50.15	0.89	25.80	9.75	0.07	1.53	1.35	1.13	3.68	0.19	0.11	5.48	11.90	293	
1.5	49.94	0.89	25.77	9.87	0.07	1.55	1.39	1.20	3.75	0.19	0.28	4.85	11.40	280	
1.8	50.54	0.88	26.14	8.92	0.07	1.57	1.41	1.21	3.79	0.17	0.26	4.83	11.30	303	
2.0	50.05	0.89	26.10	9.14	0.06	1.52	1.39	1.26	3.78	0.18	0.29	5.14	11.70	291	
2.2	50.66	0.89	24.62	9.04	0.08	1.59	1.76	1.11	3.54	0.23	0.31	5.72	17.10	284	
2.4	50.02	0.90	26.44	8.96	0.07	1.56	1.41	1.14	3.71	0.20	0.26	5.17	11.80	321	
2.6	50.11	0.88	25.38	9.31	0.06	1.49	1.50	1.25	3.66	0.21	0.37	5.48	12.10	295	
2.8	49.05	0.89	26.08	9.59	0.06	1.55	1.40	1.16	3.74	0.19	0.38	5.21	11.30	305	
2.9	49.15	0.88	26.14	9.47	0.06	1.61	1.39	1.20	3.74	0.18	0.34	5.37	11.70	305	
3.0	49.40	0.87	26.16	9.51	0.07	1.64	1.40	1.19	3.79	0.17	0.39	5.61	11.80	295	
3.2	49.42	0.90	26.30	9.25	0.07	1.57	1.36	1.13	3.74	0.18	0.42	5.45	12.80	299	
3.3	49.18	0.90	26.43	9.26	0.07	1.56	1.36	1.10	3.73	0.18	0.38	5.69	12.00	311	
3.4	49.80	0.89	26.59	9.17	0.07	1.60	1.41	1.12	3.73	0.18	0.42	5.27	12.40	302	
3.5	49.96	0.88	26.15	9.08	0.07	1.61	1.41	1.15	3.70	0.20	0.38	5.30	12.40	308	
3.7	49.49	0.89	26.06	9.44	0.06	1.60	1.37	1.11	3.71	0.19	0.44	5.13	9.10	288	
3.8	49.74	0.92	26.38	9.40	0.07	1.59	1.40	1.21	3.75	0.18	0.36	5.14	12.30	305	
3.9	50.24	0.89	26.21	9.31	0.07	1.64	1.37	1.11	3.74	0.19	0.35	5.01	12.10	296	
4.0	50.49	0.88	26.08	9.26	0.07	1.58	1.37	0.98	3.74	0.19	0.41	4.81	12.80	305	

Depth	Cr*	Mn*	Ni*	Cu*	Zn*	Rb*	Sr*	Y*	Zr*	Nb*	Ba*	Pb*	Total
0.7	131	518	82	126	150	158	268	54	190	18	821	88	99.6
0.9	140	504	119	195	128	171	258	50	182	17	828	84	100.2
1.1	134	511	112	199	125	163	252	55	180	17	781	72	100.4
1.5	146	481	120	196	125	168	250	54	185	16	802	85	100.0
1.8	138	444	112	190	120	169	261	56	181	13	747	79	100.1
2.0	145	441	120	199	120	171	263	50	180	18	796	86	100.1
2.2	144	550	107	192	147	161	255	55	189	15	742	91	99.9
2.4	139	444	117	233	123	168	270	57	178	17	764	86	100.1
2.6	139	447	120	203	129	165	263	55	180	14	803	84	100.0
2.8	142	433	123	196	123	173	264	54	176	16	798	94	99.6
2.9	141	448	111	203	122	168	255	57	180	15	753	80	99.8
3.0	125	444	110	200	120	168	249	53	181	17	792	76	100.5
3.2	138	425	113	197	123	164	252	58	180	14	761	96	100.1
3.3	139	415	117	199	120	171	256	54	178	16	774	84	100.1
3.4	135	433	105	187	109	166	252	56	179	18	755	88	100.5
3.5	140	443	109	189	116	158	252	53	176	18	777	77	100.2
3.7	138	441	121	194	117	174	256	53	182	19	786	88	99.8
3.8	137	457	111	195	112	163	250	53	178	17	810	82	100.4
3.9	140	489	113	200	118	167	256	55	182	18	773	85	100.4
4.0	131	504	115	208	114	168	253	55	184	18	766	77	100.2

Sample: Fresh PFA, Drax Power Station (Unit: % unless indicated, \*: ppm)

	SiO2	TiO2	Al2O3	Total Fe	FeO	Fe2O3	MnO	MgO	CaO	Na2O	K2O	P2O5	SO3	L.O.I.
DPFA1	53.11	0.94	25.68	7.66	1.14	5.12	0.07	1.83	2.10	1.39	3.57	0.19	0.31	3.10
DPFA2	54.16	0.95	25.29	7.15	1.04	4.84	0.08	1.66	1.73	1.58	3.79	0.21	0.27	2.75
DPFA3	53.01	0.95	26.58	7.39			0.06	1.69	1.86	1.70	3.89	0.24	0.48	0.92
	V*	Cr*	Mn*	Ni*	Cu*	Zn*	Rb*	Sr*	Y*	Zr*	Nb*	Ba*	Pb*	Total
DPFA1	272	143	481	126	135	122	153	275	51	199	20	1169	86	100.3
DPFA2	245	142	534	104	130	118	162	291	52	195	20	886	72	99.9
DPFA3	249	125	498	109	162	110	180	314	48	190	20	1134	67	99.1

Sample: Weathered PFA, Meaford ash disposal mound (Unit: % unless indicated, \*: ppm)

Analysed by XRF (Except for L.O.I., Water content, pH, FeO and Fe2O3)

(m)														Water	
Depth	SiO2	TiO2	Al2O3	Total Fe	MnO2	MgO	CaO	Na2O	K2O	P2O5	SO3	L.O.I.	Content	V*	
0.7	48.31	0.87	26.94	14.83	0.17	1.48	3.34	0.74	2.40	0.32	0.19	7.93	18.8	284	
0.9	48.72	0.88	27.61	14.08	0.15	1.50	3.28	0.73	2.43	0.35	0.15	8.07	24.5	294	
1.2	49.14	0.91	28.36	13.01	0.14	1.48	3.27	0.82	2.42	0.35	0.17	9.25	26.5	301	
1.6	46.99	0.92	28.38	14.60	0.14	1.57	3.46	0.84	2.31	0.50	0.26	10.41	24.8	310	
1.9	46.36	0.90	28.02	15.16	0.15	1.62	3.46	0.73	2.31	0.49	0.27	10.84	26.1	316	
2.4	46.43	0.90	27.72	15.70	0.15	1.61	3.46	0.72	2.26	0.49	0.25	10.54	25.9	315	
3.6	47.40	0.89	27.10	14.69	0.16	1.66	3.77	0.66	2.36	0.38	0.40	11.79	24.1	295	
4.7	47.55	0.90	27.24	14.63	0.15	1.72	3.79	0.69	2.36	0.35	0.49	10.28	23.8	303	
Depth	Cr*	Mn*	Ni*	Cu*	Zn*	Rb*	Sr*	Y*	Zr*	Nb*	Ba*	Pb*	Total		
0.7	120	1155	144	202	912	116	349	54	185	15	1187	204	100.1		
0.9	119	1077	141	203	993	121	371	56	184	14	1235	218	100.4		
1.2	126	969	138	196	1052	114	387	57	186	18	1272	221	100.6		
1.6	137	1029	166	231	1139	109	455	71	189	19	1493	285	100.5		
1.9	138	1035	169	222	1086	112	444	66	190	19	1517	284	100.0		
2.4	132	1065	173	224	1077	105	456	67	187	19	1924	308	100.3		
3.6	127	1146	166	225	1118	106	377	65	186	14	1272	311	100.0		
4.7	123	1127	174	267	1147	112	358	61	185	16	1159	294	100.4		

**Appendix C-3: Correlation matrix of data from chemical analysis of Drax weathered ash**

	SiO2	TiO2	Al2O3	Fe2O3(T)	MnO2	MgO	CaO	Na2O	K2O	P2O5	SO3	L.O.I.	V	Cr	Mn	Ni	Cu	Zn	Rb	Sr	Y	Ba
SiO2	1.000																					
TiO2	0.055	1.000																				
Al2O3	0.001	0.500	1.000																			
Fe2O3(T)	0.229	0.031	0.313	1.000																		
MnO2	0.253	-0.003	-0.120	0.127	1.000																	
MgO	-0.008	0.075	0.258	0.067	0.216	1.000																
CaO	-0.370	-0.036	-0.233	-0.089	0.304	-0.247	1.000															
Na2O	-0.445	0.085	0.155	-0.397	-0.008	0.462	0.111	1.000														
K2O	-0.013	0.436	0.846	0.117	-0.340	0.005	-0.236	0.168	1.000													
P2O5	0.225	-0.248	-0.302	-0.181	0.381	0.355	-0.156	0.068	-0.403	1.000												
SO3	-0.525	0.020	0.303	-0.173	-0.020	0.440	0.324	0.575	0.209	-0.005	1.000											
L.O.I.	-0.690	-0.197	-0.389	-0.636	-0.221	-0.149	0.282	0.345	-0.221	0.000	0.298	1.000										
V	-0.368	0.129	0.424	-0.395	-0.054	0.519	-0.120	0.685	0.378	0.215	0.661	0.333	1.000									
Cr	0.245	0.250	0.342	0.120	-0.053	0.125	-0.071	-0.035	0.377	0.189	0.114	-0.140	0.175	1.000								
Mn	0.389	-0.031	-0.124	0.299	0.716	0.270	0.267	-0.188	-0.304	0.440	-0.022	-0.255	-0.097	0.293	1.000							
Ni	-0.177	0.088	0.307	0.518	-0.253	0.166	-0.127	0.002	0.212	-0.061	0.161	-0.250	-0.019	0.372	-0.123	1.000						
Cu	-0.402	-0.021	0.361	-0.054	-0.009	0.579	-0.022	0.606	0.231	0.138	0.714	0.245	0.766	0.213	0.054	0.351	1.000					
Zn	-0.478	-0.091	-0.339	-0.500	-0.119	-0.284	0.152	0.096	-0.095	0.201	0.102	0.693	0.221	0.015	-0.124	-0.184	0.083	1.000				
Rb	-0.307	0.082	0.435	-0.041	-0.251	0.030	0.050	0.239	0.549	-0.160	0.413	0.160	0.418	0.321	-0.182	0.356	0.455	0.094	1.000			
Sr	0.084	0.249	0.269	-0.103	0.131	0.673	-0.228	0.518	0.120	0.549	0.279	-0.196	0.505	0.227	0.149	0.176	0.407	-0.151	0.013	1.000		
Y	-0.195	0.494	0.287	-0.099	-0.153	0.179	-0.045	0.140	0.268	-0.204	0.166	0.118	0.236	0.180	-0.176	0.123	0.165	0.099	-0.086	0.270	1.000	
Ba	-0.087	0.249	0.249	-0.037	0.090	0.477	-0.187	0.538	0.149	0.313	0.164	0.001	0.443	0.032	0.058	0.078	0.296	-0.004	0.060	0.636	0.068	1.000
Pb	-0.588	-0.061	-0.226	-0.517	-0.115	0.000	0.164	0.333	-0.119	0.299	0.400	0.722	0.405	0.135	-0.205	0.103	0.367	0.672	0.323	0.060	0.121	0.098

**Appendix C-4: Correlation matrix of data from the batch leaching tests (Continued-)**

	EC	Ca	Na	K	Mg	Fe	Al	B	Ba	Cd	Co	Cr	Cu	In	Li	Mn	Ni	Pb	Si	Sr	Ti	V
EC	1.000																					
Ca	0.985	1.000																				
Na	0.999	0.977	1.000																			
K	0.999	0.977	1.000	1.000																		
Mg	0.980	0.957	0.977	0.977	1.000																	
Fe	0.987	0.947	0.992	0.993	0.970	1.000																
Al	0.962	0.990	0.950	0.951	0.942	0.916	1.000															
B	0.595	0.566	0.582	0.581	0.699	0.596	0.575	1.000														
Ba	-0.082	-0.098	-0.074	-0.085	-0.089	-0.109	-0.162	-0.182	1.000													
Cd	0.993	0.959	0.996	0.997	0.982	0.998	0.932	0.612	-0.094	1.000												
Co	0.973	0.962	0.968	0.969	0.973	0.962	0.951	0.724	-0.149	0.969	1.000											
Cr	0.993	0.960	0.996	0.997	0.980	0.998	0.934	0.609	-0.105	1.000	0.970	1.000										
Cu	0.971	0.918	0.979	0.979	0.969	0.995	0.883	0.642	-0.099	0.992	0.954	0.991	1.000									
In	0.864	0.857	0.854	0.854	0.869	0.854	0.851	0.837	-0.251	0.858	0.942	0.859	0.856	1.000								
Li	0.998	0.976	1.000	1.000	0.973	0.993	0.949	0.573	-0.081	0.996	0.967	0.996	0.979	0.853	1.000							
Mn	0.931	0.956	0.917	0.916	0.940	0.870	0.956	0.584	0.037	0.897	0.905	0.894	0.846	0.774	0.911	1.000						
Ni	0.997	0.970	0.999	0.999	0.981	0.996	0.944	0.593	-0.090	0.999	0.969	0.999	0.986	0.853	0.999	0.909	1.000					
Pb	0.180	0.172	0.178	0.180	0.190	0.186	0.198	0.110	-0.280	0.187	0.166	0.188	0.187	0.130	0.178	0.155	0.185	1.000				
Si	0.938	0.957	0.925	0.926	0.956	0.889	0.961	0.624	-0.043	0.912	0.920	0.912	0.868	0.803	0.919	0.983	0.922	0.162	1.000			
Sr	0.817	0.899	0.796	0.796	0.755	0.723	0.916	0.300	-0.066	0.747	0.772	0.750	0.658	0.651	0.795	0.889	0.775	0.124	0.867	1.000		
Ti	0.960	0.967	0.949	0.949	0.962	0.928	0.963	0.741	-0.151	0.942	0.990	0.942	0.916	0.946	0.946	0.929	0.945	0.153	0.940	0.815	1.000	
V	0.363	0.375	0.350	0.350	0.364	0.363	0.402	0.630	-0.462	0.357	0.517	0.361	0.369	0.717	0.352	0.251	0.349	0.074	0.283	0.247	0.535	1.000
Zn	0.995	0.964	0.998	0.998	0.984	0.996	0.938	0.611	-0.084	1.000	0.970	0.999	0.989	0.856	0.997	0.908	1.000	0.185	0.921	0.759	0.945	0.350
Zr	0.837	0.847	0.823	0.821	0.839	0.805	0.838	0.819	-0.130	0.816	0.922	0.816	0.802	0.977	0.820	0.795	0.815	0.090	0.798	0.684	0.940	0.715
As	0.745	0.728	0.744	0.747	0.734	0.758	0.734	0.479	-0.331	0.753	0.767	0.756	0.749	0.704	0.746	0.620	0.751	0.234	0.647	0.568	0.744	0.633
Hg	0.991	0.957	0.993	0.993	0.988	0.995	0.933	0.647	-0.106	0.999	0.975	0.998	0.992	0.871	0.992	0.901	0.997	0.190	0.919	0.738	0.950	0.376
Se	0.949	0.945	0.943	0.944	0.929	0.934	0.940	0.650	-0.171	0.939	0.970	0.941	0.918	0.920	0.944	0.869	0.942	0.125	0.892	0.789	0.959	0.554
Mo	0.752	0.756	0.741	0.738	0.732	0.737	0.741	0.791	-0.242	0.736	0.838	0.738	0.736	0.954	0.741	0.644	0.732	0.092	0.666	0.577	0.854	0.722
Cl-	0.996	0.987	0.995	0.995	0.963	0.979	0.964	0.524	-0.067	0.985	0.956	0.985	0.957	0.828	0.996	0.929	0.992	0.175	0.931	0.843	0.941	0.322
NO3-	0.797	0.877	0.776	0.777	0.744	0.708	0.906	0.279	-0.097	0.733	0.753	0.736	0.645	0.614	0.775	0.868	0.759	0.129	0.851	0.980	0.791	0.234
SO4	0.830	0.811	0.821	0.820	0.863	0.825	0.800	0.908	-0.203	0.832	0.906	0.832	0.842	0.968	0.817	0.756	0.822	0.146	0.787	0.568	0.913	0.631

**Appendix C-4: Correlation matrix of data from the batch leaching tests**

	Zn	Zr	As	Hg	Se	Mo	Cl-	NO3-	SO4
Zn	1.000								
Zr	0.818	1.000							
As	0.748	0.672	1.000						
Hg	0.998	0.829	0.756	1.000					
Se	0.939	0.897	0.781	0.942	1.000				
Mo	0.734	0.939	0.573	0.747	0.808	1.000			
Cl-	0.988	0.803	0.737	0.979	0.939	0.714	1.000		
NO3-	0.744	0.639	0.612	0.726	0.776	0.518	0.825	1.000	
SO4	0.831	0.939	0.639	0.851	0.850	0.941	0.782	0.531	1.000

**Appendix C-5: Correlation matrix of data from column leaching tests,Drax fresh ash with deionised water.**

	Ca	Mg	Na	K	Fe	Al	B	Ba	Cr	Cu	Li	Mn	Ni	Pb	Mo	Sr	V	Zn	As	Si	Cl-	NO3-	
Ca	1.000																						
Mg	-0.652	1.000																					
Na	-0.739	0.891	1.000																				
K	-0.817	0.892	0.991	1.000																			
Fe	-0.051	0.173	-0.093	-0.056	1.000																		
Al	-0.477	0.882	0.931	0.886	-0.063	1.000																	
B	-0.878	0.916	0.952	0.980	0.055	0.818	1.000																
Ba	-0.901	0.808	0.781	0.843	0.117	0.623	0.900	1.000															
Cr	-0.707	0.900	0.998	0.985	-0.087	0.949	0.940	0.770	1.000														
Cu	0.016	0.262	0.159	0.131	0.659	0.243	0.149	0.040	0.179	1.000													
Li	-0.819	0.888	0.991	1.000	-0.059	0.883	0.980	0.836	0.983	0.133	1.000												
Mn	-0.847	0.822	0.915	0.945	-0.115	0.786	0.941	0.849	0.902	-0.106	0.942	1.000											
Ni	-0.410	0.546	0.480	0.492	0.447	0.504	0.515	0.524	0.478	0.207	0.490	0.419	1.000										
Pb	0.155	0.144	0.224	0.158	0.052	0.310	0.064	-0.070	0.235	0.070	0.162	-0.008	0.487	1.000									
Mo	-0.662	0.896	0.993	0.972	-0.104	0.965	0.919	0.742	0.998	0.178	0.970	0.885	0.472	0.262	1.000								
Sr	-0.258	0.700	0.828	0.752	-0.323	0.920	0.637	0.379	0.846	0.103	0.752	0.646	0.271	0.412	0.875	1.000							
V	-0.780	0.846	0.988	0.987	-0.165	0.892	0.946	0.808	0.981	0.058	0.988	0.927	0.489	0.221	0.972	0.797	1.000						
Zn	-0.047	0.230	0.093	0.090	0.743	0.134	0.138	0.089	0.109	0.972	0.090	-0.105	0.145	-0.057	0.100	-0.040	-0.006	1.000					
As	-0.594	0.717	0.909	0.878	-0.308	0.856	0.791	0.656	0.910	0.058	0.879	0.765	0.341	0.365	0.914	0.842	0.926	-0.038	1.000				
Si	-0.855	0.850	0.975	0.991	-0.068	0.832	0.977	0.833	0.960	0.088	0.993	0.948	0.473	0.152	0.942	0.710	0.981	0.056	0.861	1.000			
Cl-	-0.632	0.901	0.986	0.961	-0.099	0.974	0.906	0.730	0.994	0.192	0.959	0.871	0.470	0.267	0.999	0.885	0.961	0.111	0.908	0.925	1.000		
NO3-	-0.796	0.943	0.918	0.938	0.028	0.842	0.959	0.902	0.917	0.159	0.934	0.878	0.563	0.051	0.903	0.641	0.908	0.126	0.764	0.906	0.900	1.000	
SO4	-0.230	0.323	0.255	0.246	0.101	0.283	0.264	0.191	0.254	0.000	0.252	0.279	0.218	0.015	0.256	0.199	0.251	0.011	0.222	0.265	0.246	0.231	

**Appendix C-6: Correlation matrix of data from column leaching tests, Drax weathered ash with deionised water.**

	Ca	Mg	Na	K	Fe	Al	B	Ba	Cr	Cu	Li	Ni	Pb	Mo	Sr	V	Zn	As	Si	Cl-	NO3-	SO4	
Ca	1.000																						
Mg	0.999	1.000																					
Na	0.993	0.990	1.000																				
K	0.989	0.985	0.999	1.000																			
Fe	0.565	0.573	0.588	0.594	1.000																		
Al	0.862	0.867	0.869	0.867	0.873	1.000																	
B	0.819	0.814	0.856	0.866	0.603	0.822	1.000																
Ba	0.130	0.136	0.114	0.109	0.492	0.417	0.034	1.000															
Cr	0.902	0.898	0.914	0.912	0.613	0.875	0.820	0.168	1.000														
Cu	0.630	0.641	0.583	0.564	0.061	0.395	0.374	-0.095	0.371	1.000													
Li	0.859	0.853	0.904	0.913	0.672	0.841	0.869	0.108	0.809	0.497	1.000												
Ni	0.621	0.631	0.632	0.621	0.812	0.805	0.563	0.449	0.603	0.276	0.668	1.000											
Pb	0.370	0.382	0.325	0.311	-0.014	0.244	0.189	-0.123	0.186	0.799	0.303	-0.022	1.000										
Mo	0.728	0.714	0.776	0.793	0.453	0.662	0.811	0.049	0.707	0.469	0.875	0.471	0.220	1.000									
Sr	1.000	1.000	0.991	0.985	0.573	0.867	0.313	0.135	0.900	0.636	0.854	0.631	0.377	0.714	1.000								
V	0.666	0.660	0.710	0.723	0.778	0.847	0.786	0.302	0.790	0.114	0.787	0.490	0.194	0.658	0.661	1.000							
Zn	0.979	0.977	0.985	0.985	0.599	0.891	0.888	0.169	0.931	0.578	0.892	0.638	0.313	0.813	0.977	0.725	1.000						
As	0.435	0.433	0.472	0.489	0.804	0.753	0.699	0.406	0.624	-0.102	0.551	0.519	-0.150	0.541	0.434	0.813	0.559	1.000					
Si	0.772	0.756	0.837	0.855	0.570	0.740	0.855	0.108	0.831	0.201	0.911	0.533	0.022	0.863	0.759	0.800	0.836	0.596	1.000				
Cl-	0.993	0.996	0.978	0.970	0.585	0.874	0.795	0.148	0.885	0.658	0.834	0.653	0.405	0.671	0.996	0.638	0.965	0.422	0.715	1.000			
NO3-	0.894	0.878	0.923	0.934	0.441	0.717	0.802	0.087	0.851	0.420	0.864	0.434	0.180	0.848	0.880	0.704	0.906	0.433	0.913	0.836	1.000		
SO4	0.995	0.998	0.982	0.974	0.591	0.878	0.804	0.155	0.891	0.645	0.839	0.649	0.393	0.681	0.997	0.652	0.970	0.438	0.728	1.000	0.847		

**Appendix C-7: Correlation matrix of data from column leaching tests, Meaford weathered ash with deionised water.**

	Ca	Mg	Na	K	Fe	Al	B	Ba	Cr	Cu	Li	Mn	Pb	Mo	Sr	V	Zn	As	Se	Si	Cl-	NO3-	
Ca	1.000																						
Mg	0.959	1.000																					
Na	0.975	0.954	1.000																				
K	0.503	0.494	0.424	1.000																			
Fe	0.422	0.459	0.403	0.575	1.000																		
Al	0.799	0.909	0.795	0.636	0.505	1.000																	
B	0.463	0.407	0.379	0.339	0.257	0.467	1.000																
Ba	0.919	0.873	0.932	0.415	0.314	0.689	0.267	1.000															
Cr	-0.017	0.020	-0.062	0.114	-0.195	0.115	-0.060	-0.285	1.000														
Cu	0.732	0.703	0.704	-0.086	0.086	0.463	0.300	0.680	-0.027	1.000													
Li	0.704	0.702	0.560	0.685	0.577	0.662	0.468	0.552	-0.005	0.423	1.000												
Mn	-0.491	-0.441	-0.515	-0.130	0.041	-0.382	-0.326	-0.554	0.236	-0.286	-0.221	1.000											
Pb	0.742	0.702	0.695	0.407	0.067	0.559	0.272	0.849	-0.273	0.661	0.569	-0.325	1.000										
Mo	0.998	0.967	0.971	0.515	0.413	0.824	0.484	0.916	-0.011	0.733	0.714	-0.494	0.756	1.000									
Sr	0.781	0.739	0.804	0.140	0.325	0.562	0.353	0.849	-0.430	0.680	0.456	-0.759	0.627	0.778	1.000								
V	0.913	0.965	0.894	0.462	0.435	0.910	0.560	0.824	-0.071	0.725	0.708	-0.405	0.732	0.931	0.719	1.000							
Zn	0.076	0.083	0.005	-0.304	0.175	-0.108	-0.095	-0.091	0.162	0.280	0.272	0.312	-0.182	0.053	-0.081	0.048	1.000						
As	0.936	0.852	0.874	0.483	0.280	0.714	0.595	0.817	0.084	0.702	0.679	-0.495	0.702	0.937	0.689	0.833	0.056	1.000					
Se	0.929	0.944	0.910	0.704	0.538	0.932	0.500	0.850	0.022	0.550	0.710	-0.475	0.672	0.940	0.693	0.915	-0.101	0.859	1.000				
Si	0.643	0.551	0.636	-0.091	-0.115	0.289	0.467	0.698	-0.411	0.738	0.299	-0.417	0.743	0.644	0.681	0.629	0.023	0.646	0.424	1.000			
Cl-	0.806	0.766	0.722	0.861	0.556	0.796	0.503	0.693	0.133	0.382	0.786	-0.399	0.586	0.815	0.523	0.728	-0.141	0.816	0.908	0.219	1.000		
NO3-	0.956	0.976	0.918	0.604	0.423	0.912	0.486	0.847	0.072	0.650	0.779	-0.477	0.725	0.968	0.689	0.951	0.031	0.895	0.958	0.529	0.849	1.000	